EJA

European Journal of Anatomy

Volume 27 - Number 3 May 2023

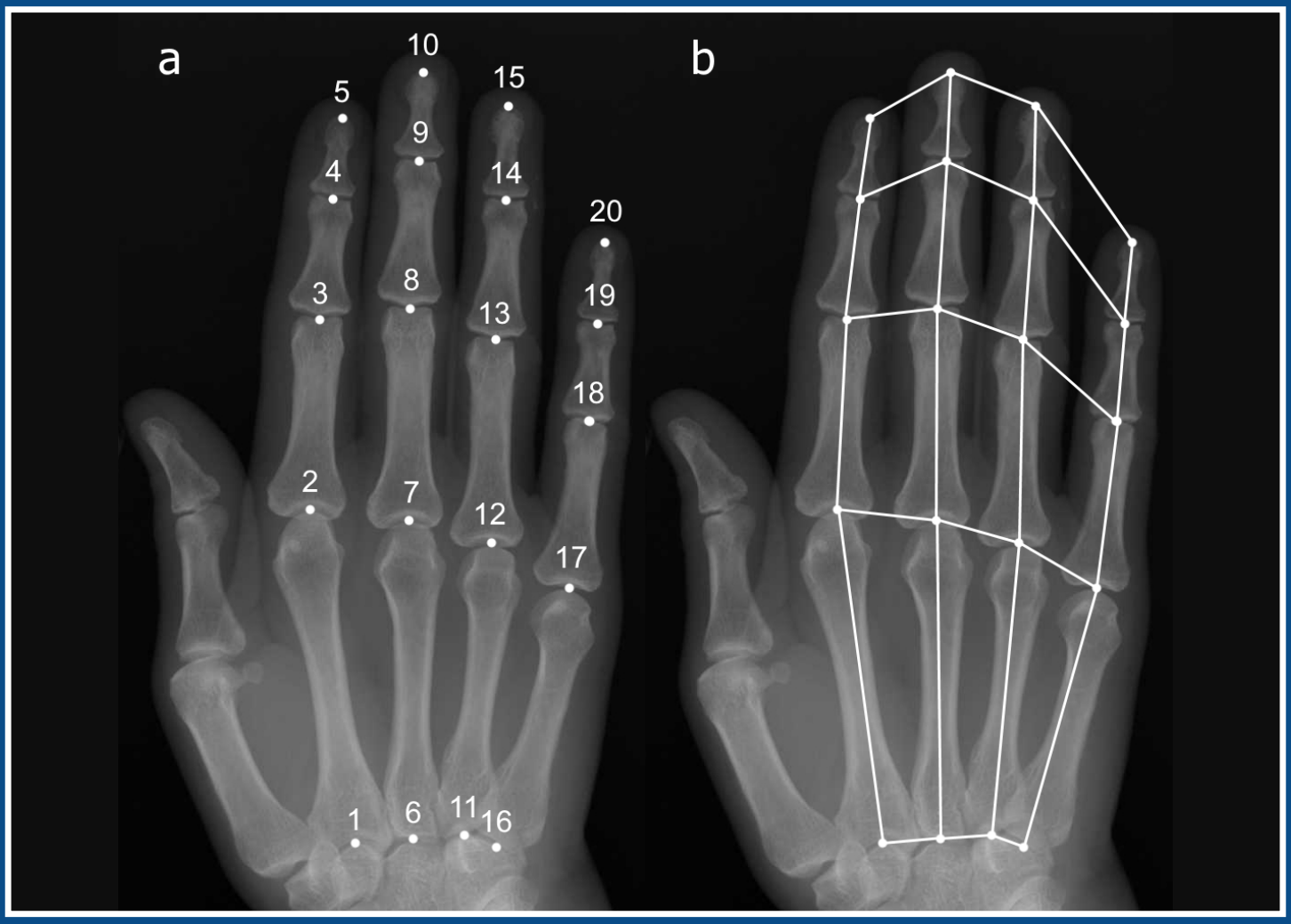

Indexed in:

CLARIVATE
- JCR:2020
- Q4 (21/23)
- I.F. J.C.I.: 0.19

DIALNET

EMBASE / Excerpta Medica

SCOPUS
- SJCR: 2020
- Q4 (31/39)
- I.F.: 0.162

Emerging Sources Citation Index

LATINDEX. Catálogo v1.0 (2002-2017)

Official Journal of the Spanish Society of Anatomy

Published by: **LOKI & DIMAS**

www.eurjanat.com

EJA
European Journal of Anatomy

Volume 27 - Number 3 May 2023

ORIGINAL ARTICLES

CASE REPORTS

BOOK REVIEW

Possible environment influence in spine segmentation anomalies

Manuel D. D'Angelo del Campo[1, 2, 3], Sara Pastor[3], Laura Medialdea[3], Mónica Caballero Grijalba[3], Pamela García Laborde[2], Mónica Salemme[4], Manuel Campo Martín[3], Armando González Martín[3], Verónica Seldes[5], Ricardo Anibal Guichón[1, 2]

[1] Consejo Nacional de Investigaciones Científicas y Técnicas, Centro Científico Tecnológico-Tandil (CONICET, CCT Tandil). Provincia de Buenos Aires, Argentina

[2] Universidad Nacional del Centro de la Provincia de Buenos Aires (UNCPBA), Facultad de Ciencias Sociales (FACSO), Laboratorio de Ecología Evolutiva Humana (LEEH), Unidad de Enseñanza Universitaria Quequén (UEUQ). Provincia de Buenos Aires, Argentina

[3] Laboratorio de Poblaciones de Pasado (LAPP), Departamento de Biología, Facultad de Ciencias, Universidad Autónoma de Madrid (UAM), Madrid, España

[4] Centro Austral de Investigaciones Científicas (CADIC). Ushuaia, Argentina

[5] Instituto Ciencias Antropológicas (ICA), Sección Antropología Biológica, Facultad de Filosofía y Letras, Universidad de Buenos Aires (UBA). Ciudad Autónoma de Buenos Aires, Argentina

SUMMARY

Segmentation anomalies of the spine transformations are relatively common in humans, mainly in adjacent regions. Its aetiology is multifactorial, a combination of genetic, environmental, and epigenetic interaction. A sample of 50 adult individuals of both sexes from two different sites and chronologies of the current Argentine territory was examined. This work proposes a new approach to analyse segmentation anomalies, considering the taphonomic characteristics of the spine, together with the most common occasional contour shifts of such anomalies. Likewise, a bibliographic review was conducted to compile the knowledge achieved to date on this topic. The results showed different patterns of expression of segmentation anomalies among the analysed samples, with the lumbosacral transformations being the most prevalent. The similarities and disparities observed between Southern Patagonian samples and Inuit populations suggest that cold, as an environmental factor, could play an important role in the phenotypic plasticity of human populations. Similarly, hypoxia could influence the sample from Pukará de Tilcara. Due to the scarce existing methodological standardization for addressing segmentation anomalies, a systematization of the methods used to analyse segmentation anomalies is recommended; our approach is a proposal for this purpose.

Key words: Argentina – Boundary regions – Sacralization – Cold – Hypoxia – Holocene

Corresponding author:
Manuel Domingo D'Angelo del Campo. CONICET, CCT Tandil, provincia de Buenos Aires, Argentina; UNCPB, FACSO, LEEH, UEUQ, provincia de Buenos Aires, Argentina; LAPP, Dept. Biología, Fac. Ciencias, UAM, Madrid, España. Phone: 0034 6993381891. E-mail: manueldomingodangelo@gmail.com

Submitted: November 2, 2022. **Accepted:** December 14, 2022

https://doi.org/10.52083/RRXI5320

INTRODUCTION

The alteration of the spine may occur in terms of its number of vertebrae and morphology, which are often related but not necessarily (ten Broek et al., 2012). When these variations occur between two regions of the spine, they are considered segmentation anomalies (SAs), relatively common among humans (White and Folkens, 2005; ten Broek et al., 2012; Singh et al., 2015). Along with genetic factors, the development of the spine can be affected by other effects such as those caused by nutritional, hormonal, or mechanical agents. Variations and spine malformations have a multifactorial origin, resulting from congenital anomalies that arise due to intrinsic (genetic and hormonal) and extrinsic (environmental) factors, or a combination of both (epigenetic interaction). Therefore, it is difficult to determine the aetiology of such pathologies due to the complexity of determining the underlying cause (Barnes, 1994; Sarfo, 2014; Tancock, 2014; Karapetian and Makarov, 2019).

It is important to note that archaeological human bones are often affected by taphonomic processes. Good preservation conditions depend on various extrinsic and intrinsic factors. Vertebral elements are among the skeletal elements most vulnerable to taphonomic process (Holland et al., 1996; Manifold, 2012). Therefore, these processes are a limiting factor in paleopathological analysis, but even more so in paleopathological examination of the spine.

The aim of this study was to explore SAs in two Argentine populations from different periods: a) hunter-gatherers from Southern Patagonia (SP), and b) prehispanic farmers from the Argentinean prepuna. Considering that the first population lived in a cold environment at the sea level and the second in high altitude ecosystems with a large temperature range, the hypothesis of this work is that differences among these two populations are expected for the prevalence of different SAs due to the different microevolutionary processes of adaptation to the environment adopted by each of these populations.

MATERIAL AND METHODS

Two samples of adults from different parts of Argentina were analysed (Fig. 1): 1) a sample of hunter-gatherers from SP; 2) skeletal remains from the Argentinean prepuna, from the *Pukará de Tilcara* site (PT). In the present study, a total of 126 individuals (98 SP and 28 PT) were initially analysed; 50 of them met the desired standards of completeness and preservation: at least the last four thoracic vertebrae, the entire lumbar region and the sacrum, which were used to carry out a more in-depth analysis. Therefore, the final sample for analysis comprised 37 from SP and 13 PT individuals.

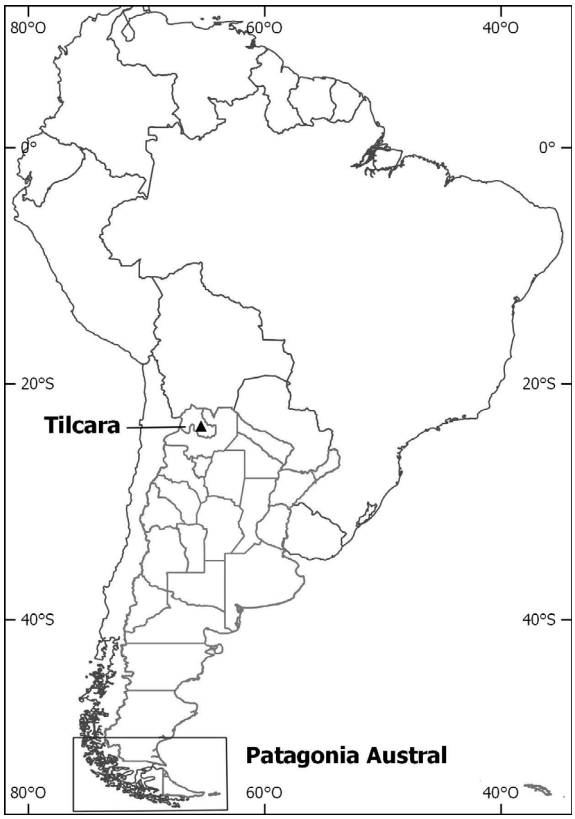

Fig. 1.- Map of South America with the two samples located in Argentina. *Patagonia Austral* (SP) shows the localisation of the hunter-gatherers from SP. Tilcara shows the localization of *Pukará de Tilcara* site (PT).

SP sample (13 women, 22 men and 2 with sex not available -NA), dated from Holocene, between 5000 years B.P. and the 20th century, from different archaeological sites (Table 1) excavated in SP, area behind the 50th parallel South, including the last foothills of the American continent. The bioanthropological information on these individuals comes from *Base de Información Bioantropológica de*

Patagonia Austral -B.I.B.P.A.- (D'Angelo del Campo et al., 2020). These populations were maritime or terrestrial hunter-gatherers, and presented a high degree of isolation from other American populations as shown by previous genetic (Lalueza, 1997a; Pérez et al., 2009; de la Fuente et al., 2015, 2018; Crespo et al., 2018), morphological (Cocilovo and Guichón, 1986, 1999-2000; Guichón, 1993; Varela et al., 1993-94; Lalueza et al., 1996; González-José et al., 2002; Pérez et al., 2007, 2009) and archaeological studies (Borrero, 2001). However, there is an internal homogeneity between them reported both genetically (Lalueza, 1997a; García-Bour et al., 2004; Crespo et al., 2017) and morphometrically (Hernández et al., 1997; González-Jose, 2003; Bernal et al., 2010). With the arrival of allochthonous people at the end of the 19th century, the lifestyle changed drastically, and a great demographic decline took place (García-Moro et al., 1997).

Therefore, the individual SP were classified according to the period and the specific region to which they belonged. The periods were divided according to the arrival of the colonizers, differentiating between 1) precontact, before 1.520 A.D., when the Magellan expedition crossed the Strait of Magellan; 2) post-contact, after that date; and 3) pericontact: because dating methodologies inevitably have precision errors, individuals dated around 1,520 A.D. cannot be classified as pre- or post- contact (Table 1). In addition, we divided the period of post-contact into: (i) individuals who lived at Salesian the Mission "*Nuestra Señora de La Candelaria*" – SMLC – (lat. -53,72º, long. -67,79º) near to Río Grande city (North of Tierra del Fuego, Argentina); and (ii) individuals who lived out of SMLC. To analyse the regional factor, the classification by Borrero et al. (2001) was used. According to it, the SP region is divided the region into six areas: Beagle Channel (BC), San Gregorio-Brunswick (SGB), North of *Isla Grande de Tierra del Fuego* (NIG), Mitre Peninsula (MP), Continent (C) and *Última Esperanza* Mountain (UEM) (see Table 1). However, due to the low number of individuals present in some of these areas, we had to modify this classification and regroup the 6 areas into 3 as follows (Fig. 2): (**1**) Beagle Channel (**BC**); (**2**) *Isla Grande* (**IG**), made up by the union of North of *Isla Grande de Tierra del Fuego* (NIG) and Mitre Peninsula (MP); and (**3**) Continent (**C**), made up by the union of Continent (C), *Ultima Esperanza* Mountain (UEM) and San Gregorio-Brunswick (SGB).

PT sample (6 female, 5 male and 2 NA; Table 2) from the *Pukará de Tilcara*, site from Argentinian prepuna, located in the central sector of the *Quebrada de Humahuaca*, a valley sited in the province of Jujuy connecting the Eastern plains to the Puna and the Southern Mountain hills area. This

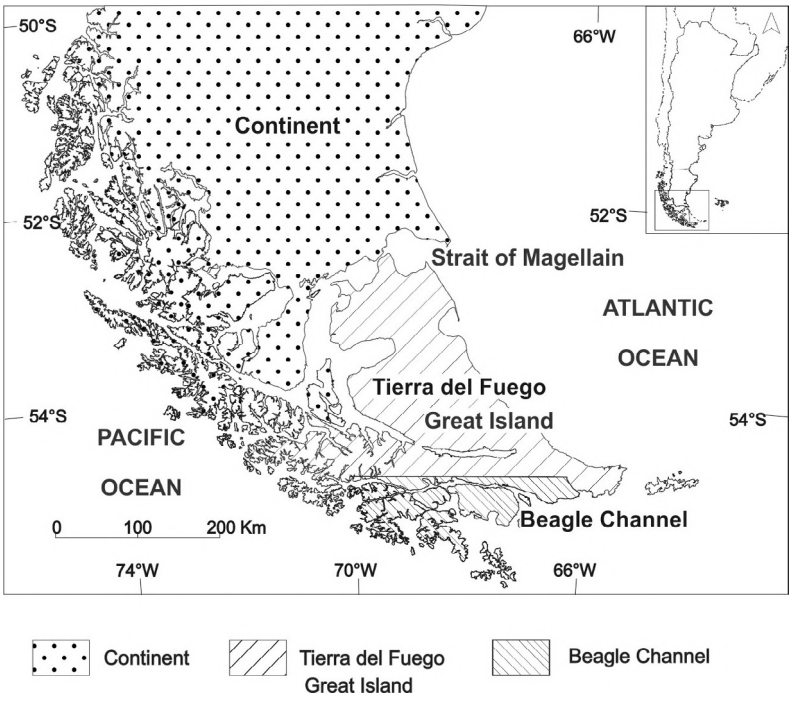

Fig. 2.- Map of SP divided in three regions: Continent (C), Beagle Chanel (BC) and *Isla Grande* (IG). Modified from Borrero et al. (2001).

Table 1. Skeletal remains from Southern Patagonia (SP) analysed in this work.

	Individual		Institution[a]	IC[b]	Chronology (years BP)	Region[c]	Sex[d]	Age	C vert.	T vert.	L vert.	S vert.	Co vert.	Total vert.	References
1	La Arcillosa 2		CADIC	-	5205 ± 58	NIG	F	24-28	7	12	5	6	0	29	Saleme et al., 2007a
2	Bahía Felipe 2		IP	50103	1608 ± 45	NIG	M	35-50	7	12	5	5	0	29	Suby, 2014
3	Shamakush 6		MFM	SH-6	1536 ± 46	CB	M	35-45	7	12	5	5	0	29	Suby et al., 2011
4	Paishauaia I		MFM	857	1504 ± 46	CB	F	35-45	7	12	5	5	0	29	Suby et al., 2011
5	Punta Daniel		IP	33949	1090 ± 30	SGB	M	30-40	7	12	5	5	0	29	Suby, 2014
6	Cabo Nose		IP	89014	980 ± 40	NIG	M	20-35	3	11	5	5	1	25	Alfonso-Durruty et al., 2011
7	Caleta Falsa, site 8 (1)		MFM	S8-1	820 ± 40	PM	M	18-23	6	11	5	5	0	27	Guichón & Suby, 2011
8	Seno Lauta 2		IP	288	Pre-contact	CB	F	35-40	7	12	5	6	0	30	Guichón, 1994
9	Isla Hoste (12590)		ME	12590	Pre-contact	CB	M	36	6	12	5	5	0	28	Guichón, 1994
10	Isla Hoste (12589)		ME	12589	Pre-contact	CB	F	A	3	12	5	7	0	27	Guichón, 1994
11	Aleph 3		ME	-	450 ± 60 (Peri-contact)	PM	M	30-39	0	9	5	6	0	20	Lanata, 1995
12	Brazo Norte, Cerro Johny		IP	6784	390 ± 60/480 ± 70 (Peri-contact)	SGB	M	30-50	7	12	5	7	0	31	Guichón, 1994
13	Puesto Pescador		CADIC	-	335 ± 35	NIG	M	22-28	7	12	5	6	0	31	Suby et al., 2008
14	Lengua de Vaca		IP	6780	251 ± 41	NIG	F	30-40	7	12	5	5	1	30	Suby, 2014
15	Las Mandíbulas 1		LEEH	QQN002	1770-1950 A.D.	NIG	M	20-34	7	12	5	5	0	29	Guichón et al., 2000
16	Caverna 3, Puerto Natales		IP	50109	Post-contact	UEM	M	20-25	2	11	5	5	0	23	Prieto 1993-94
17	Cementerio Haberton		MFM	CH 95	Post-contact	CB	M	25-35	5	11	5	5	0	26	Piana et al., 2006
18	Akathusún		MFM	-	Post-contact	CB	F	30-40	4	12	5	5	1	27	Piana et al., 2006
19	Salesian Mission	C11 (1)	LEEH	QQN0058	Post-contact	NIG	M	20-30		12	5	6	0	23	García Laborde, 2016
20		D-C 9-10	LEEH	QQN0053	Post-contact	NIG	M	25-40	7	12	5	7	0	31	García Laborde, 2016
21		C 13	LEEH	QQN0026	Post-contact	NIG	F	25-35		8	5	5	0	18	García Laborde, 2016
22		E 10-11 (1)	LEEH	QQN0049	Post-contact	NIG	M	25-30	7	12	5	6	0	30	García Laborde, 2016
23		E 10-11 (2)	LEEH	QQN0055	Post-contact	NIG	F	18-25	7	12	5	5	0	29	García Laborde, 2016
24		E 12-13	LEEH	QQN0023	Post-contact	NIG	M	35-45	7	12	5	5	0	29	García Laborde, 2016
25		C 14 (2)	LEEH	QQN0033	Post-contact	NIG	F	19-20	7	12	5	5	0	29	García Laborde, 2016
26		D 16 (bis)	LEEH	QQN0039	Post-contact	NIG	F	21-53	7	12	5	6	0	31	García Laborde, 2016
27		E 15-16 2 (bis)	LEEH	QQN0045	Post-contact	NIG	M	30-40	3	12	5	5	1	26	García Laborde, 2016
28		D 15-16	LEEH	QQN0030	Post-contact	NIG	F	35-49	2	10	5	6	0	23	García Laborde, 2016
29	Ushuaia		ME	13276	-	CB	-	A	2	*9	5	5	0	21	Guichón, 1994
30	Zona Industrial, Ushuaia		MFM	2670	-	CB	M	A	7	12	4	6	0	29	This work
31	Parque Nac. La Patria		MFM	2403 (2)	-	CB	M	35-49		12	5	5	0	22	This work
32	Close to SMLC		ME	25884	-	NIG	M	30-35	6	12	5	5	0	28	Schindler, 2001
33	Estancia María Behety		MFM	2667	-	NIG	M	35-49	7	12	5	5	0	29	This work
34	Bahía Chilota		IP	73722	-	NIG	F	A	7	12	5	5	1	30	Alfonso-Durruty et al., 2015
35	Bahía Santiago 4		IP	50112	-	SGB	-	A	7	12	5	5	1	30	This work
36	2671		MFM	2671	-	-	F	20-34	2	*11	5	5	1	19	This work
37	2405		MFM	2405	-	-	M	50		12	5	5	0	22	This work

[a] **CADIC:** *Centro Austral de Investigaciones Científicas,* Ushuaia; Argentina. **IP:** *Instituto de la Patagonia,* Punta Arenas, Chile. **MFM:** *Museo del Fin del Mundo,* Ushuaia, Argentina. **ME:** *Museo Etnográfico Juan B. Ambrosetti,* Universidad de Buenos Aires, Buenos Aires, Argentina, **LEEH:** *Laboratorio de Ecología Evolutiva Humana,* Quequén, Buenos Aires, Argentina.
[b] **IC**: Institution code.
[c] *Norte de Isla Grande de Tierra del Fuego* (NIG); San Gregorio-Brunswick (SGB); Mitre Peninsula (PM); Beagle Channel (CB); *Última Esperanza* Mountain (UEM).
[d] F: Female; M: male.
Vert.: vertebrae.

settlement is placed at a plateau with a maximum height of 2525 m in the middle of the valley in a complex topography, with ladders and fertile valleys. PT can be considered a high-altitude place, with the consequent effects of altitude produce in human physiology. As Frisancho (1993) noted, the results of altitude are perceived at 2000 m during physical activity and 2500 m during rest. The first settlements in this area happened before the 1st millennium A.D., and it was a densely populated area during late pre-Hispanic times (11th to 16th centuries A.D.), reaching its largest size and becoming the main hierarchical center of the region during the Inca period (Debenedetti, 1930; Otero, 2015). Thus, those settlements are pre-contact. Moreover, the sample is composed of individuals whose lifestyle was majorly a combination of farming and shepherding. The collection is located at *Museo Etnografico "J. B. Ambrosetti", Facultad de Filosofía y Letras* at *Universidad de Buenos Aires* (UBA). The analysed individuals have been classified according to their sex as male (M) or female (F), based on the study of the cranium and the hip bones, according to the method proposed by Buikstra and Ubelaker (1994). Age was classified as over and under 30 years at death, estimated by the study of pubic symphyses (Todd 1921a, b; Brooks and Suchey, 1990), auricular surface (Lovejoy et al., 1985) epiphyseal fusion (Buikstra and Ubelaker, 1994) and the metamorphosis of the fourth sternal rib end (Isçan et al., 1984).

SAs changes in transitional vertebrae, column units that are in the boundary regions of the spine, comprise cervicothoracic, thoracolumbar, lumbosacral and sacrococcygeal. The definitions that we have used in this study are the following: Jankauskas (2001); Sarfo (2014); ten Broek et al. (2017) and Karapetian et al. (2019). They all describe: 1) Cranial shift: the vertebra acquires the typical characteristics of the immediately inferior section; 2) Caudal shift: the vertebra acquires the typical characteristics of the immediately superior section of the spine. Caudal and cranial shift diversity are illustrated in Fig. 3, based on previous works (Jankauskas, 2001; Sarfo, 2014; ten Broek et al. (2017; Karapetian and Makarov, 2019). In order to analyse the SAs, a macroscopical study was carried out in all spines to identify each vertebral region, observing the presence or absence of each vertebral element (Fig. 3). Vertebrae were examined attending to the diverse characteristics of each segment (White and Folkens, 2005): foramen, body, arch, pedicle, lamina, spinous process, transverse process, articular facets (superior and inferior) and costal fovea. In the case of the *sacrum*, the promon-

Table 2. Skeletal remains from *Pukará de Tilkara* (PT) analysed in this work.

Individual		Institution[a]	Sex[b]	Age	C vert.	T vert.	L vert.	S vert.	Co vert.	Total vert.
1	17823 (box 132)	ME	F	18-22	7	12	5	5	0	29
2	17846 (box 171)	ME	M	28-45	7	12	5	5	0	29
3	17825 (box 24)	ME	M	35-55	6	12	5	5	0	28
4	17828 (box 26)	ME	I	-	7	12	5	5	1	30
5	17954 (box 50)	ME	F	20-38	6	12	5	6	0	29
6	17952 (box 49)	ME	M	24-55	7	12	4	6	0	29
7	17955 (box 51)	ME	I	18-25	7	12	5	5	0	29
8	17949 (box 47)	ME	F	22-48	7	12	5	6	0	30
9	17951 (box 48)	ME	F	A	6	11	5	6	0	28
10	17852 (box 40)	ME	F	>40	6	12	5	5	0	28
11	17853 (box 41)	ME	M	25-35		12	5	5	0	22
12	17855 (box 43)	ME	F	20-40	6	12	5	5	0	29
13	17833 (box 31)	ME	M	20-27	5	12	5	5	0	29

[a] **ME:** Museo Etnográfico Juan B. Ambrosetti, Universidad de Buenos Aires, Facultad de Filosofía y Letras, Buenos Aires, Argentina.
[b] F: Female; M: male; I: indeterminate.
Vert.: vertebrae.

tory, alae, sacroiliac joint, anterior sacral foramina, transverse lines, superior articular facets, dorsal wall, and median crest were observed. Finally, in the *coccyx*, the articular and transverse processes superiorly and the *cornua* were identified. To identify each vertebra into specific vertebral region, a good preservation of vertebral elements is important. However, preservation of all the vertebral elements is complex because the spine is especially sensitive to taphonomic processes (Manifold, 2012), fundamentally the coccygeal region (Stodder, 2019). Another factor to consider in the study of SAs is where these alterations occur, usually in boundary regions, being the lumbosacral region the most affected (Konin and Walz, 2010) and the cervicothoracic region the least affected (Jankauskas, 2001). Based on these two factors, and since there is still no methodological standardization to study SAs, this work proposes a new approach to study these anomalies by analysing specific regions of the spine instead of the entire structure. In addition, considering the current limitations of preservation of archaeological samples and the high prevalence of SAs existing in lumbosacaral and boundary regions (Fig. 3), this new approach requires a minimal preservation condition of the spine to have the last four thoracic vertebrae, the entire lumbar region and the sacrum. Therefore, in this work, those individuals who did not present the minimum preservation requirements were excluded from the study.

Descriptive analyses were carried out in the SA analysed with the new approach proposed constructing contingency tables for caudal thoracicallization, lumbarization and cranial sacralization, considering sex, grouped age, region (CB, IG and C) and period (precontact, peri-contact, post-contact – out of SMLC and post-contact – in SMLC). Number of Sacral Vertebrae (NSV) frequencies were also studied considering the same factors. Results were in contingency tables. Hypothesis testing for the different levels of the factors contained in the contingency tables was performed with two-sided Fisher's exact test with a confidence level of 95% (α <0.05). This statistical test is recommended for small samples such as our case.

In order to contextualize the results of SP and PT, this paper reviews the literature on SAs in ancient populations, including information from different studies carried out on all continents since the beginning of the 20th century (Table 3).

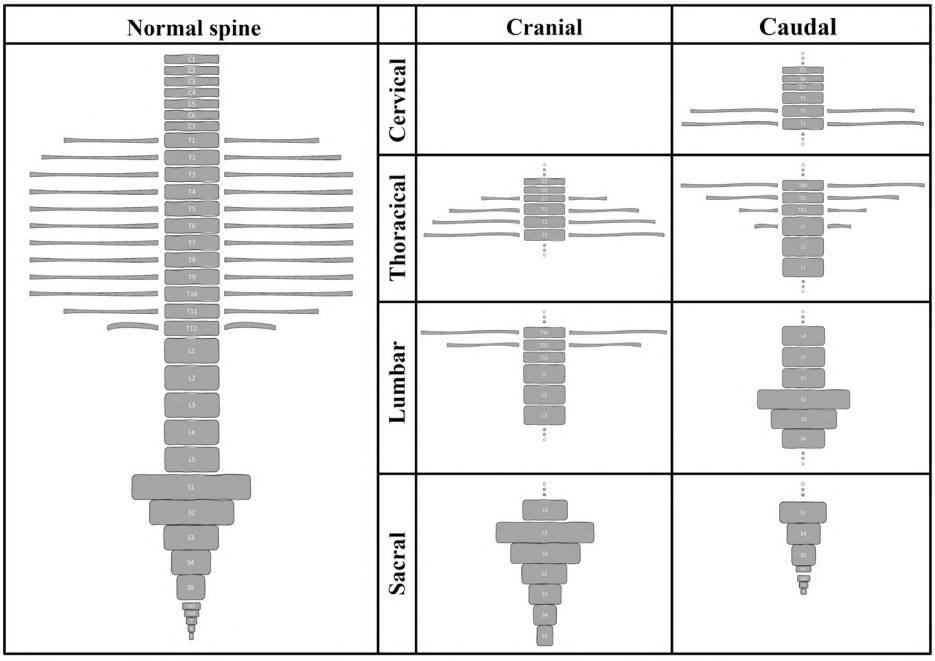

Fig. 3.- Schema of the spine, both normal (left) and with SAs (middle and right): **Caudal cervicalization**: T1 transformation to cervical morphology without ribs. **Cranial dorsalization**: presence of rib facets on the vertebral body of C7. **Caudal dorsalization**: ribs at L1 and/or superior articular process of dorsal type. **Cranial lumbarization**: T12 without rib facets and/or inferior articular process of lumbar type. **Caudal lumbarization**: S1 acquires lumbar form and remains separate from the sacrum. **Cranial sacralization**: L5 is assimilated by the *sacrum* or modify its shape assuming S1 form. **Caudal sacralization**: Co1 acquires sacral vertebrae shape and usually is assimilated by the *sacrum*.

Table 3. Bibliographic information on SAs variation in different skeletal samples around the world. Rows colored in grey represent data from current work. Those cells where no information about the variable is provided remain clear.

Continent	Collection or sample (Country)	Period	Lifestyle	Total individuals	Sacralization						Lumbarization						Dorsalization						References	Observations
					n	Cranial		Methodology	Caudal		Methodology	n	Cranial		Methodology	Caudal		Methodology	n	Cranial		Methodology	Caudal		Methodology	
						n	%		n	%			n	%		n	%			n	%		n	%			
AMERICA	Hamann-Tod Osteological Collection, Cleveland (USA). **Documented collection**	20th century	Urban	Total: 748																				Willis, 1923	
	Departmental collections of Washington University and Western Reserve University	20th century	Urban	Total: 201	Total: 201	28	0,14	Sacralization of L5 (total or partial)																Lanier, 1939	
	Sadlemiurt, Southampton island. Museum of Man, Ottawa (Canada)	Several hundred years - 20th century	HG	♂: 33	♂: 33	1			22	0		♂: 33	1		Kühne (1936)	14		Kühne (1936)	♂: 33	0		Kühne (1936)	18	0	Kühne (1936)	Merbs, 1974	
				♀: 37	♀: 37	2			13	0		♀: 37	1			10			♀: 37	0			10	0			
				Total: 70	Total: 70	3			35	0		Total: 70	2	8,6		24			Total: 70	0			28	0			
	Northwest Coast Indian (Haida, Kwakiutl, Nootka). Field Museum of Natural History, Chicago (USA)	Before 19th century	ND	Total: 70	Total: 70	3		Kühne (1936)	26		Kühne (1936)	♂: 33	4			23			Total: 70	3			18	0			
												♀: 37															
												Total: 70															
	Eskimo skeletons from the American Museum of Natural History, New York (USA)	1th century A.D	ND	Total: 295	Total: 295	11	3.7																	Lester & Shapiro, 1968	
	Hamann-Tod Osteological Collection, Cleveland (USA) and Robert J. Terry Anatomical Skeletal Collection, Missouri (USA). **Documented collections**	19th- 20th centuries	Urban	♂: 1048	White: 487	36	7.3	High Assimilation of the Sacrum																	Tague, 2009	
					Black: 495	30	6																				
				♀: 1038	White: 433	20	4.6																				
					Black: 540	45	8.3																				
				Total: 2086	Total: 1955	131	6.7																				
	Skeletal sample from the Ryan Mound site, south-eastern side of the San Francisco Bay, San José (USA)	2180 - 250 BP	HG	♂: 66	♂: 50			Barnes (1994)				♂: 50				4	8	Barnes (1994)								Weiss, 2009	
				♀: 66	♀: 41							♀: 41				0	0										
				Total: 146	Total: 91							Total: 91				4	4,4										
	Skeletal remains from the Sully site (39SL4), Arikara natives. National Museum of Natural History (NMNH), Smithsonian Institution, Washington D.C. (USA)	11th-18th centuries a.C.	Horticultural (Agriculture)	♂: 39	Total: 52	4	7,7	Cranial sacralization	5	9,6	Sacralization of coccygeal vertebra	Total: 52	1	1,9	T12 lumbarization	2	3,8	S1 lumbarization (total or partial)					3	5,8	L1 thoracization	Kimmerle, 2010	
				♀: 33																							
				Total: 172																							

Continent	Collection or sample (Country)	Period	Lifestyle	Total individuals	Sacralization						Lumbarization						Dorsalization						References	Observations
					n	Cranial		Methodology	Caudal		Methodology	n	Cranial		Methodology	Caudal		Methodology	n	Cranial		Methodology	Caudal		Methodology		
						n	%		n	%			n	%		n	%			n	%		n	%			
EUROPE	Hamann-Todd Osteological Collection, Cleveland (USA) and Robert J. Terry Anatomical Skeletal Collection, Missouri (USA). **Documented collections**	19th- 20th centuries	Urban	♂: 1617	♂: 1617					43,4	Sacralization of coccygeal vertebra													Tague, 2011	
				♀: 737	♀: 737					37															
				Total: 2354	Total: 2354				703 273 976	41,5															
	Hamann-Todd Osteological Collection, Cleveland (USA) and Robert J. Terry Anatomical Skeletal Collection, Missouri (USA). **Documented collections**	19th- 20th centuries	Urban	♂: 569	♂: 569	59	0,104	High Assimilation of the Sacrum																Tague, 2011b	This work presents a different percentage compared to Tague (2009), because only individuals between 20 and 49 years were considered
				♀: 392	♀: 392	46	0,117																		
				Total: 961	Total: 961	105	10,9																		
AMERICA	European ancestry north american: Robert T. Terry Anatomical Skeletal Collection, Missouri (USA) and Grant Collection, Toronto (Canada). **Documented Collections**	20th century	Urban	Total: 232	Total: 232		3,3	Cranial shift L5-S1				Total: 232		7	Caudal shift L5-S1		3,1	Presence of ribs at L1 level	Total: 232					0,7	Reduction of 12th pair of ribs	Karapetian & Makarov, 2019	
	African ancestry north american: Robert J. Terry Anatomical Skeletal Collection, Missouri (USA). **Documented Collection**			Total: 70	Total: 70	0	4,5					Total: 70		0			0		Total: 70					3			
	Tilcara's Pukará necropolis. Tilcara (Argentina)	Pre-contact	Agriculture	♂: 2	♂: 2	1	50	Sacralization of L5 (total or partial)	0	0	Sacralization of coccygeal vertebra (total or partial)	♂: 2	0	0	T12 lumbariaztion (total or partial)	0	0	S1 lumbarization (total or partial)					0	0	L1 thoracization (total or partial)	This work	
				♀: 5	♀: 5	1	20		2	40		♀: 5	0	0		0	0						0	0			
				Total: 13	Total: 13	2	15,4		3	23		Total: 13	0	0		0	0						0	0			
	Southern Patagonia (Argentina / Chile)	5.200 B.P. 20th centuries	HG	♂: 22	♂: 22	3	1,3		4	18,2		♂: 22	0	0		0	0						0	0			
				♀: 13	♀: 13	1	7,9		3	23,1		♀: 13	1	7,7		0	0						0	0			
				Total: 37	Total: 37	4	10,8		7	18,9		Total: 37	1	2,7		0	0						0	0			
EUROPE	North-eastern Scottish. Department of Anatomy of the University of Aberdeen (Scotland). **Documented Collection**	20th centuries	Urban	♂: 19					13	68,42	Sacralization of coccygeal vertebra													Saluja, 1988	
				♀: 15					10	66,6															
				Total: 34																					
	Crypt of St. Bride's Church, Fleet Street, London (England). **Documented collection**	18th - 19th centuries		♂: 54					22	40,7															
				♀: 40					9	22,5															
				Total: 94																					

Continent	Collection or sample (Country)	Period	Lifestyle	Total individuals	Sacralization						Lumbarization						Dorsalization						References	Observations
					n	Cranial		Methodology	Caudal		Methodology	n	Cranial		Methodology	Caudal		Methodology	n	Cranial		Methodology	Caudal		Methodology		
						n	%		n	%			n	%		n	%			n	%		n	%			
EUROPE	Skeletal remains from Monte Bibele, Bologna (Italy)	6100-5500 AC (Neolitic)	HG	Total: 95	♂: 50	1	2	Sacralization of L5 (total or partial)																	Brasili, 1997	
					♀: 35	1	2,8																			
					Total: 89	2	2,5																			
	Skeletal sample from Pompeii, Naples (Italy)	79 A.D	Urban	♂: 70	♂: 70	16	23	Sacralization of L5 (total or partial)	8	11	Sacralization of coccygeal vertebra														Henneberg & Henneberg, 1999	Only sacral bones has been examined for this study
				♀: 54	♀: 54	7	13		1	2																
				Total: 124	Total: 124	23	19		9	7,2																
	Skeletal series from Oslonki site, near Wloclawek in Kujawy region (Poland)	4300-4000 B.C.	Agriculture	Total: 92		8	13,11	Sacralization of L5 (total or partial)																	Garlowska, 2001	
	Skeletal remains from the Great Moravia cemeteries. Devín-Hrad (Slovakia)	11th-12th centuries	ND	Total: 217	♂: 46	7	15	Sacralization of L5 (total or partial)	6	7,4		♂: 46				1	0,46	S1 lumbarization (total or partial)							Masnicova & Benus, 2003	
					♀: 53	1	2					♀: 53				1	0,53									
					Total: 112	9	8					Total: 112				2	2,24									
	Skeletal remains from the Great Moravia cementeries. Devín-Za costolom (Slovakia)	9th century		Total: 112	♂: 16	1	6					♂: 16				0	0									
					♀: 13	1	8					♀: 13				0	0									
					Total: 29	2	7					Total: 29				0	0									
	Byzantine populations from Eleutherna. Crete island (Greece)	8th-11th centuries	Rural	♂: 52		1	1,9	Sacralization of L5 (total or partial)																	Bourbon, 2010	
				♀: 21																						
				Total: 100		1	1																			
	Byzantine populations from Kefali. Crete island (Greece)	8th-11th centuries		♂: 18		1	5,6																			
				♀: 11																						
				Total: 49		1	2																			
	Human skeletons from the necropolis in the Eastern part of the Princely Court. Curtea domneasca (Romania)	17th centuries	Urban	♂: 70	♂: 66	2	3	Sacralization of L5: sacral bone with an extra foramen				♂: 66				1	1,5	S1 lumbarization (total or partial)							Groza *et al.*, 2012	
				♀: 26	♀: 25	0	0					♀: 25														
				Total: 111	Total: 91	2	2,2					Total: 91				1	1,1									
	Saint-Urnel necropolis, south Finistere (France)	5th - 11th centuries	Rural		Total: 30	1	3,33	Sacralization of L5 (total or partial)								1	3,3	S1 partial lumbarization							Zemirline *et al.*, 2012	
	Bone material from Drustar (Bulgaria)	9 th-15 th centuries	Rural	Total: 147	Total: 103	3	2,8	Sacralization of L5 (total or partial)																	Toneva & Nikolova, 2013	
	Pamplona muslim cemetery (*maqbara*). Pamplona (Spain)	7th cementery	Urban	Total:177		2	2,25	Sacralization of L5 (total or partial)																	Ibañez, 2016	
						2	2,25																			
	Anthropological Department, Lomonosov Moscow State University, Moscow (Russia). Documented Collection	1950th	Urban	♂: 66	♂: 66		2,8	Craneal shift L5-S1				Total: 232		4,4	Caudal shift L5-S1		1,3	Presence of ribs at L1 level	Total: 232					2,7	Reduction of 12th pair of ribs	Karapetian & Makarov, 2019	
				♀: 14	♀: 14																					
				Total: 80	Total: 80																					
	Kozino village cementery, Moscow region, Lomonosov Moscow State University, Moscow (Russia)	18th century	ND	♂: 78	♂: 78		0					Total: 70		2,8			0		Total: 70					1,9		
				♀: 53	♀: 53																					
				Total: 131	Total: 131																					

Continent	Collection or sample (Country)	Period	Lifestyle	Total individuals	Sacralization						Lumbarization							Dorsalization							References	Observations
					n	Cranial		Methodology	Caudal		Methodology	n	Cranial		Methodology	Caudal		Methodology	n	Cranial		Methodology	Caudal		Methodology		
						n	%		n	%			n	%		n	%			n	%		n	%			
AFRICA	Guanche sample, Canary islands (Spain)	15th century	HG			6		Sacralization of L5 (total or partial)		3							5									Rodríguez, 1995	
	Bantu natives skeletons. Anthropological Museum of Anatomy Department of the University of Witwatersrand (South Africa)	ND	ND	♂: 63 ♀: 17 Total: 82	Total: 81	1	1,2									3	3,7								Shore, 1930	
	Exhumed skeletal of Boksburg Municipality, University of the Witwatersrand (South Africa)	20th centuries	Urban	Total: 36		400%	12	Sacralization of L5 (total or partial)																	Meyer, 2013	
	Vertebral columns from the Anthropological Collection in the Department of Anatomy, Marekere College (Uganda)	ND	ND	♂: 179 ♀: 27 Total: 206	Total: 200	22	11	Sacralization of L5 (total or partial)																	Allbrook, 1955	
	Human remains excavated in the Bahriyah Oasis (Egypt)	Greco-Roman period	ND	♂: ♀: 1 Total: 77	Total: 36	1 2	2,8 2,9					♂: 41 ♀: - Total: 41				1 1	2,4 2,4								Hussien *et al.*, 2009	
	Skeletons excavated from Giza and belong to the Old Kingdom (Egypt)	2686 a.C. - 2181 a. C	Elithe and Rural town	♂: 147 ♀: 125 Total: 272	135	♂: 1 ♀: 3 Total: 4	0,74 2,3 2,96	Sacralization of L5 (total or partial)				Total: 135				♂: 1 ♀: 1 Total: 2	0,7 0,7 1,5	Lumbarization total or partial of S1							Sarry el din, 2006	
	Kelis II Cemendety, Dakhleh Oasis (Egyp)	332 BC-4th century	Urban	♂: 82 ♀: 119 Total: 201	♂: 82 ♀: 119 Total: 201	7 10 17	8,5 8,4 8,5																		Sarfo, 2014	
ASIA	Thai skeletons from the Bone Collection Unit, Department of Anatomy, Faculty of Medicine, Khon Kaen University (Thailand). **Documented Collection**	ND	ND	♂: 114 ♀: 92 Total: 206	♂: ♀: Total:	7 2 9	6,1 2,2 4,4	Sacralization of L5 (total or partial)																	Chaijaroonkhanarak *et al.*, 2006	Only cranial sacralization had been analyzed
	Human remains from the archaeological site of Jiangjaliang (China)	7000-3000 BP	Elithe and Rural town	Total: 66	Total: 66	4	6,1	Sacralization of L5 (total or partial)																	Hernández, 2009	
	Human remains from the archaeological site of Minhe X, Minhe M and LGS (China)	3000 BP		Total: 96	Total: 96	2	2,1																			
	Human remains from the archaeological site of MXY (China)	3000 BP		Total: 40	Total: 40	3	7,5																			

Continent	Collection or sample (Country)	Period	Lifestyle	Total individuals	Sacralization						Lumbarization						Dorsalization						References	Observations
					n	Cranial		Methodology	Caudal		Methodology	n	Cranial		Methodology	Caudal		Methodology	n	Cranial		Methodology	Caudal		Methodology	
						n	%		n	%			n	%		n	%			n	%		n	%		
ASIA	Chinese sacra from the Department of Anatomy, School of Basic Medical Sciences, Southern Medical University (China). **Documented collection**	20th century	Urban	Total: 208	♂: 129	12	9,3	Sacralization of L5 (total or partial)								6	4,6	Lumbarisation S1							Wu *et al.*, 2009	
					♀: 74	13	17,6									3	4									
					Total: 203	25	12,3									9	4,4									
	Dried human sacra collected from repositories of medical institutions across the central and western provinces of the Indian union (India). **Documented collections**	20th century	Urban	Total: 256	♂: 30	16	53,3	Castelvi (1984)																Mahato, 2011	
					♀: 33	4	12,1																			
					Total 63	20	31,7																			
	Department of Anatomy and Forensic Medicine and Regional Medicolegal Institute of Bhopal and Raipur (India).	20th century	Urban	♂: 124	♂:	20	9,8	Castelvi (1984)	9	4,4	Sacralisation of coccygeal vertebra					♂: 6	2,9	Lumbarisation S1							Sharma, 2011	
				♀: 82	♀:	9	4,3		7	3,4						♀: 3	1,4									
				Total: 206	Total:	29	14,1		16	7,8						Total: 9	4,3									
	Human sacra from Department of Anatomy, Medical college Vadodara and Government Medical college Surat in Gujarat (India)	20th century	Urban	♂: 115	♂: 115	14	12,2	Sacralization of L5 (total or partial)																Dharati *et al.*, 2012	
				♀: 74	♀: 74	7	9,4																			
				Total: 189	Total: 189	21	11,1									3	1,3	Lumbarisation S1								
	Department of Anatomy, Medical college Vadodara and Government Medical college Surat in Gujarat (India)	20th century	Urban	♂: 115	♂: 115					22,6	Sacralization of coccygeal vertebra													Nagar, 2012	
				♀: 74	♀: 74				26 19 45	25,7																
				Total: 189	Total: 189					23,8																
	Sacral bones from the Department of Anatomy, ESIC Medical College & PGIMSR, Chennai (India). **Documented Collection**	20th century	Urban	Total: 50		3	6																	Krishnamurthy & Adibatti, 2016	Only cranial sacralization had been analyzed
	Sacra human bone from the Department of Anatomy and Department of Forensic Medicine, Velammal Medical College Hospital and Research Institute, Madurai (India)	21th century	Urban	♂: 41		7	17,1	Castelvi (1984)																Suman & Mahato, 2016	
				♀: 29		4	13,8																			
				Total: 70		11	15,7									1	1,4	Lumbarization total or parcial S1								
	Harappa or Indus Valley (Pakistan)	2600 – 1900 BC.	Urban	Total: 84	Total: 19	1	5,26	Sacralization of L5 (total or partial)																Lovell, 2014	

Continent	Collection or sample (Country)	Period	Lifestyle	Total individuals	Sacralization						Lumbarization						Dorsalization						References	Observations
					n	Cranial		Methodology	Caudal		Methodology	n	Cranial		Methodology	Caudal		Methodology	n	Cranial		Methodology	Caudal		Methodology		
						n	%		n	%			n	%		n	%			n	%		n	%			
ASIA	Skeleton remains recovered from the Pokrovskiy necropolise. Krasnoyarsk State Medical University (Russia)	17th-20th centuries	Rural/ urban	Total: 327	♂: 61																			Dabernat *et al.*, 2013	
					♀: 31																				
					Total: 213																				
	Skeleton remains recovered from the Voskressens-ko-Preobrajens-kiy necropolise. Krasnoyarsk State Medical University (Russia)			Total: 182	♂: 59																				
					♀: 38																				
					Total: 101																				
	Skeleton remains recovered from the Pokrovskiy and Voskresens-ko-Preo-brazhenskiy necropolises. Krasnoyarsk State Medical University (Russia)			Total: 509	♂: 120																				
					♀: 99																				
					Total: 224	3	1,3		3	1,3															
	Ekven Eskimo collection, Re-search Institute and Museum of the Lomonosov Moscow State University, Mos-cow (Russia)	Old Bering Sea / Okvik culture	HG	♂: 30	♂: 23	0	0					♂: 24	4			2			♂: 30	0	0		0	0		Karapetian & Makarov, 2019	
				♀: 29	♀: 25	0	0	Craneal shift L5-S1				♀: 23	2		Caudal shift L5-S1	1		Presence of ribs at L1 level	♀: 29	0	0	Presence of ribs at C7 level	0	0	Reduction of 12th pair of ribs	
				Total: 59	Total: 48	0	0					Total: 61	6			3			Total: 61	0	0		0	0		
OCEANÍA	Australian Aborigenes from Trench A in Roonka II Flat Dune (Australia)	4000-220 BP	HG	Total: 92		1	1,1	Sacralization of L5 (total or partial)																	Pretty & Kricun, 1989	
	Archaeological survey in Tamuning Municipality, Agana, Guam (USA)	10th-16th centuries a.C.	HG	Total: 152	♂: 11	0	0	Sacralization of L5 (total or partial)				♂: 9				0	0	Lumbarization total or partial of S1							Douglas, 1997	
					♀: 7	0	0					♀: 4				0	0									
					Total: 18	0	0					Total: 13				0	0									

ND*: No Data

RESULTS

From the initial 126 individuals, those without spine (42 SP and 7 PT) were discarded, remaining 56 and 21 individuals, respectively (Table 4). Afterwards, individuals presenting all vertebrae elements and meeting the minimum preservation requirements proposed by the present work were analysed. Thus, 37 SP (37,7%) and 13 PT (46,4%) individuals were finally examined for SAs. 60,3% of the individuals were discarded due to preservation and taphonomical challenges. 37.8% of SP and 30.8% of PT populations presented *coccyx*; 57.1% (8/14) and 75% (3/4), respectively had it fused to the *sacrum* (Table 5). The rest of the analyses were performed with this last sample.

Table 4. Number of individuals according to vertebrae preservation. Results of Fisher Exact Test (FET) in SP and PT samples for sex, age, period, and region variables.

Samples	Initial sample	Individuals with spine	Methodology proposed	Complete column
PT	28	21 (75)	13 (46,4)	6 (21,4)
SP	98	56 (57,1)	37 (37,7)	20 (20,4)

Number of cases and prevalence: n (%).

Table 5. Coccix preserved.

Sample	Coccix	Coccix fused
PT	4/13 (30,8)	3/4 (75)
SP	14/37 (37,8)	8/14 (57,1)

Number of cases and prevalence: n (%).

Results in SP sample showed a prevalence of cranial sacralization (Fig. 4) of 10.8% (4/37), from which 7.9% were women (1/13) and 13.6% men (3/22), more frequent in individuals over 30 years old (15.8%, 3/9) with respect to those under 30 years old (7.9%, 1/13). Regarding chronological differences, 10% (1/10) of pre-contact individuals and 33.3% (3/9) with unknown values for such variable presented the variation, while no positive results were found for other periods. According to regional differences, 4.7% of individuals in IG (1/21), 25% in C (1/4) and 5.4% in NA (2/37) showed this type of sacralisation. Caudal sacralisation was observed in 18.9% (7/37) of the sample, 23.1% (3/13) women and 18.2% (4/22) men, with higher prevalence in older individuals (21%, 4/22) than in younger (7.9%, 1/13), together with two more cases (5.4%) of unknown age. In terms of chronology, 10% (1/10) of pre-contact individual, 50% (1/2) of peri-contact individuals, 25% (4/16) of post-contact individuals (post - out of SMLC: 16.7% -1/6- and post - in SMLC: 30% -3/10-) and 11.1% (1/9) NA presented caudal sacralisation. One case of cranial lumbarization was found in the sample (2.7%, 1/37) – individual C13, a young woman in SMLC from IG region – showing a typical last thoracic arc, as well as a superior articular process reflecting a lumbar conformation with no rib facets (Tables 6 and 7).

Table 6. Sacralization in PT and SP samples according to sex and age.

Sacralization		Sex			Age (years)			Σ
		F	M	ND	≤ 30	>30	ND	
PT	n	6	5	2	6	4	2	13
	Cranial	-	-	-	-	-	-	-
	Caudal	3 (60)	-	-	1 (16.7)	1 (25)	1 (50)	3 (23)
SP	n	13	22	2	13	19	5	37
	Cranial	1 (7,9)	3 (13,6)	-	1 (7,9)	3 (15,8)	-	4 (10,8)
	Caudal	3 (23,1)	4 (18,2)	-	1 (7,9)	4 (21)	2 (40)	7 (18,9)
NSV		**F**	**M**	**ND**	**≤ 30**	**>30**	**ND**	**Σ**
PT	n	6	5	2	6	5	2	13
	5	3 (50)	5 (100)	2 (100)	5 (83.3)	4 (80)	1 (50)	10 (77)
	6	3 (50)	-	-	1 (16.7)	1 (20)	1 (50)	3 (23)
SP	n	13	19	5	13	22	2	37
	5	9 (69,2)	13 (68,4)	3 (60)	8 (61,5)	15 (68,2)	2 (100)	25 (67,6)
	6	4 (30,8)	4 (21,1)	1 (20)	4 (30,8)	5 (22,7)	-	9 (24,3)
	7	-	2 (10,5)	1 (20)	1 (7,7)	2 (9,1)	-	3 (8,1)

Number of cases and prevalence: n (%).
ND: No Data.

Within the numerical variation of the sacrum, 67.6% (25/37) of the total sample showed 5 sacral vertebrae. The 24.3% (9/37) resulted in 6 sacral vertebrae and 8.1% (3/37) in 7 sacral vertebrae. Regarding the period, 70% of peri-contact individuals (7/10) have presented 5 sacral vertebrae, 20% (2/10) 6 sacral vertebrae and 10% (1/7) 7

Table 7. SAs in SP sample according to chronology and region.

	Period						Region				Σ
			Post-contact			ND	CB	IG (NIG + PM)	C (SGB + CUE)	ND	
Sacralization	**Pre-contact**	**Peri-contact**	**Out of SMLC**	**SMLC**	**Total**						
n	10	2	6	10	16	9	10	21	4	2	37
Cranial	1 (10)	-	-	-	-	3 (33,3)	-	1 (4,7)	1 (25)	2 (100)	4 (10,8)
Caudal	1 (10)	1 (50)	1 (16,7)	3 (30)	4 (25)	1 (11,1)	2 (20)	4 (19)	1 (25)	-	7 (18,9)
NSV	**Pre-contact**	**Peri-contact**	**Post-contact**			**ND**	**CB**	**IG (NIG + PM)**	**C (SGB + CUE)**	**ND**	**Σ**
			Out of SMLC	**SMLC**	**Total**						
n	10	2	6	10	16	9	10	21	4	2	37
5	7 (70)	-	5 (83,3)	5 (50)	10 (62,5)	8 (88,9)	7 (70)	13 (61,9)	3 (75)	2 (100)	25 (67,6)
6	2 (20)	1 (50)	1 (16,7)	4 (40)	5 (31,2)	1 (11,1)	2 (20)	7 (33,3)	-	-	9 (24,3)
7	1 (10)	1 (50)	-	1 (10)	1 (6,2)	-	1 (10)	1 (4,8)	1 (25)	-	3 (8,1)

Number of cases and prevalence: n (%).
ND: No Data.

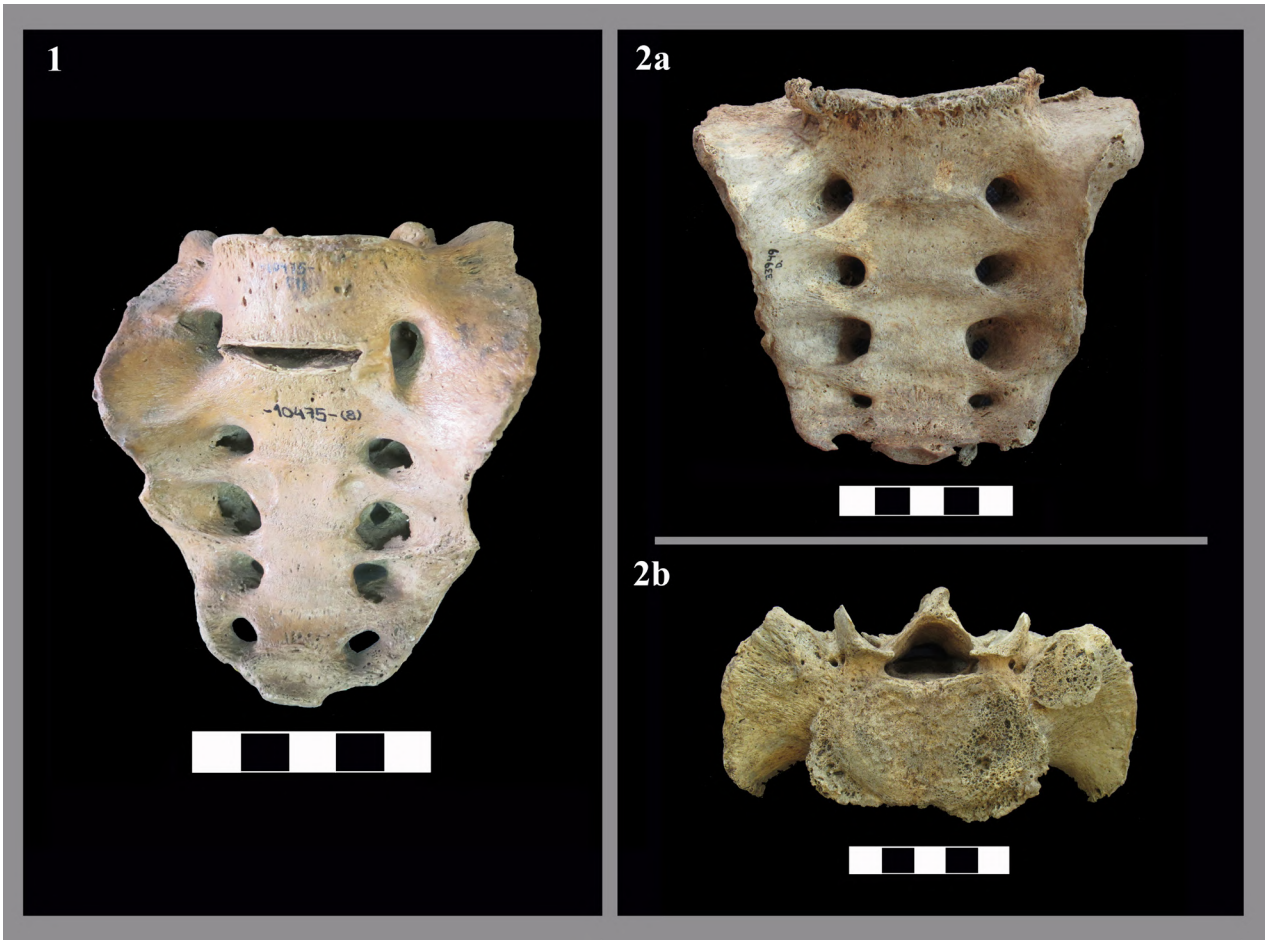

Fig. 4.- Two cases of cranial sacralization: **1**) Complete, individual 10.475/17952 from PT sample. **2 a-b**) Partial, individual 33.949 (*Punta Daniel*) from SP sample.

sacral vertebrae. In the peri-contact period, one case of two (50%) showed 6 sacral vertebrae and the other 7 sacral vertebrae. In post-contact remains, 83.3% (5/6) of out of SMLC exhibited 5 sacral vertebrae and 16.7% 6 sacral vertebrae, while 50% (5/10), 40% (4/10) and 10% (1/10) of post -in SMLC presented 5, 6 and 7 sacral vertebrae respectively. From the 9 individuals identified as NA for chronology, 88.9% (8/9) had 5 sacral vertebrae and 11.1% (1/9) 7 sacral vertebrae. Regarding the regional location, 70% of individuals from the Beagle Channel region (7/10) presented 5 sacral vertebrae, 20% (2/10) 6 sacral vertebrae and 10% (1/10) 7 sacral vertebrae. The IG region registered 61.9% (13/21) individuals with 5 sacral vertebrae, 33.3% (7/21) with 6 sacral vertebrae and 4.8% (1/21) with 7 sacral vertebrae. In the Continent region, 75% (3/4) had 5 sacral vertebrae and 25% (1/4) 7 sacral vertebrae. Two NA individuals were described for such factor, showing 5 sacral vertebrae each (Table 4). No significant differences were found between the levels of the different factors analysed when using Fisher's statistical test (Table 8).

Table 8. Results of Fisher Exact Test (FET) in SP and PT samples for sex, age, period, and region variables.

		p-value (FET)
Sacralization		
Sex	SP	1
	PT	1
Age	SP	1
	PT	1
Period		1
Region		0,4286
NSV*		
Sex	SP	0,5023
	PT	0,1818
Age	SP	0,8605
	PT	1
Period		0,24
Region		0,4553

*Number of Sacral Vertebrae

Results in the PT sample showed an incidence of caudal sacralisation of 23% of the sample (3/13), from which 50% were women (3/6) and no cases were observed in men, less frequent in subjects under 30 years old (16,7%, 1/6) than those over 30 years (25%, 1/4). No cases of cranial sacralization, thoracicalization or lumbarization were observed (Table 3). Regarding the variations in the number of sacral vertebrae, 77% of the total sample (10/13) presented 5 sacral vertebrae and 23% (3/13) showed 6 sacral vertebrae. No cases of sacrum with 4 or 7 vertebrae were observed in the PT sample (Table 3). However, in the sample presenting spine a high prevalence of individuals with 4 sacral vertebrae (9,5%, 2/21) was observed.

The bibliographic review accounted for 40 works reporting evidence on 53 samples, describing a total of 91 SAs distributes among the different types analysed in the present work (Table 3). Most of the studies were performed on American (28.3%), Asian (30.2%) and European (24.5%) samples, being Africa (13.2%) and Oceania (3.8%) the least studied. Cranial sacralization received most of the attention in these works (90%), followed by caudal lumbarization (45%), caudal sacralization (25%), cranial lumbarization (12.5%), caudal thoracicalization (12.5%), and cranial thoracicalization (2.5%), see Table 3. The prevalence of cranial sacralization, under 40% in all works examined, was analysed by means of continent and lifestyle (Figs. 5 and 6). Asian samples presented the highest prevalence, also showing the wider range of frequencies for this SAs, followed by the European, American, African, and Oceanian samples, whose prevalence was the lowest, close to zero. Twenty-one methodologies were described in those studies to describe the five SAs addressed in this work. Seven different methodologies have been used up to date to study cranial sacralization, four for caudal lumbarization, three for cranial lumbarization, three for caudal thoracicalization description, two for cranial lumbarization and two for caudal sacralization research (Table 9).

DISCUSSION

The present work registered information on SAs, considering cranial and caudal lumbarization and sacralization together with caudal thoracicalization. Spine elements are among the most damaged by taphonomic processes, explaining the severely

Table 9. SAs Bibliographic review. considering the type of SAs, methodologies used and the country from where the study was done.

		Continent					Lifestyle						
		Africa	**America**	**Asia**	**Europe**	**Oceania**	**AG**	**HG**	**MIX**	**NA**	**RU**	**UR**	**Methodologies (n)**
Sacralization	Cranial	7	10	13	10	2	3	5	5	9	5	15	7
	Caudal	0	7	3	2	0	2	1	1	2	1	5	2
Lumbarization	Cranial	0	6	1	0	0	2	1	0	1	1	2	3
	Caudal	3	7	5	4	1	2	3	1	5	2	7	4
Dorsalization	Cranial	0	2	1	0	0	0	0	0	1	0	2	2
	Caudal	0	6	1	0	0	2	1	0	1	1	2	3

n = number of studies. Lifestyle: AG (agriculture), HG (hunter-gatherer), MIX (urban and rural), NA (not available), RU (rural) and UR (urban).

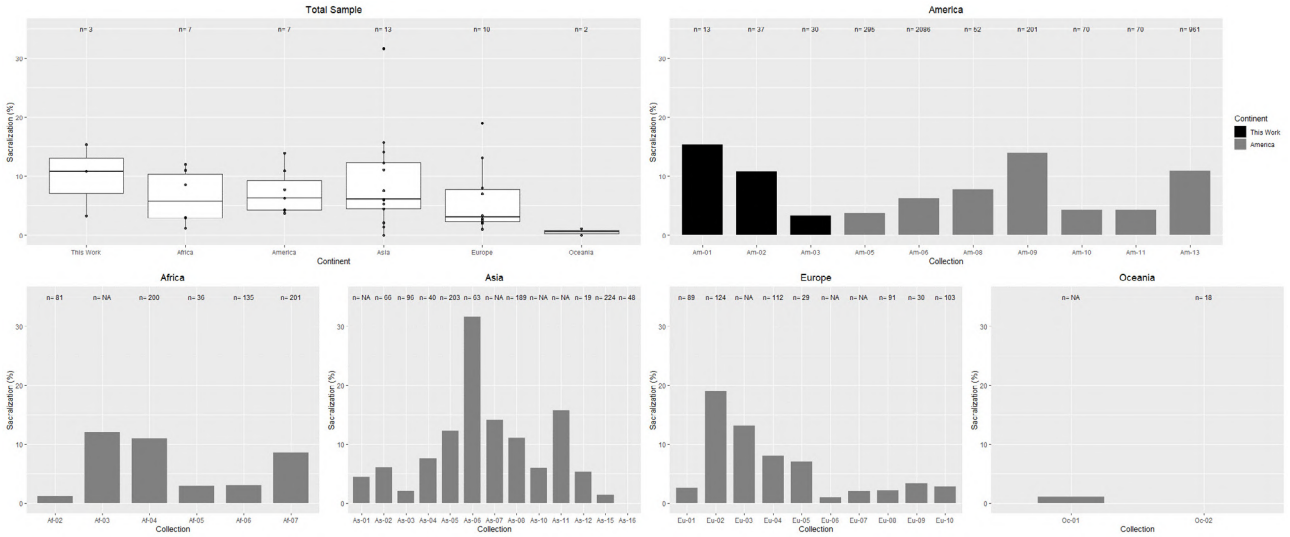

Fig. 5.- Sacralization prevalence worldwide (left and above), considering inter-continental variations (right above and below) for America (Am), Africa (Af), Asia (As) Europe (Eu) and Oceania (Oc); after conducting a bibliographic review (grey columns), including our sample (black columns). Check Table 3 for details about individuals (columns).

limited column regions showed in this work (Holland et al., 1996; Manifold, 2012). In addition, it should be considered that cervical vertebrae and coccyx are usually worse preserved than those located in other regions (Stodder, 2019; Vilas-Boas et al., 2019). Regarding to the coccyx, the results here reported agree with the data of low preservation found in other archaeological sites, as this segment of the column is also difficult to find well preserved in these contexts (Stodder, 2019). The fact that most of the coccyx described by the present study were fused to the sacrum suggests that this kind of fusion is better preserved than the coccyx alone, presumably due to its connection with another bigger bone. Besides, the most common border shifts are in the lumbosacral region, with a presence of 4%-36% in the global population (Barnes, 1994; Bulut et al., 2013; Delport et al., 2006; French et al., 2014; Jankauskas, 2001; Kimmerle, 2010; Konin and Walz, 2010; Nardo et al., 2012; Tang et al., 2014). Furthermore, cervicothoracic shifts show the lowest prevalence, under 3%, reaching 0% in some populations (Aly et al., 2016; Anap et al., 2013; Bost et al., 2011; Galis et al., 2006; Jankauskas, 2001). Such pattern could be related to high frequencies of cranial thoracicalization shifts – characterized by cervical ribs – found in stillbirths (Bots et al., 2011; ten Broek

et al., 2012). All these factors make the approach proposed in this study adequate to address this challenge. The present study shows all the stages conducted to achieve the sample selection, allowing to estimate the loss of specimens due to the taphonomic and preservation effects. However, it is difficult to compare our results in this subject with other existing studies, since they do not usually register this variable. In future works, it would be highly advisable to start registering this topic, since it would allow addressing the current taphonomical and preservation bias when analysing the complete spine.

SAs performed in this work show that thoracicalization prevalence is null. Absence or low presence of these alterations coincides with data showed by other authors (Aly et al., 2016; Anap et al., 2013; Chengetanai et al., 2017) that presented values near 1% at the thoracolumbar border. However, higher prevalence closer to 6% has been reported (Kimmerle, 2010). Although slight, an incidence of cranial lumbarization has been described in the current study, between the values of 1.9% and 5% indicated in the analysis of other samples (Jankauskas, 2001; Kimmerle, 2010). No cases of caudal lumbarization are described, which is not surprising, since previous studies have reported values between 0% and 11.4% (Shore, 1930; Masniková and Benus, 2003; Weiss, 2009; Kimmerle, 2010; Karapetian and Makarov, 2019). Sacralizations are the main studied SAs, especially cranial cases (Kimmerle, 2010), with prevalence that varies from 0% to 40% (Jankauskas, 2001; Delport et al., 2006; Kimmerle, 2010; Konin and Walz, 2010; Sharma et al., 2011; Nagar et al., 2012; Nardo et al. 2012; Bulut et al., 2013; Dabernat et al., 2013; French et al., 2014; Tang et al., 2014). The results of the Argentine samples studied oscillate between 3.3% and 18.8%, staying within the range set in previous works. The prevalence of cranial sacralization presented in our samples ranged from 0% to 23%, according to previous works.

SP sample has the particularity that it is possible to study differences between periods and regions as indicated above. Pre-contact individuals present lower values of vertebral alterations than post-contact, and especially those found in SMLC. It is known that these individuals suffered great changes in their lifestyle and were exposed to diseases and situations never lived before (García-Moro et al., 1997; Casali, 2011). These changes are in line with the increase in pathologies, both in number of cases and in different typologies, observed in previous studies (Guichón et al., 2006; García Laborde et al., 2010; Moreno Estefanell et al. 2018; D'Angelo del Campo et al., 2017, 2021). Regarding the region, it seems that this factor has less influence in SAs than chronology.

Numerical variability of the sacrum observed in the present work is comprised within the global ranges of variation previously reported (Table 10, Fig. 6). Thus, the most common number of vertebrae is 5 (60%-86% of the cases), then 6 (4%-28%) and, finally, the least common (0%-4%) is the sacrum with 4 and 7 vertebrae (Shore, 1930; Tulsi, 1972; Jankauskas, 2001; Tancock 2014; Singh, 2015). Infranumerary variations are less common than supranumerary variations (Barnes, 1994), as has been observed in the results of this work. However, there are also studies in which higher percentages of 4SV have been found, close to 7% (Singh, 2015). No cases of infranumerary variations have been found in the initial sample analysed.

The bibliographic review here presented describes different patterns of prevalence for cranial sacralization. Regarding the origin of the studied samples, it would be especially useful to deepen in the study of African and Oceanian populations in order to provide more data to be compared with other populations. That would enormously contribute to the knowledge of spine SAs patterns among populations. Besides, the number of different methodologies applied to determine the different type of variations varies depending on the variation addressed. Thus, cranial sacralization is the topic with more methodologies proposed. On the one hand, it is logic that the most studied variation has more variety of methods for assessing it. On the other hand, it is surprising that almost for every five works there is a new methodology proposed. This fact complicates the discussion of the results obtained by the different works. The high number of methodologies used to study the rest of

Table 10. Numerical variability of the sacrum in different samples around the world.

Continent	Collection	Period	n	SV				Reference
				S4	S5	S6	S7	
Africa	Bantu population. Housed at Raymond A. Dart. Collection, Witwatersrand University (South Africa).	ND	81	0	81 (79)	17 (21.0)	0	Shore, 1930
America	Yukon River, Alaska (USA)	ND	179	2 (1.1)	126 (70.4)	50 (27.9)	1 (0.1)	Stewart, 1932
	Pukará de Tilcara	1000 - 1520 A.D.	♀: 6	0	3(50)	3(50)	0	This work
			♂: 5	0	5 (100)	0	0	
			ND: 2	0	2 (100)	0	0	
			Total: 13	0	10 (77)	3 (23)	0	
	Southern Patagonia	5200 BP - 20th cent.	♀: 15	0	10 (66.7)	4 (26.7)	1 (6.7)	
			♂: 29	0	20 (69)	7 (24.1)	1 (4)	
			Total: 48	0	34 (70.8)	11 (22.9)	3 (6.3)	
Europe	Archaeological remains from Lituania (Lituania)	1000-2000 A.D.	633	7 (1.1)	378 (59.8)	225 (35.5)	23 (3.7)	Jankauskas, 2001
	Populations from Rural and Urban Northeast England (England)	18th-19th cent.	130	2 (1.5)	122 (93.8)	6 (4.6)	0	Tancock, 2014
Oceanía	Australian Aborigens. South Australian Museum and Department of Anatomy, University of Adelaide (Australia)	ND	♀: 48	0	46 (95.8)	2 (4.2)	0	Tulsi, 1972
			♂: 63	1 (1.6)	50 (79)	12 (19)	0	
			Total: 125	1 (0.9)	96 (86.5)	14(12.6)	0	

Number of cases and prevalence: n (%).
ND: No Data.

variations described in the present work face the same challenge. Final considerations regarding previous studies on SAs: First, most authors focus their attention on the study of cranial sacralization, which has been reported to present a prevalence under 40% (Table 3). This may be because many of the studies are done exclusively with the sacrum (Henneberg and Henneberg, 1999; Sharma et al., 2011; French et al., 2014; Singh et al., 2015). Besides, unlike the rest of the alterations, there are specific methodologies for its study and comparison (Castellvi et al., 1984). These facts

Fig. 6.- Numerical variability of the *sacrum*. **1**) 4 SV, individual 12589 from PT sample. **2**) 5 SV, individual 17844 from PT sample. **3**) 6 SV, individual 796 from SP sample. **4**) 7 SV, individual E 10-11 (1) from SP sample.

may cause the authors to prefer to focus their studies on the sacrum.

Extrinsic factor, environment

Environment influence on development becomes of greater importance, instead of the consideration of genetics by itself. For example, it has been observed that when pregnant women are exposed to several environmental conditions in their early stages of gestation, the proper development of the spine of the embryo may result challenging (Sparrow et al., 2012). It has been also shown that some environmental factors like cold or high-altitude environments can cause lasting changes over generations at the physiological and genetic level (Bigham, 2016; Leonard, 2018).

Results of SP sample showed the highest values in the percentage of 7 sacral vertebrae (8.1%) when comparing to other works (Table 5). With respect to sacral numerical variation, similar prevalence was observed between Inuit and SP populations. Existing similarities between both populations have been previously described regarding skull (Lahr et al., 1995; Hernández et al., 1997; Lalueza et al., 1997b), nasal cavity (Noback et al., 2011) long bones (Pearson and Millones, 2005) and rib morphology (García-Martínez et al., 2018), spine pathologies prevalence like spondylolysis (D'Angelo del Campo et al., 2017), sacrum pathologies (D'Angelo del Campo et al., 2021), oral pathologies (Pérez-Pérez and Lalueza Fox, 1992), metabolism, height, stature, body proportions and robustness (Hernández et al., 1997; Pearson and Millones, 2005; Pérez and Monteiro, 2009; Leonard, 2018). However, these populations showed clear differences in DNA analysis (Chiaroni et al., 2009; de Saint-Pierre et al., 2012; Marangoni et al., 2014; de la Fuente et al., 2015). For these reasons, some authors propose that the environment, especially when influenced by cold, could play an important role in the morphological and physiological variation observed, thus resulting in phenotypical plasticity or environmental and climate changes (Hernández et al., 1997; Lalueza et al., 1997b; Pérez et al., 2007, 2011; Pérez and Monteiro, 2009). Regarding SAs occurring in Inuit and SP populations, it is important to note that, while Inuit show high values of caudal lumbarization and low values of cranial sacralization (Karapetian and Makarov, 2019), SP do not show cases of caudal lumbarization but present high prevalence of cranial sacralization. Thus, both samples show high variation in lumbosacral region, however depicting a different shift pattern: cranial-directed in SP and caudal-directed in Inuit. Such observed differences could be also related to a "*possible impact of environmental factors on the pattern of cranio-caudal shifts*" among human populations, as has been already stated by Karapetian and Makarov (2019: 195).

Sacral variation numbers from the PT sample were within the global range. However, if the number of sacral vertebrae in the individuals in the sample presenting spine is considered, the prevalence of individuals exhibiting a sacrum with 4 vertebrae (9.5%) is relevant, since it is the highest observed up to date. The PT sample is considered to come from a high-altitude settlement, highlands regions which are characterized by numerous environmental challenges as cold climate, powerful solar radiation, limited nutritional availability and low oxygen conditions, i.e., hypoxia. The latter is one of the many stressors for human populations, because the partial pressure of oxygen in the atmosphere decreases proportionally with increasing altitude, thereby limiting the passage of gas molecules from the atmosphere to the tissues and the respiratory, cardiovascular, and haematological systems (Beall, 2007; Weinstein, 2007; Frisancho, 2013). Native highlanders are characterized by slow growth and small adult body size, delayed sexual and physical maturation, expanded chest dimensions and functional adaptation to hypoxia conditions – increased lung volume and lung diffusion capacity, along with more efficient transport and diffusion of oxygen to the tissues, among others (Frisancho, 1993, 2013; Beall, 2007; Leonard, 2018). Besides, chest expansion implies clear modifications in thoracic skeletal morphology, sternal and clavicular proportions and rib areas and curvatures (Weinstein, 2007). Furthermore, chronic hypoxia has a critical role on embryonic development orchestrating cellular differentiation and organogenesis (Moore et al., 2011). On one hand, experiments with mice have shown that gestational

hypoxia can induce congenital malformations of the spine, an experience that has turned out to be like clinical situations in humans (Ingalls and Curley, 1975; Hou et al., 2018). On the other hand, hypoxia would trigger the alteration of the expression of certain genes involved in somatogenesis, resulting in an example of a congenital defect mediated by the interaction of genetic and environmental factors. (Giampietro et al., 2012; Sparrow et al., 2012). Therefore, it is plausible to think that under hypoxic conditions any type of SA could be expressed at the level of the spine. However, knowledge on this topic is still scarce. The variations observed in this work at sacral level could be a first hint on this matter.

It is difficult to know to what extent environmental, genetic, and epigenetic factors influence the human vertebral alterations in this work due to their multi-etiological nature (Sarfo, 2014). However, the SAs examined in prepuna and SP suggest that the environmental factor plays an important role in their expression. This phenotypic variability observed in response to cold and high-altitude conditions can be explained by microevolutionary responses, since it is possible that genotypic plasticity has limitations when it comes to explaining these phenotypes adapted to extreme conditions. Nevertheless, further studies are recommended to better understand the environmental effect on the expression of phenotypic plasticity among humans.

CONCLUSION

This work describes the variability in the prevalence of five segmentation anomalies located in the spine between two Argentine archaeological populations, Southern Patagonia and Pukará de Tilcara. The most frequent SA was cranial sacralization while no caudal thoracicalization or cranial lumbarization cases were reported. The SP sample presented the highest prevalence for all identified SAs, being the only one to outline caudal lumbarization. Furthermore, this sample showed the highest prevalence of cranial sacralization among different American samples.

Similarities between the SP sample and Inuit populations have been previously reported, proposing environmental factors as modulators of phenotypic expression in humans. In this work, we describe similar patterns in the prevalence of lumbosacral SAs between both populations but with different directions. Although environmental factors such as cold climate could be involved in the expression of similar morphological and physiological characteristics, the different directionality of the shift could be triggered by the effect of other factors, not yet unaddressed, which encourage us to continue with this approach. In PT another environmental factor, hypoxia, could be involved in the variations observed in sacral bones.

Due to a scarce methodological standardization in this field, it is challenging to make any comparison or generation of knowledge about it. In addition, the optimal preservation conditions to carry out this type of study, which include the complete spine, are scarce in past population samples. That is why this paper proposes a new methodology to analyse SAs in archaeological samples. It is easy to replicate and build on previous studies, as well as on insights from the review conducted here, with the aim of establishing a starting point to increase our knowledge about SAs and their aetiology.

AKNOWLEDGEMENTS

We would like to express our gratitude to museums and research institutions of Argentina (*Museo del Fin del Mundo*, Ushuaia; CADIC, Ushuaia; *Museo Etnográfico Juan B. Ambrosetti, Facultad de Filosofía y Letras*, *Universidad de Buenos Aires*) and Chile (*Instituto de la Patagonia, Punta Arenas*) for the permission to study the human remains housed at those places. We thank Patricia I. Palacio for her help with the design of the figures. This research was supported by FONCyT-PICT 0575, PIP 112 201201 00359 CO of Argentina and a CONICET postdoctoral fellowship awarded to one of the authors (MDDdC). The research group *Laboratorio de Poblaciones del Pasado* (LAPP) has been supported by Projects HAR2016-78036-P, HAR2016-74846-P, HAR2017-82755-P, HAR2017-83004-P (Spanish Government) and a grant (ref. 38360) from The Leakey Foundation.

REFERENCES

ALY I, CHAPMAN JR, OSKOUIAN RJ, LOUKAS M, TUBBS RS (2016) Lumbar ribs: A comprehensive review. *Childs Nerv Syst*, 32: 781-785.

ANAP D, KACHEWAR S, PRABHAKAR A, DIWATE A, GANVIR SD (2013) Lumbar rib: An uncommon causation of a common manifestation. *Rev Rom Kinetoterapie*, 19(31): 19-22.

BARNES E (1994) *Developmental defects of the axial skeleton in paleopathology*. University Press of Colorado, Colorado, USA.

BEALL C (2007) Two routes to functional adaptation: Tibetan and Andean high-altitude natives. *Proc Natl Acad Sci*, 104(1): 8655-8660.

BERNAL V, PÉREZ SI, GONZÁLEZ PN, SARDI ML, PUCCIARELLI HM (2010) Spatial patterns and evolutionary processes in southern South America: A study of dental morphometric variation. *Am J Phys Anthropol*, 142(1): 95-104.

BIGHAM AW (2016) Genetics of human origin and evolution: high-altitude adaptations. *Curr Opin Genet Dev*, 41: 8-13.

BORRERO LA (2001) *El poblamiento de Patagonia. Toldos, milodones y volcanes*. Emecé Editores, Buenos Aires, Argentina.

BORRERO LA, GUICHÓN RA, TYKOT R, KELLY J, PRIETO A, CARDENAS P (2001) Dieta a partir de isótopos estables en restos óseos humanos de Patagonia Austral. Estado actual y perspectivas. *Magallania (Punta Arenas)*, 29: 119-127.

BOTS J, WIJNAENDTS LCD, DELEN S, VAN DOGEN S, HEIKINHEIMO K, GALIS F (2011) Analysis of cervical ribs in a series of human fetuses. *J Anat*, 219: 403-409.

BROOKS ST, SUCHEY (1990) Skeletal age determination based on the os pubis: a comparison of the Acsádi-Nemeskéri and Suchey-Brooks methods. *Hum Evol*, 5: 227-238.

BUIKSTRA JE, UBELAKER DH (1994) *Standards for Data Collection from Human Skeletal Remains*. Arkansas Archaeological Survey Research Series No.44, Arkansas, USA.

BULUT M, UÇAR BY, UÇAR D, AZBOY I, DEMIRTAS A, ALEMDAR C, GEM M, ÖZKUL E (2013) Is sacralization really a cause of low back pain? *ISRN Orthop*, 839013: 1-4.

CASALI R (2011) *Contacto Interétnico en el norte de Tierra del Fuego. La Misión Salesiana de La Candelaria y la salud de la población Selk´nam. (1895-1931)*. PhD, Universidad Nacional de Mar del Plata (UNMdP), Mar del Plata, Argentina.

CASTELLVI AE, GOLDSTEIN LA, CHAN DP (1984) Lumbosacral transitional vertebrae and their relationship with lumbar extradural defects. *Spine*, 9(5): 493-495.

CHENGETANAI S, NCHABELENG EK, BACCI N, BILLINGS BK, MAZENGENYA P (2017) Supernumerary lumbar ribs: a rare occurrence on an adult African male skeleton. *Anat Cell Biol*, 50(2): 155-158.

CHIARONI J, UNDERHILL PA, CAVALLI-SFORZA L (2009) Y chromosome diversity, human expansion and cultural evolution. *Proc Natl Acad Sci*, 106(48): 20174-20179.

COCILOVO J, GUICHÓN RA (1986) Propuesta para el estudio de las poblaciones aborígenes del extremo austral de Patagonia. *Magallania (Punta Arenas)*, 6: 111-123.

COCILOVO J, GUICHÓN RA (1999-2000) La variación geográfica y el proceso de microdiferenciación de las poblaciones aborígenes de Patagonia Austral y de Tierra del Fuego. *Rev Chil de Antrop*, 15: 9-28.

CRESPO CM, RUSSO MG, HAJDUK A, LANATA JL, DEJEAN CB (2017) Variabilidad mitocondrial en muestras pre-colombinas de la Patagonia Argentina: hacia una visión de su poblamiento desde el ADN antiguo. *Rev Argent Antropol Biol*, 19(1): 1-21.

CRESPO CM, LANATA JL, CARDOZO DG, AVENA SA, DEJEAN CB (2018) Ancient maternal lineages in hunter-gatherer groups of Argentinean Patagonia. Settlement, population continuity and divergence. *J Archaeol Sci Rep*, 18: 689-695.

DABERNAT H, REIS T, TARASOV T, ARTYUKHOV L, NIKOLAEV V, MEDVEDEVA A, GAVRILYUK O, NIKOLAEV M, CRUBÉZY E (2013) Paleopathology of the population of Krasnoyarsk, central Siberia. *Archaeol Ethnol Anthrop Eurasia*, 41(13): 140-150.

D'ANGELO DEL CAMPO MD, SUBY JA, GARCÍA-LABORDE P, GUICHÓN RA (2017) Spondylolysis in the past: A case study of hunter-gatherers from Southern Patagonia. *Int J Paleopathol*, 19: 1-17.

D'ANGELO DEL CAMPO MD, CURTI H, GERVASIO LÓPEZ M, GARCÍA-LABORDE P, VALENZUELA LO, MOTTI JMB, MARTUCCI M, PALACIO PI, GONZÁLEZ MARTÍN A, GUICHÓN RA (2020) Base de información bioantropológica de Patagonia Austral (B.I.B.P.A.). *Rev Argent Antropol Biol*, 22(2): 1-13.

D'ANGELO DEL CAMPO MD, MEDIALDEA L, GARCÍA-LABORDE P, SALEMME M, SANTIAGO F, CAMPO MARTÍN M, GONZÁLEZ MARTÍN A, GUICHÓN RA (2021) Sacrum paleopathology in hunter-gatherers' from Southern Patagonia. *Chungará,* 53(4):647-663.

DE LA FUENTE C, GALIMANY J, KEMP BM, JUDD K, REYES O, MORAGA M (2015) Ancient marine hunter-gatherers from Patagonia and Tierra del Fuego: diversity and differentiation using uniparentally inherited genetic markers. *Am J Phys Anthropol*, 158(4): 719-729.

DE LA FUENTE C, ÁVILA-ARCOS MC, GALIMANY J, CARPENTER ML, HOMBURGUER JR, BLANCO A, CONTRERAS P, CRUZ DÁVALOS D, REYES O, SAN ROMÁN M, MORENO-ESTRADA A, CAMPOS PF, ENG C, HUNTSMAN S, BURCHARD EG, MALASPINAS A-S, BUSTAMANTE CD, WILLERSLEV E, LLOP E, VERDUGO RA, MORAGA M (2018) Genomic insigSAs into the origin and diversification of late maritime hunter-gatherers from Chilean Patagonia. *Proc Natl Acad Sci*, 115(17): e4006-e4012.

DE SAINT PIERRE M, BRAVI CM, MOTTI JMB, FUKU N, TANAKA M, LLOP E, BONATTO SL, MORAGA M (2012) An alternative model for the early peopling of Southern South America revealed by analyses of three mithocondrial DNA Haplogroups. *PLoS One*, 7(9): e43486.

DEBENEDETTI S (1930) Las ruinas del Pukará, Tilcara, Quebrada de Humahuaca (Provincia de Jujuy). *Arch Museo Etnogr*, 11.

DELPORT EG, CUCUZZELLA TR, KIM N, MARLEY J, PRUITT C, DELPORT AG (2006) Lumbosacral transitional vertebrae: Incidence in a consecutive patient series. *Pain Physician*, 9: 53-56.

FRENCH HD, SOMASUNDARAM AJ, SCHAEFER NR, LAHERTY RW (2014) Lumbosacral transitional vertebrae and its prevalence in the Australian population. *Global Spine J*, 4: 229-232.

FRISANCHO AR (1993) *Human adaptation and accommodation*. University of Michigan Press, Ann Arbor, USA.

FRISANCHO AR (2013) Developmental functional adaptation to high altitude: Review. *Am J Hum Biol*, 25(2): 151-168.

GALIS F (1999) Why do almost all mammals have seven cervical vertebrae? Developmental constraints, Hox genes, and cancer. *J Exp Zool*, 285(1): 19-26.

GARCÍA-BOUR J, PÉREZ-PÉREZ A, ÁLVAREZ S, FERNÁNDEZ E, LÓPEZ-PARRA AM, ARROYO-PARDO E, TURBÓN D (2004) Early population differentiation in extinct aborigines from Tierra del Fuego-Patagonia: ancient mtDNA sequences and Y-chromosome STR characterization. *Am J Phys Anthropol*, 123(4): 361-370.

GARCÍA-MARTÍNEZ D, NALLA S, FERREIRA MT, BASTIR M, D'ANGELO DEL CAMPO MD, GUICHÓN RA (2018) Eco-geographic adaptations in the human ribcage throughout a 3D geometric morphometric approach. *Am J Phys Anthropol*, 166(2): 323-336.

GARCÍA LABORDE P, SUBY JA, GUICHÓN RA, CASALI R (2010) El antiguo cementerio de la misión de Río Grande, Tierra del Fuego. Primeros resultados sobre patologías nutricionales-metabólicas e infecciosas. *Rev Argent Antropol Biol*, 12(1): 57-69.

GARCÍA-MORO C, HERNÁNDEZ M, LALUEZA C (1997) Estimation of the optimum density of the Selk'nam from Tierra del Fuego: inferences about human dinamics in extreme environments. *Am J Hum Biol*, 9(6): 699-708.

GIAMPIETRO PF, RAGGIO CL, BLANK RD, MCCARTY C, BROECKEL U, PICKART MA (2013) Clinical, genetic and environmental factors associated with congenital vertebral malformations. *Mol Syndromol*, 4: 94-105.

GONZÁLEZ-JOSÉ R, GARCÍA MORO C, DAHIN S, HERNÁNDEZ M (2002) Origin of Fueguian-Patagonians: an approach to population history and structure using R matrix and matrix permutation methods. *Am J Hum Biol*, 14(3): 308-320.

GONZÁLEZ-JOSÉ R (2003) *El Poblamiento de la Patagonia. Análisis de la Variación Craneofacial en el contexto del Poblamiento Americano*. PhD, Universitat de Barcelona, Barcelona, Spain.

GUICHÓN RA (1993) *Antropología Física de Tierra del Fuego. Caracterización Biológica de las Poblaciones Prehispánicas*. PhD, Universidad de Buenos Aires, Buenos Aires, Argentina.

GUICHÓN RA, SUBY JA, CASALI R, FUGASSA MH (2006) Health at the time of native-european contact in Southern Patagonia. First steps, results and prospects. *Mem Inst Oswaldo Cruz*, 101(Suppl. II): 97-105.

HENNEBERG R, HENNEBERG M (1999) Variation in the closure of the sacral canal in the skeletal sample from Pompeii, Italy, 79 ad. *Perspect Hum Biol*, 4(1): 177-188.

HERNÁNDEZ M, LALUEZA C, GARCÍA-MORO C (1997) Fueguian cranial morphology: the adaptation to a cold, harsh environment. *Am J Phys Anthropol*, 103(1): 103-117.

HOLLAND TD, ANDERSON BE, MANN RW (1996) Human variables in the postmortem alteration of human bone: Examples from U.S. War casualties. In: Sorg MH, Haglund WD (eds). *Forensic Taphonomy, The Postmortem Fate of Human Remains*. CRC Press, Boca Ratón, Florida, USA, pp 263-273.

HORAN GSB, RAMÍREZ-SOLÍS R, FEATHERSTONE MS, WOLGEMUTH DJ, BRADLEY A, BEHRINGER RR (1995) Compound mutants for the paralogous hoxa-4, hoxb-4, and hoxd-4 genes show more complete segmentation anomalies and a dose-dependent increase in the number of vertebrae transformed. *Genes Dev*, 9: 1667-1677.

HOU D, KANG N, YIN P, HAI Y (2018) Abnormalities associated with congenital scoliosis in high-altitude geographic regions. *Int J Orthop*, 42: 575-581.

INGALLS TH, CURLEY FJ (1957) Principles governing the genesis of congenital malformations induced in mice by hypoxia. *N Engl J Med*, 257: 1121-1127.

ISÇAN MY, LOTH SR, WRIGHT RK (1984) Metamorphosis at the sternal rib end: a new method to estimate age at death in white males. *Am J Phys Anthropol*, 65(2): 147-156.

JANKAUSKAS R (2001) Variations and anomalies of the vertebral column in Lithuanian palaeoosteological samples. *Anthropol Anz*, XXXIX(1): 33-37.

KARAPETIAN MK, MAKAROV SV (2019) Restudying variations of axial skeleton patterning in skimo groups with new data from ancient Chukotka (Ekven archaeological site). *Eur J Anat*, 23(3): 187-199.

KIMMERLE EH (2010) A comparative study of developmental defects and metabolic diseases among the Arikara and earlier Northern plains populations. *Plain Anthropol*, 55(215): 225-234.

KONIN GP, WALZ DM (2010) Lumbosacral transitional vertebrae: Classification, imaging findings, and clinical relevance. *Am J Neuroradiol*, 31(10): 1778-1786.

LAHR MM (1995) Patterns of modern human diversification: implications for Amerindian origins. *Yearb Phys Anthropol*, 38: 163-198.

LALUEZA C, HERNÁNDEZ M, GARCÍA-MORO C (1996) Craniometric analysis in groups from Tierra del Fuego/Patagonia and the peopling of the south extreme of the Americas. *Hum Evol*, 11: 217-224.

LALUEZA C, PÉREZ-PÉREZ A, PRATS E, CORNUDELLA L, TURBON D (1997a) Lack of founding Amerindian mitochondrial DNA lineages in extinct aborigines from Tierra de Fuego Patagonia. *Hum Mol Gen*, 6(1): 41-46.

LALUEZA C, HERNÁNDEZ M, GARCÍA-MORO C (1997b) La morfología facial de las poblaciones fueguinas: ¿reflejo de una adaptación al frío? *Magallania (Punta Arenas)*, 25: 45-58.

LEONARD WR (2018) Centennial perspective on human adaptability. *Am J Phys Anthropol*, 165: 813-833.

LOVEJOY CO, MEINDL RS, PRYZBECK TR, MENSFORTH RP (1985) Chronological metamorphosis of the auricular surface of the ilium: a new method for the determination of adult skeletal age at death. *Am J Phys Anthropol*, 68(1): 15-28.

MALLO M, WELLIK DM, DESCHAMPS J (2010) Hox genes and regional patterning of the vertebrate body plan. *Dev Biol*, 344(1): 7-15.

MANIFOLD BM (2012) Intrinsic and extrinsic factors involved in the preservation of non-adult skeletal remains in archeology and forensic science. *Bull Int Assoc paleodont*, 6(2): 51-69.

MARANGONI A, CARAMELLI D, MANZI G (2014) Homo Sapiens in the Americas. Overview of the earliest human expansion in the New World. *J Anthropol Sci*, 92: 79-97.

MORENO ESTEFANELL L, D'ANGELO DEL CAMPO MD, CAMPO MARTÍN M, GARCÍA LABORDE P, CAMBRA-MOO O, GONZÁLEZ MARTÍN A, GUICHÓN RA (2018) Aproximación a la paleopatología de la columna vertebral en el cementerio de la Misión Salesiana "Nuestra Señora de La Candelaria" (s. XIX-XX, Río Grande, Argentina). *Rev Argent Antropol Biol*, 20(2): 1-18.

NAGAR S, KUBAVAT D, MALUKAR O, VALEKAR P, RATHOD H, CHAUHAN P (2012) Study of sacralisation of coccygeal vertebra in Gujarat. *Natl J Integr Res Med*, 3(3): 39-42.

NARDO L, ALIZAI H, VIRAYAVANICH W, LIU F, HERNÁNDEZ A, LYNCH JA, NEVITT MC, MCCULLOCH C, LANE NE, LINK TM (2012) Lumbosacral transitional vertebrae: Association with low back pain. *Radiol*, 265(2): 497-503.

NOBACK ML, HARVATI K, SPOOR F (2011) Climate-related variation of the human nasal cavity. *Am J Phys Anthropol*, 145(4): 599-614.

OTERO C (2015) Distribución y consumo de cerámica inca en el Pukará de Tilcara (Quebrada de Humahuaca, Argentina). *Chungara*, 47(3): 401-414.

PEARSON OM, MILLONES M (2005) Rasgos esqueletales de adaptación al clima y la actividad entre los habitantes aborígenes de Tierra del Fuego. *Magallania (Punta Arenas)*, 33(1): 37-50.

PELLETIER F, COLTMAN DW (2018) Will human influences on evolutionary dynamics in the wild pervade the Anthropocene? *BMC Bio*, 16: 7.

PÉREZ SI, BERNAL V, GONZÁLEZ P (2007) Morphological differentiation of aboriginal human populations from Tierra del Fuego (Patagonia): Implications for South American peopling. *Am J Phys Anthropol*, 133(4): 1067-1079.

PÉREZ SI, BERNAL V, GONZÁLEZ P, SARDI M, POLITIS G, O'ROURKE D (2009) Discrepancy between cranial and DNA data of Early Americans: Implications for American Peopling. *PLoS One*, 4(5): e5746.

PÉREZ SI, MONTEIRO LR (2009) Nonrandom factor in modern human morphological diversification: a study of craniofacial variation in Southern South America populations. *Hum Evol*, 63(4): 978-993.

PÉREZ SI, LEMA V, DINIZ-FILHO JAF, BERNAL V, GONZÁLEZ P, GLOBBO D, PUCCIARELLI HM (2011) The role of diet and temperature in shaping cranial diversifications of South American human populations: an approach based on spatial regression and divergence rate tests. *J Biogeogr*, 38(1): 148-163.

PÉREZ-PÉREZ A, LALUEZA FOX C (1992) Indicadores de presión ambiental en aborígenes de Fuego-Patagonia. Un reflejo de la adaptación a un ambiente adverso. *Magallania (Punta Arenas)*, 21:99-108.

RAWLS A, FISHER R (2018) Developmental and functional anatomy of the spine. In: Kusumi K, Dunwoodie S (eds). *The Genetics and Development of Scoliosis*. Springer, Strasbourg, France, pp 21-46.

SARFO TA (2014) *A statistical investigation of nonmetric vertebral traits with a skeletal population sample from the Dakhleh Oasis, Egypt*. PhD, Occidental Ontario University, Canada.

SHARMA VA, SHARMA DK, SHUKLA CK (2011) Oesteogenic study of lumbosacral transitional vertebra in Central India region. *J Anat Soc Ind*, 60(2): 212-217.

SHORE LR (1930) Abnormalities of the vertebral column in a series of skeletons of Bantu natives of South Africa. *J Anat*, 64(2): 207-238.

SINGH ID, AJITA R, NARANBABU SINGH T (2015) Variation in the number of sacral pieces. *Hum Biol Rev*: 88-94.

SPARROW DB, CHAPMAN G, SMITH AJ, MATTAR MZ, MAJOR JA, O'REILLY VC, SAGA Y, ZACKAI EH, DORMANS JP, ALMAN BA, MCGREGOR L, KAGEYAMA R, KUSUMI K, DUNWOODIE SL (2012) A mechanism for gene-environment interaction in the etiology of congenital scoliosis. *Cell*, 149(2): 295-306.

STODDER A (2019) Taphonomy and the nature of archaeological assemblages. In: Katzenberg A, Grauer A (eds). *Biological anthropology of the human skeleton*. Wiley Blackwell, Oxford, England, pp 73-115.

TANCOCK D (2014) *Congenital defects in 18th and 19th century populations from rural and urban Northeast England*. PhD, Durham University, England.

TANG M, YANG X, YANG S, HAM P, MA Y, YU H, ZHU B (2014) Lumbosacral transitional vertebra in a population-based study of 5860 individuals: Prevalence and relationship to low back pain. *Eur J Radiol*, 83(9): 1679-1682.

TEN BROEK CMA, BAKKER AJ, VARELA-LASHERAS I, BUGIANI M, VAN DONGEN S, GALIS F (2012) Evo-Devo of the human vertebral column: on homeotic transformations, pathologies and prenatal selection. *Evol Biol*, 39: 456-471.

TODD TW (1921a) Age changes in the pubic bone I: the male white pubis. *Am J Phys Anthropol*, 3: 285-334.

TODD TW (1921b) Age changes in the pubic bone III: the pubis of the white female. *Am J Phys Anthropol*, 4: 1-70.

TULSI RS (1972) Vertebral column of the Australian aborigine: Selected morphological and metrical features. *Z Morp Anthrop*, 64(2): 117-144.

VARELA H, COCILOVO A, GUICHÓN RA (1993-1994) Evaluaciones de la información somatométrica por Gusinde sobre los aborígenes de Tierra del Fuego. *Magallania (Punta Arenas)*, 22: 193-205.

VILAS-BOAS D, WASTERLAIN SN, D'OLIVEIRA COELHO J, NAVEGA D, GONÇALVES D (2019) SPINNE: an app for human vertebral height estimation based on artificial neural networks. *Forensic Sci Int*, 298: 121-130.

WEINSTEIN KJ (2007) Thoracic skeletal morphology and high-altitude hypoxia in Andean prehistory. *Am J Phys Anthropol*, 134: 36-49.

WELLIK DM, CAPECCHI MR (2003) Hox10 and Hox11 genes are required to globally pattern the mammalian skeleton. *Science*, 301(5631): 363-367.

WHITE TD, FOLKENS PA (2005) *The human bone manual*. Elsevier Academics Press, Amsterdam, Netherlands.

An irrefutable unambiguous insight into zygomatic air cell defect (ZACD)

Karthikeya Patil[1], Sanjay C.J.[1], Lakshminarayana Kaiyoor Surya[1], Vidya Gowdappa Doddawad[2], Girish MS[3], Shilpa Padar Shastry[4]

[1] Department of Oral Medicine and Radiology, JSS Dental College and Hospital, JSS Academy of higher Education and Research, SS Nagar, Mysore - 570 015, India

[2] Department of Oral Pathology & Microbiology, JSS Dental College and Hospital, JSS Academy of higher Education and Research, SS Nagar, Mysuru - 570 015, India

[3] Department of Pedodontics &Preventive Dentistry, JSS Dental College and Hospital, JSS Academy of higher Education and Research, SS Nagar, Mysuru - 570 015, India

[4] Department of Oral Medicine & Radiology, Vydehi Institute of Dental Sciences and Research Centre, Nallurhalli, Whitefield, Bangalore 560066, India

SUMMARY

Zygomatic air cell defect (ZACD) of the temporal bone, has been characterized as the auxiliary air cells in the zygomatic process and articular eminence of the temporal bone. They present as unresectable findings in the zygomatic process of the temporal bone and articular tubercle. They are crucial, as they signify regions of weak resistance and the spread of disease. Comprehension of the decrepit regions in the zygomatic bones with Cone Beam Computed Tomography (CBCT), and the imaging of choice in maxillofacial disorders for its superior 3D anatomical reconstruction and minimal distortion, are indispensable in the diagnosis, treatment planning and placement of endosseous or basal dental implants to elude complications. 154 CBCT images of subjects aged between18 and 70 years with optimal diagnostic quality and area coverage satisfying the selection criteria without the history of maxillofacial fractures, pathologies, anomalies involving the middle one third of the face were analysed. The overall prevalence of ZACD was in 16 (10.4%) subjects, with 9 in females (56.25%) and in 7 males (43.75%). The men-to-women ratio was 1:1.28. It was also revealed that bilateral incidence of ZACD was more common and the prevalence of ZACD the highest 8 (50%) in the age group of 21-30 years. This study highlights the importance of research on the prevalence of the ZACD on CBCT, which was exiguous in the past, and compares with similar studies done using panoramic radiographs. This study paves the way for more studies employing CBCT to justify the findings we have expressed.

Key words: Zygomatic air cell defect – Cone Beam Computed Tomography – Prevalence – TMJ – Endosseous implants

Corresponding author:
Dr Sanjay CJ, MDS. Department of Oral Medicine and Radiology, JSS Dental College and Hospital, JSS Academy of higher Education and Research, SS Nagar, Mysore - 570 015, India. Phone: +91 9742565566. E-mail: drsanjaycj_dch@jssuni.edu.in

Submitted: November 28, 2022. **Accepted:** December 16, 2022

https://doi.org/10.52083/QUSG8782

INTRODUCTION

Growth and development of the skull occurs concomitantly with pneumatization. This process is governed by various vital anatomic factors (Diamant,1954). Zygomatic air cell defect is an addendum of such pneumatization of the temporal bone anteriorly to the articular tubercle. These cells, which imitate the mastoid cells of Lenoir, have been characterized as the auxiliary air cells in the zygomatic process and articular eminence of the temporal bone. It was Tyndall and Matteson that introduced pneumatized articular eminence, later coined as Zygomatic Air Cell Defect (ZACD) in 1987 (Tremble, 1934). There is an array of information which describes air cells that extend up to the Zygomatic process involving the articular eminence. But there is no consensus on the exact classification of Zygomatic Air cell defect, Pneumatized Articular Tubercle (PAT) and Pneumatized Roof of the Glenoid Fossa (PRGF). They present as unresectable, non-protractible, non-disparaging, tangential findings in the zygomatic process of the temporal bone and articular tubercle, which do not project beyond the zygomatic-temporal suture line.

Although ZACD are considered mere anatomical variations without any cortical destruction, knowledge of the same is crucial as they signify regions of weak resistance and the spread of disease into the temporomandibular complex. Common occurrence of otitis and mastoiditis can spread rapidly to the temporomandibular complex leading to joint ankylosis and detrimental effects on the development of mandible. The risk of TMJ surgeries may be increased, as there can be iatrogenic penetrations into the dura and leakage of CSF. Skull fractures can enter into the glenoid fossa, so adequate preoperative identification is necessary to avoid untoward complications. Comprehension of the decrepit regions in the Zygomatic bones is indispensable in the planning and placement of Endosseous or Basal Dental implants to elude complications.

An incidental finding on a panoramic radiograph indicates the presence of ZACD, which originates in the zygomatic arch and displays as an innocuous, radiolucent, non-destructive, non-expansile defect. (Gupta, D et al., 2013). Tyndall and Matteson segregated ZACD into three different types: (a) unilocular type, (b) multilocular type, and (c) trabecular type. The prevalence of ZACD may entail absolute contraindications to complex surgeries pertaining to mandibular dislocations such as eminoplasty or eminectomy.

Cone Beam Computed Tomography (CBCT) is a breakthrough diagnostic tomographic practice of recent times with the ability to appreciate inconspicuous lesions in 3 dimensions whose inherent qualities are the absence of superimposition of the anatomic structures and the absence of obscurity of the resultant images. It is capable of providing millimetric resolution images of superior quality with shorter scanning times. It has greater dimensional accuracy and significantly lesser radiation exposure, compared to conventional CT scans. CBCT has evolved into the imaging of choice in maxillofacial disorders for its superior 3D anatomical reconstruction and minimal distortion.

Until the present date, there are a few studies which bring to the fore the importance of in-depth understanding of the pneumatization and development of ZACD. Existing data about ZACD might be underestimated owing to the limitations of the conventional radiographs. Detailed studies of ZACD with novel and avant-garde imaging techniques like CBCT offer precedence in understanding the disease spread from the mastoid and the mesotympanum to the zygomatic process, and hence the lateral skull base. It provides an insight in the surgical management of the temporomandibular joint disorders. This study helps to spell out the supremacy of accurately estimating the prevalence of ZACD in CBCT, as well as and precise understanding of the entity in comparison with conventional panoramic radiographs.

MATERIAL AND METHODS

This is an invitro survey orchestrated in the Oral Medicine and Radiology department, JSS Dental College and Hospital, JSS Academy of Higher Education and Research, Mysuru, India. The study was envisaged to consider the various presentation of pneumatization like ZACD, PAT and PRGF as ZACD to avoid perplexity in the study.

Purposive sampling was used to collect the sample, and the study sample size was computed using the formula: N = (Z2) P(1-P)/d2, where n = study sample size, and z = level of confidence, P = Prevalence, and d = allowable error. This formula assumes that P and d are decimal values, but it would also be correct if they are percentages, with the exception that the term (1-P) in the numerator would become (100-P).

Prior to the investigation, an ethical clearance was obtained by the university's IEC (IEC No 26/2021). The source of data collection was done in two parts, retrospectively from the archive of CBCT images, which were satisfying the eligibility criteria and prospectively following CBCT examination of the patients for their own dental treatment purpose at the Department of Oral Medicine and Radiology. 154 patients were selected between 18 to 70 years of age satisfying the selection criteria. All the images were taken with PLANMECA Promax 3D mid and analysed using ROMEXIS VIEWER software.

Selected images were considered in sagittal, axial and coronal planes; the attributes of ZACD were examined by an experienced Oral and Maxillofacial radiologist twice with an interval of 4 weeks, and average was considered to avoid intra examiner variability. Mean and standard deviation were used for continuous data, and Chi square test with $p<0.05$ was used for categorical data. SPSS 22 software was used for statistical analysis.

Inclusion criteria:

- CBCT images taken for the purpose of evaluation of third molar, extensive restorative dental procedures, mixed dentition analysis, implant planning in orthodontic and orthognathic procedures.
- Ideal CBCT images with optimal diagnostic quality.
- CBCT images exhibiting structures like zygomatic arch, zygomatic process of maxilla and encompassing TMJ.

Exclusion criteria:

- CBCT images of Subjects with history of maxillofacial fractures, pathologies, anomalies involving the middle one-third of the face involving temporal and the zygomatic bones.
- Images with poor diagnostic quality and with image artefacts.
- Images in which zygomatic arch is not clearly or partially visualised.
- CBCT images with evidence of previous surgeries of TMJ and zygomatic arch and process.
- Images obtained by erratum in the CBCT exposure of Maxillofacial region.
- Images of subjects below 18 years of age, as the pneumatization occurs in adulthood.

RESULTS

Out of 154 patients who were part of the study, 91(59%) were women and 63(41%) were men. (Fig. 1 showing the Sex distribution of ZACD study sample). The 154 subjects were divided into 6 age groups: i.e., up to 20 years, 21 to 30, 31 to 40, 41 to 50, 51 to 60, 61 to 70 years, with sample size distribution of 5 (Male 2 + Female 3) in up to 20 age group, 64 (Males 23 + Females 41) in 21 to 30, 38 (Males 15 + Females 23) in 31 to 40, 25(Males 10 + Females 15) in 41 to 50, 16 (Males 10 + Females 6) in 51 to 60 and 6 (Males 3 + Females 3) in 61 to 70. The average age of the sample size was 33.69 +/- 13.43yrs.

The overall prevalence of ZACD was in 16 (10.4%) subjects, with 7 in males and 9 in females, with 0 up to 20 years of age, 8(50%) in 21-30 years, 3 (18.75%) in 31- 40 years of age, 3 (18.75%) in 41- 50 years, 2(12.5%) in 51-60 years, 0 in 61-70 years of age. The highest incidence was noted in the group of 21-30 years. (Table 1: Age wise distribution of ZACD) (Fig. 2: Age-wise distribution of ZACD).

ZACD was noted bilaterally in 8(5.20%) of the subjects, unilaterally on the right side in 6 (3.90%) and on left side in 2 (1.30%) of the patients. (Table 2: ZACD cell distribution).

In the detailed radiological examination, the distribution of ZACD was as follow:

- Bilateral Multilocular type of ZACD was seen in 6 (25%) subjects on Right side and in 6(25%) on Left side.

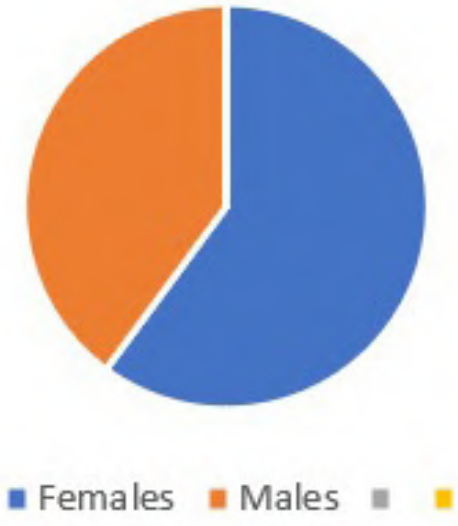

Fig. 1.- Sex Distribution of ZACD study sample.

Table 1. Age wise distribution of ZACD.

Age_Wise_Distribution

Years	Males	Females	Prevalence
11-20	0	0	0
21-30	3	5	8-50%
31-40	1	2	3-18.75%
41-50	2	1	3-18.75%
51-60	1	1	2-12.50%
61-70	0	0	0

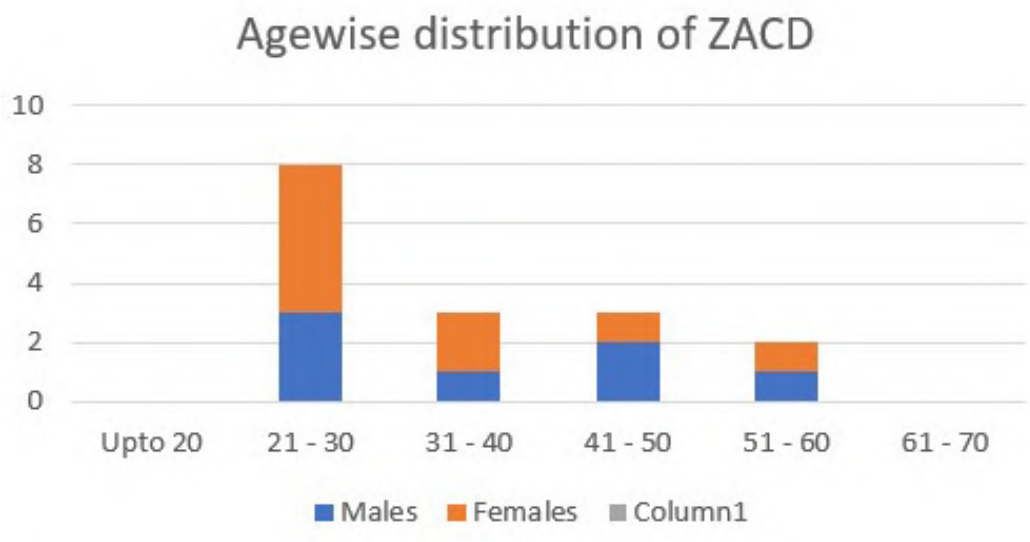

Fig. 2.- Age wise distribution of ZACD.

Table 2. ZACD distribution.

Zacd_distribution

ZACD_cell_distribution	Number	Percentage
Not present	138	89.60%
Bilateral	8	5.20%
Unilateral Right	6	3.90%
Unilateral Left	2	1.30%

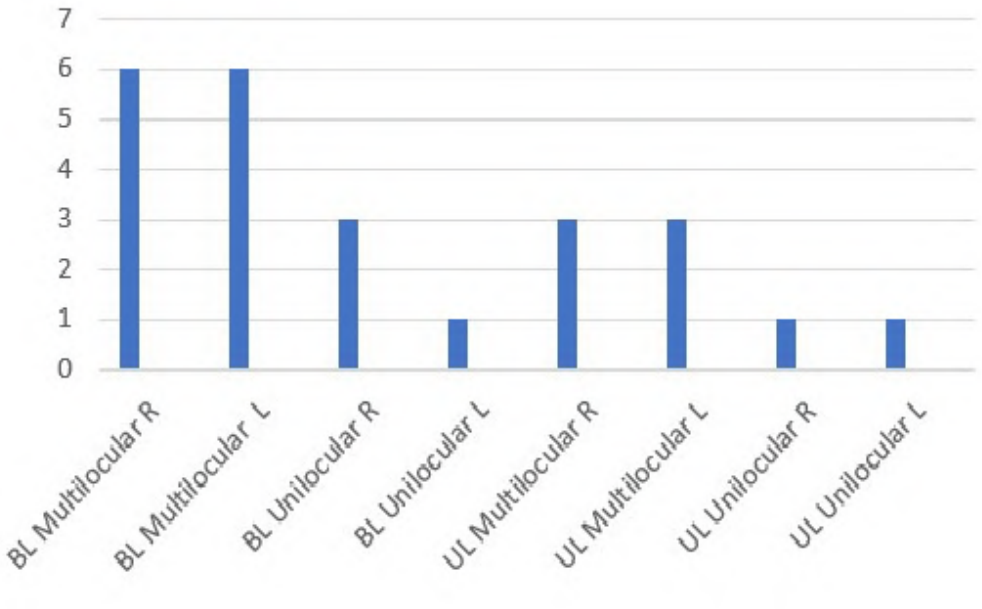

Fig. 3.- ZACD pattern of prevalence. (BL = Bilateral, UL = Unilateral, R = Right, L = Left).

- Bilateral Unilocular type of ZACD was seen in 3 (12.5%) on Right side and in 1 (4.2%) on Left side.
- Unilateral Multilocular type of ZACD was seen in 3 (12.5%) on Right side and in 3 (12.5%) on Left side.
- Unilateral Unilocular type of ZACD was seen in 1 (4.2%) on Right side and in 1 (4.2%) on Left side. (Table 3. ZACD pattern of prevalence) (Fig. 3 ZACD pattern of prevalence).

The Bilateral multilocular type of ZACD was the most common pattern noticed.

DISCUSSION

Tremble organized 10 regions of Air Cells (AC) in the temporal bone with particular quotation to emphasize alleyway of mastoid infection (Tremble, 1934). The root of the zygomatic process, which creates the glenoid fossa, is one of the temporal bone's AC sites. Often the AC of the zygomatic process can even approach the arch (Tremble, 1934). Tyndall and Matteson (1985) re-inscribed the circumstance of the pneumatized articular eminence from a radiological point of view. On panoramic radiographs with an appearance similar to the mastoid AC, they characterized it as an asymptomatic radiolucent "defect" in the zygo-

Table 3. ZACD pattern of prevalence. BL= Bilateral, UL= Unilateral, R= Right, L= Left.

ZACD_pattern

ZACD	Number	Percentage
BL Multilocular R	6	25%
BL Multilocular L	6	25%
BL Unilocular R	3	12.5%
BL Unilocular L	1	4.2%
UL Multilocular R	3	12.5%
UL Multilocular L	3	12.5%
UL Unilocular R	1	4.2%
UL Unilocular L	1	4.2%

matic process of the temporal bone. They assert that the 'defect' optionally approximates up to the temporo-zygomatic suture but never crosses it. Furthermore, they established that the zygoma was in normal shape with no deformation or altered outline.

Tyndall and Matteson (1987) proposed a categorization of ZACD into three types: unilocular, multilocular, and trabecular type. A well-defined oval radiolucency is alluded to as unilocular; multiple small cavities resembling mastoid air cells are considered multilocular; and the trabecular variant is a multilocular defect with internal bony striations.

CBCT has evolved into the prime design of choice in imaging complex structures of maxillofacial regions owing to its superior 3D anatomical reconstruction and minimal distortion. Previously, multitudinous studies of ZACD with Panoramic radiographs were executed. In the analysis designed by Patil et al. (2012), the pervasiveness of ZACD was noted to be 1.82% in a series of panoramic radiographs. On the other hand, the studies conducted by Gupta et al. (2013), Tyndall and Matteson (1987), and Arora et al. (2016) divulged the prevalence rate of ZACD as 5.7%, 1.5%, and 1.94% respectively on panoramic radiographs. A study by De Rezende et al. (2014) revealed a prevalence of 7.57% in the study population based on digitalized skull CT images. These researchers state that, because of its three-dimensional imaging and enhanced spatial resolution of the region of interest, CBCT scans would be a more viable approach. Overall, they demonstrate in their study that ZACD incidence was much lower in panoramic radiographs (1-3.5%) compared to those by CBCT (8%). This finding with CBCT is comparable with the present study, where the prevalence of ZACD was found to be 10.4% (in 16 subjects), which is proportionally higher owing to the superior imaging by CBCT when compared to conventional radiographs. Principally, CBCT is superior to conventional radiographs in visualization of anatomic structure in thin slices, and in meticulous perception of the exact anatomic details.

In this study, ZACD was found in 9 women (56.25%) and in 7 men (43.75%). The men to women ratio was 1:1.28 although there was negative statistical significance difference between the genders. In the scrutiny conducted by Miloglu et al. (2011), the prevalence was found to be 1:1.6; an independent study done by Carter et al. (1999) (M:F= 1:1.2) showed no such predilection, suggesting a panoramic insight in this aspect, whereas in the study by Patil et al. (2012) the prevalence was 0.8:1. The predominant female population attending the dental department for cosmetic purposes and the willingness for volunteering for the research attributable to the heightened perception about the oral health in the developing countries could be a reason for the higher number of females in the sample size.

According to this study, the prevalence of ZACD was zero (0) during the first decade of life, and the highest was 8 (50%) in the age group of 21-30 years. As the age increases, we noticed that the prevalence decreased. The completion of pneumatization by second decade of life could be a major factor in the occurrence. This study was in conformity with the analysis of ZACD by Carter et al.

(1999), who demonstrated that 16.3 % prevalence was seen in the age group of 20-29 years, followed by 30-39 (13.1%), and the least being 0.3% in the age group of 80-89 years.

This is in conformity with the inquiry done by Park et al. (2002) and Patil et al. (2012). The prevalence rate is lesser in older age groups, maybe owing to the remodelling process of the matured bone. Further scientific research is imperative in this respect.

On further evaluation, it was revealed that bilateral incidence of ZACD was more common in 8 (5.20%) than unilateral on right, in 6 (3.9%), and left, in 2 (1.3%). This is in accordance with the survey done by Yavuz et al. (2009). It is contradictory to the review done by Arora et al. (2016) and Patil et al. (2012), where unilateral occurrence was more commonly noticed. This discrepancy may be due to the underestimation of the ZACD prevalence by the conventional technique.

After researching in detail, it was found that bilateral multilocular (Fig. 4: multilocular ZACD in CBCT images) was the most common type of ZACD noted. The unilateral multilocular type of ZACD was more prevalent in the scrutinies done by Patil et al. (2012) and Yavuz et al. (2009). This contradicts the surveys done by Gupta et al. (2013) and Arora et al. (2016), where the unilateral, unilocular (Fig. 5, unilocular ZACD in CBCT images) type was more prevalent, whereas the study by Tyndall and Matteson (1987) gave an equal number of variations. This imbalance in the demonstration of the ZACD in various studies calls for more standardized scientific exploration with CBCT.

Occurrence of pneumatization might be an incidental finding as a routine anatomic variant, but is critical in the planning of surgeries of the temporomandibular joint. Recurrent temporomandibular joint disease could be the result of extensive pneumatization and spread of infection.

An extensive knowledge of pneumatization of Zygomatic air cells is important in understanding the inflammatory process in the lateral skull base.

In-depth comprehension of the anatomy and development of the zygomatic process of the temporal bone is a prerequisite in understanding the pathology of lateral skull base diseases. In addition, there are lot of studies about ZACD, PAT, and PGRF, but not a comprehensive inquiry. In some studies, the terms are interchangeable, but a precise demarcation is the need of the hour. Additionally, it is a quintessential guide for surgery on temporomandibular joint disorders. CBCT is an identifiable implement in scrutinizing

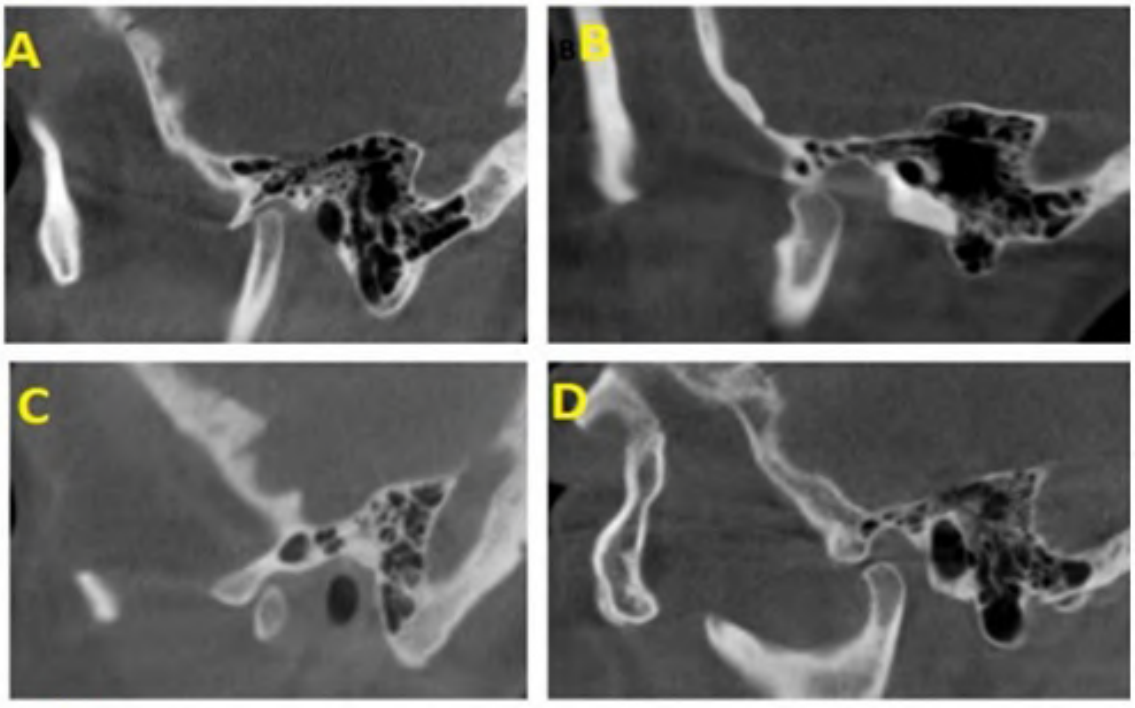

Fig. 4.- Multilocular ZACD in CBCT images.

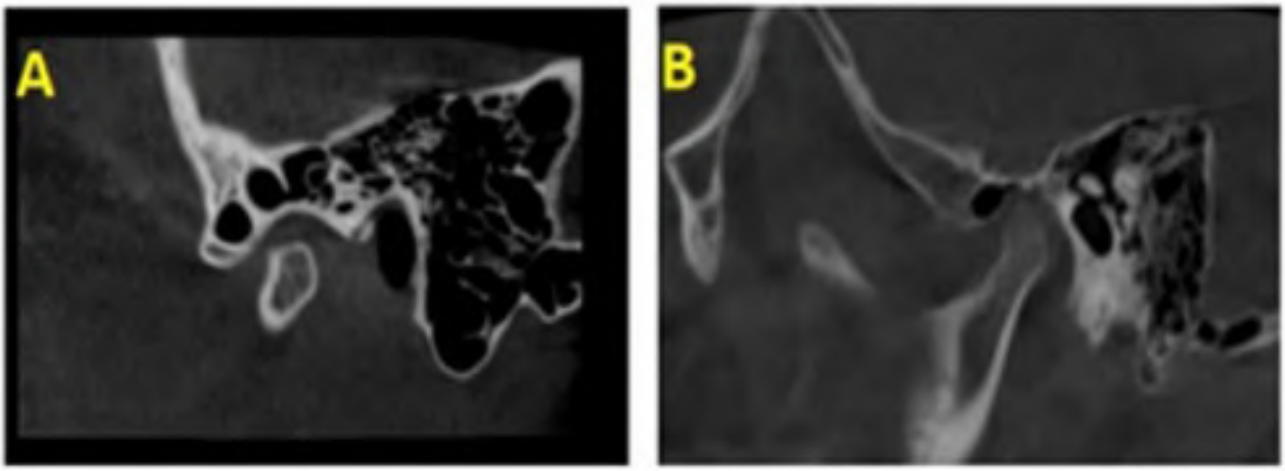

Fig. 5.- Unilocular ZACD in CBCT images.

the anatomical structures of the maxillofacial region by virtue of its inherent qualities. This study highlights the importance of further research on the prevalence of the ZACD on CBCT, which was exiguous in the past, and compares with similar studies done using panoramic radiographs; it also paves the way for more studies employing CBCT to justify the findings we have expressed.

DECLARATIONS

Ethical Approval: Ethics are upheld in conformity with the 1964 Helsinki Declaration and its following revisions Prior to the investigation, an ethical clearance was obtained by the university's IEC (IEC No 26/2021). (JSS DENTAL COLLEGE AND HOSPITAL INSTITUTIONAL ETHICAL COMMITTEE). Informed consent taken from all the participants involved in the study.

Availability of Data and Materials: The complete data base pertaining to the study is preserved as electronic database with the corresponding author and can be retrieved at any point of time.

ACKNOWLEDGEMENTS

We are grateful to all the patients who gave us written consent to compile this scientific typescript and to herald the same. We wouldlike to thank our co-workers for helping us with this project.

REFERENCES

ARORA KS, KAUR P, KAUR K (2016) ZACD: a retrograde panoramic analysis among Indian population with new system of classification. *J Clin Diagn Res*, 10(1): ZC71.

CARTER LC, HALLER AD, CALAMEL AD, PFAFFENBACH AC (1999) Zygomatic air cell defect (ZACD). Prevalence and characteristics in a dental clinic outpatient population. *Dentomaxillofac Radiol*, 28(2): 116-122.

DE REZENDE BARBOSA G, NASCIMENTO MDO C, LADEIRA DB, BOMTORIM VV, DA CRUZ AD, ALMEIDA SM (2014) Accuracy of digital panoramic radiography in the diagnosis of temporal bone pneumatization: a study in vivo using cone-beam computed tomography. *J Craniomaxillofac Surg*, 42(5): 477-481.

DIAMANT M (1954) Size variation of the mastoid air cell system according to Wittmaack, Schwarz and Diamant. *Acta Oto-Laryngologica*, 43(suppl 118): 54-67.

GUPTA D, SHEIKH S, PALLAGATTI S, AGGARWAL A, GOYAL G, CHIDANANDAPPA RN, PARNAMI P (2013) Zygomatic air cell defect: a panoramic radiographic study of a North Indian population. *J Invest Clin Dentistry*, 4(4): 247-251.

MILOGLU O, YILMAZ AB, YILDIRIM E, AKGUL HM (2011) Pneumatization of the articular eminence on cone beam computed tomography: prevalence, characteristics and a review of the literature. *Dentomaxillofac Radiol*, 40(2): 110-114.

PARK YH, LEE SK, PARK BH, SON HS, CHOI M, CHOI KS, AN CH (2002) Radiographic evaluation of the zygomatic air cell defect. *Imag Sci Dentistry*, 32(4): 207-211.

PATIL K, MAHIMA VG, MALLESHI SN, SRIKANTH HS (2012) Prevalence of zygomatic air cell defect in adults—a retrospective panoramic radiographic analysis. *Eur J Radiol*, 81(5): 957-959.

TREMBLE GE (1934) Pneumatization of the temporal bone. *Arch Otolaryngol*, 19(2): 172-182.

TYNDALL DA, MATTESON SR (1985) Radiographic appearance and population distribution of the pneumatized articular eminence of the temporal bone. *J Oral Maxillofac Surg*, 43(7): 493-497.

TYNDALL DA, MATTESON SR (1987) The zygomatic air cell defect (ZACD) on panoramic radiographs. *Oral Surg, Oral Med, Oral Pathol*, 64(3): 373-376.

YAVUZ MS, ARAS MH, GÜNGÖR H, BÜYÜKKURT MC (2009) Prevalence of the pneumatized articular eminence in the temporal bone. *J Craniomaxillofac Surg*, 37(3): 137-139.

The possible ameliorative effects of vitamin E against cisplatin-induced injury on adult rat liver and testes

Sally M.M.H. Omar[1], Marwa M.A. Ahmed[2], Ola A.E-S.M. Khalil[1], Marwa M. Mady[1]

[1] Department of Anatomy and Embryology, Faculty of Medicine, Alexandria University, Alexandria, Egypt

[2] Pathology Department, Faculty of Medicine, Alexandria University, Alexandria, Egypt

SUMMARY

Cisplatin is one of the most potent cytotoxic drugs used to treat cancer, but clinical use is linked to testicular and liver damage. According to a number of studies, antioxidant supplementation may have an impact on the toxicity caused by cisplatin. The purpose of the current investigation was to determine how vitamin-E supplementation protected rats from cisplatin-induced damage. Thirty laboratory adult male albino rats were divided into three groups: Group I received saline orally, once daily for 21 days. Group II received cisplatin on day 0, 7, 14 and were sacrificed on day 21. Group III received cisplatin on day 0, 7, 14 and received orally vitamin E daily, starting 5 days before the first dose of cisplatin until day 21. Liver and both testes were obtained and fixed. Sections from the liver and both testes were stained by H&E and Trichrome stain, and then examined under light microscope.

Alterations included a significant increase in malondialdehyde (MDA) level in the cisplatin group compared with the other groups (p value for comparing between control and each other group, statistically significant at $p \leq 0.05$). Histopathologically, cisplatin induced signs of hepatic injury; it also showed signs of testicular degeneration in all rats. However, the cisplatin induced disturbances significantly improved by treatment with Vitamin E. Statistical analysis showed a significant difference among the three groups in all signs of injury ($p<0.001$). According to this research, cisplatin has a toxic impact on the liver and testicles, and when it is administered along with vitamin E, a noticeable improvement is seen.

Key words: Cisplatin – Liver – Testes – Vitamin E – Oxidative stress

INTRODUCTION

One of the most powerful anticancer medications is cisplatin (cis-diammine dichloroplatinum II CDDP). It is a successful anti-cancer drug used to treat a variety of malignancies, including ovarian, gastric, pulmonary, head-and-neck, prostate, bladder, and cervical cancers, lymphoma, and osteosarcoma (Lirdi et al.,2008; Roldan-Fidalgo et al., 2016). Cisplatin is frequently used to treat cancer, either alone or in combination with other medications (Pectasides et al., 2009; Takeshita et al., 2013).

Corresponding author:
Dr. Sally Mahmoud Mohamed Hussein Omar. Department of Anatomy and Embryology, Faculty of Medicine, Alexandria University, Alexandria, Egypt. E-mail: saliy.hessen@alexmed.edu.eg - ORCID ID: 0000-0001-6601-4243

Submitted: October 2, 2022. **Accepted:** December 24, 2022

https://doi.org/10.52083/PUIH6269

By enabling a covalent bond between purine bases and the platinum molecule, which causes G2 cell cycle arrest and initiates death, cisplatin produces its lethal action through contact with DNA (Pil et al.,1992).

CDDP has a number of toxic side effects, including ototoxicity, nephrotoxicity, myelotoxicity, and gastrointestinal toxicity, as well as serious side effects affecting the neurologic, hematologic, and reproductive systems, despite having promising results, particularly in the treatment of testicular cancer (Beytur et al., 2012; Kaya et al., 2015). One of the cisplatin side effects that is frequently observed is long-lasting testicular dysfunction (Colpi et al., 2004). Due to the high rate of spermatogenic cell proliferation in the testis, the adverse effects of chemotherapy on the testis may be severe and irreversible, resulting in the death of spermatogenic cells during the process of spermatogenesis and changes in the sperm DNA, which may result in oligozoospermia, azoospermia, or even prolonged sterility (Ekinci Akdemir et al 2019).

When Cisplatin is used at large dosages, liver damage might ensue (Santos et al., 2007; Martins, 2008). Signs of harm are present in the abnormalities in liver function brought on by cisplatin. Cisplatin can deplete reduced glutathione (GSH) and produce reactive oxygen species (ROS), (Yilmaz et al., 2004; Wozniak et al., 2004) which can cause tissue damage through reactions with cellular macromolecules such as proteins, nucleic acids, and lipids, leading to cell injury and death, despite the paucity of information on the underlying mechanisms causing its hepatotoxic effect (Halliwell, 2006). Strengthening intracellular survival pathways is the key to protection against cisplatin-induced testicular injury. Studies have shown that antioxidant compounds protect against the damage caused by cisplatin (Kaya et al., 2015; Anand et al., 2015). Alpha-tocopherols like vitamin E have the strongest antioxidant action. It is a crucial non-enzymatic antioxidant defense system that can only be supplied by food or supplementation, and it performs a wide range of biological tasks including enzymatic activity, gene regulation, and platelet aggregation inhibition (Schneider, 2005; Villacorta et al., 2003; Atkinson et al., 2008). Due to its lipophilic action, vitamin E is found in the membrane-rich cell components and is a membrane-specific antioxidant. It possesses anticancer, cardiovascular, neurological, anti-diabetic, osteoprotective, immunomodulatory, and gastroprotective properties (Aggarwal et al., 2010). As a very potent antioxidant, it forms the first defense line that protects unsaturated fatty acids in the structure of phospholipids from the effects of free radicals. It removes the lipid peroxyl radicals, and terminates lipid peroxidation chain reactions. Therefore, it is also known as chain-breaking antioxidant (Aggarwal et al., 2010).

Since it is a very potent antioxidant, it works as the first line of defense against the effects of free radicals for the unsaturated fatty acids contained in the structure of phospholipids. Lipid peroxidation is stopped in its tracks by the elimination of the lipid peroxyl radicals. The phrase "chain-breaking antioxidant" is another term for it (Abdel-Daim et al., 2018; Ourique et al., 2016).

In this study, we aim to investigate the role of Vitamin-E in the protection against cisplatin-induced liver and testes injury. The aim of the current study was to examine the protective effects of vitamin E against Cisplatin induced liver and testes injury in adult albino rat.

MATERIALS AND METHODS

Chemicals

Cisplatin was used in a 1 mg/ml intravenous infusion (Cisplatin Mylan Pharma 1 mg/ml solution à diluer pour perfusion). Vitamin E was purchased as soft gelatin capsules from PHARCO pharmaceuticals Company, Egypt. Each capsule contained 400mg of vitamin E.

Experiment animals

Thirty laboratory adult male albino Wistar rats, 7-9 weeks old. Each of 180-220 g average weight were obtained from the Animal house center, Faculty of Medicine, Alexandria University. The animals were allowed to acclimatize for two weeks before the experiment. The animals were maintained under standard laboratory conditions of temperature, humidity and 12 hours light/dark cycle. First injection of cisplatin is considered as day 0.

Experimental design

Male albino rats were randomly separated into three equal groups of ten each. Group I (control group) received saline (the vehicle) orally, once daily for 21 days. Group II (Cisplatin group) received cisplatin (single dose of 6.5 mg/kg intraperitoneal) on day 0, 7, 14 and were sacrificed on day 21. Group III received cisplatin (single dose of 6.5 mg/kg intraperitoneal) on day 0, 7, 14 and then received orally by gavage vitamin E at a dose of 100 mg/kg body weight daily, starting 5 days before first dose of cisplatin till day 21. They were sacrificed on day 21 (Li et al., 2020; Moneim et al., 2019; Park et al., 2012; Erdemli et al.,2019).

Estimation of malondialdehyde (MDA)

At the end of the 21-day period, the animals were then sacrificed, and the liver and testes tissues were removed. MDA levels in the liver and testes tissues homogenate were measured. The measured outcomes were presented as MDA nmol/g tissue (Biochemistry lab, El Mowasah, Faculty of Medicine, Alexandria University).

Preparation of tissue homogenates

1. Prior to dissection, perfuse tissue with a PBS (phosphate buffered saline) solution, PH 7.4 containing 0.16 mg/ ml heparin to remove any red blood cells and clots.
2. Homogenize the tissue in 5-10 ml cold buffer (i.e, 50 mM potassium phosphate, PH 7.5) per gram tissue.
3. Centrifuge at 4000r.p.m for 15 minutes.
4. Remove the supernatant for essay and store on ice. If not assaying on the same day, freeze the sample at -80C. The sample will be stable for at least one month (Satoh, 1978; Ohkawa et al., 1979).

Histopathological investigations

At the end of the experiment, the animals were sacrificed by decapitation under mild anesthesia using 50 mg/kg of sodium pentobarbital. The liver and both testes were obtained and fixed in 10% neutral buffered formalin and Bouin's solution respectively. Ascending grades of ethanol (70%, 90% and 100%) were used for dehydration, followed by clearing in xylene. Embedding was done using soft and hard paraffin. The resulting paraffin blocks were sectioned at a thickness of 5-7 micrometers, using a rotatory microtome, then cut and immersed in xylene for dewaxing, followed by descending grades of ethanol (100%, 90% and 70%) for rehydration. Sections from the liver and both testes were stained by Harris Hematoxylin & Eosin (H&E) and Masson Trichrome stain. All sections were examined under light microscope (Olympus CX23).

Sections from the liver were examined for signs of hepatic injury including feathery degeneration, lytic necrosis, portal inflammation, congestion, and cholestasis. Portal expansion and fibrosis were assessed by Masson Trichrome.

The testes were examined for signs of degeneration of the seminiferous tubules. The spermatogenesis was assessed, and the following was recorded whenever encountered: 1) Active spermatogenesis; 2) Maturation arrest; 3) Germ cell aplasia.

Statistical analysis of the data

Data were uploaded to the computer and analyzed using IBM SPSS software package, version 20.0. (Armonk, NY: IBM Corp). For continuous data, they were tested for normality by the Shapiro-Wilk test. Quantitative data were expressed as range (minimum and maximum), mean, standard deviation and median. ANOVA was used for comparing the three studied groups, followed by Post Hoc test (Tukey) for pairwise comparison. Significance of the obtained results was judged at the 5% level.

RESULTS

MDA Measurement

The changes in the MDA are shown in Table 1, Fig. 1. The MDA concentrations in the tissues were used as an index of lipid peroxidation. The MDA levels in the liver and testes tissue were significantly higher in the cisplatin-treated group when compared to control group. On the other hand, it was observed that the MDA levels in liver and testes tissue significantly decreased in cisplatin and Vitamin E-treated rats compared to the cisplatin group. These data were consistent with the histopathological findings.

Table 1. Comparison between the three studied groups according to MDA in tissue homogenate.

MDA in Tissue homogenate (nmol/g)	Group I (n = 10)	Group II (n = 10)	Group III (n = 10)	F (p)	Significance between groups
Liver					
Mean ± SD	57.8 ± 10.3	207 ± 42.7	113 ± 13.3	80.925* (<0.001*)	p_1<0.001*, p_2<0.001*, p_3<0.001*
Median (Min – Max)	56 (44 – 76)	197 (155 – 287)	112 (95 – 131)		
Testes					
Mean ± SD	57.5 ± 11.4	170 ± 37.8	75 ± 17.1	59.461* (<0.001*)	p_1<0.001*, p_2=0.274, p_3<0.001*
Median (Min – Max)	57.5 (40 – 78)	170 (112 – 222)	75 (51 – 101)		

SD: **Standard deviation**
F: **F for One way ANOVA test**, Pairwise comparison between each 2 groups was done using **Post Hoc Test (Tukey)**
p: p value for comparing between the three studied groups
p_1: p value for comparing between **Control** and **Cisplatin**
p_2: p value for comparing between **Control** and **Vitamin E**
p_3: p value for comparing between **Cisplatin** and **Vitamin E**
*: Statistically significant at p ≤ 0.05

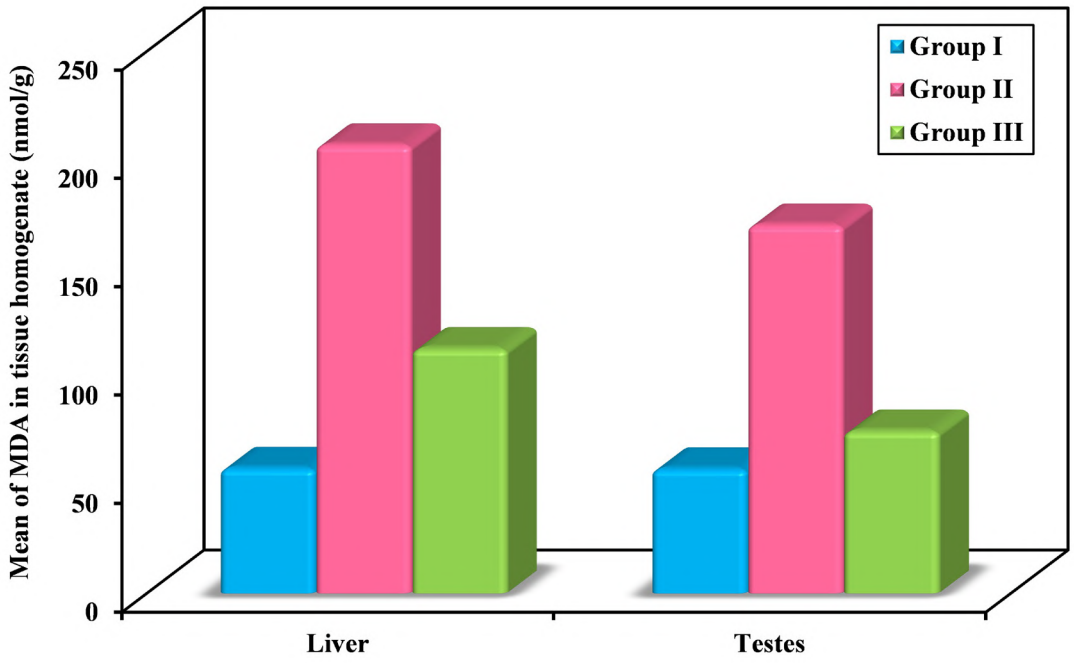

Fig. 1.- Comparison between the three studied groups according to MDA in tissue homogenate.

Histological findings

Liver:

Group I showed preservation of the hepatic architecture without detectable fibrosis or inflammation. Neither cholestasis nor congestion was observed (Fig. 2a, b).

Group II showed signs of hepatic injury including congestion in 4/10 rats (40%), feathery degeneration in 7/10 rats (70%), lytic necrosis in 5/10 rats (50%), cholestasis in 5/10 rats (50%), and portal inflammation in 3/10 rats (30%). Trichrome stain revealed portal expansion in 4/10 rats (40%) and bridging fibrosis in 4/10 rats (40%) (Fig. 2c-g).

Group III showed a remarkable improvement whereby neither lytic necrosis nor cholestasis were detected in any of the rats (0%). Trichrome stain revealed neither portal nor bridging fibrosis in all rats (0%). However, congestion and feathery degeneration were detected in 7/10 rats (70%) and portal inflammation was detected in 6/10 rats (60%) (Fig. 2h, i).

Statistical analysis showed a significant difference among the three groups according to signs of liver injury (Table 2, Fig. 3).

Testis:

Group I The seminiferous tubules showed normal morphology with active spermatogenesis (Fig. 4a).

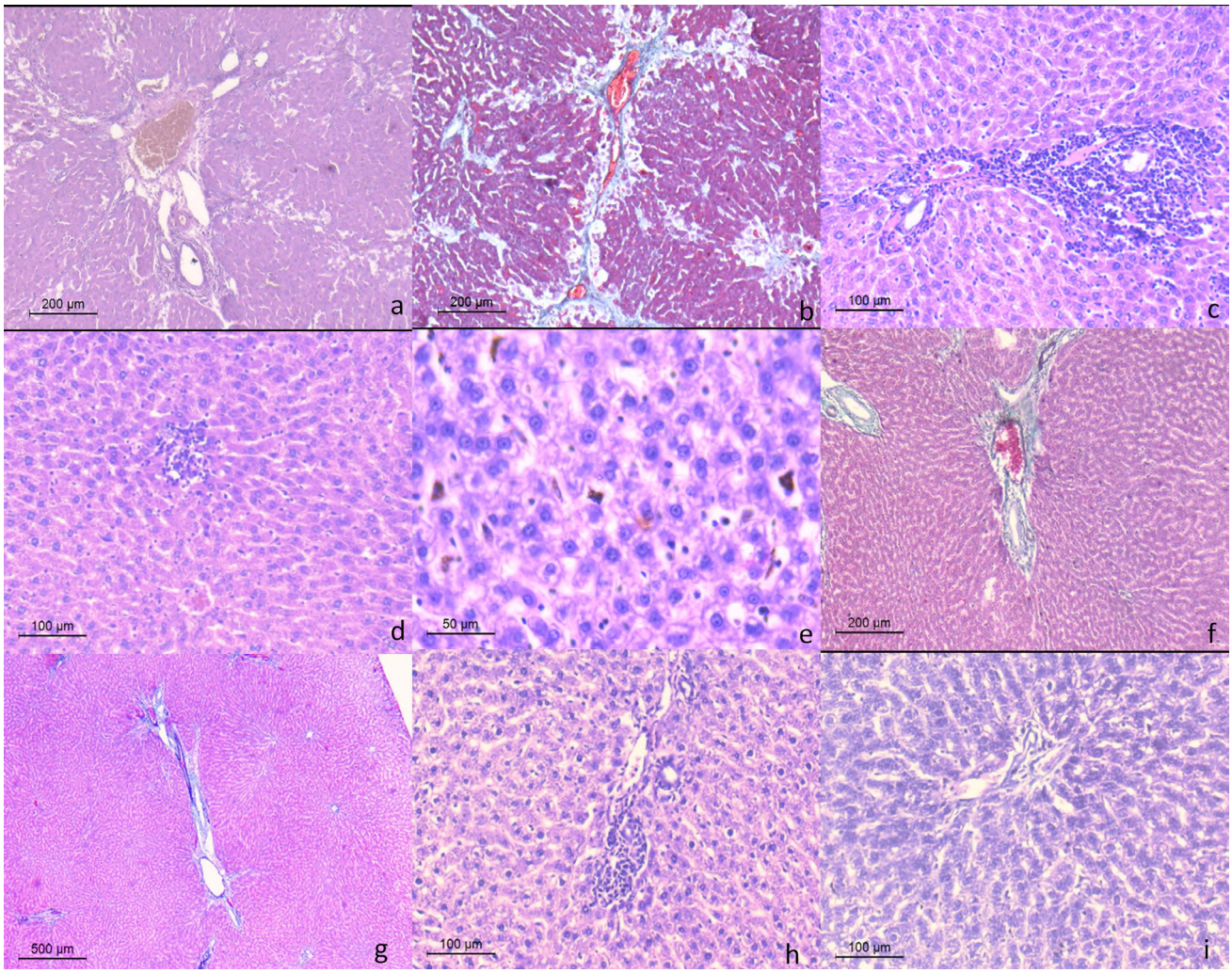

Fig. 2.- Group I (control rats) shows preserved hepatic architecture with no signs of injury (**a:** H&E) and no fibrosis (**b:** Trichrome). Group II (rats receiving cisplatin) shows portal inflammation (**c:** H&E), lytic necrosis (**d:** H&E), feathery degeneration and cholestasis (**e:** H&E), portal expansion and fibrosis (**f:** trichrome) and bridging fibrosis (**g:** Trichrome). Group III (rats receiving Cisplatin + vitamin E) shows portal inflammation and feathery degeneration (**h:** H&E) but no portal fibrosis (**i:** trichrome). p: p value for comparing between the studied groups; *****: Statistically significant at $p \leq 0.05$. Scale bars: a, b, f = 200 µm; c, d, h, i = 100 µm; e = 50 µm; g = 500 µm.

Table 2- Comparison between the three studied groups according to signs of liver injury.

Parameter	Group I (n=10)	Group II (n=10)	Group III (n=10)	χ^2	^{MC}p
Congestion	0 (0.0%)	4 (40.0%)	7 (70.0%)	11.101*	0.006*
Feathery degeneration	0 (0.0%)	7 (70.0%)	7 (70.0%)	14.040*	0.001*
Lytic necrosis	0 (0.0%)	5 (50.0%)	0 (0.0%)	9.441*	0.006*
Cholestasis	0 (0.0%)	5 (50.0%)	0 (0.0%)	9.441*	0.006*
Portal inflammation	0 (0.0%)	3 (30.0%)	6 (60.0%)	8.622*	0.017*
Portal expansion (Tri)	0 (0.0%)	4 (40.0%)	0 (0.0%)	6.876*	0.022*
Bridging fibrosis (Tri)	0 (0.0%)	4 (40.0%)	0 (0.0%)	6.876*	0.022*

χ^2: **Chi square test**; MC: **Monte Carlo**
p: p value for comparing between the studied groups
*: Statistically significant at $p \leq 0.05$

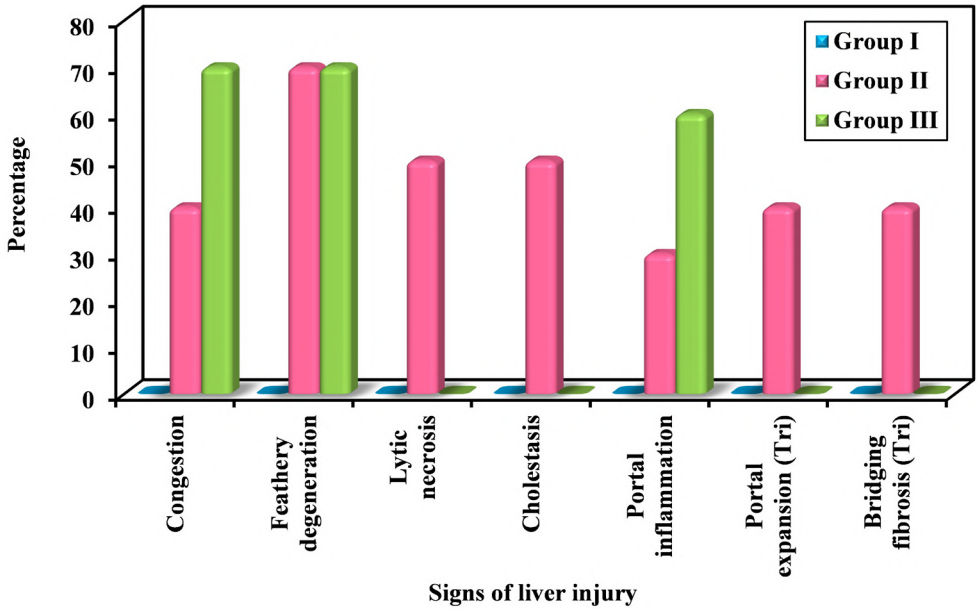

Fig. 3.- Comparison between the three studied groups according to signs of liver injury.

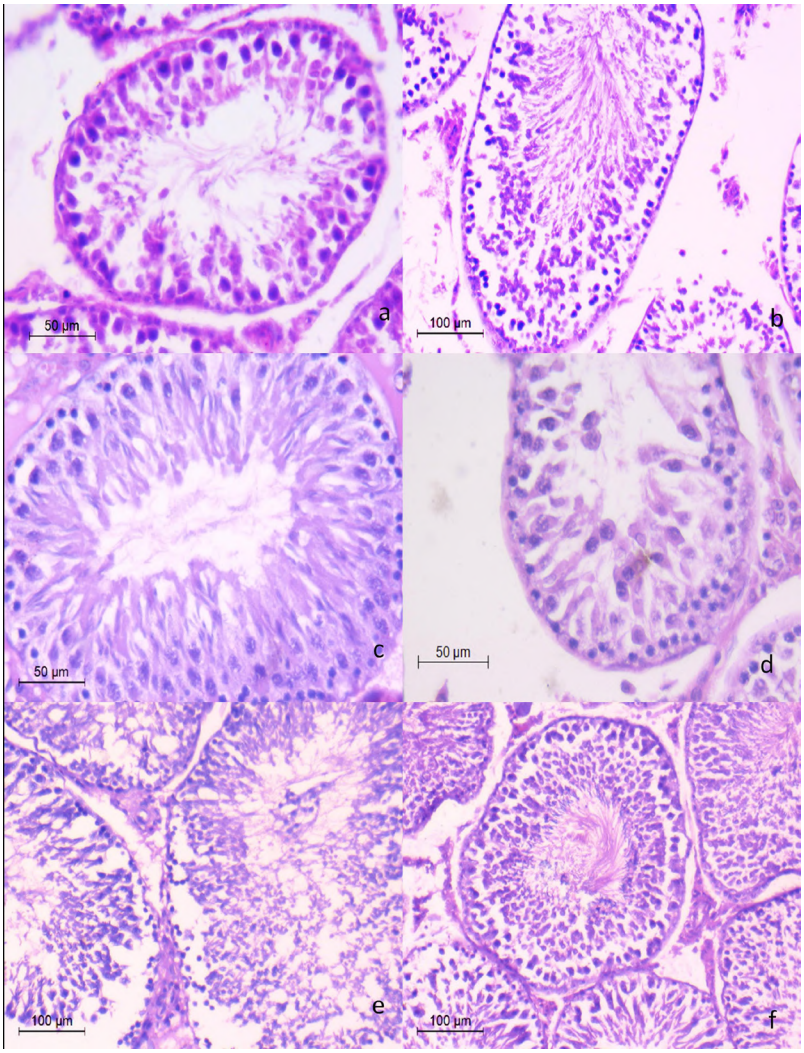

Fig. 4.- Group I (control rats) shows active spermatogenesis without degeneration (**a:** H&E). Group II (rats receiving cisplatin) shows degeneration (**b**), germ cell aplasia with only Sertoli cells and no spermatogonia (**c**), maturation arrest with spermatogonia, primary spermatocytes and Sertoli cells (**d**) and active spermatogenesis (**e**). Group III (rats receiving Cisplatin + vitamin E) showing active spermatogenesis without degeneration (**f**: H&E). p: p value for comparing between the studied groups; *: Statistically significant at $p \leq 0.05$. Scale bars: a, c, d = 50 µm; b, e, f = 100 µm.

Table 3.- Comparison between the three studied groups according to signs of testicular injury.

Parameter	Group I (n=10)	Group II (n=10)	Group III (n=10)	χ^2	^{MC}p
Degeneration	0 (0.0%)	10 (100.0%)	0 (0.0%)	30.262*	<0.001*
Spermatogenesis	10 (100.0)	1 (10.0%)	10 (100.0%)	24.286*	<0.001*
Maturation arrest	0 (0.0%)	6 (60.0%)	0 (0.0%)	12.377*	0.001*
Germ cell aplasia	0 (0.0%)	4 (40.0%)	0 (0.0%)	6.876*	0.022*

χ^2: **Chi square test**; MC: **Monte Carlo**
p: p value for comparing between the studied groups
*: Statistically significant at $p \leq 0.05$

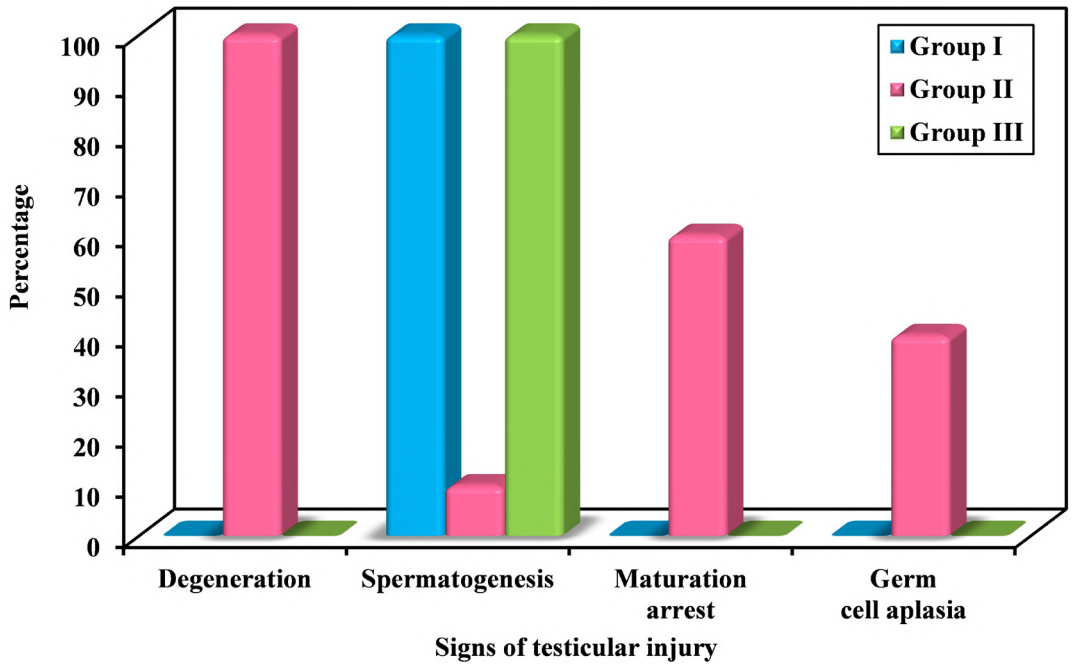

Fig. 5.- Comparison between the three studied groups according to signs of testicular injury.

Group II showed signs of degeneration in all rats (100%). Active spermatogenesis was detected in only one rat (10%), maturation arrest was seen in 6 rats (60%) while germ cell aplasia with only Sertoli cells seen lining the seminiferous tubules was found in 4 rats (40%) (Fig. 4b-e).

Group III showed a remarkable histological improvement without any signs of degeneration in any of the 10 rats (0%) and active spermatogenesis in all 10 rats (100%) (Fig. 4f).

Statistical analysis showed a significant difference among the three groups with degeneration and active spermatogenesis showing the highest significance ($p<0.001$, Monte Carlo significant test) (Table 3, Fig. 5).

DISCUSSION

One of the very efficient chemotherapy medications used to treat many cancer types is cisplatin. However, due to its numerous severe side effects, its clinical application is limited. [1] Sertoli cells, interstitial Leydig cells, seminiferous tubule epithelium, and notably germ cells are the main targets of its toxic effects on the male reproductive system and liver (Boekelheide, 2005). Because of this, avoiding cisplatin side effects is crucial, and there is ongoing discussion on how to do so when using the drug in clinical settings.

Cisplatin has been especially interesting since it has shown anticancer activity in a variety of tumors. It was discovered to have cytotoxic prop-

erties in the 1960s, and by the end of the 1970s it had earned a place as the key ingredient in the systemic treatment of germ cell cancers. Among many chemotherapy drugs that are widely used for cancer, Cisplatin is one of the most compelling ones. It was the first FDA-approved platinum compound for cancer treatment in 1978 (Kelland, 2007). This has led to interest in platinum (II) - and other metal-containing compounds as potential anticancer drugs (Frezza et al., 2010).

As compared with gemcitabine alone, cisplatin plus gemcitabine was associated with a significant survival advantage without the addition of substantial toxicity. Cisplatin plus gemcitabine is an appropriate option for the treatment of patients with advanced biliary cancer (Valle et al., 2010).

In this study, it has been detected that cisplatin-induced signs of testicular degeneration, maturation arrest, germ cell aplasia with only Sertoli cells and no spermatogonia. Also cisplatin-induced liver changes such as portal inflammation, feathery degeneration and cholestasis, which matched the results of many other studies (Beytur et al,. 2012; Ateşşahin et al., 2006b; Custódio et al., 2009; Iraz et al., 2006).

Oxidative stress is brought on by reactive oxygen species, which can form naturally as a consequence of metabolism, or more commonly as a result of ischemia situations, radiation, inflammation, ageing, chemicals, medicines, and exposure to electromagnetic fields. Oxidative stress targets DNA double-bond bases, as well as protein and lipid double-bond groups that contain double-bonds. As a result, macromolecules such as intracellular lipid, protein, and DNA are harmed, and cellular injury-induced apoptosis takes place (Yan, 2014). Testes are one among the organs that oxidative stress targets, since they have higher levels of polyunsaturated membrane lipids than other tissues (Beytur et al., 2012). Therefore, oxidative chemicals like cisplatin commonly affect the testes. However, due to their lower circulatory supply and low oxygen pressures, testes may still protect themselves from oxidative damage, albeit to a lesser extent. The testes are given the capacity to resist oxidative stress because of this situation (Aitken and Roman, 2008).

After developing oxidative damage from a variety of causes, such as radiation therapy, varicocele, chemotherapy, torsion, infections, and smoking, testicular tissue and spermatogenesis are hindered. Numerous investigations have shown that cisplatin causes harmful alterations in testicular tissue. Additionally, in our investigation, testes from the rats that received cisplatin showed signs of histological damage: this was consistent with a number of investigations (Fazile et al., 2019; Ateşşahin et al., 2006a; Alves Favareto et al., 2011; Schweyer et al., 2004). Additionally, it has been shown that cisplatin treatment causes alterations in the liver; this was consistent with a number of investigations (Custódio et al., 2009; Iraz et al., 2006; Nazıroglu et al., 2004).

These findings revealed that lipid peroxidation and free radical production were involved. Cisplatin causes lipid peroxidation and produces ROS, such such superoxide anion and hydroxyl radicals (Halliwell and Gutteridge, 1999). It is accepted that both are related to oxidative stress and lead to an imbalance between the capacity of the organism's antioxidant system and the production of oxygen-derived radicals. The administration of cisplatin has been linked in several studies to enhanced free radical production and significant oxidative stress (Antunes et al., 2001; Mora et al., 2003). The natural equilibrium between radical creation and defence against them in cells is upset as a result of an increase in free radical formation in cisplatin-induced toxicity (Conklin, 2000). As a result, proteins, lipids, and nucleic acids will sustain oxidative damage (Packer et al., 1990).

Various methods have been suggested to reduce the toxicity caused by cisplatin. The development of treatments to stop the production of free radicals may affect the development of oxidative renal damage as well as the emergence of acute renal damage brought on by cisplatin. Supplementing with natural vitamin E makes it simple and safe to enhance its levels in tissues. In this study, we looked at how vitamin E affected cisplatin-treated rats (Packer et al., 1990).

The present study has indicated that treatment with vitamin E may have protective effects against cisplatin-induced testicular degeneration. This condition was demonstrated by remarkable improvement by

analyses of general histological images of hematoxylin-eosin stained sections of testicular tissue.

According to reports, vitamin E includes tocopherol, tocotrienol, and free radical scavengers and reduces the toxicity of endothelial cells and nephrotoxicity caused by cisplatin (Aggarwal et al., 2010; Paksoy et al., 2011). In addition, vitamin E serves as a potential inhibitor of lipid peroxidation reactions and guards against free radical damage to the fatty acids that make up unsaturated phospholipid membranes (Paksoy et al., 2011; Villani et al., 2016). Kalkanis et al. (2004) found that vitamin-E supplementation reduced the toxicity of cisplatin in rats. Our study's findings are corroborated by a previous study that found dexamethasone and vitamin E supplements to be particularly beneficial in reducing the negative effects of cisplatin therapy (Paksoy et al., 2011).

In our study, where we investigated protective effects of vitamin E in cisplatin-induced toxicity, we detected that these antioxidant molecules alleviated cellular injuries induced by cisplatin administration, which was similar to the results of other studies (Soyalıç et al., 2016; De Freitas et al., 2009). Based on this literature information, we can say that vitamin E may ameliorate damage caused by cisplatin thanks to its antioxidant, free-radical scavenger and similar activities.

CONCLUSION

Based on biochemical and histological analyses, the overall results of this study demonstrated that CDDP caused damage to the liver and testicles. Vitamin E supplementation provided excellent adverse effect prevention in addition to concurrent treatment for CDDP. In order to stop CPPD-induced damage and oxidative stress from continuing, vitamin E may act as an antioxidant by scavenging free radicals.

Ethical approval

The present study was approved by the Ethical guidelines of Alexandria University on laboratory animals and the national institute for the care and use of laboratory animals. Further the Alexandria Faculty of Medicine ethical committee approval was obtained.

REFERENCES

ABDEL-DAIM MM, ABDEEN A (2018) Protective effects of rosuvastatin and vitamin E against fipronil-mediated oxidative damage and apoptosis in rat liver and kidney. *Food Chem Toxicol*, 114: 69-77.

AGGARWAL BB, SUNDARAM C, PRASAD S, KANNAPPAN R (2010) Tocotrienols, the vitamin E of the 21st century: its potential against cancer and other chronic diseases. *Biochem Pharmacol*, 80: 1613-1631.

AITKEN RJ, ROMAN SD (2008) Antioxidant systems and oxidative stress in the testes. *Oxid Med Cell Longev*, 1: 15-24.

ALVES FAVARETO AP, DAL BIANCO FERNANDEZ C, FOSSATO DA SILVA DA, ANSELMO-FRANCI JA, DE GRAVA KEMPINAS W (2011) Persistent impairment of testicular histology and sperm motility in adult rats treated with cisplatin at peri-puberty. *Basic Clin Pharmacol Toxicol*, 109(2): 85-96.

ANAND H, MISRO MM, SHARMA SB, PRAKASH S (2015) Protective effects of Eugenia jambolana extract versus N-acetyl cysteine against cisplatin-induced damage in rat testis. *Andrologia*, 47: 194-208.

ANTUNES LMG, DARIN JDC, BIANCHI M DE LP (2001) Effects of the antioxidants curcumin or selenium on cisplatin-induced nephrotoxicity and lipid peroxidation in rats. *Pharmacol Res*, 43: 145-150.

ATEŞŞAHIN A, SAHNA E, TÜRK G, CERIBAŞI AO, YILMAZ S, YÜCE A, BULMUŞ O (2006a) Chemoprotective effect of melatonin against cisplatin-induced testicular toxicity in rats. *J Pineal Res*, 41: 21-27.

ATEŞŞAHIN A, KARAHAN I, TÜRK G, GÜR S, YILMAZ S, CERIBAŞI AO (2006b) Protective role of lycopene on cisplatin-induced changes in sperm characteristics, testicular damage and oxidative stress in rats. *Reprod Toxicol*, 21(1): 42-47.

ATKINSON J, EPAND RF, EPAND RM (2008) Tocopherols and tocotrienols in membranes: a critical review. *Free Radic Biol Med*, 44(5): 739-764.

BEYTUR A, CIFTCI O, OGUZ F, OGUZTURK H, YILMAZ F (2012) Montelukast attenuates side eVects of cisplatin including testicular, spermatological, and hormonal damage in male rats. *Cancer Chemother Pharmacol*, 69(1): 207-213.

BOEKELHEIDE K (2005) Mechanisms of toxic damage to spermatogenesis. *J Natl Cancer Inst Monogr*, 34: 6-8.

COLPI GM, CONTALBI GF, NERVA F, SAGONE P, PIEDIFERRO G (2004) Testicular function following chemo-radiotherapy. *Eur J Obstet Gynecol Reprod Biol*, 113(Suppl 1): S2-6.

CONKLIN KA (2000) Dietary antioxidants during cancer chemotherapy: impact on chemotherapeutic effectiveness and development of side effects. *Nutr Cancer*, 37: 1-18.

CUSTÓDIO JBA, CARDOSO CMP, SANTOS MS, ALMEIDA LM, VICENTE JAF, FERNANDES MAS (2009) Cisplatin impairs rat liver mitochondrial functions by inducing changes on membrane ion permeability: Prevention by thiol group protecting agents. *Toxicology*, 259(1-2): 18-24.

DE FREITAS MR, FIGUEIREDO AA, BRITO GA, LEITAO RF, CARVALHO JUNIOR JV, GOMES JUNIOR RM, DE ALBURQUERQUE RIBEIRO R (2009) The role of apoptosis in cisplatin-induced ototoxicity in rats. *Braz J Otorhinolaryngol*, 75: 745-752.

EKINCI AKDEMIR FN, YILDIRIM S, KANDEMIR FM, AKSU EH, GULER MC, OZMEN HK, KUCUKLER S, ESER G (2019) The antiapoptotic and antioxidant effects of eugenol against cisplatin-induced testicular damage in the experimental model. *Andrologia*, 51(9): e13353.

ERDEMLI ME, ERDEMLI Z, TURKOZ Y, BAG HG, SELAMOGLU Z (2019) The effects of acrylamide and vitamin E administration during pregnancy on adults' ovarian tissue: An experimental study. *Ann Med Res*, 26(9): 1856-1860.

FAZILE NEA, YILDIRIM S, KANDEMIR FM, AKSU EH, GULER MF, OZMEN HK, KUCUKLER S, ESER G (2019) The antiapoptotic and antioxidant effects of eugenol against cisplatin-induced testicular damage in the experimental model. *Andrologia*, 51(9): e13353.

FREZZA M, HINDO S, CHEN D, DAVENPORT A, SCHMITT S, TOMCO D, DOU QP (2010) Novel metals and metal complexes as platforms for cancer therapy. *Curr Pharm Des*, 16: 1813-1825.

HALLIWELL B (2006) Reactive species and antioxidants: redox biology is a fundamental theme of aerobic life. *Plant Physiol*, 141: 312-322.

HALLIWELL B, GUTTERIDGE JMC (1999) Lipid peroxidation: a radical chain reaction. In: Halliwell B, Gutteridge JMC (Eds.) *Free radicals in biology and medicine*. Clarendon Press, Oxford, UK, pp 188-276.

IRAZ M, OZEROL E, GULEC M, TASDEMIR S, IDIZ N, FADILLIOGLU E, NAZIROGLU M, AKYOL O (2006) Protective effect of caffeic acid phenethyl ester (CAPE) administration on cisplatin-induced oxidative damage to liver in rat. *Cell Biochem Funct*, 24: 357-361.

KALKANIS JG, WHITWORTH C, RYBAK LP (2004) Vitamin E reduces cisplatin ototoxicity. *Laryngoscope*, 114: 538-542.

KAYA K, CIFTCI O, CETIN A, DOGAN H, BASAK N (2015) Hesperidin protects testicular and spermatological damages induced by cisplatin in rats. *Andrologia*, 47: 793-800.

KAYA K, CIFTCI O, CETIN A, DOGAN H, BASAK N (2015) Hesperidin protects testicular and spermatological damages induced by cisplatin in rats. *Andrologia*, 47: 793-800.

KELLAND L (2007) The resurgence of platinum-based cancer chemotherapy. *Nat Rev Cancer*, 7: 573-584.

LI XW, FENG LX, ZHU XJ, LIU Q, WANG HS, WU X, YAN P, DUAN XJ, XIAO YQ, CHENG W, PENG JC, ZHAO F, DENG YH, DUAN SB (2020) Human umbilical cord blood mononuclear cells protect against renal tubulointerstitial fibrosis in cisplatin-treated rats. *Biomed Pharmacother*, 121: 109662.

LIRDI LC, STUMPP T, SASSO-CERRI E, MIRAGLIA SM (2008) Amifostine protective effect on cisplatin-treated rat testis. *Anat Rec*, 291: 797-808.

MARTINS NM, SANTOS NAG, CURT C, BIANCHI MLP, SANTOS AC (2008) Cisplatin induces mitochondrial oxidative stress with resultant energetic metabolism impairment, membrane rigidification and apoptosis in rat liver. *J Appl Toxicol*, 28: 337-344.

MONEIM LMA, HELMY MW, EL-ABHAR HS (2019) Co-targeting of endothelin-A and vitamin D receptors: a novel strategy to ameliorate cisplatin-induced nephrotoxicity. *Pharmacol Rep*, 71(5): 917-925.

MORA LO, ANTUNES LMG, FRANCESKOCATO HDC, BIANCHI MLP (2003) The effects of oral glutamine on cisplatin-induced nephrotoxicity in rats. *Pharmacol Res*, 47: 511-522.

NAZIROGLU M, KARAOGLU A, AKSOY AO (2004) Selenium and high dose vitamin E administration protects cisplatin-induced oxidative damage to renal, liver and lens tissues in rats. *Toxicology*, 195: 221-230.

OHKAWA H, OHISHI W, YAGI K (1979) Assay for lipid peroxides in animal tissues by thiobarbituric acid reaction. *Anal Biochem*, 95(2): 351-358.

OURIQUE GM, SACCOL EM, PÊS TS, GLANZNER WG, SCHIEFELBEIN SH, WOEHL WM, BALDISSEROTTO B, PAVANATO MA, GONÇALVES PB, BARRETO KP (2016) Protective effect of vitamin E on sperm motility and oxidative stress in valproic acid treated rats. *Food Chem Toxicol*, 95; 159-167.

PACKER L, LANDVIK S (1990) Vitamin E in biological systems. In: Emerit I, Packer L, Auclair C (eds). *Antioxidants in therapy and preventive medicine*. Plenum Press, New York, pp 93-104.

PAKSOY M, AYDURAN E, SANLI A, EKEN M, AYDIN S, OKTAY ZA (2011) The protective effects of intratympanic dexamethasone and vitamin E on cisplatin-induced ototoxicity are demonstrated in rats. *Med Oncol*, 28: 615-621.

PARK JW, CHO JW, JOO SY, KIM CS, CHOI JS, BAE EH, MA SK, KIM SH, LEE JU, KIM SW (2012) Paricalcitol prevents cisplatin-induced renal injury by suppressing apoptosis and proliferation. *Eur J Pharmacol*, 683(1-3): 301-309.

PECTASIDES D, PECTASIDES E, PAPAXOINIS G, SKONDRA M, GEROSTATHOU M, KARAGEORGOPOULOU S, KAMPOSIORAS C, TOUNTAS N, KOUMARIANOU A, PSYRRI A, MACHERAS A, ECONOMOPOULOS T (2009) Testicular function in poor-risk nonseminomatous germ cell tumors treated with methotrexate, paclitaxel, ifosfamide, and cisplatin combination chemotherapy. *J Androl*, 30(3): 280-286.

PIL PM, LIPPARD SJ (1992) Specific binding of chromosomal protein HMG1 to DNA damaged by the anticancer drug cisplatin. *Science*, 256: 234-237.

ROLDAN-FIDALGO A, MARTIN SALDANA S, TRINIDAD A, OLMEDILLA-ALONSO B, RODRIGUEZ-VALIENTE A, GARCIA-BERROCAL JR, RAMIREZ-CAMACHO R (2016) In vitro and in vivo effects of lutein against cisplatin-induced ototoxicity. *Exp Toxicol Pathol*, 68(4): 197-204.

SANTOS NAG, MARTINS NM, CURTI C, BIANCHI MLP, SANTOS AC (2007) Dimethylthiourea protects against mitochondrial oxidative damage induced by cisplatin in liver of rats. *Chem Biol Int*, 170: 177-186.

SATOH K (1978) Serum lipid peroxide in cerebrovascular disorders determined by a new colorimetric method. *Clin Chim Acta*, 90(1): 37-43.

SCHNEIDER C (2005) Chemistry and biology of vitamin E. *Mol Nutr Food Res*, 49(1): 7-30.

SCHWEYER S, SORURI A, MESCHTERO, HEINTZE A, ZSCHUNKE F, MIOSGE N (2004) Cisplatin-induced apoptosis in human malignant testicular germ cell lines depends on MEK/ERK activation. *Brit J Cancer*, 91: 589-598.

SOYALIÇ H, GEVREK F, KOÇ S, AVCU M, METIN M, ALADAĞ İ (2016) Intraperitoneal curcumin and vitamin E combination for the treatment of cisplatin-induced ototoxicity in rats. *Int J Pediatr Otorhinolaryngol*, 89: 173-178.

TAKESHITA H, CHIBA K, KITAYAMA S, MORIYAMA S, OMURA R, NORO A (2013) Triplet chemotherapy with paclitaxel, gemcitabine, and cisplatin as second-line therapy for advanced urothelial carcinoma. *Mod Chemother*, 2: 1.

VALLE J, WASAN H, PALMER DH, CUNNINGHAM D, ANTHONEY A, MARAVEYAS A, MADHUSUDAN S, IVESON T, HUGHES S, PEREIRA SP, ROUGHTON M, BRIDGEWATER J (2010) Cisplatin plus gemcitabine versus gemcitabine for biliary tract cancer. *N Engl J Med*, 362: 1273-1281.

VILLACORTA L, GRAÇA-SOUZA AV, RICCIARELLI R, ZINGG JM, AZZI A (2003) α-Tocopherol induces expression of connective tissue growth factor and antagonizes tumor necrosis factor-α-mediated downregulation in human smooth muscle cells. *Circ Res*, 92(1): 104-110.

VILLANI V, ZUCCHELLA C, CRISTALLI G, GALIE E, BIANCO F, GIANNARELLI D, CARPANO S, SPRIANO G, PACE A (2016) Vitamin E neuroprotection against cisplatin ototoxicity: Preliminary results from a randomized, placebo-controlled trial. *Head Neck*, 38(Suppl 1): E2118-2121.

WOZNIAK K, CZECHOWSKA A, BLASIAK J (2004) Cisplatin-evoked DNA fragmentation in normal and cancer cells and its modulation by free radical scavengers and the tyrosine kinase inhibitor STI571. *Chem Biol Interact*, 147: 309-318.

YAN LJ (2014) Positive oxidative stress in aging and aging-related disease tolerance. *Redox Biol*, 2: 165-169.

YILMAZ HR, IRAZ M, SOGUT S, OZYURT H, YILDIRIM Z, AKYOL O, GERGERLIOGLU S (2004) The effects of erdosteine on the activities of some metabolic enzymes during cisplatin-induced nephrotoxicity in rats. *Pharmacol Res*, 50: 287-290.

Morphological and clinical significance of the suprameatal region: a topographic study

Berin Tuğtağ Demir[1], Dilara Patat[1], Davut Akduman[2]

[1] Ankara Medipol University, Faculty of Medicine, Department of Anatomy, Ankara, Turkey

[2] Department of Otorhinolaryngology, Ankara Atatürk Sanatoryum Training and Research Hospital, Gulhane Faculty of Medicine, University of Health Science Turkey, Ankara, Turkey

SUMMARY

The suprameatal approach, which does not require mastoidectomy, uses the method of tunneling over the facial nerve to enter the middle ear in cochlear implantation. Even if the SMA approach is also used to drain the mastoid antrum, the depth of the triangle and protrusion types may be important for surgical approaches in this region. This descriptive study was conducted with 58 dry skulls found in the laboratories of the University Faculty of Medicine. Important landmarks were used on the left and right sides of the skulls. All the distances were measured with a vernier caliper to the nearest millimeter.

No statistical significance was found between the right and left sides (*p>0.05*). The border lengths of the suprameatal triangle were respectively 14.88±1.67 mm, 18.17±1.09 mm, 14.56±1.59 mm on the right and 15.34±1.65 mm, 19.01±0.56 mm, 15.89±0.52 mm on the left. Consequently, it was determined that the left side was wider than the right, and there was statistical significance between the sides. The mean ST area was found to be 112.7±16.90 mm^2. The crest was observed mostly on the right side (n=30 (51.72%)), and the triangular suprameatal protrusion was observed mostly on the right side (n=10 (31.03%)). We think that knowing this area's borders and morphological features well, nominated before the surgical procedure, will be a guide in preventing possible operative and postoperative complications.

Key words: Suprameatal approach – Mastoid antrum – Suprameatal triangle – Middle cranial fossa surgery

INTRODUCTION

Cochlear implants are surgically implanted devices for the treatment of patients with severe to profound sensorineural hearing loss in children and adults. Cochlear implantation is conventionally performed via mastoidectomy posterior tympanotomy approach (MPTA) since House first introduced it in 1961 (House, 1976). Although it is easily performed, temporary injury to the facial nerve and chorda tympani may be troublesome for both the surgeon and the patients (Cohen and Hoffman, 1991). Some alternatives to this classic approach are the endomeatal approach, the middle fossa, the canal wall down technique, and a technique using a tunnel drilled in the mastoid area without mastoidectomy to approach the middle ear. All the described techniques have their

Corresponding author:
Berin Tuğtağ Demir, PhD. Department of Anatomy, Ankara Medipol University, Faculty of Medicine, Ankara, Turkey. E-mail: berrintugtag@hotmail.com ORCID No: 0000-0001-8301-9257

Submitted: December 11, 2022. **Accepted:** December 24, 2022

https://doi.org/10.52083/JVQJ5380

own difficulties and complications. The suprameatal approach (SMA), based on the retroauricular tympanotomy approach as an access to the middle ear and cochleostomy site, was developed by Kronenberg et al. as an alternative technique to the classic approach. In this technique, the electrode is inserted into the middle ear in a suprameatal route without a mastoidectomy. As stated in the editor's commentary by Robert K. Jackler, the majority of surgeons today are trained in the conventional retroauricular and mastoidectomy approaches, either canal wall up or down. SMA requires skills developed exclusively for this procedure. A good understanding of anatomy is the key point of this route, and training in this technique is a prerequisite for avoiding complications (Kronenberg et al., 2001). Herein we designed an anatomical study to contribute to the understanding of the anatomy of this region.

The area called the foveola suprameatalis (Mac Ewen's triangle, suprameatal triangle) located between the posterior upper part of the external acoustic meatus and the supramastoid crest in the temporal bone is a clinically important region that defines the lateral wall of the mastoid antrum.The suprameatal depression is a narrow space located between the anterior end of the supramastoid process and the posterosuperior quadrant of the external acoustic meatus (Grays, 2016; Turgut et al., 2002). Since the mastoid antrum, the lateral wall of the suprameatal triangle, lies approximately 12-15 mm below, it is generally considered a reference anatomical site for surgical access (Cummings, 1993). In addition, the mastoid cortex behind the bony prominence called the suprameatal prominence guides the lateral wall of the mastoid antrum and is located at a depth of 15 mm in adults and approximately 2 mm in newborns (Peker et al., 1998). In classical anatomy books, it is stated that this protrusion serves as an additional attachment point for ligaments that fix the cartilaginous parts of the external acoustic meatus and temporal fascia and muscles (Sagosu et al., 2013). Due to their anatomical location, both the suprameatal triangle and the ridge are of clinical importance for otological surgeons (Acar et al., 2020; Peker et al., 1998). The morphological position of the suprameatal triangle is also clinically important for the localization of the mastoid antrumand tegmen tympani. Because this triangle is an important topographic region that separates the middle cranial fossa and the mastoid antrum (Romanes, 1992; Bender et al., 2018). The cribriform area in the suprameatal (Mac Ewen's triangle) triangle is pierced by numerous small foramens that serve as a passage for the vessels of the mastoid antrum mucosa. For this reason, it is stated that dissection on the sides of the triangle is safer due to the absence of neurovascular structures (Belsare, 2014; Bender et al., 2018).

The postauricular incision described by Wilde (1853) is still a widely used surgical approach to the temporal bone (Belsare et al., 2014). The temporal line is the apex of this postauricular incision. However, a clear determination of the suprameatal triangle is clinically important for the localization of the mastoid antrum and tegmen tympani, as it is an important topographical landmark that separates the middle cranial fossa and the mastoid antrum. In addition, the morphology of the suprameatal triangle can be used in cochlear implantation procedures as one of the markers in the process of mastoidectomy and posterior tympanotomy. Therefore, we believe that the analysis of the morphometric and topographic features of the suprameatal triangle, suprameatal protrusion and depression in the skulls will guide not only anatomists but also neurosurgeons for middle cranial fossa surgeries, and otolaryngologists for middle ear surgeries. This study is aimed to define the guide points for the surgical interventions to be performed in the region by analyzing the morphometric and topographic features of the suprameatal triangles, suprameatal protrusions and depressions in the skulls.

MATERIALS AND METHODS

This descriptive study was conducted with dry skulls found in the Anatomy laboratories of Ankara Medipol University and Erciyes University Faculty of Medicine.

Samples

In order to determine the number of samples, power analysis was performed using the G*Power (v3.1.9.7) program. The power of the study is ex-

pressed as 1-β (β = probability of type II error). In the calculation made, the effect size (d) was found to be 0.630 to obtain 85% power at the α=0.05 level. Accordingly, it was calculated that there should be 58 skulls (a total of 116 temporal bones on the right and left) in the study.

Inclusion criteria: Bones with preserved bone integrity and no structural defects were included in the study.

Exclusion criteria: Bones with fractures in the processus mastoideus, tuberculum anterius, tuberculum posterius, porus acusticus externus, trigonum suprameatica areas were excluded from the study.

Study Design

Important landmarks were used on the left and right sides of the skulls. All the distances were measured with a vernier caliper to the nearest millimeter. The following morphometric measurements were taken (Fig. 1):

- *Mastoid length (ML)*
- *Distance between anteior tubercle and tip of mastoid (AT-TM)*
- *Distance between posterior tubercle and tip of mastoid (PT-TM)*
- *The outer opening of the external acoustic meatus width (EMA width)*
- *The outer opening of the external acoustic meatus length (EMA Length)*
- *Mastoid triangle measurements which include (Fig. 1):*
  - *Upper border of suprameatal triangle (ST1)*
  - *Anteroinferior border of suprameatal triangle (ST2)*
  - *Posterior border of suprameatal triangle (ST3)*
  - *Distance between Henle's spine and midpoint of suprameatal triangle (ST4),*
  - *Distance between porion and midpoint of suprameatal triangle (ST5),*
- *Area of the suprameatal triangle (STA)*
- *Types of suprameatal spine*
- *The size of suprameatal spine (small, medium and large size)*
- *Suprameatal triangle depression*

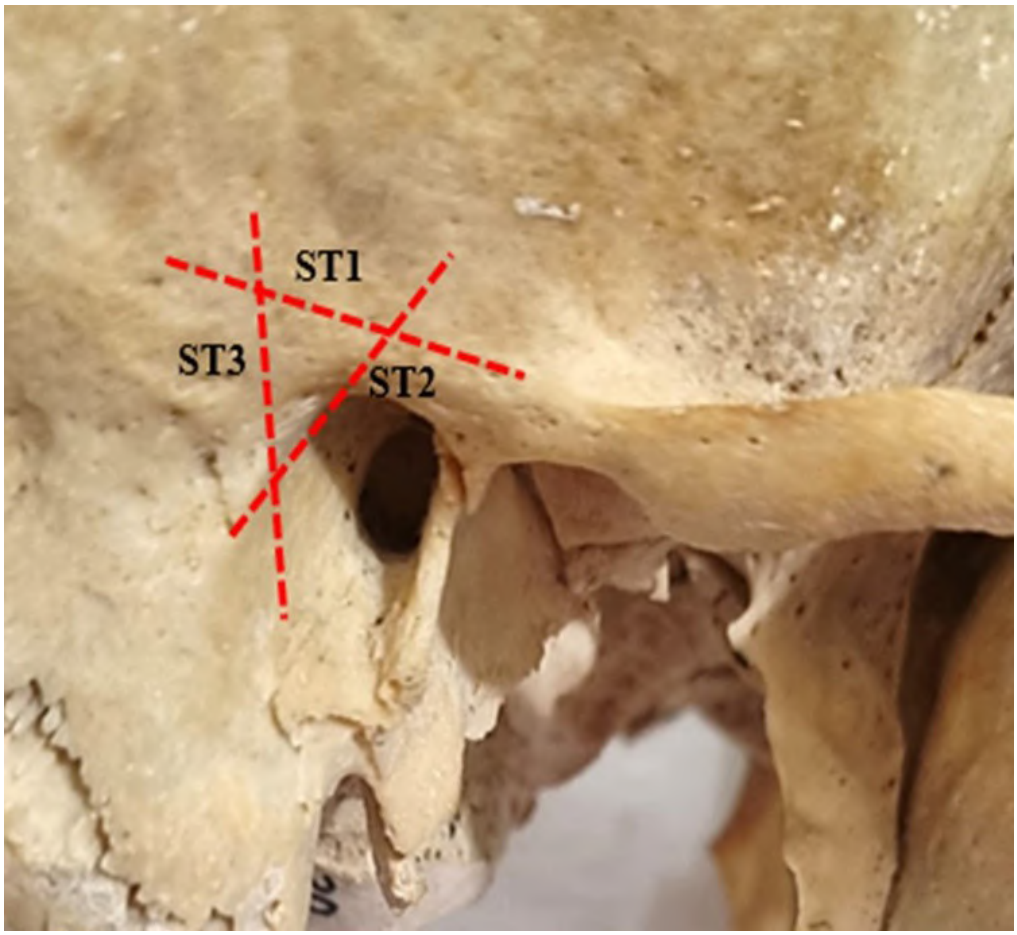

Fig. 1.- Border line of suprameatal triangle (ST1 superior border, ST2 anteroinferior border, ST3 posterior border).

Statistical analyses

Basic descriptive statistics were used to analyze the data made by the computer software SPSS. Mean, standard deviation and range were evaluated for each measurement. A comparison of the values of all measurements was made between the flanks of each subject. All measurements and frequencies of the data are tabulated and separated according to the sides. The relationship between the two categorical variables was analyzed by the linear correlation between the variables measured with the Pearson correlation coefficient. P values less than 0.05 significance level were considered as statistically significant.

RESULTS

This study was conducted on 58 adult Turkish human dry skulls. The studied skulls were 30 male skulls and 28 female skulls. Mastoid length was 37.6±2.34 mm on the right and 34.6±3.01 mm on the left; the distance between the anterior tubercle and the mastoid process was 48.4±1.78 mm on the right and 46.0±7.44 on the left; the distance between the posterior tubercle and the mastoid process was 45.0±12.6 mm on the right and 46.7±7.23 mm on the left. The mean width and length of outer opening of the external acoustic meatus were; 14.9±06.9 mm and 20.4±9.2 mm; respectively. No statistical significance was found between the right and left sides (*p>0.05*).

Considering the data of the suprameatal triangle, ST1 was 14.88±1.45 mm on the right, 15.34±1.65 mm on the left, ST2 was 18.27±1.09 mm on the right and 19.01±0.56 mm onthe left, ST 3 was 14.56±1.59 mm on the right and 15.89±0.52 mm on the left. It was determined that the left side was wider than the right and there was statistical significance between the sides ($p<0.05$). The mean ST area was found to be 112.78±16.90 mm^2 (Table 1).

In Fig. 2, the side lengths of the suprameatal triangle and the comparison of the right and left side areas are given.

According to Table 2; It was determined that there was no spinal protrusion at the rate of 17.24% on the right side and 24.13% on the left side. Suprameatal spine was observed on the right side with a rate of 51.72% and mostly in form of crest (Fig. 3).

It was determined that the crest was observed mostly on the right side (n=30 (51.72%)), and the triangular suprameatal protrusion was observed most on the right side (n=18 (31.03%)).

The dimensions of the suprameatal prominence are given in Table 3. It was determined that the supra-meatal protrusion was absent at a rate of 34.48%, and it was medium in size at the maximum rate of right side 52.86%. On the other hand, it was determined that the small-sized spinal protrusion was 12.06% on the right side and 15.51% on the left side; there were no statistical signifi-

Table 1. Descriptive information of the suprameatal region and the relationship between the sides.

		Average(mm)	Right (mm)	Left (mm)	p
Mastoid length		36.0±9.01	37.6±2.34	34.6±3.01	.494
Distance between anterior tubercle and tip of mastoid		47.7±18.0	48.4±1.78	46.0±7.44	.292
Distance between posterior tubercle and tip of mastoid		44.8±17.5	45.0±12.6	46.7±7.23	.130
The outer opening of the external acoustic meatus width		14.9±06.9	15.0±7.6	14.5±6.59	.895
The outer opening of the external acoustic meatus length		19.8±10.8	19.95±5.66	19.6±09.87	.184
The borders of suprameatal triangle (mm)	ST1	15.09±1.65	14.88±1.67	15.34±1.65	**.030**
	ST2	19.03±1.06	18.27±1.09	19.01±0.56	**.044**
	ST3	15.25±1.14	14.56±1.59	15.89±0.52	**.010**
	ST4	29.12±5.24	30.97±4.15	30.61±9.67	.234
	ST5	12.52±0.19	11.16 ± 0.17	12.16 ± 0.19	.690
	STA (mm^2)	112.78±16.90	99.65±9.89	116.56±11.01	**.002**

Test: Mann whitney U, p<0.05

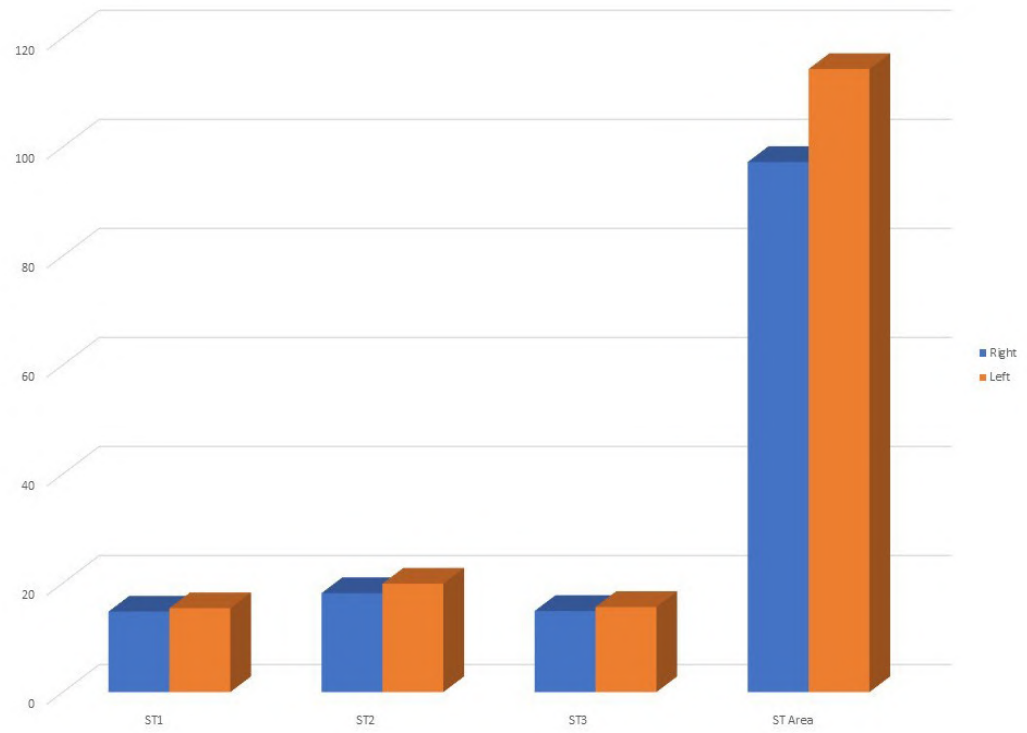

Fig. 2.- Column chart of suprameatal triangle dimensions.

Table 2. Variation of suprameatal spine.

Types of supremeatal spine	Right			x^2	p	Left			x^2	p
	Female	Male	Total			Female	Male	Total		
Absent	5 (17.85)	5 (16.66)	10 (17.24)	1.58	.071	10 (35.71)	4 (13.33)	14 (24.13)	1.89	.124
Crest	15 (53.57)	15 (50)	30 (51.72)	1.40	.564	12 (42.85)	17 (56.66)	29 (50)	2.43	.349
Triangular	8 (28.57)	10 (33.33)	18 (31.03)	1.10	.897	6 (21.42)	9 (30)	15 (25.86)	1.98	.128
Total	28 (100)	30(100)	58(100)			28 (100)	30(100)	58(100)		

Test: chi-square, p<0.05

cance between the sides (p>.05). In other dimensions, as gender, statistical significance was found between absent, medium and large (p>.05).

SMD was shallow in 6 male skulls (20%) and in 9 female skulls (32.4%) on the right side while it was shallow in 6 male skulls (20%) and in 6 female skulls (21.4%) on the left side. According to the evaluation of the suprameatal depression on the right and left sides, it was determined that there was no suprameatal depression in 27.58% on the right and 22.41% on the left, deep in the left side in 56.89% and shallow in the right side in 25.86%. Statistical significance was found between the dimensions of the right and left sides and the absent and deep (p<.05) (Fig. 4, table 4).

DISCUSSION

The suprameatal triangle is the focal point of the suprameatal approach (SMA), which does not require mastoidectomy and uses the method of tunneling over the facial nerve to enter the middle ear in cochlear implantation (Zernotti et al., 2012). Mastoidectomy with posterior tympanotomy was started to be used for cochlear implantation by House (1961), but it has been reported

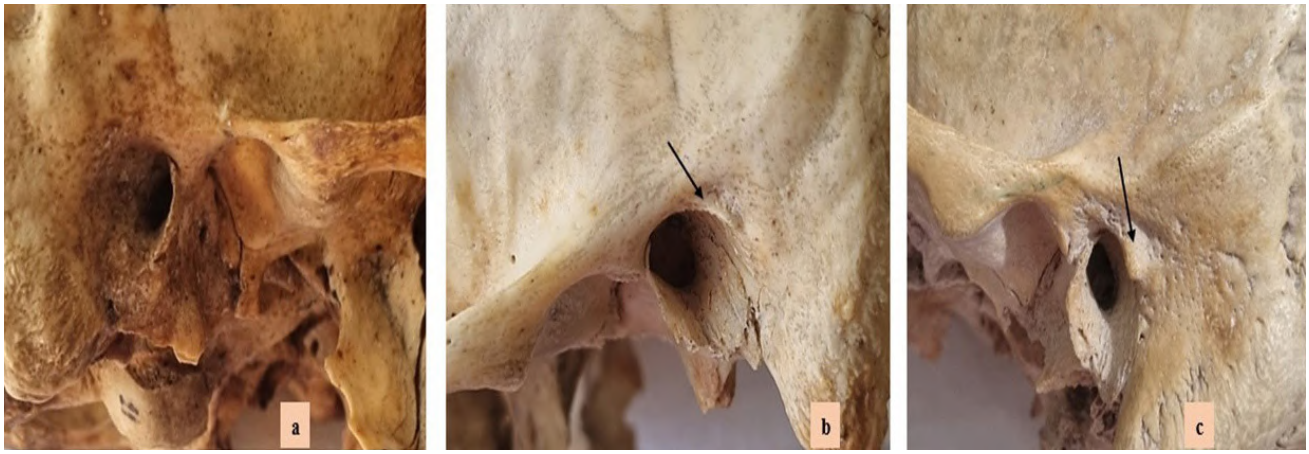

Fig. 3.- Types of suprameatal protrusions. **a:** Absent, **b:** Crest, **c:** Triangle.

Table 3. Dimensions of the suprameatal spine.

Dimensions of the suprameatal spine	Right					Left				
	Female	Male	Total	x^2	p	Female	Male	Total	x^2	p
Absent	12 (42.85)	8 (26.66)	20 (34.48)	.097	.147	14 (24.13)	6 (20)	20 (34.48)	8.12	**.037**
Small	3 (10.71)	4 (13.33)	7 (12.06)	0.90	.645	5 (17.85)	4 (13.33)	9 (15.51)	0.14	.061
Medium	9 (32.14)	6 (20)	15 (25.86)	1.81	.872	5 (17.85)	17 (56.66)	22 (37.93)	9.89	**.019**
Large	4 (14.28)	12 (40)	16 (27.58)	6.67	**.041**	4 (14.28)	3 (10)	7 (12.06)	0.97	.891
Total	28 (100)	30(100)	58(100)			28 (100)	30(100)	58(100)		

Test: chi-square, p<0.05

that the possibility of damage to the facial nerve and chorda tympani during surgery is quite high in this approach (Öztürk et al., 2016). Because of these complications, new techniques have been developed to reach the middle and inner ear via the suprameatal triangle rather than mastoidectomy, and studies have begun to report that the safest approach to the target area is the suprameatal triangle without damaging the chorda tympani and facial nerve (Postelman et al., 2011; Kronenberg et al., 2001). Moreover, in chronic bone disease, the bony cortex in the suprameatal triangle region may be deceptively thick, while in diseases such as acute mastoiditis, the bony cortex may be lost secondary to the disease (Jain et al., 2019). Since the SMA approach is also used to drain the mastoid antrum, the depth of the triangle and protrusion types may be important for surgical approaches in this region (Peker et al., 1998). Despite the stated clinical importance of the suprameatal triangle, little research has been done regarding the morphology of the triangle. Therefore, this study was carried out with the aim of revealing the morphological features of the suprameatal triangle and protrusion and the relationship of these structures according to size and shape in the Turkish population.

In advanced infectious cases, the mastoid antrum is evacuated from the suprameatal triangle with a surgical approach, but due to its complicated structure, it is extremely important to know the anatomy of the temporal region and related structures, both surgically and anatomically (Selman, 2011). In addition, in case of vascular compression, trigeminal neuralgia can be treated and the suprameatal region can be preferred to approach the cerebellopontine region and surgical treatment of trigeminal neuralgia in the cisterna can be performed (Piilai et al., 2009). Kronenberg and Migiro (2006), on the other hand, reported that the suprameatal approach for cochlear implantation is very safe without damaging the facial

nerve and without limited operative time, so the borders of the triangle should be known.In this study, the suprameatal triangle was positioned by drawing imaginary lines and the borders of the triangle were measured between the right and left sides. Considering the data of the suprameatal triangle, it was determined that the upper border was 14.88±1.67 mm on the right side, 15.34±1.65 mm on the left side, the lower anterior margin was 18.27±1.09 mm on the right side, 19.01±.56 mm on the left side, the posterior margin was 14.56±1.59 mm on the right side and 15.89±0.52 mm on the left side. It was determined that the left side was larger than the right and there was statistical significance between the sides (*p<0.05*). The mean ST area was found to be 112.78±16.90 mm^2. It was determined that ST1-2 and 3 were longer on the left side than the right. Antony et al. (2019) determined the right- and left-side lengths of the upper border as 13.71 ± 1.86 mm and 13.76 ± 1.74 mm, the anteroinferior margin lengths on the right and left sides as 14.46 ± 1.63 mm and 14.30 ± 1.46 mm; the rear border lengths on the right and left sides as 14.12 ± 2.02 mm and 17.73 ± 1.74 mm.

Apart from the dimensions of the suprameatal triangle, the lengths of ST4 (middle of the suprameatal triangle-henle protrusion) and ST5 (middle of the suprameatal triangle-porion) are measured to preserve the facial nerve and chorda tympani in mastoidectomy, and the depth of the sigmoid sinus can be determined by additional measurements (Turgut et al., 2003; Kumar, 2021). In our study, the mean ST4 was 29.12±5.24 mm, and the ST5 was 12.52±0.19 mm. Kumar (2021), who made the same measurements, determined the ST4 as 32.27±0.14 mm and the ST5 as 12.2±0.19 mm.

In our study, we determined the area of the suprameatal triangle as 99.65±9.89 mm^2 on the right and as 116.56±11.01 mm^2 on the left, and we found that the triangle area on the left side was significantly wider. In a similar study conducted in a Turkish population, it was stated that the left suprameatal triangle area was 112.73±15.57 mm^2 on the left and 112.73±15.57 mm^2 on the right, but there was no difference between the sides (Açıkgöz et al., 2021). Sogasu et al. (2019) reported a much smaller (right-81.37±26.13 mm^2, left-

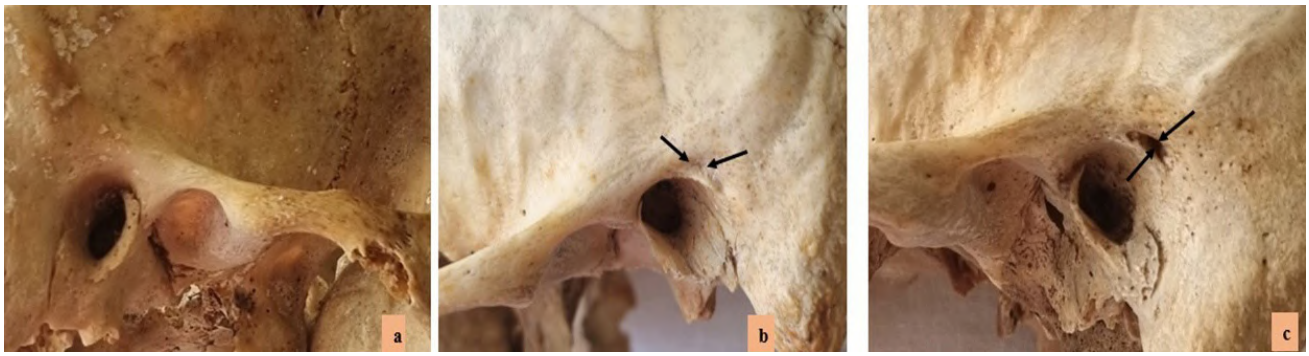

Fig. 4.-Types of suprameatal depressions. **a:** Absent, **b:** Shallow, **c:** Deep.

Table 4. The depth of suprameatal depression (SMD) on both sides.

Suprameatal depression	Right			x^2	p	Left			x^2	p
	Female	Male	Total			Female	Male	Total		
Absent	11 (39.28)	5 (16.66)	16 (27.58)	2.343	**.049**	12 (42.85)	1 (3.33)	13 (22.41)	8.541	**.025**
Shallow	9 (32.14)	6 (20)	15 (25.86)	.341	.090	6 (21.42)	6 (20)	12 (20.68)	.561	.970
Deep	8 (28.57)	19 (63.33)	27 (46.55)	6.44	**.026**	10 (35.71)	23 (76.66)	33 (56.89)	7.306	**.038**
Total	28 (100)	30 (100)	58 (100)			28 (100)	30(100)	58(100)		

Test: chi-square, p<0.05

73.74±23.26 mm^2) suprameatal triangular area in their study of 50 human skulls from the Indian population (Vinay et al., 2016). In surgical approaches, it is thought that the area of the region can create significant differences between populations and intraoperative planning should be done accordingly.

Clear identification of the suprameatal prominence with the suprameatal triangle is clinically extremely important for the localization of the mastoid antrum and tegmen tympani, as it is an important topographic landmark that separates the middle cranial fossa and mastoid antrum. In most of the previous studies, it was stated that the suprameatal protrusion was mostly observed as the crest type (Peker et al., 1998; Hauser and De stefano, 1989). Shalaby et al. (2016) stated that there was spinal protrusion in all skulls in their research and that the most common protrusion type was crest with 45%. Aslan et al. (2004) found that the percentage of crest type (40%) was equal to the percentage of triangular type (40%) in Turkish skulls. In our study, it was determined that there was no spinal protrusion in the suprameatal process with a rate of 17.24% on the right and 24.13% on the left, and it was mostly observed in the form of a crest and on the right side.

Another important feature of the suprameatal triangle in neurological and otological approaches is the presence and dimensions of the suprameatal protrusion in this region. Peker et al. (1998) reported the dimensions of the suprameatal prominence as, 6.6% (absent), 39.9% (small), 31.3% (medium), 22.2% (large), 4.4 (absent) on the right side, and 40.9% (small), 32.8% (medium), 21.8% (large) on the left side. They stated that it has a small distribution on the right and a medium size distribution on the left. Açıkgöz et al. (2021) reported that the distribution of suprameatal prominence dimensions was 12.06%, 25.86 each small- and medium-sized on the right side, and 37.93% as medium-sized on the left side. In our study, it was found that the suprameatal protrusion was absent at a rate of 34.48%, and it was medium-sized at the maximum rate of 37.93%.According to the sides, it was determined that the small-sized spinal protrusion was found in 12.06% on the right and 15.51% on the left, and statistical significance was observed between the sides ($p<0.05$). In other dimensions, statistical significance was not found between the sides ($p>0.05$). In a study on the subject, it was reported that the suprameatal prominence was mostly medium in size, less frequently in large size, and at least in small size, and the small size was more common on the left (Shalaby, 2019). In our study, it was found that the small type was seen more on the left side.

We evaluated the suprameatal depression on the right and left sides as absent, shallow and deep. Accordingly, the rates were as 27.58%, 25.86% and 46.55% on the right side, and 22.41%, 20.68% and 56.89% on the left side; respectively. No statistical significance was found between the dimensions of the right and left sides and the suprameatal triangle. In the study of Açıkgöz et al. (2021) reported the depth of the suprameatal depression as 45.5% shallow on the right side, and as 39.4% both shallow and medium-depth on the left side. Peker et al. (1998) found the suprameatal depression depth as 4.5% (absent), 32.5% (shallow), 31.6% (medium) and 31.4% (deep) on the right side, and 4.9% (absent), 31.3% (shallow), 35.5% (medium) and 28.3% (deep) on the left side. The study result of Shalaby et al. (2019) stating that the incidence of deep suprameatal depression is higher on both the right and left sides, are similar to our study.

SMA provides a wider exposure of the operative field, better localization of the cochleostomy site, and an approach without the risk of facial nerve injury. However, morphometric analysis of the suprametal region alone is not sufficient for SMA. In summary, the use of a non-mastoidectomy approach, such as SMA, in CI surgery allows for extensive exposure of the middle ear and allows easier puncture of the cochleostomy and better control of electrode entry in cases of deformity and deformity. Better visibility of the cochleostomy site allows preservation of residual hearing, and allows placement of the electrode in the scala tympani. Exclusion of mastoidectomy in SMA reduces operative time to approximately 1 hour, improves aesthetic outcomes without retroauricular bone defect, and eliminates possible facial nerve and chorda tympani injury. Damage to the chorda tympani has become a very important issue due

to the increasing number of patients with bilateral implants. Therefore, the surgeon's knowledge of where and at what angle the suprameatal triangle should be started for the surgical intervention to be performed in CI surgery, the length of the canal to be opened, and the position of the dura mater, will increase the success of CI and prevent nerve damage.

CONCLUSION

The suprameatal triangle has anatomical variations that can assist neurosurgeons and otology surgeons in procedures involving access to structure in the posterior cranial fossa and mastoid air system. Knowing the borders, area, depression depth and topographic anatomy of the suprameatal protrusion types of the suprameatal triangle is very important for the suprameatal approach, especially in surgical operations such as mastoidectomy, petroclival meningioma, petrotentorial meningioma and cochlear implantation. Therefore, in line with the results we have obtained, we think that knowing the borders and morphological features of this area well, especially before the surgical procedure, will be a guide in preventing possible operative and postoperative complications. The success rate of surgery can be increased by using a trans-channel approach to the middle ear and cochlea for CI and by opening a direct tunnel through the postero-superior bone canal wall.

REFERENCES

AÇAR G, ÇİÇEKCİBAŞI AE (2020) Surgical anatomy of the temporal bone. *Oral Maxillofac Surg. IntechOpen,* 1-23.

ASLAN A, MULTU C, CELİK O, GOVSA F, OZGUR T (2004) Surgical ımplication of anatomical landmarks on the lateral surface of mastoid bone. *Surg Radiol Anat,* (26): 263-267.

BELSARE GS (2014) Step by step temporal bone dissection. Jaypee Brothers Medical Publishers, New Delhi, India.

BENDER ME, LİPİN RB, GOUDY SL (2018) Development of the pediatric temporomandibular joint. *Oral Maxillofac Surg*, 30(1): 1-9.

COHEN NL, HOFFMAN RA (1991) Complications of cochlear implant surgery in adults and children. *Ann Otol Rhinol Laryngol*, 100: 708-711.

CUMMİNGS CW, FREDRİCKSON JM, HARKER LA, KRAUSE CJ, SCHULLER DE (1993) Otolaryngology head and neck surgery, 2nd edn. Mosby Yearbook, St Louis.

GRAY SS (2016) Gray's Anatomy: The Anatomical Basis of Clinical Practice. Elsevier, Philadelphia.

HAUSER G, DE STEFANO GF (1989) Epigenetic variants of the human skull. E. Schweizerbartsche, Stuttgart, pp 188-191, 193-194.

HOUSE WF (1976) Cochlear implant. *Ann Otol Rhinol Laryngol*, 85(Suppl 27): 2-6.

JAİN S, DESHMUKH PT, LAKHOTİA P, KALAMBE S, CHANDRAVANSHİ D, KHATRİ M (2019) Anatomical study of the facial recess with ımplications in round window visibility for cochlear ımplantation: personal observations and review of the literature. *Int Arch Otorhinolaryngol,* 23(3): e281-e291.

KRONENBERG J, MİGİROV L, DAGAN T (2001) Suprameatal approach: New surgical approach for cochlear implantation. *J Laryngol Otol,* 115: 283-285.

KUMAR B, SENTHİL (2021) Morphometric study of Macewan's Triangle in relation to depth of the sigmoid sinus plate. *Indian J Forensic Med Toxicol,* 15: 640-645.

ÖZTÜRK K, GÖDE S, ÇELİK S (2016) Revisiting the Anatomy of the facial recess: the boundaries of the round window exposure. *Balkan Med J,* 33(05): 552-555.

PEKER TV, PELİN C, TURGUT HB, ANİL A, SEVİM A (1998) Various types of suprameatal spinesand depressions in the human temporal bone. *Eur Arch Otorhinolaryngol,* 255(8): 391-395.

PİLLAİ P, SAMMET S, AMMİRATİ M (2009) Image-guided, endoscopic assisted drilling and exposure of the whole length of the internal auditory canal and its fundus with preservation of the integrity of the labyrinth using a retrosigmoid approach: A laboratory investigation. *Neurosurgery,* 65 Suppl 6: 53-59.

POSTELMANS JT, VAN SPRONSEN E, GROLMAN W, STOKROOS RJ, TANGE RA, MARÉ MJ (2011) An evaluation of preservation of residual hearing using the suprameatal approach for cochlear implantation: Can this implantation technique be used for preservation of residual hearing? *Laryngoscope,* 121: 1794-1799.

ROMANES GJ (1992) Cunningham's manual of practical anatomy, vol III. Head and neck and brain. Oxford University Press, London.

SELMAN MO (2011) Metric study on depth of the sigmoid sinus plate in relation to suprameatal (Macewen's) triangle. *Iraqi J Med Sci,* 9: 86-91.

SHALABY SA, EİD EM, ALLAM OA, SARG NA, METWALLY AG (2016) Morphometric study of mastoid canal and suprameatal triangle of human Egyptian skull, with gender determination. *Nat Sci*, 14(4): 67-73.

SOGASU D, THENMOZHİ MS, LAKSHMANAN G (2019) Suprameatal trigone and its relation to the length of the sigmoid sinus. *Drug Invent Today,* 12(8): 1802-1805.

TURGUT HB, ANİL A, PEKER T, PELİN C, GULEKON IN (2003) Supraarticular, supramastoid and suprameatal crests on the outer surface of the temporal bone and the relation between them. *Surg Radiol Anat,* 25(5-6): 400-407.

VİNAY KV, SWATHİ, DENİA MY, SACHİN KS (2016) Morphometrıc study of hypoglossal canal of occıpıtal bone ın dry skulls of South Indıa. *Int J Anat Res,* 4(4): 3016-3019.

WİLLİAMS PL, WARWİCK R, DYSON M, BANNİSTER LH (1993) Gray's anatomy, 37th edn. Elsevier BV Churchill Livingstone, Edinburgh.

ZERNOTTİ ME, SUÁREZ A, SLAVUTSKY V, NİCENBOİM L, Dİ GREGORİO MF, SOTO JA (2012) Comparison of complications by technique used in cochlear implants. *Acta Otorrinolaringol Esp,* 63(05): 327-331.

Anti-oxidative and anti-inflammatory role of naringin against vanadium-induced neurotoxicity in adult Wistar rats

Adeshina O. Adekeye, Adedamola A. Fafure, Darell E. Asira, Ayoola E. Ogunsemowo

Department of Anatomy, College of Medicine and Health Sciences, Afe-Babalola University, Ado-Ekiti, Ekiti State, Nigeria

SUMMARY

Vanadium is a trace element that can induce oxidative damage in the brain due to excess accumulation, which leads to programmed neuronal cell death. Naringin as a natural flavonoid has been reported to have a broad range of pharmaceutical bioactivities. We aimed to explore the therapeutic effects of naringin against oxidative stress and inflammation induced by vanadium exposure. Forty adults male Wistar rats were indiscriminately distributed into four (4) groups (n = 10). The groups received the followinh treatments: 5 ml/kg double distilled water (control), Naringin (Intraperitoneally, 30mg/kg BW), Vanadium & Naringin (Vanadium at 10mg/kg & Naringin at 30mg/kg respectively), Vanadium (Intraperitoneally, 10mg/kg BW). The result of vanadium administration showed an increase in oxidative stress, as seen in the reduction of glutathione peroxidase and catalase level of the brain (hippocampus), a decrease in numbers of viable cells and significant increase in inflamed cells. A decrease in memory function following vanadium administration was also observed. Therapeutic administration with naringin following vanadium exposure showed an elevation of glutathione peroxidase levels and catalase level of the hippocampus, a significant decrease in the number of inflamed cell and an improvement in memory function. This study is a proof that naringin can serve as a neuroprotective agent against oxidative stress and inflammation following vanadium toxicity in the brain.

Key words: Naringin – Vanadium – Antioxidant – Inflammation – Neurotoxicity – Glutathione peroxidase

INTRODUCTION

Dietary and occupational exposure is a public health hazard that has been linked to oxidative damage in the liver, kidney, and neurological damage (Xiong et al., 2021; Adekeye et al., 2020). Vanadium exposure can be through infected food and water; it can also be through air, or typical factory systems. Recent studies on health risk assessment of heavy metals have explore cognition, memory and the motor system following exposure to this chemical metal known as vanadium (Adekeye et al., 2020).

There have been recent reports of global environment problems on contamination of water with heavy metal, owing to the advancement of economy and development of industry. One of the contaminants that research has reported to pose

Corresponding author:
Fafure Adedamola Adediran. Neuroscience Unit, Department of Anatomy, College of Medicine and Health Sciences, Afe Babalola University, Ado-Ekiti, Nigeria. Phone: +2348069501996. E-mail: adedamolaf@abuad.edu.ng

Submitted: September 2, 2022. **Accepted:** January 11, 2023

https://doi.org/10.52083/EUNF6102

a potential threat to animals and human beings is vanadium (Eze et al., 2022). This has become a major concern because increasing mining, smelting, weathering of rocks and sediments rich in vanadium have resulted in a high concentration of vanadium in the groundwater (Usende et al., 2017). Ways by which the concentration of vanadium in soil and natural water have been increased are through the uses of pesticides and fertilizers, as well as other human activities such as industrial production, mining, fossil fuel combustion and recycling of household waste. Vanadium can enter the body through either the lungs or the stomach and can be uptaken via the blood stream, cross the blood brain barrier and deposit in the brain. Its accumulation in the brain might be linked with the pathological processes of some nervous system disorders. After a long-term exposure, its deposition can result in more severe pathologies (Adekeye et al., 2020).

Vanadium is a trace element (atomic number 23), and is the 21st most abundant element in the outer regions of our planet. Vanadium is a special element that can interrelate with diverse physiological substrates that are otherwise put into work by phosphate as the tetrahedral anion vanadate (V) (Rehder, 2015). It can switch between the oxidation states +2, +3, and +4 in a physiological environment and can efficiently increase its sphere beyond tetrahedral coordination (Rehder, 2015; Olaolorun et al., 2021). The most stable oxidation state is the quadrivalent salts (VO^{2+}, vanadyl) (Barceloux and Barceloux, 1999). Vanadium is a heavy metal and is specially stored in certain organs, mainly in the bones, the kidneys, and the liver (Cortizo et al., 2000). The daily uptake of vanadium compounds via breathing air, drinking water and nutrients in nonpolluted areas varies between 10 µg and 2 mg (Rehder, 2013). The absorption of its compounds hinges on their solubility as well as the route of entry (Barceloux and Barceloux, 1999). Upon uptake, vanadium compounds undergo speciation by redox interaction and ligand removal/exchange with ingredients of body fluids in the various body compartments (Rehder, 2016). Dietary vanadium occurs either as vanadyl or as vanadate, with the latter being absorbed about 3 times more adequately by the digestive tract than the former (Barceloux and Barceloux, 1999). Critical exposure to vanadium compounds is confined to inhalation of vanadium oxides, and are readily absorbed in the lungs. It easily enters the respiratory tree deep into the airways, crossing the blood–gas barrier and reaching the bloodstream (Ghosh et al., 2014). Once in the bloodstream, high-molecular mass transporters such as transferrin (plasma) serum albumin (Ab) and immunoglobulin G (Ig) form binary complexes and ternary complexes with vanadium (Rehder, 2013). Further distribution from blood to the inner compartments (heart, liver and kidneys), the outer compartments (tissue and brain) and the bone structure occurs. Ultimately, vanadium is excreted via feces and urine (Ghosh et al., 2014). At nutritional concentrations, intoxication with vanadium is unlikely (Rehder, 2016). Vanadium compounds have the ability to interchange into different species constantly within the cell in the presence of ROS, which makes it a powerful inducer of cell death (necrosis) (Rojas-Lemus et al., 2020). Neurotoxic metals such as vanadium cause blood brain barrier disruption, neuropathology, and neuronal damage, which can trigger CNS alterations. The hippocampus, being a part of the limbic system, performs several brain functions such as learning, memory, and spatial coding

The hippocampus is vulnerable to oxidative stress, especially the subfields CA1 and CA3, and granule cells of DG are highly influenced by oxidative damage (Avila-Costa et al., 2006).

Thus, oxidative damage to this brain area can cause impairment in multiple brain functions. The management of hippocampal neurons' normal redox state is essential in the management and prevention of cognitive decline (Marosi et al., 2012). The living framework is known to have a natural antioxidant defense framework to neutralize the ROS produced within the metabolic handle (Viswanatha et al., 2017). The antioxidant defense is constituted by the antioxidant enzymatic actions. When this natural antioxidant defense falls brief, the antioxidants ought to be supplemented from an outside source by implies of supplements (Marosi et al., 2012). Flavonoids such as naringin possess antioxidant, anti-inflammatory, anti-apoptotic, anti-ulcer, anti-oste-

oporotic and anti-carcinogenic properties (Chen et al., 2016). Naringin is one natural flavanone, and reports have shown that it has a broad range of pharmaceutical bioactivities against oxidative stress, hyperlipidemia, and neurodegeneration (Chen et al., 2018). Orally administered naringin is deglycosylated into naringenin by hydrolytic enzymes of the epithelium of the oral cavity, or epithelial cells of the small intestine and by the intestinal microflora (Zou et al., 2015; Memariani et al., 2020). Research have shown that naringenin is not properly absorbed in the human digestive track, with merely 15% oral bioavailability (Josh et al., 2018). NGE is partially absorbed and then metabolized to glucuronide and sulfate metabolites through stage I and stage II metabolic reactions (Memariani et al., 2020). After absorption, Flavanones are bound to the albumin in the blood and immediately circulated to the thoroughly perfused organs like liver, kidney, heart, spleen, and cerebellum. Peng et al., 1998, reported the apparent permeability of Naringenin to be between 250-350 nm/s. Subsequently, Naringenin have high porousness across in situ BBB

models as well as in vitro examinations. Naringin has proven to be effective in the reduction of expression of signaling factors associated with the inflammatory response, such as, interleukin-6 (IL-6), interleukin-8 (IL-8), inducible nitric oxide synthase (Inos), nuclear factor erythroid 2-related factor 2 and tumour necrosis factor alpha (Chen et al.,2016). Protective genes against oxidative stress, inflammation, and accumulation of toxic metabolites contain a promoter element known as antioxidant response element (ARE). Nuclear factor erythroid 2- related factor-2 (Nrf2) binds to antioxidant response element (ARE). This action leads to the induction of cytoprotective genes, which reports have shown to play a protective role in central nervous system diseases (Gopinath et al., 2012). Continuous exposure to vanadium and its accumulation in the brain can result in a series of health conditions, and this might be linked with the pathogenesis of some specific neurological disorders. The consequence of the long- period exposure can even be more severe pathologically, and this in-turn may affect day-to-day activities and safety at workplace (Adekeye et al., 2020). This study gives us a chance to see the antioxidant effect of naringin on neurotoxicity caused by oxidative stress from vanadium oxides.

MATERIALS AND METHODS

Ethical approval and experimental design

All the procedures performed during this experiment are in accordance with the National institute of Health Guide for care and use of Laboratory Animals (NIH, 1985) and the Department of Human Anatomy, College of Medical and Health Sciences, Afe Babalola University Ado Ekiti, Nigeria (AB/EC/22/01/95). We endeavor to minimize the number of animals used for this experiment, as well as their suffering. Forty healthy male Wistar rats weighing 150-180 g were purchased from the Animal Holdings of the Department of Anatomy, Afe Babalola University, Ado-Ekiti. The rats were placed in a standard laboratory rat cage. They were given access to water and standard rat chow ad libitum. After a two-week acclimatization period, animals were randomly divided into four (4) groups with n = 10 per group. This included: Control as group CTL (received H_2O), Naringin as group NAR (received 30 mg/kg bw of naringin orally for 14 days), Vanadium + Naringin as group NAR+VAN (received 10 mg/kg of vanadium intraperitoneally for 7 days and 30 mg/kg bw of naringin orally for 14 days), and Vanadium as group VAN (received 10 mg/kg bw of vanadium Intraperitoneally for 7 days).

The oral administrations were carried out with an oral cannula and the Vanadium was administered intraperitoneally. The duration of the experiment was 21 days (Fafure et al., 2020; Yang et al., 2021).

Chemicals and reagents

RBFOX3 polyclonal antibody (Elabscience China, Cat No- E-AB-70267, 1:150), NLRP3 inflammasome polyclonal antibody (Elabscience China, Cat No- E-AB-65952, 1:200), 2- step plus poly-HRP Anti-mouse/rabbit IgG Detection system, DAB solution (Elabscience China, Cat No- E-IR-R217), Triton-X (Elabscience China, Cat No- E-IR-R122), phosphate buffered solution (Elabscience China, Cat No- EP-CM-L0007), Naringin (Sigma-Aldrich,

St. Louis, MO, USA; Cat No-N1376), Vanadium (Chembid, Germany, Cat No- 13718-26-8).

Neurobehavioral study

Memory index were assessed in the animals using novel object recognition (NOR) (IITC Life Science, Woodland Hills, CA, USA), and Y-maze test. These tests carried out in a sound- controlled behavior analysis room with a proper illumination as previously described by (Lueptow, 2017; Kraeuter et al., 2019). A practice session was conducted at the beginning of the experiment, and the final test for both NOR and Y-maze was done at the end of the treatment.

Animal sacrifice and sample preparation

The animals were anesthetized with 50 mg/kg bw of sodium pentobarbital (intraperitoneally) 48 hours after the last administration, followed by intra-cardiac perfusion fixation with normal saline and 4% paraformaldehyde respectively. The animals meant for biochemical analysis were perfused intracardially with phosphate buffered solution. The brain was removed, and the region of the hippocampus was homogenized in phosphate buffer solution and centrifuged at 10,000 rpm for 10 min at 4°C (Olaniyi and Areloegbe, 2022). The supernatant was collected and frozen until it was needed for the biochemical assay (Glutathione Peroxidase and Catalase). The brain meant for histological analysis was post-fixed in 4% paraformaldehyde, In addition, the region of the hippocampus (interaural 3.72 mm: 5.28 mm away from the Bregma) was grossed using rat brain atlas (Paxinos and Watson, 2017), and passed through routine tissue processing. Sections from the embedded blocks were obtained for immunohistochemical analysis.

Immunohistochemical procedure

For immunohistochemistry studies, Sections from 5 animals were routinely prepared for immunohistochemistry and quantified using the cell counter plug-in of ImageJ (Version 1.53). Sections of the CA1 field of the hippocampus (5 µm thick) were coronally cut with a microtome. Antigen retrieval with citrate buffer was done using the microwave (15 min) immediately after hydrating the sections, after which endogenous peroxidase activity was blocked by incubating the sections in 3% hydrogen peroxide solution for 10 min. Sections were washed with phosphate buffered solution for 2 min, 3 times. Normal goat serum was used to block the nonspecific binding sites with incubation time of 20 min. Sections were immunolabelled with primary antibodies directed against RBFOX3 (for neuronal cell distribution) and NLRP3 (for inflammation) polyclonal antibodies (NLRP3 1:200; RBFOX3 1:150, Elabscience, China), with incubation time of 2 hours at a room temperature or 37°C. Sections were incubated in Polyperoxidase-anti-Mouse/Rabbit IgG (E-IR-R217) secondary antibody for 20 min (Fafure et al., 2022). Sections were washed with phosphate buffered solution for 2 min, 3 times. A fresh prepared DAB working solution was added to the section, rinsed after obtaining the desired coloration, followed by counterstaining in Hematoxylin solution, dehydrating, transparentizing and sealing were carried out. Sections were photographed using an OPTU-EDU light microscope.

Data and statistical analysis

Image J was used to count the number of neurons present in each group after the experiment using a grid of 20000-60000 depending on the size of neurons. Statistical group analysis was performed using the Graphpad prism 8.01. Data are presented as means ± SD. One-way ANOVA was used to compare the mean values of variables and post hoc analysis was performed with post hoc Turkey test. Statistically significance was considered at $p < 0.05$.

RESULTS

Effects of Naringin on memory alteration following vanadium induction

The NOR test was used to assess non-spatial short-term working memory, while Y-maze test is used to evaluate short-term spatial working memory in the animals. The analysis showed that exposure to vanadium decreased memory index as seen in the vanadium (VAN) group and treatment with Naringin was effective in improving memory impairment as seen in the naringin and vanadi-

um (NAR+VAN) group. A decrease in memory index after exposure to vanadium can be seen in the vanadium (VAN) group and treatment with Naringin was effective in ameliorating these changes, as seen in the naringin and vanadium (NAR+VAN) group.

Effect of Naringin on Oxidative stress changes following vanadium induction

Glutathione peroxidase (GPX) and Catalase (CAT) levels were assessed in a section of hippocampus of rat following the administration of vanadium to induce neurotoxicity and treatment with naringin. Significant decreased in the glutathione peroxidase levels upon exposure to vanadium was seen in the vanadium (VAN) group. Treatment with Naringin showed a significant increase in GPX levels (GPX) levels as seen in the naringin and vanadium (NAR+VAN) group. Also, a reduction in the catalase activity upon exposure to vanadium was noticed in the vanadium (VAN) group. An improvement in catalase levels was noticed after treatment with Naringin as seen in the naringin and vanadium (NAR+VAN) group. Catalase levels in NAR+VAN group when compared to VAN group. There is also an increase in the hippocampal catalase level, when exposed to just Naringin in the NAR group when compared to VAN group.

Immunohistochemistry demonstration of Inflammasome and neuronal cells in the CA1 field of the hippocampus

RBFOX3 antibodies are used to identify mature neurons in cell cultures and tissue sections. This stain was used to identify viable neuronal cell bodies in the CA1 field of the hippocampus proper of the rats. The VAN group showed very little number of viable neuronal cells, while the CTL and NAR group revealed a lot of viable neuronal cells, as shown in the photomicrograph. In the NAR+VAN group also showed a lesser number of viable cell bodies when compared to the CTL and NAR groups, but showed a higher number of viable cell bodies when compared to the VAN group.

NLRP3 inflammasome is used as a marker for inflamed or damaged cell in the CA1 field of the hippocampus. The CTL and NAR groups showed very little NLRP3immuno-positive cells, whereas the VAN group showed the highest number of NLRP3 immuno-positive cells as seen in the photomicrograph below. Also, the NAR + VAN group showed expression of NLRP3 immuno-positive cells.

DISCUSSION

Metals are the most distributed pollutants globally with a propensity to amass in some human tissues and with huge toxic potentials at relatively low concentration. Vanadium is a heavy metal and is specially stored in certain organs, mainly in bone, kidney, and liver (Cortizo et al., 2000). Vanadium compounds have the ability to interchange into different species constantly within the cell in the presence of ROS, which makes it a powerful inducer of cell death (necrosis) (Rojas-Lemus et al., 2020). Neurotoxic metals such as vanadium cause blood brain barrier disruption, neuropathology and neuronal damage, which can trigger CNS alterations.

The hippocampus, being a part of the limbic system, performs several brain functions such as learning, memory, and spatial coding (Avila-Costa et al., 2006). The hippocampus is vulnerable to oxidative stress and oxidative damage (Salim et al., 2016). Thus, oxidative damage to this brain area can disrupt normal synaptic neurotransmission, cause impairment in memory function, cell proliferation and degeneration; it can alter structural changes, and distort neurogenesis. Therefore, the maintenance of a normal redox state in hippocampal neurons is crucial in the impediment of memory decline (Marosi et al., 2012).

Oxidative stress is a result of a mismatch between the generation of faulty reactive oxygen species (ROS) and the organism's capacity to moderate their harmful effects (Viswanatha et al., 2017). The antioxidant defense is made up by the antioxidant enzymatic actions.

Superoxide radicals are converted to hydrogen peroxide (free radical), and the hydrogen peroxide is eliminated by glutathione peroxidase (GPx) and/or catalase (CAT). These enzymes are responsible for the destruction of excess hydrogen peroxide formed in the nervous tissue. However, when

this intrinsic antioxidant defense is low, supplementation from an external source is required to strengthen the antioxidant (Marosi et al., 2012).

Naringin possesses various pharmacological properties such as antioxidant, anti-inflammatory, neuroprotective, hepatoprotective, anti-diabetic, anti-atherosclerotic, anti-hyperlipidemic, reno- protective, cardio-protective properties, and so on (Viswanatha et al., 2017). Several published papers have reported the protective role of naringin through modulations of antioxidant in numerous parts of the brain (Viswanatha et al., 2017).

Behavioral analysis result, using the Novel Object Recognition (NOR) test and the Y maze test to assess spatial memory. The results from the Y maze analysis shows a significant decrease in the percentage of alteration in the vanadium-only (VAN) group as compared to the other groups, as shown in Fig. 1A. This result is in correspondence with the study by Franklin et al. (2021) on the ameliorative role of Khaya anthotheca in vanadium-induced cognitive dysfunction in mice. Vanadium elicits its harmful reactions through the formation of free radicals, when it crosses the blood brain barrier and in turns leads to lipid peroxidation and a damage in the antioxidant defense of the tissue. In the study by Franklin et al. (2021), it was reported that the vanadium-induced animals had the least number of arms entries in the Y maze. The Novel Object Recognition test (NOR) is also widely used to evaluate recognition memory in mice. In Fig. 1B, it can be noted that there was a steady decrease in percentage of memory index, with the least value being the vanadium only (VAN) group. This has been proven in the study by Khadija et al. (2018) on how short-term exposure to titanium, aluminum, and vanadium (Ti 6Al 4V) alloy powder extremely affects behavioral and antioxidant metabolites in male albino mice. The study reported significant decrease and compromise in the animals' novel object recognition capability. In this current study, it is noted that the decline in memory index between all four groups were progressive, as seen in Fig. 1B.

In the results of the biochemical analysis, it was noted that a decrease in glutathione peroxidase and catalase (Cat) level was observed in the vanadium-only (VAN) group, as seen in Fig. 2A. This was in accordance with Folarin et al. (2017a), who studied changes in the central nervous system antioxidant level following chronic vanadium

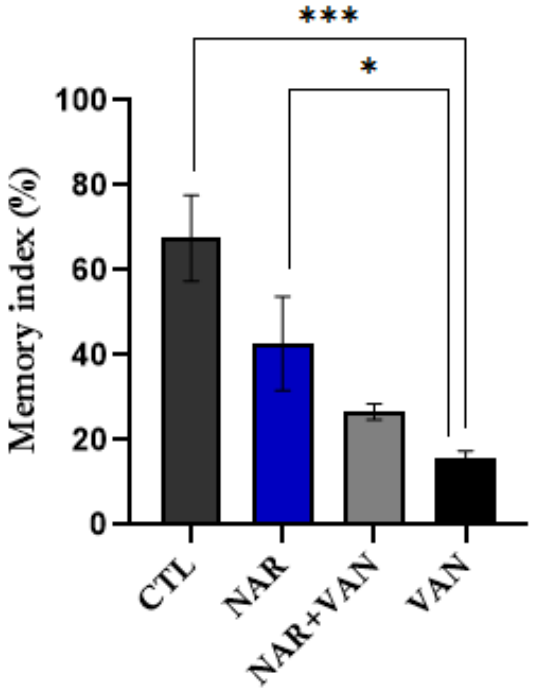

Fig. 1A.- Bar chart representation showing changes in non-spatial memory function from the NOR test following exposure to VAN and treatment with Naringin, comparison between groups by one-way ANOVA followed by Tukey's multiple comparison test shows significant decrease in memory index in VAN group (***p< 0.0001) when compared with CTL group. Administration of naringin only showed an increase in memory index of the NAR only group when compared to VAN. Legend: CTL = control group; NAR = naringin group; NAR+VAN= Naringin + Vanadium group; VAN = vanadium group.

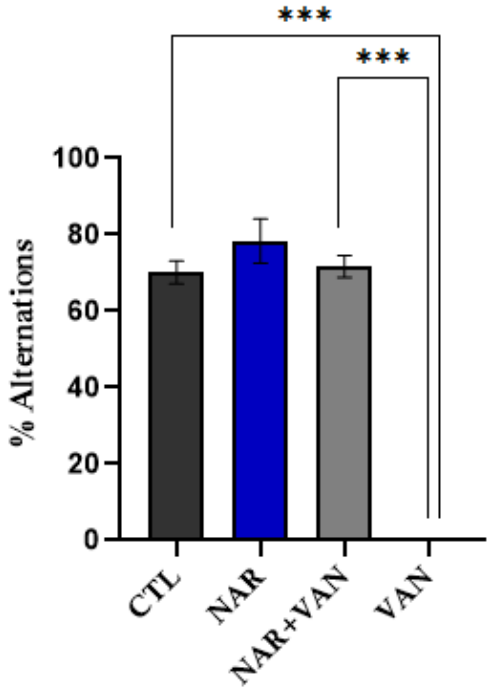

Fig. 1B.- Bar chart representation showing changes in short term spatial memory following exposure to VAN and treatment with Naringin. Comparison between groups by one-way ANOVA followed by Tukey's multiple comparison test shows significant decrease in memory index in VAN group (***p<0.0001) when compared with CTL group. Treatment with Naringin significantly increased memory index in NAR+VAN group (***p<0.0001) when compared to CTL. Legend: CTL = control group; NAR = naringin group; NAR+VAN= Naringin + Vanadium group; VAN = vanadium group.

exposure in mice. It was reported that chronic vanadium administration led to oxidative damage shown by significant increase nitric oxide, Malondialdehyde, and hydrogen peroxide production, associated with a reduction in the activities of intrinsic antioxidant system, superoxide dismutase (SOD), Glutathione peroxidase (GPX), and Glutathione (GSH) in the brain. An increase in glutathione peroxidase and catalase (Cat) level was observed in the naringin + vanadium (NAR + VAN) group after treatment with naringin following exposure to vanadium as seen in Fig. 2B. This is in correspondence with the research by Kumar et al. (2010) in the study of Naringin's attenuation of memory impairment, and oxidative stress induced by d-galactose in mice. Results from the immunohistochemistry analysis showed changes in numbers of viable cells and numbers of inflamed cells. The RBFOX3 marker was used to evaluate the number of viable neuronal cells in the CA1 region of the hippocampus. From Fig. 3A, the vanadium-only (VAN) group shows a decrease in number of viable cells. In accordance with Folarin et al. (2017b) study on neuro-inflammatory profiles and metal distribution after chronic vanadium administration and withdrawal in mice, where he revealed that damaged pyramidal cells, with morphological alterations including cell clustering, loss of layering pattern and cytoplasmic vacuolation in the vanadium-exposed brains. The naringin + vanadium (NAR + VAN) group showed an increase in number of viable cells after administration of naringin following vanadium exposure. The NLRP3 Inflammasome marker used to detect NLRP3 positive cell. Fig. 3B showed that the vanadium-only (VAN) group had the largest amount of NLRP3 positive cell. Inflammation is a protective response of an organism to the biologically, chemically, or physically mediated injury. The process is initiated by inflammatory mediators, including cytokines and chemokines that are released by injured tissue, which attract leukocytes to the damaged site (Zwolak, 2013). Therapeutic treatment with naringin following vanadium administration as seen in the naringin + vanadium (NAR+VAN) group showed a lower amount of NLRP3 positive cells. The anti-inflammatory effect of Naringenin was linked to the activation of transcription factor Nrf2, which functions as an agonist of aryl-hydrocarbon receptors, and subsequently reduces the formation of ROS and inflammatory mediators in the cells (Joshi et al., 2018).

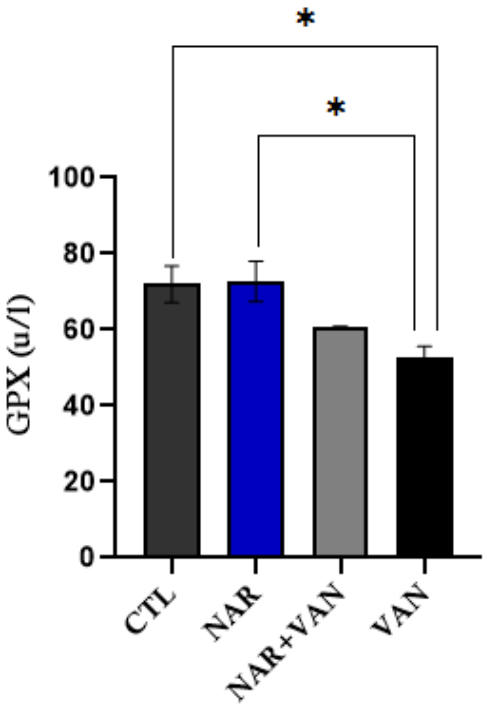

Fig. 2A.- Bar chart representation showing changes in glutathione peroxidase level in the hippocampus across all the groups of rats used in the experiment. The groups were compared by one-way ANOVA followed by Tukey's multiple comparison test. A decrease in the hippocampal glutathione peroxidase level in (VAN) group when compared with control (CTL) group (*p<0.01). Treatment of the (VAN) group with Naringin show an increase in the glutathione peroxidase levels as seen in NAR+VAN group when compared to VAN group. There is an increase in the hippocampal glutathione level in rat exposed to just Naringin in the NAR group when compared to VAN group (*p<0.02).

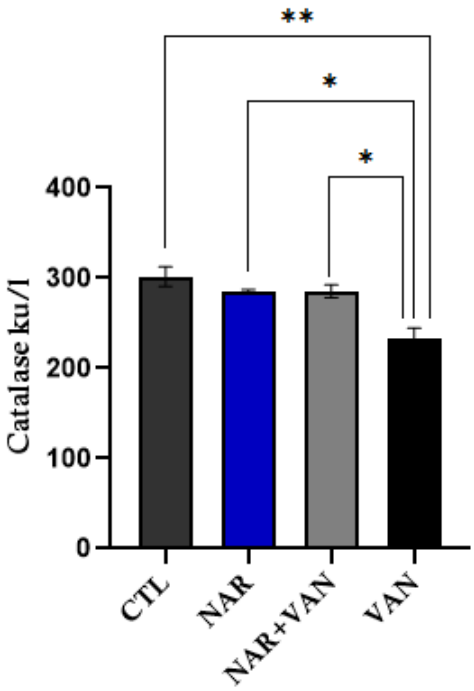

Fig. 2B.- Bar chart showing changes in hippocampal catalase level using one-way ANOVA followed by Tukey's multiple comparison test to compare between the group. The result of the analysis showed a decrease in the hippocampal catalase level in VAN group when compared with CTL group(**p<0.05). Upon treatment with Naringin, there is an increase in hippocampal catalase levels in NAR+VAN group when compared to VAN group. There is also an increase in the hippocampal catalase level, when exposed to just Naringin in the NAR group when compared to VAN group.

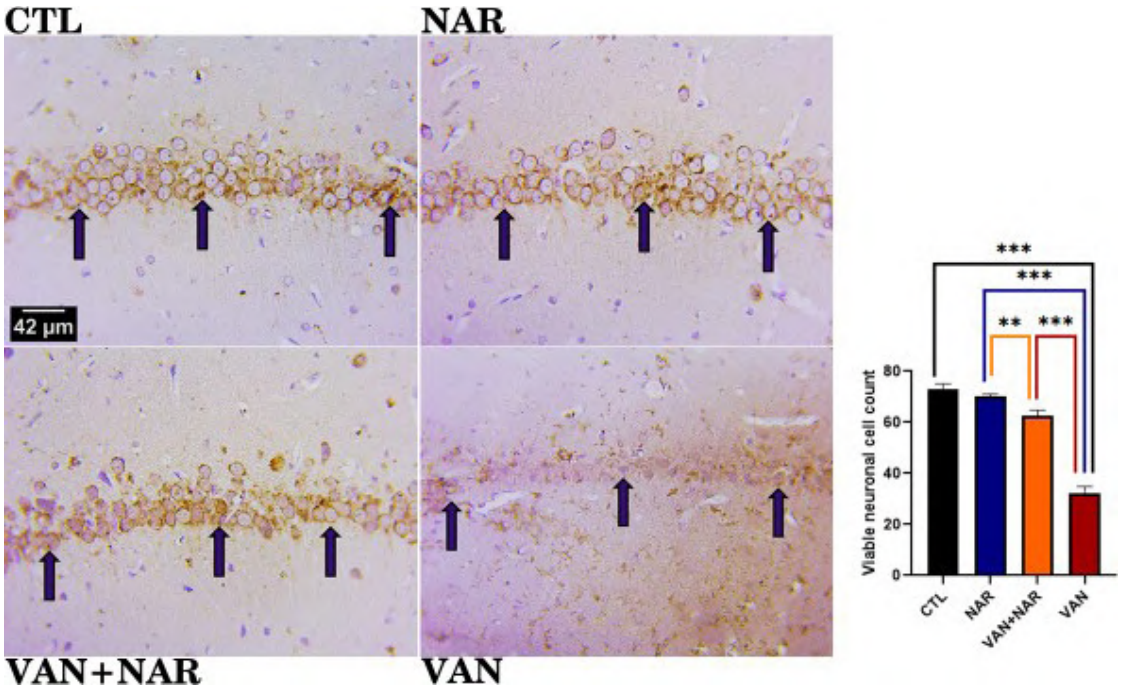

Fig. 3A.- Photomicrograph showing RBFOX3 viable cell bodies in the CA1 region. Dark brownish round cells indicate the viable nerve cell bodies. Bar chart representation showing viable neuronal cell count following exposure to VAN and treatment with naringin. Comparison by one-way ANOVA followed by Tukey's multiple comparison test showed a significant decrease in viable neuronal cells in VAN group when compared with CTL group(***p<0.0001). Upon treatment with Naringin, an increase in the number of viable neuronal cell count in NAR+VAN group was observed when compared to VAN group (***p<0.0001). There is also an increase in the viable neuronal cell count in rat the NAR group when compared to VAN group (***p<0.0001). x1200 (Scale bar: 42µm).

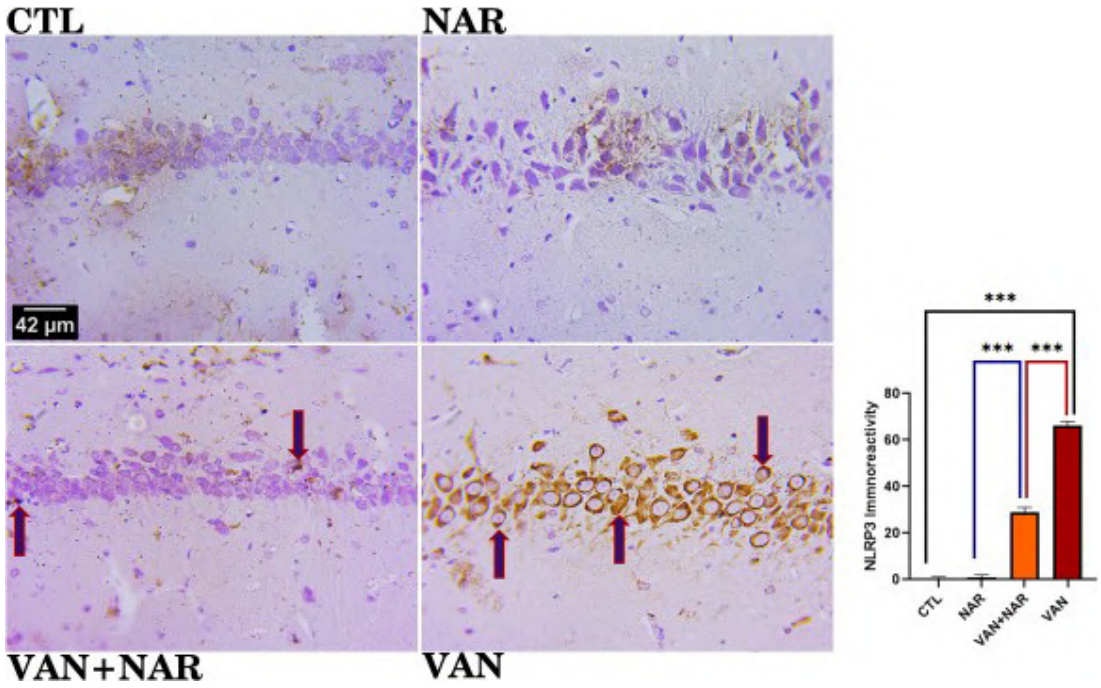

Fig. 3B.- Photomicrograph showing NLRP3 immuno-positive cells in the CA1 region. Dark brownish round cells indicate the cells that expressed inflammasome. Bar chart representation showing the cell count following exposure to VAN and treatment with naringin. Comparison between groups by one-way ANOVA followed by Tukey's multiple comparison test shows a significant increase in inflammasome in VAN group when compared with CTL group (***p<0.001). Treatment with Naringin reduced the immunopositive cell count in NAR+VAN group when compared to VAN group (***p<0.001). There is equally a statistically significant reduction in the immunopositive cell count in rat exposed to just Naringin in the NAR group when compared to VAN group (***p<0.001). x1200 (Scale bar: 42µm).

CONCLUSION

This study has proven the adverse effects of chronic vanadium exposure on the body. It has also shown the therapeutic effects of naringin as an antioxidant and anti-inflammatory agent in mitigating the neurotoxic of oxidative stress by heavy metals, especially vanadium.

ACKNOWLEDGEMENTS

The authors appreciate the support of histology and immunohistochemistry unit of Afe Babalola University, Ado-Ekiti, Nigeria, and the technical support of Mrs Oluwabukola Fafure.

REFERENCES

ADEKEYE AO, IRAWO GJ, FAFURE AA (2020) Ficus exasperata Vahl leaves extract attenuates motor deficit in vanadium-induced parkinsonism mice. *Anat Cell Biol*, 53(2): 183-193.

AVILA-COSTA MR, FORTOUL TI, NIÑO-CABRERA G, COLÍN-BARENQUE L, BIZARRO-NEVARES P, GUTIÉRREZ-VALDEZ AL, ORDÓÑEZ-LIBRADO JL, RODRÍGUEZ-LARA V, MUSSALI-GALANTE P, DÍAZ-BECH P, ANAYA MARTÍNEZ V (2006) Hippocampal cell alterations induced by the inhalation of vanadium pentoxide (V2O5) promote memory deterioration. *Neurotoxicology*, 27(6): 1007-1012.

BARCELOUX DG, BARCELOUX D (1999) Vanadium. *J Toxicol Clin Toxicol*, 37(2): 265-278.

CHEN L, ZHANG C, HAN Y, MENG X, ZHANG Y, CHU H, MA H (2019) Gingko biloba extract (EGb) inhibits oxidative stress in neuro 2A cells overexpressing APPsw. *BioMed Res Int*, 2019: 1-9.

CHEN T, SU W, YAN Z, WU H, ZENG X, PENG W, GAN L, ZHANG Y, YAO H (2018) Identification of naringin metabolites mediated by human intestinal microbes with stable isotope-labeling method and UFLC-Q-TOF-MS/MS. *J Pharm Biomed Anal*, 161: 262-272.

CORTIZO AM, BRUZZONE L, MOLINUEVO S, ETCHEVERRY SB (2000) A possible role of oxidative stress in the vanadium induced cytotoxicity in the MC3T3E1 osteoblast and UMR 106 osteosarcoma cell lines. *Toxicology*, 147(2): 89-99.

EZE VC, OKEKE DO, NWABUDIKE AR, ADUAKA CN (2022) Assessment of vanadium pollution and ecological risk in some selected waste dumpsites in Southeastern Nigeria. *Health Environ*, 3(1): 169-175.

FAFURE AA, EDEM EE, OBISESAN AO, ENYE LA, ADEKEYE AO, ADETUNJI AE, NEBO KE, OLUSEGUN AA, FAFURE OE (2022) Fermented maize slurry (Ogi) and its supernatant (Omidun) mitigate elevated intraocular pressure by modulating BDNF expression and glial plasticity in the retina-gut axis of glaucomatous rats. *J Complement Integr Med*, 19(4): 887-896.

FOLARIN OR, ADARAMOYE OA, AKANNI OO, OLOPADE JO (2017a) Changes in the brain antioxidant profile after chronic vanadium administration in mice. *Metab Brain Dis*, 33(2): 377-385.

FOLARIN OR, SNYDER AM, PETERS DG, OLOPADE F, CONNOR JR, OLOPADE JO (2017b) Brain metal distribution and neuro-inflammatory profiles after chronic vanadium administration and withdrawal in mice. *Front Neuroanat*, 11: 58.

FRANKLIN ZG, LADAGU AD, GERMAIN JEAN MAGLOIRE KW, FOLARIN OR, SEFIRIN D, TASHARA TG, DIEUDONNE N, OLOPADE JO (2021) Ameliorative effects of the aqueous extract of Khaya anthotheca (Welw.) C.DC (Meliaceae) in vanadium induced anxiety, memory loss and pathologies in the brain and ovary of mice. *J Ethnopharmacol*, 275: 114099.

GHOSH SK, SAHA R, SAHA B (2014) Toxicity of inorganic vanadium compounds. *Res Chem Intermed*, 41(7): 4873-4897.

GOPINATH K, SUDHANDIRAN G (2012) Naringin modulates oxidative stress and inflammation in 3-nitropropionic acid-induced neurodegeneration through the activation of nuclear factor-erythroid 2-related factor-2 signalling pathway. *Neuroscience*, 227: 134-143.

JOSHI R, KULKARNI YA, WAIRKAR S (2018) Pharmacokinetic, pharmacodynamic and formulations aspects of Naringenin: An update. *Life Sci*, 215: 43-56.

KHADIJA G, SALEEM A, AKHTAR Z, NAQVI Z, GULL M, MASOOD M, IQBAL F (2018) Short term exposure to titanium, aluminum, and vanadium (Ti 6Al 4V) alloy powder drastically affects behavior and antioxidant metabolites in vital organs of male albino mice. *Toxicol Rep*, 5: 765-770.

KRAEUTER AK, GUEST PC, SARNYAI Z (2019) The Y-maze for assessment of spatial working and reference memory in mice. In: *Preclinical models*. Humana Press, New York, pp 105-111.

KUMAR A, PRAKASH A, DOGRA S (2010) Naringin alleviates cognitive impairment, mitochondrial dysfunction and oxidative stress induced by d-galactose in mice. *Food Chem Toxicol*, 48(2): 626-632.

LUEPTOW LM (2017) Novel object recognition test for the investigation of learning and memory in mice. *J Vis Exp*, 126: 55718.

MAROSI K, BORI Z, HART N, SÁRGA L, KOLTAI E, RADÁK Z, NYAKAS C (2012) Long-term exercise treatment reduces oxidative stress in the hippocampus of aging rats. *Neuroscience*, 226: 21-28.

MEMARIANI Z, ABBAS SQ, UL HASSAN SS, AHMADI A, CHABRA A (2020) Naringin and naringeninin as anticancer agents and adjuvants in cancer combination therapy; efficacy and molecular mechanisms of action, a comprehensive narrative review. *Pharmacol Res*, 2020: 105264.

OLANIYI KS, ARELOEGBE SE (2022) Suppression of PCSK9/NF-kB-dependent pathways by acetate ameliorates cardiac inflammation in a rat model of polycystic ovarian syndrome. *Life Sci*, 300: 120560.

OLAOLORUN FA, OLOPADE FE, USENDE IL, LIJOKA AD, LADAGU AD, OLOPADE JO (2021) Neurotoxicity of vanadium: In: *Advances in Neurotoxicology,* Vol. 5. Academic Press, pp 299-327.

PAXINOS G, WATSON C (2007) The rat brain in stereotaxic coordinates/George Paxinos: Charles Watson, Amsterdam.

PENG H (2019) A literature review on leaching and recovery of vanadium. *J Environ Chem Engineer*, 7(5): 103313.

REHDER D (2015) The role of vanadium in biology. *Metallomics*, 7(5): 730-742.

ROJAS-LEMUS M, BIZARRO-NEVARES P, LÓPEZ-VALDEZ N, GONZÁLEZ VILLALVA A, GUERRERO PALOMO G, CERVANTES-VALENCIA ME, FORTOUL-VAN DER GOES T (2020) Oxidative stress and Vanadium. *Genotoxicity Mutagenicity Mech Test Methods*, 3: 1-19.

USENDE IL, EMIKPE BO, OLOPADE JO (2017) Heavy metal pollutants in selected organs of African giant rats from three agro-ecological zones of Nigeria: evidence for their role as an environmental specimen bank. *Environment Sci Pollution Res*, 24(28): 22570-22578.

VISWANATHA GL, SHYLAJA H, MOOLEMATH Y (2017) The beneficial role of Naringin- a citrus bioflavonoid, against oxidative stress-induced neurobehavioral disorders and cognitive dysfunction in rodents: A systematic review and meta-analysis. *Biomed Pharmacother*, 94: 909-929.

XIONG Z, XING C, XU T, YANG Y, LIU G, HU G, CAO H, ZHANG C, GUO X, YANG F (2021) Vanadium induces oxidative stress and mitochondrial quality control disorder in the heart of ducks. *Front Vet Sci*, 8: 756534.

ZOU W, LUO Y, LIU M, CHEN S, WANG S, NIE Y, CHENG G, SU W, ZHANG K (2015) Human intestinal microbial metabolism of naringin. *Eur J Drug Metab Pharmacokinet*, 40(3): 363-367.

ZWOLAK I (2013) Vanadium carcinogenic, immunotoxic and neurotoxic effects: a review of in vitro studies. *Toxicol Mech Methods*, 24(1): 1-12.

Willingness toward donation in Mexico and the influence of personality

Daniela C. Gonzalez-Cruz*, Rodrigo E. Elizondo-Omaña*, Alejandro Quiroga-Garza, Javier H. Martinez-Garza, David de la Fuente-Villarreal, Oscar de la Garza-Castro, Katia Guzman-Avilan, Jorge Gutierrez-de-la-O, Santos Guzman-Lopez

Department of Human Anatomy, School of Medicine, Universidad Autonoma de Nuevo Leon, Monterrey, Nuevo León, México

SUMMARY

Organ and body donation are key elements in health sciences. This study examines the perception of the population toward organ and body donation and how it may be influenced by personality traits. A cross-sectional study was designed, in which a questionnaire including items of demographic data and attitudes toward organ and body donation were distributed among the general population. A validated questionnaire for the screening of personality disorders was applied as well. 202 questionnaires were obtained, 76 (37.6%) from men and 126 (62.4%) from women. A total of 95.2% of women and 93.4% of men responded to be in favor of organ donation (p>0.05). However, only 40.3 % of women and 37.8% of men were in favor of body donation. Sixty-eight percent of participants had a probable personality disorder. Of those against body donation, 67% had a probable personality disorder. Body donation is not a well-known option among the Mexican population. However, for a program to be feasible, it is necessary to raise public awareness regarding donation and its implications to achieve greater engagement.

Key words: Donation – Organ donation – Body donation – Dissection – Motivation for donation – Human anatomy – Education

INTRODUCTION

Donation is a key element in medicine. Organ donation is widely accepted around the world and improves the quality of life of thousands every year (Milaniak et al., 2018). Not only is organ donation the ultimate way of contributing to medicine in an altruistic manner; body donation is too, in particular in research and education. The use of the human body has been a fundamental tool for teaching and studying gross anatomy for centuries (Biassuto et al., 2006; Jeyakumar et al., 2020; Tapia-Nañez et al., 2022). Students develop anatomical and surgical knowledge directly from the body, as well as professionalism and empathy (Papa and Vaccarezza, 2013; Quiroga-Garza et al., 2017; Reyes-Hernandez et al., 2016; Riederer, 2016; del Campo, 2016). Donation programs contribute to transplantation, medical education, and

Corresponding author:
Dr. Santos Guzmán López. E-mail: dr.santos.anato@gmail.com / Dr. Jorge Gutiérrez de la O. E-mail: jorgegdelao@yahoo.com. Departamento de Anatomia Humana, Facultad de Medicina, Ave. Francisco I. Madero y Aguirre Pequeño, s/n, Col. Mitras Centro, Monterrey, Nuevo León, México. Phone: +521 81 8329 4171.

* These authors participated equally in the study and both should be considered first authors of this study

Submitted: October 20, 2022. **Accepted:** January 16, 2023

https://doi.org/10.52083/XXES3736

research (Garment et al., 2007; Querevalú-Murillo et al., 2012). However, many countries still lack a formal donation program. (Quiroga-Garza et al., 2017; Wainman and Cornwall, 2019; Salinas-Alvarez et al., 2020).

Along with history, there have been changes concerning the methods used to study medicine and anatomy (Korf et al., 2008; McBride and Drake, 2018; Salinas-Alvarez et al., 2020). The recent COVID-19 outbreak disrupted the traditional education settings and challenged medical schools to adopt the use of available tools and innovative technologies (Iwanaga et al., 2021; Krebs et al., 2021; Muñoz-Leija et al., 2020; Pather et al., 2020). The use of imaging studies, virtual and augmented reality, 3D impression, and simulation models, have been increasing in popularity for anatomy education (Baskaran et al., 2016; Chytas et al., 2020; Fernández-Reyes et al., 2022; Gadaleta et al., 2020). However, many anatomists argue the importance of donors for dissection and prosection to actively complement learning. Students develop anatomical and surgical knowledge directly from the body, as well as professionalism and empathy (Papa and Vaccarezza, 2013; Sanchez del Campo, 2015; Reyes-Hernández et al., 2016; Riederer, 2016; Quiroga-Garza et al., 2017; Guerrero-Mendivil et al., 2023).

Current, legislation, costs, and ethics have influenced the dissection practice in gross anatomy laboratories. There is a limitation in the availability of bodies, primarily in countries without body donation programs, as is the case in most of Mexico (Quiroga-Garza et al., 2022, 2017; Salinas-Alvarez et al., 2020). Most medical schools continue to use unclaimed bodies for dissection and prosection as teaching tools in the laboratory while lacking formal donation programs (Quiroga-Garza et al., 2017; Salinas-Alvarez et al., 2020; Wainman and Cornwall, 2019). Research regarding perspectives is scarce (Elizondo-Omaña et al., 2005). Mexico has a low rate of organ donation, below the necessities of the healthcare system, due to a low donation culture (Centro Nacional de Trasplantes, 2021; Ríos et al., 2014). To strengthen and implement current organ donation programs, it is important to consider the psychological aspects and the lack of information of the general population (Hernández Rivera et al., 2020; Irving et al., 2012; Marván et al., 2017; Quiroga-Garza et al., 2017).

The objective of this study was to evaluate the perspective of the general population toward organ and body donation, as well as the personality spectrum of potential donors.

MATERIALS AND METHODS

A cross-sectional, descriptive study was designed with the purpose of evaluating the perception of the population toward organ and body donation after death. Simultaneously, the presence of personality disorders and their relation with the perception toward organ and body donation were assessed. Two questionnaires were applied voluntarily and anonymously to the general population. Age of ≥18 years was required for inclusion. Those who were healthcare professionals and students were excluded.

The Salamanca questionnaire was used for screening personality disorders. The result of the Salamanca questionnaire is obtained by a score of ≥ 4, which indicates a probable personality disorder, although further evaluation by a psychiatrist is necessary to confirm a diagnosis (García-Portilla et al., 2011; Giner Zaragoza et al., 2015). To assess attitudes and perceptions toward organ and body donation, a questionnaire was designed and validated by the Delphi method, in which demographic information was obtained as well (Supplement File 1). During recruitment of participants, the questionnaire and its purpose were explained by members of the research study, obtaining verbal informed consent. The questionnaires were printed and distributed at our University Hospital "Dr. José Eleuterio González", a tertiary level healthcare institution in the north of Mexico.

Responses from all questionnaires were registered in a database using 2020 Microsoft Excel for Mac, version 16.43 (Microsoft Corp., Redmond, WA). These were then analyzed using SPSS statistical package, version 25.0 (SPSS Inc., Chicago, IL). For the statistical analysis, the variables were divided into positive ("strongly agree" or "agree") and negative ("strongly disagree" or "disagree") responses. Those who answered "neither agree nor disagree" were considered neutral. The sam-

ple size was decided by availability. Quantitative variables are summarized in measures of central tendency and dispersion, and qualitative variables in frequencies and percentages. Associations in qualitative variables were tested using Pearson's Chi-Squared test and by calculating the odds ratio (OR) and associated 95% confidence intervals (CI) to measure the degree of association. Variables with a p-value of <0.05 were considered statistically significant.

The study was previously reviewed and approved by the ethics and research committees of our institution, with the registration AH18-005, certifying that it adheres to the guidelines of the General Health Law on Health Research in Human Beings of our country, as well as international guidelines and the Declaration of Helsinki. No external funding was used. Due to the design and intervention of the study, informed consent was approved to be given verbally from all participants. The authors declare no conflicts of interest. All authors have reviewed the final version of the manuscript and certify their responsibility for the work.

RESULTS

A total of 202 questionnaires were collected: most of the respondents, 126 (62.4%), were female and 76 (37.6%) were male. Ages ranged from 18 to 75 years and the mean age was of 32 ± 15 years. Catholicism was the most prevalent religion (83%), and 62.8% of participants have a graduate educational level (Table 1). Knowledge of the terms "organ donation" and "body donation", the willingness of participants to donate after death, and the spectrum of personality disorders were evaluated (Table 2). No statistical differences were identified among these variables and willingness toward donation.

Knowledge of donation

The term "organ donation" was recognized by 92.7% of female respondents and 89% of male respondents, in contrast to "body donation" which was known by only half of female respondents (51.2%) and 45.3% of male respondents (Table 2).

Table 1. Epidemiological characteristics of the study population as a whole.

Characteristic		**All participants n = 202**
Sex	Male	76 (37.6%)
	Female	126 (62.4%)
Age	mean±SD (years)	32 ±15.14
Religion	Catholic	151 (83%)
	Christian	15 (8.2%)
	Atheist	11 (6%)
	Other	5 (2.7%)
Education	Elementary	9 (4.5%)
	Middle	21 (10.6%)
	High School	34 (17.1%)
	Graduate	125 (62.8%)
	Postgraduate	10 (5%)

N: sample size; SD: standard deviation.

Willingness toward donation

High acceptance toward organ donation was given in contrast to acceptance of body donation. Over 90% of male and female respondents expressed being in favor of organ donation after death, while more than 50% were unwilling towards body donation. However, of those who had a negative response toward donating their body after death (n 106), over half (n 59, 55.7%) lacked knowledge of the term.

Screening for personality disorders

Sixty-eight percent of participants (n 137) had highly marked personality traits, which are classified as probable personality disorders. Of the 78 patients who were in favor of body donation after death, 51 (65.4%) had a probable personality disorder. Of the 191 participants who were in favor of organ donation, 130 (68%) had a probable personality disorder. Of those who answered to be against donating their organs after death (n 2), 1 had a probable personality disorder. Of those 106 participants who answered to be against body donation, 71 (67%) had a probable personality disorder. No statistical difference was found.

Table 2. Organ and Body Donation knowledge, willingness, and personality correlation.

		Organ Donation (%)					Body Donation (%)				
		n	**P**	**U**	**N**	***p***	**n**	**P**	**U**	**N**	***p***
Knowledge	Women	123	114 (92.7)	0 (0)	9 (7.3)	0.360	121	62 (51.2)	5 (4.1)	54 (44.6)	0.706
	Men	73	65 (89)	1 (1.4)	7 (9.6)		75	34 (45.3)	4 (5.3)	37 (49.3)	
Willingness	Women	126	120 (95.2)	5 (4)	1 (0.8)	0.850	124	50 (40.3)	9 (7.3)	65 (52.4)	0.920
	Men	76	71 (93.4)	4 (5.3)	1 (1.3)		74	28 (37.8)	5 (6.8)	41 (55.4)	
Personality	No PPD	65	61 (93.8)	3 (4.6)	1 (1.5)	0.860	65	27 (41.5)	3 (4.6)	35 (53.8)	0.625
	PPD	137	130 (94.9)	6 (4.4)	1 (0.7)		133	51 (38.3)	11 (8.3)	71 (53.4)	

n: sample population. P: Positive (knowledge of what the term means, in favor and strongly in favor to donate); U, Undecided; N, Negative (no knowledge of what the term means, against and strongly against to donate); Body donation was specified for a period of 1 year. PPD, Probable Personality Disorder (4 or more points on an item of the questionnaire is considered to have a probable personality disorder which must be corroborated by a mental health professional). Presence or absence of a personality disorder was studied with the willingness toward donation. Statistical analysis: chi-squared test.

Perceptions of body destination

Perception regarding what is considered appropriate regarding body destination after death was assessed as a multiple-choice question, but an open-ended option was included as well (Figure 1). Most participants (70%) consider it important to respect the wishes of the deceased. Twenty-eight percent of participants answered that burial or cremation with a religious ceremony was the preferred option. Only 2% reported it as "not relevant".

DISCUSSION

Our results demonstrate high knowledge and willingness towards organ donation. However, body donation is still a widely unknown term by the Mexican population. Most of the participants had strongly marked personality traits, which places them in a probable personality disorder category. However, we did not find statistically significant differences in trends toward donation among those with or without a probable personality disorder.

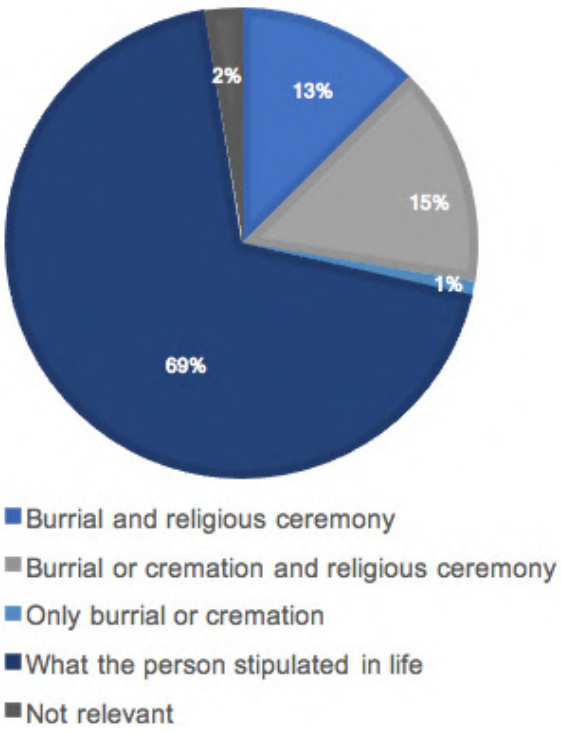

Fig. 1.- Participants' perception about what is considered appropriate regarding body destination after death.

Despite an apparent high willingness for organ donation from previous studies (Quiroga-Garza et al., 2017), the most recent data from the National Transplants Center CENATRA report 22,988 individuals on the waiting list for a transplant. Additionally, regarding the kidney –which is the most frequent organ transplanted– less than half (49%) in 2019 and less than a third (31.1%) in 2020 were from deceased-donor donations (Centro Nacional de Trasplantes, 2021).

In 2016, the first body donation program in Mexico was launched by the Universidad Nacional Autónoma de Mexico. Since then, the program has been marked by its success and advances in education, research, and innovation through the use of donors (Michel Olguin, 2019). Quiroga-Garza et al. (2017) researched willingness towards organ and body donation among anatomy students, near-peers, and educators in the medical school of Universidad Autónoma de Nuevo León. They report a high favor towards both types of donation (Quiroga-Garza et al., 2017), in contrast to our results of the general population, who are mostly compliant towards organ donation, but not body donation. Similar results were reported in India (Rokade and Gaikawad, 2012).

The Netherlands legislation on human body disposal mentions donating one's body to science as an alternative to burial or cremation, which has led to an increase of body donor candidates (Bolt et al., 2010). These findings support the importance of raising public awareness about the possibility of willingly donating one's body after death (Aneja et al., 2013; Cornwall et al., 2012; Winkelmann, 2016), as well as the benefits of a donation program (Cornwall et al., 2012; O'Neill, 2009). Altruism and empathy play an important role in motivation for donation (Hill, 2016; Milaniak et al., 2018), and the creation of a socially accepted donation program ruled by the law would support those interested in contributing to science to willingly register (Bolt et al., 2011).

Body donors aid in the education of future generations, research in anatomical sciences, development of new surgical techniques, patient safety, development of prostheses and medical equipment (Houser and Kondrashov, 2018; Korf et al., 2008; Riederer, 2016; Tapia-Nañez et al., 2022).

The limitations of this study include the omission of the calculation of the minimum sample size. Our sample was too small to be representative of the general community, which also made it impossible to analyze the personality traits individually. Considering that we did not find statistically significant differences among our results, we encourage future research where the number of participants might be expanded to search for the association between attitudes toward donation and personality traits. The use of a highly sensitive test to assess personality traits categorizes most of the sample in a probable personality disorder. The psychological outcomes from this study must be interpreted with caution.

Strategies to improve the current panorama

The International Federation of Associations of Anatomists published recommendations of good practice for the donation of human bodies and tissues for anatomical examination in 2012 (Jones, 2014). These include establishing a legal framework detailing the procedures and time frames; transparency and clear communication between the institution, potential donors, and their relatives; and encouragement for donors to discuss their intentions with their relatives to ensure that their wishes be carried out (Jones, 2014).

Cornwall et al. (2012) reported spouses, own children, and other closer relatives were the primary people who were consulted regarding donation. Donors' knowledge of body donation programs was primarily obtained through friends and family. A positive experience will provide a positive response among relatives that will help raise awareness of donation programs (Cornwall et al., 2012; El-Haddad et al., 2021).

Special lectures in ethics to students and healthcare professionals handling human remains for anatomical education and research must be held. Potential donors have experienced negative feelings when thinking of the potential type of treatment given to their bodies during laboratory practice (Hu and Huang, 2015; Richardson and Hurwitz, 1995; Rokade and Gaikawad, 2012), which highlights the importance of following ethical standards that promote respect, transparency, and trust (Jones, 2014).

Programs must target the population depending on demographics (da Rocha et al., 2017; Mueller et al., 2021). Gender does not influence willingness to donate. However, white single women seem to be the most prevalent donors in some programs (da Rocha et al., 2017; El-Haddad et al., 2021; Mueller et al., 2021). Most donors report an altruistic motive, although aiding medical sciences for research purposes and worry of costs have also been reported (Cornwall et al., 2012; da Rocha et al., 2017; Gürses et al., 2019; Jiang et al., 2020).

Local, social, and cultural aspects as these may influence attitudes towards donation (El-Haddad et al., 2021; Habicht et al., 2018). Body donation programs should be in collaboration with mental health professionals to aid in the assessment, needs, and preferences of potential donors, to offer a vast and dignified program (Bolt et al., 2011; McClea and Stringer, 2013; Riederer, 2016). Commemoration services for those who donated their bodies for medical education and research should be performed (Jones, 2014; Pawlina et al., 2011). These commemoration ceremonies can also be shared with relatives and registered living donors (El-Haddad et al., 2021; Quiroga-Garza et al., 2017). Future studies should evaluate attitudes and perspectives of family members of donors.

In a study by Štrkalj et al. (2020), of the universities of 71 countries surveyed only one-third used exclusively donated bodies. Unclaimed bodies are still widely used (Caplan and DeCamp, 2019; Habicht et al., 2018; Salinas-Alvarez et al., 2020). This still implies uncertain ethical and legal parameters that must be updated through awareness of the populations (Chia and Oyeniran, 2020; Cornwall et al., 2012; Sasi et al., 2020).

CONCLUSION

We found a positive outcome regarding attitudes toward organ donation. However, body donation in Mexico is a topic that remains unexplored and highly unaccepted. Our findings demonstrate that this population might show a positive response to a donation program that is well-funded and promoted. We suggest encouraging health professionals to explore donations and raise awareness among the surrounding community. Future studies are needed to determine factors influencing attitudes toward organ and body donation in underdeveloped countries. Efforts should be undertaken to change the mindset of the wider society toward body donation.

REFERENCES

ANEJA PS, BANSAL S, SOOD KS, SAXENA A (2013) Body donation - a dilemma among doctors. *J Evol Med Dent Sci*, 2. https://doi.org/10.14260/jemds/582

BASKARAN V, ŠTRKALJ G, ŠTRKALJ M, DI IEVA A (2016) Current applications and future perspectives of the use of 3D printing in anatomical training and neurosurgery. *Front Neuroanat*, 10: 69.

BIASSUTO SN, CAUSSA LI, CRIADO DEL RÍO LE (2006) Teaching anatomy: Cadavers vs. computers? *Ann Anat*, 188: 187-190.

BOLT S, VENBRUX E, EISINGA R, KUKS JBM, VEENING JG, GERRITS PO (2010) Motivation for body donation to science: More than an altruistic act. *Ann Anat*, 192(2): 70-74.

BOLT S, EISINGA R, VENBRUX E, KUKS JBM, GERRITS PO (2011) Personality and motivation for body donation. *Ann Anat*, 193(2): 112-117.

CAPLAN I, DECAMP M (2019) Of discomfort and disagreement: unclaimed bodies in anatomy laboratories at United States Medical Schools. *Anat Sci Educ*, 12(4): 360-369.

CENTRO NACIONAL DE TRASPLANTES (2021) Reporte Anual 2021 Receptores, Donación y Trasplantes en México. [https://www.gob.mx/cms/uploads/attachment/file/692109/ Anual2021.pdf] Accessed: 01 May 2022.

CHIA T, OYENIRAN O (2020) Ethical considerations in the use of unclaimed bodies for anatomical dissection: a call for action. *Ulutas Med J*, 6. doi.org/10.5455/umj.20201229101758

CHYTAS D, JOHNSON EO, PIAGKOU M, MAZARAKIS A, BABIS GC, CHRONOPOULOS E, NIKOLAOU VS, LAZARIDIS N, NATSIS K (2020) The role of augmented reality in Anatomical education: An overview. *Ann Anat*, 229: 151463.

CORNWALL J, PERRY GF, LOUW G, STRINGER MD (2012) Who donates their body to science? An international, multicenter, prospective study. *Anat Sci Educ*, 5(4): 208-216.

DA ROCHA AO, DE CAMPOS D, FARINA MA, PACINI GS, GIROTTO MC, HILBIG A (2017) Using body donor demographics to assist the implementation of donation programs in Brazil. *Anat Sci Educ*, 10(5): 475-486.

EL-HADDAD J, PRVAN T, ŠTRKALJ G (2021) Attitudes of Anatomy students toward commemorations for body donors: a multicultural perspective. *Anat Sci Educ*, 14(1): 89-98.

ELIZONDO-OMAÑA RE, GUZMÁN-LÓPEZ S, DE LOS ANGELES GARCÍA-RODRÍGUEZ M (2005) Dissection as a teaching tool: Past, present, and future. *Anat Rec B New Anat*, 285(1): 11-15.

FERNÁNDEZ-REYES BA, FLORES-GONZÁLEZ AK, ALVAREZ-LOZADA LA, GUERRERO-ZERTUCHE JT, ARRAMBIDE-GARZA FJ, QUIROZ-PERALES XG, QUIROGA-GARZA A, ELIZONDO-OMAÑA RE, GUZMÁN-LÓPEZ S (2022) The importance of simulation training in surgical sciences. *Int Surg J*, 9: 1289-1293.

GADALETA DJ, HUANG D, RANKIN N, HSUE V, SAKKAL M, BOVENZI C, HUNTLEY CT, WILLCOX T, PELOSI S, PUGLIESE R, KU B (2020) 3D printed temporal bone as a tool for otologic surgery simulation. *Am J Otolaryngol*, 41(3): 102273.

GARCÍA-PORTILLA M, BASCARÁN M, SÁIZ P, PARELLADA M, BOUSOÑO M, BOBES J (2011) Instrumentos de evaluación para la personalidad y sus trastornos. Cuestionario Salamanca de Trastornos de la Personalidad. *Banco Instrumentos Básicos para la Práctica la Psiquiatría Clínica*, 6: 204-223.

GARMENT A, LEDERER S, ROGERS N, BOULT L (2007) Let the dead teach the living: the rise of body bequeathal in 20th-century America. *Acad Med*, 82(10): 1000-1005.

GINER ZARAGOZA F, LERA CALATAYUD G, VIDAL SÁNCHEZ ML, PUCHADES MUÑOZ MP, RODENES PÉREZ A, CÍSCAR PONS S, CHICLANA ACTIS C, MARTÍN VIVAR M, GARULO IBÁÑEZ T, TAPIA ALCAÑIZ J, DÍAZ ESTEBAN E, FERRER FERRER L (2015) Diagnóstico y prevalencia de trastornos de la personalidad en atención ambulatoria: estudio descriptivo. *Rev Asoc Esp Neuropsiquiatría*, 35. https://doi.org/10.4321/s0211-57352015000400007

GUERRERO-MENDIVIL FD, ELIZONDO-OMAÑA RE, JACOBO-BACA G, QUIROZ-PERALES XG, SALINAS-ALVAREZ Y, MARTINEZ-GARZA JH, DE LA FUENTE-VILLARREAL D, QUIROGA-GARZA A, GUZMAN-LOPEZ S (2023) Payment with knowledge – a method for a training program of anatomy near-peer teachers and formation of future anatomists. *Anat Sci Edu*, doi: 10.1002/ase.2253. Online ahead of print.

GÜRSES İA, ERTAŞ A, GÜRTEKIN B, COŞKUN O, ÜZEL M, GAYRETLI Ö, DEMIRCI MS (2019) Profile and motivations of registered whole-body donors in Turkey: Istanbul University Experience. *Anat Sci Educ*, 12(4): 370-385.

HABICHT JL, KIESSLING C, WINKELMANN A (2018) Bodies for anatomy education in medical schools: An overview of the sources of cadavers worldwide. *Acad Med*, 93(9): 1293-1300.

HERNÁNDEZ RIVERA JCH, MOJICA OD, MENDOZA MS, BARBOSA LS, ALEJANDRI LS, SILVA RUEDA RI, PÉREZ LÓPEZ MJ, COVARRUBIAS LG, ÁLVAREZ CRUZ NL, MEJÍA VELÁZQUEZ JL, MENDOZA CG, GUTIÉRREZ WN, PANIAGUA SIERRA JR (2020) Factors that influence the attitude of the population to be a donor in Mexico. *Transplant Proc*, 52(4): 1036-1041.

HILL EM (2016) Posthumous organ donation attitudes, intentions to donate, and organ donor status: Examining the role of the big five personality dimensions and altruism. *Pers Individ Dif*, 88. https://doi.org/10.1016/j.paid.2015.09.021.

HOUSER JJ, KONDRASHOV P (2018) Gross anatomy education today: the integration of traditional and innovative methodologies. *Mo Med*, 115(1): 61-65.

HU D, HUANG H (2015) Knowledge, attitudes, and willingness toward organ donation among health professionals in China. *Transplantation*, 99(7): 1379-1385.

IRVING MJ, TONG A, JAN S, CASS A, CHADBAN S, ALLEN RD, CRAIG JC, WONG G, HOWARD K (2012) Community attitudes to deceased organ donation: A focus group study. *Transplantation*, 93(10): 1064-1069.

IWANAGA J, LOUKAS M, DUMONT AS, TUBBS RS (2021) A review of anatomy education during and after the COVID-19 pandemic: Revisiting traditional and modern methods to achieve future innovation. *Clin Anat*, 34(1): 108-114.

JEYAKUMAR A, DISSANAYAKE B, DISSABANDARA L (2020) Dissection in the modern medical curriculum: an exploration into student perception and adaptions for the future. *Anat Sci Educ*, 13(3): 366-380.

JIANG J, ZHANG M, MENG H, CUI X, YANG Y, YUAN L, SU C, WANG J, ZHANG L (2020) Demographic and motivational factors affecting the whole-body donation programme in Nanjing, China: A cross-sectional survey. *BMJ Open*, 10(9): e035539.

JONES G (2014) Recommendations of good practice for the donation and study of human bodies and tissues for anatomical examination. *Plexus*, 12-14.

KORF HW, WICHT H, SNIPES RL, TIMMERMANS JP, PAULSEN F, RUNE G, BAUMGART-VOGT E (2008) The dissection course - necessary and indispensable for teaching anatomy to medical students. *Ann Anat*, 190(1): 16-22.

KREBS C, QUIROGA-GARZA A, PENNEFATHER P, ELIZONDO-OMAÑA RE (2021) Ethics behind technology-enhanced medical education and the effects of the COVID-19 pandemic. *Eur J Anat*, 25(4): 515-522.

MARVÁN ML, ÁLVAREZ DEL RÍO A, JASSO K, SANTILLÁN-DOHERTY P (2017) Psychosocial barriers associated with organ donation in Mexico. *Clin Transplant*, 31(11). doi: 10.1111/ctr.13112.

MCBRIDE JM, DRAKE RL (2018) National survey on anatomical sciences in medical education. *Anat Sci Educ*, 11: 7-14.

MCCLEA K, STRINGER MD (2013) Why do potential body donors decide against donating? *N Z Med J*, 126(1377): 51-58.

MICHEL OLGUIN FM (2019) Programa de Donación de Cuerpos, único en México. Gac. UNAM.

MILANIAK I, WILCZEK-RUŻYCZKA E, PRZYBYŁOWSKI P (2018) Role of empathy and altruism in organ donation decisionmaking among nursing and paramedic students. *Transplant Proc*, 50(7): 1928-1932.

MUELLER CM, ALLISON SM, CONWAY ML (2021) Mississippi's whole body donors: Analysis of donor pool demographics and their rationale for donation. *Ann Anat*, 234: 151673.

MUÑOZ-LEIJA M, ZARATE-GARZA P, JACOBO-BACA G, QUIROGA-GARZA A, SALINAS-ALVAREZ Y, MARTINEZ-GARZA J, ELIZONDO-OMAÑA R, GUZMÁN-LÓPEZ S (2020) Modifications to the delivery of a gross anatomy course during the COVID-19 pandemic at a Mexican medical school. *Eur J Anat*, 24: 507-512.

O'NEILL FK (2009) Giving from our bodily belongings: Is donation an appropriate paradigm for the giving of bodies and body parts?: What else might be considered? *HEC Forum*, 21(2): 151-174.

PAPA V, VACCAREZZA M (2013) Teaching anatomy in the XXI century: New aspects and pitfalls. *Sci World J*, 2013: 310348.

PATHER N, BLYTH P, CHAPMAN JA, DAYAL MR, FLACK NAMS, FOGG QA, GREEN RA, HULME AK, JOHNSON IP, MEYER AJ, MORLEY JW, SHORTLAND PJ, ŠTRKALJ G, ŠTRKALJ M, VALTER K, WEBB AL, WOODLEY SJ, LAZARUS MD (2020) Forced disruption of anatomy education in Australia and New Zealand: An acute response to the Covid-19 pandemic. *Anat Sci Educ*, 13(3): 284-300.

PAWLINA W, HAMMER RR, STRAUSS JD, HEATH SG, ZHAO KD, SAHOTA S, REGNIER TD, FRESHWATER DR, FEELEY MA (2011) The hand that gives the rose. *Mayo Clin Proc*, 86(2): 139-144.

QUEREVALÚ-MURILLO W, OROZCO-GUZMÁN R, DÍAZ-TOSTADO S, HERRERA-MORALES KY, LÓPEZ-TELIZ T, MARTÍNEZ-ESPARZA AC (2012) Iniciativa para aumentar la donación de órganos y tejidos en México. *Rev Fac Med*, 55(1): 12-17.

QUIROGA-GARZA A, REYES-HERNÁNDEZ CG, ZARATE-GARZA PP, ESPARZA-HERNÁNDEZ CN, GUTIERREZ-DE LA O J, DE LA FUENTE-VILLARREAL D, ELIZONDO-OMAÑA RE, GUZMAN-LOPEZ S (2017) Willingness toward organ and body donation among anatomy professors and students in Mexico. *Anat Sci Educ*, 10: 589-597.

QUIROGA-GARZA A, GARZA-CISNEROS AN, ELIZONDO-OMAÑA RE, VILCHEZ-CAVAZOS JF, DE-OCA-LUNA RM, VILLARREAL-SILVA E, GUZMAN-LOPEZ S, GONZALEZ-GONZALEZ JG (2022) Research barriers in the Global South: Mexico. *J Glob Health*, 12: 03032.

REYES-HERNÁNDEZ CG, DE LA O-GUTIÉRREZ J, DE LA FUENTE-VILLARREAL D, JACOBO-BACA G, QUIROGA-GARZA A, SALINAS-ZERTUCHE A, ELIZONDO-OMAÑA RE, GUZMAN-LÓPEZ S (2016) Students helping students: Five years of experience. *Anat Sci Educ*, 9(4): 400-401.

RICHARDSON R, HURWITZ B (1995) Donors' attitudes towards body donation for dissection. *Lancet*, 346(8970): 277-279.

RIEDERER BM (2016) Body donations today and tomorrow: What is best practice and why? *Clin Anat*, 29(1): 11-18.

RÍOS A, LÓPEZ-NAVAS A, AYALA-GARCÍA MA, SEBASTIÁN MJ, ABDO-CUZA A, ALÁN J, MARTÍNEZ-ALARCÓN L, RAMÍREZ EJ, MUÑOZ G, SUÁREZ-LÓPEZ J, CASTELLANOS R, RAMÍREZ R, GONZÁLEZ B, MARTÍNEZ MA, DÍAZ E, RAMÍREZ P, PARRILLA P (2014) Spanish-Latin American multicenter study of attitudes toward organ donation among personnel from hospital healthcare centers. *Cir Esp*, 92(6): 393-403.

ROKADE SA, GAIKAWAD AP (2012) Body donation in India: Social awareness, willingness, and associated factors. *Anat Sci Educ*, 5(2): 83-89.

SALINAS-ALVAREZ Y, QUIROGA-GARZA A, MARTINEZ-GARZA JH, JACOBO-BACA G, ZARATE-GARZA PP, RODRÍGUEZ-ALANÍS KV, GUZMAN-LOPEZ S, ELIZONDO-OMAÑA RE (2020) Mexican educators survey on anatomical sciences education and a review of world tendencies. *Anat Sci Educ*, 11: 1-11.

SANCHEZ DEL CAMPO F (2015) El cadáver en la enseñanza de la Medicina. *Ann Real Acad Med Comunitat Valencia*, 16: 1-4.

SASI A, HEGDE R, DAYAL S, VAZ M (2020) 'Life after Death – the dead shall teach the living': a qualitative study on the motivations and expectations of body donors, their families, and religious scholars in the South Indian city of Bangalore. *Asian Bioeth Rev*, 12(2): 149-172.

ŠTRKALJ G, EL-HADDAD J, HULME A (2020) A global geography of body acquisition for anatomy education: issues, challenges and prospects. In: Chan LK, Pawlina W (eds). *Teaching Anatomy*. Springer, Cham, pp 223-235. https://doi.org/10.1007/978-3-030-43283-6_24

TAPIA-NAÑEZ M, QUIROGA-GARZA A, GUERRERO-MENDIVIL FD, SALINAS-ALVAREZ Y, JACOBO-BACA G, DE LA FUENTE-VILLARREAL D, GUZMAN-LOPEZ S, ELIZONDO-OMAÑA RE (2022) A review of the importance of research in Anatomy, an evidence-based science. *Eur J Anat*, 26: 477-486.

WAINMAN BC, CORNWALL J (2019) Body donation after medically assisted death: an emerging consideration for donor programs. *Anat Sci Educ*, 12(4): 417-424.

WINKELMANN A (2016) Consent and consensus—ethical perspectives on obtaining bodies for anatomical dissection. *Clin Anat*, 29(1): 70-77.

The radioanatomization of the Nasopalatine canal on Cone Beam Computed Tomography – an eloquent study

Lakshminarayana Kaiyoor Surya, Karthikeya Patil, V.G. Mahima, C.J. Sanjay

Department of Oral Medicine and Radiology, JSS Dental College and Hospital, JSS Academy of Higher Education and Research, SS Nagar, Mysore - 570 015, India

SUMMARY

The Nasopalatine Canal (NPC) was investigated using Cone Beam Computed Tomography (CBCT) to better comprehend its significance and semantic attributes in the diagnosis and treatment of pathologies and reconstructive surgeries involving the premaxilla, as it is more susceptible to progressive resorption and alterations in the morphometrics of the NPC, which increases its clinical significance. Axial, coronal, and sagittal CBCT sections were analysed in a sample of 60 individuals between the ages of 18 and 70. The chi-square test was used to examine differences between categorical variables, while the independent t test and the ANOVA test were used to examine differences between continuous variables.

A statistically significant adjudication vis-à-vis the transverse and longitudinal diameters of the Stensen foramen in the axial section, the transverse dimension of the NPC at Level C, and the labial bone length and labial bone width at Level 2 in the sagittal section bequeathed scientific acreage to this study. The Labial bone length and Labial bone width at Level 2, which were not contemplated in other researches, constitute this study as yardstick for imminent inquiries of NPC in these demeanours. This interpretation made an assay of various parameters of NPC, elaborated on the relevance of NPC in the anterior maxilla, and emphasised chartering a protocol to facilitate excellent surgical planning techniques in the placement of dental implants and surgical implants in the premaxillary region, admonishing maxillofacial trauma impacting the aesthetics, and ministration of the various pathologies.

Key words: Nasopalatine canal – Cone Beam Computed Tomography – Maxillae – Morphology – Analysis

INTRODUCTION

The Nasopalatine canal (NPC) is a paramount structure in the premaxilla that forms a conduit between the nasal and oral cavities (Lake et al., 2018). It is stationed posteriorly to the maxillary incisors, terminates beneath the incisive papilla, and unfurls into the external nasal cavity on each side as Stensen foramina, just 2 cm behind the posterior margin of the nostril. It transmits the anterior septal branch of the sphenopalatine

Corresponding author:
Dr Karthikeya Patil, MDS. Department of Oral Medicine and Radiology, JSS Dental College and Hospital, JSS Academy of Higher Education and Research, SS Nagar, Mysore 570015 India. Phone +91 94498 22498. E-mail: dr.karthikeyapatil@jssuni.edu.in

Submitted: December 7, 2022. **Accepted:** January 17, 2023

https://doi.org/10.52083/HJND9247

artery, which forms a crucial part of the arterial plexus in the Littles area.

The maxilla, being more trabecular, is more susceptible to progressive resorption and alters the morphometrics of the NPC. Cysts very commonly occur in the canal from epithelial cell remnants secondary to trauma, infection, and constant irritation due to poorly fitting dentures, which enhances their clinical consideration.

The mid facial region is a housing of complex bony structures which are fragile and delicate and prone for fracture due to trauma. The sheer proficiency of the NPC's presentation is of enormous assistance in admonishing maxillofacial trauma affecting aesthetics and preventing post-surgical neurosensory afflictions. Dysesthesia and post-septal surgery complications can be avoided by a careful spurectomy in the antero-inferior part of the body of the nasal septum, owing to the conscientious knowledge of NPC.

Although the maxillary incisors form an indispensable implement for mastication and also contribute to high aesthetic merits for facial appearance due to their strategic location, they often need to be replaced due to their deficits secondary to trauma, caries, and infection. Careful consideration of the anatomy of the NPC and the labial cortical bone is essential in dental implant science. A better perspective on implant replacement is overtly achieved by thorough knowledge of the anatomy, thus avoiding oversized implants.

Cone Beam Computed Tomography (CBCT) is the image of choice in dentistry, otolaryngology, and interventional radiology diagnosis, planning, and treatment because it displays images in all three dimensions without superimposition in sparse sections.

Hence, this study was designed to review the NPC with CBCT with a view to understanding the primary importance of the architectural and semantic attributes of the NPC that are altered due to age, sex, ethnicity, tooth loss, and trauma (Lake at el., 2018), to aid in the diagnosis and treatment of pathologies and reconstructive surgeries involving the midface region, including dental implants.

MATERIALS AND METHODS

This inquiry was organised in the Department of Oral Medicine and Radiology, JSS Dental College and Hospital, India. Subjects between the ages of 18 and 70 who visited the outpatient clinic, met the inclusion criteria, and volunteered to participate in the study by providing written consent were chosen. The inquiry was executed in complete compliance with the Declaration of Helsinki. The inquiry was validated by the Institutional Ethical Committee, with research protocol number JSSDCH IEC 29/2020.

The sample size was estimated using SPSS software version 20 for hypothesis testing. The sample size derived was 54, with 27 males and 27 females, assuming a 97% confidence interval and 90% power by employing the credo

$$n = (z^2)\, P(1\text{-}P) / d^2,$$

in which n stands for sample size, z for the statistic indicating degree of confidence, P for the anticipated prevalence, and d for the permitted error. Despite the fact that this formula assumes P and d to be decimal numbers, it would be still accurate if they were percentages, with the exception that the phrase (1-P) in the numerator would change to (100-P). The sample size was then rounded to 60, with 30 males and 30 females, anticipating a 10% allowable error. A difference of 1.92 with pooled Standard Deviance was assumed.

Individuals between the age groups of 18 and 70 years without any morbidities, possessing both intact maxillary central incisors, and who are undergoing CBCT (PlanmecaPromexis 3D Mid, Planmeca Oy, Helsinki, Finland) evaluation for any mandibular arch pathologies, pre- and post-treatment assessment for the placement of mandibular implants, evaluation of TMJ disorders, and computation for orthognathic surgery on the mandible were encompassed in the study.

Subjects with a previous history or radiographic evidence of surgical implants of the maxilla, orthodontic treatment, dental implants, trauma and surgery, cysts, tumours, and central lesions in the premaxilla, peri-apical cysts, and maxillary cen-

tral incisor apicoectomies after root canal treatment were precluded from the study.

Diagnostic CBCT Axial, Coronal, and Sagittal Section Images of the Anterior Maxilla, Nasopalatine Canal, and Hard Palate without any artefacts related to inherent, subject, or exposure were designated for the study.

The corporeal characters of the NPC were appraised using the axial, coronal, and sagittal sections of CBCT independently by two experienced oral and maxillofacial radiologists twice, at an interval of 2 weeks to avoid inter- and intra-examiner variability, and the average was considered.

In the axial view, the Incisive Foramen (IF) and Stensen Foramen (SF) were located, and their longitudinal and transverse diameters were measured. The Labial Bone Thickness (LBT) of the maxillary bone antecedent to the NPC at both IF and SF levels was gauged with the transverse diameter as the yardstick. The end points of the transverse diameter line were designated as points A and C, whereas the midpoint of the diameter was designated as point B. LBT was calculated from points A, B, and C on the labial bone plate.

In the case of multiple foramina, the dominant foramen was used for study. If two or more foramina were present, then the average of their individual diameters was considered.

In the coronal section, variations in the canal morphology, such as single canals, two parallel canals, or Y-shaped canals with variants, were appreciated (Bornstein et al., 2011). Given the nature of bilateral superior terminations and the single end point at the Incisive Foramen, the canal has a characteristic Y or V shape (Lake et al., 2018).

In the sagittal view, the configuration of the NPC was assessed and segregated as Cylindrical (labial and palatal parts are parallel) or Funnel (increased anteroposterior dimension at one end), Hourglass (the antero-posterior dimension is the smallest near the centre) and Spindle (the antero-posterior dimension is the widest at the centre). The transverse dimensionality of the IF, SF, and midlevel of the NPC were calculated. (Etoz and Sisman, 2014; Safi et al., 2017).

The Labial Bone Width (LBW) from the Naso Palatine Canal to the Labial Cortical plate was measured at IF, midlevel, and SF level. This provides the dimension of the labial antecedent bone to the NPC. The Labial Bone Length (LBL) was calculated by tracing the corresponding lines from the NPC that estimated the LBW to the cortical bone at the IF and SF levels. The distance between the two foramina along a line originating from the midpoint of the transverse dimensionality of the Stensen foramen to the midpoint of the transverse dimensionality of the Incisive foramen gave the length of NPC. In the case of the curved NPC, the length was measured in two parts: from one end to the middle part and from there to the other end.

The angulation of the NPC to the horizontal palatine bone gave the inclination of the NPC and was measured in degrees.

RESULTS

The study sample comprised of 30 males and 30 females (Fig. 1), who were classified into 6 age groups (Fig. 2) (Table 1), and the CBCT images of NPC in Axial, Coronal, and Sagittal planes were analysed.

Table 1. Age wise distribution of the study sample.

Age group	Males	Females	Total
11-20	4(13.2%)	3(10%)	7(11.7%)
21-30	8(26.7%)	8(26.7%)	16(26.7%)
31-40	8(26.7%)	7(23.3%)	15(25%)
41-50	5(16.7%)	5(16.7%)	10(16.7%)
51-60	3(10%)	7(23.3%)	10(16.7%)
61-70	2(6.7%)	0	2(3.2%)

The IF and SF of the NPC were located in the Axial view and their longitudinal and transverse dimensions were appraised (Table 2) (Figs. 3, 4).

Table 2. Transverse and longitudinal dimensions of the IF and SF.

Dimensions	Males	Females
Transverse diameter IF	3.57+/-1.07 mm	3.17+/-0.8 mm
Longitudinal diameter IF	3.07+/-0.94 mm	2.97+/-0.8 mm
Transverse diameter SF	3.40 +/-1.27mm	3.33+/-1.24 mm
Longitudinal diameter SF	2.83 +/-0.93mm	2.63+/-0.76 mm

(IF = Incisive foramen, SF = Stensen foramen)

Fig. 1.- Study Sample Size (Blue= Males, Orange= Females).

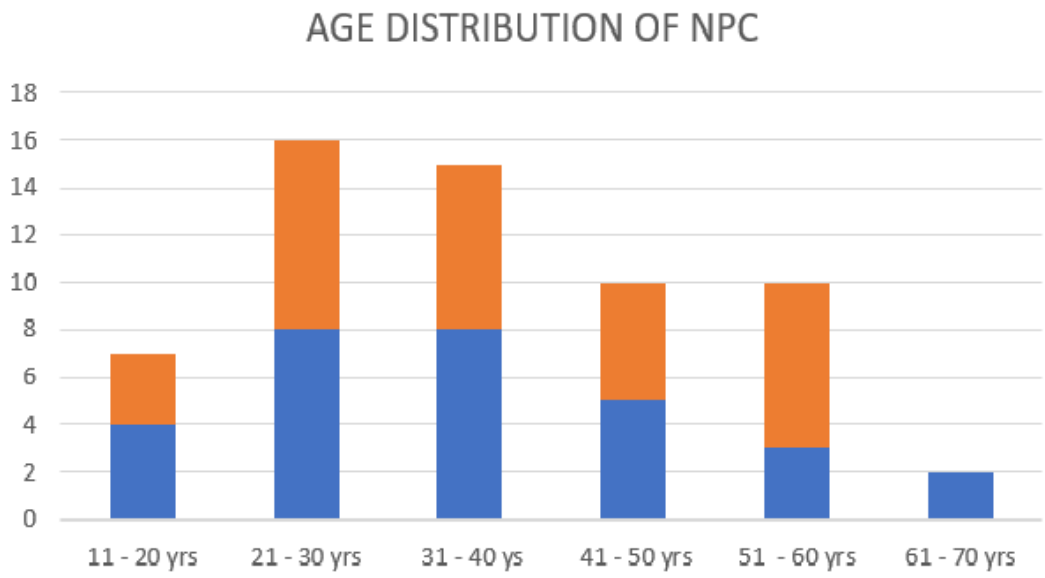

Fig. 2.- Age wise distribution of study sample.

The Labial Bone Thickness antecedent to the NPC at the IF level (Table 3) and at the SF level (Table 4) were tabulated.

In the Coronal section, the diverse morphological presentation of NPC as Single, Parallel, and Y-shaped canal was along these lines (Table 5) (Figs. 5, 6).

Table 3. Labial bone thickness in relation to IF in males and females.

LBT (IF)	Males	Females
Level A	8.00+/-1.46 mm	7.40+/-1.27 mm
Level B	8.30 +/-1.36mm	7.67 +/-1.21mm
Level C	8.07+/-1.48 mm	7.53 +/-1.43mm

(IF = Incisive foramen)

Fig. 3.- CBCT image of the Incisive foramen (**A** = Incisive foramen, **B** = Longitudinal and Transverse Diameters of IF, **C** = Labial Bone Thickness in relation to IF).

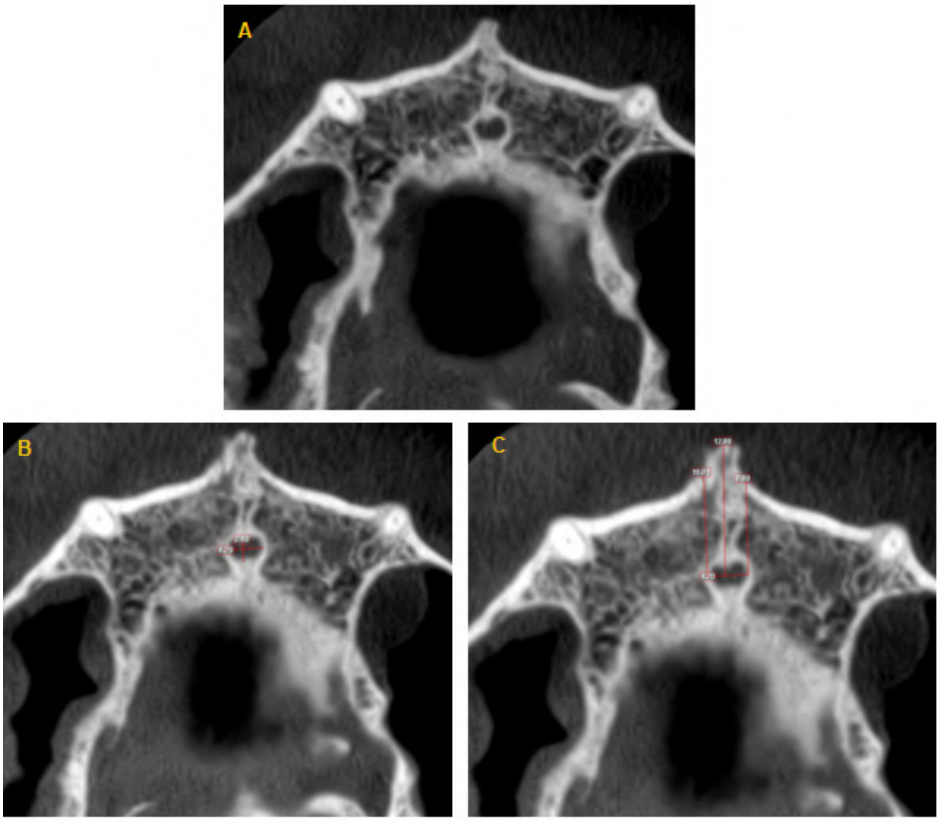

Fig. 4.- CBCT images of the Stensen foramen (**A** = Stensen foramen, **B** = Longitudinal and Transverse diameters of SF, **C** = Labial Bone Thickness in relation to SF).

Table 4. Labial Bone Thickness in relation to SF in males and females.

LBT (SF)	Males	Females
Level A	7.93+/-2.08 mm	7.07+/-1.81 mm
Level B	8.73 +/-1.63 mm	8.20 +/-1.91 mm
Level C	8.23+/-1.83 mm	7.63+/-1.92 mm

(SF = Stensen foramen)

Table 5. Morphology of NPC in coronal plane.

Morphology (Coronal)	Males	Females	Total
Parallel	2 (6.67%)	2 (6.67%)	4 (6.67%)
Single	25 (83.33%)	25 (83.33%)	50 (83.33%)
Y Type	3 (10%)	3 (10%)	6 (10%)

(NPC = Nasopalatine canal)

In the Sagittal plane, the variegated presentation of NPC was tabulated as Cylindrical, Funnel, Hour glass, and Spindle shaped. (Table 6) (Figs. 7, 8).

The Morphometric dimensions of NPC like Length, Transverse diameter at different strata, angulation of NPC to the palate, and the configuration of Labial bone width were systemized. (Table 7) (Fig. 9).

DISCUSSION

The motive of the current inquiry was primarily to analyse the anatomical constitution and the morphometric proportions of the NPC with the high-calibre imaging technique, CBCT, to contemplate the outcome of age and sexual role on the NPC. Excellent knowhow about the NPC is required to plan surgical techniques in the treatment of maxillofacial trauma for the therapeutics of various pathologies in order to avoid neural damage due to inadvertent administration of local anaesthetics, and to recognise neural damage that may occur as a sequel to maxillofacial trauma.

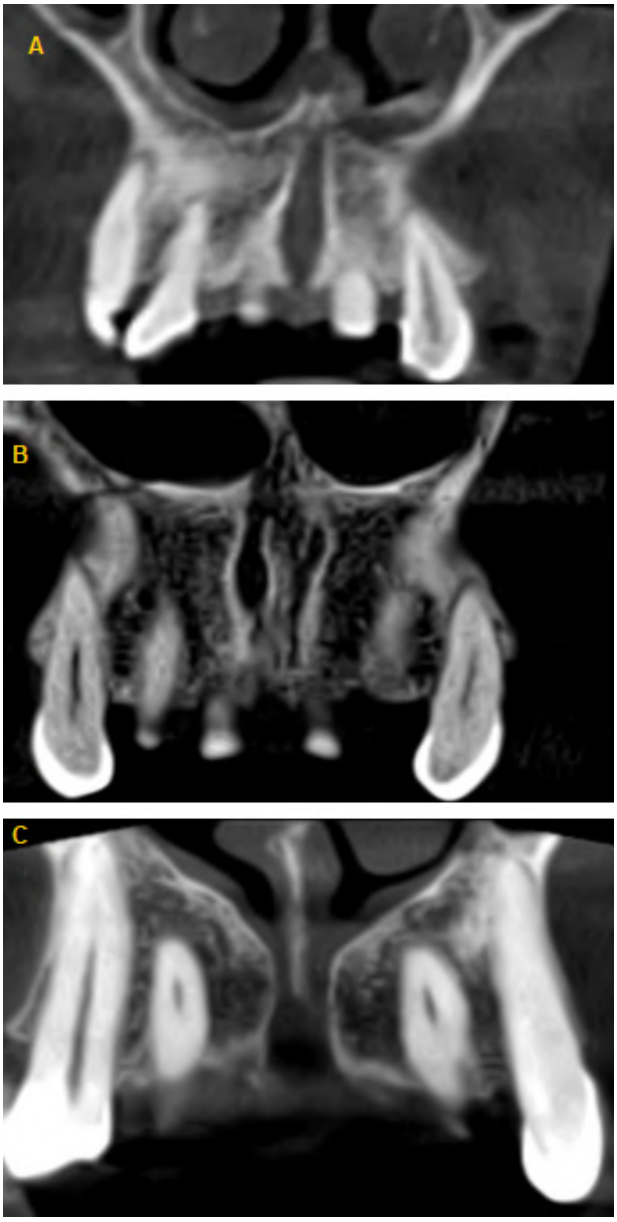

Fig. 5.- CBCT images of NPC in coronal section (**A** = Single canal, **B** = Parallel canals, **C** = Y shaped canal).

The study group comprised 60 subjects aged between 10 and 70 years. The greater proportion of the subjects in the study were in their 2nd to 4th decades of life, owing to increased awareness of dental health, access to the modern amenities of dental practice, increased ventures into appre-

Table 6. Morphology of NPC in sagittal plane.

Morphology (Sagittal)	Males	Females	Total
Cylindrical	8 (26.67%)	11(36.67%)	19 (31.67%)
Funnel	14 (46.67%)	9 (30%)	23 (38.33%)
Hour glass	6 (20%)	6 (20%)	12 (20%)
Spindle	2 (6.67%)	4 (13.33%)	6 (10%)

(NPC = Nasopalatine canal)

Table 7. Dimensions of different parameters of NPC in Sagittal sections in males and females.

Morphology Sagittal	Males	Females
Labial Bone WidthL1	6.7 mm	6.27 mm
Labial Bone Width L2	6.93 mm	6.03 mm
Labial Bone Width L3	7.80 mm	6.93 mm
Labial Bone Length	10.57+/-2.7 mm	8.57+/-2.73 mm
NPC Length	13.87+/-6.5 mm	9.5+/-2.1 mm
Transverse Diameter Level A	3.27+/-0.94 mm	2.67+/-0.82 mm
Transverse Diameter Level B	2.67+/-1.02 mm	2.50+/-0.77 mm
Transverse Diameter Level C	2.93+/-1.08 mm	2.50+/-0.9 mm
Angulation of NPC	119+/-9°	154.43+/-21.3°

(NPC = Nasopalatine canal)

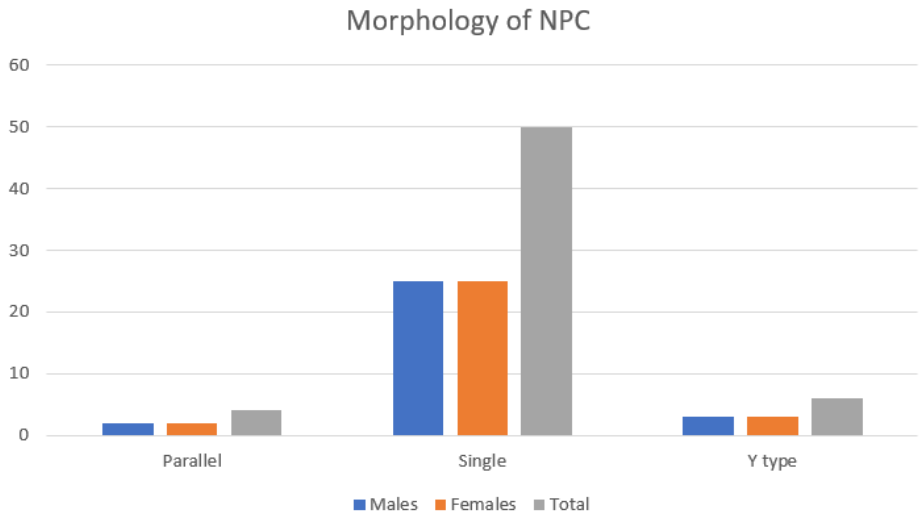

Fig. 6.- Morphology of NPC in Coronal plane.

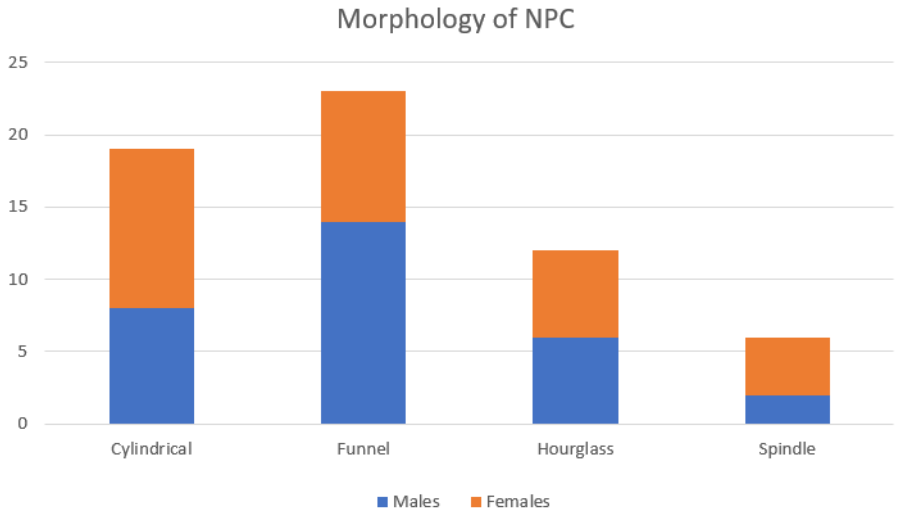

Fig. 7.- Morphology of NPC in Sagittal plane.

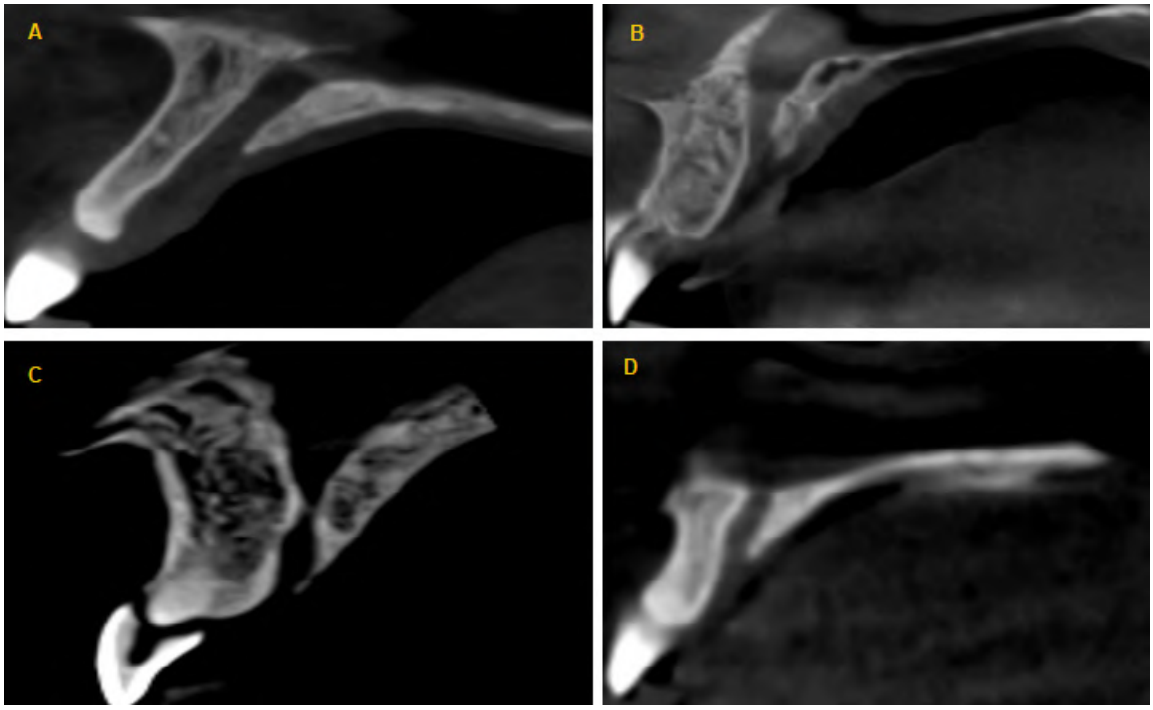

Fig. 8.- CBCT Images of NPC configuration in Sagittal section. (**A** = Cylindrical canal, **B** = Funnel canal, **C** = Hour glass canal, **D** = Spindle canal).

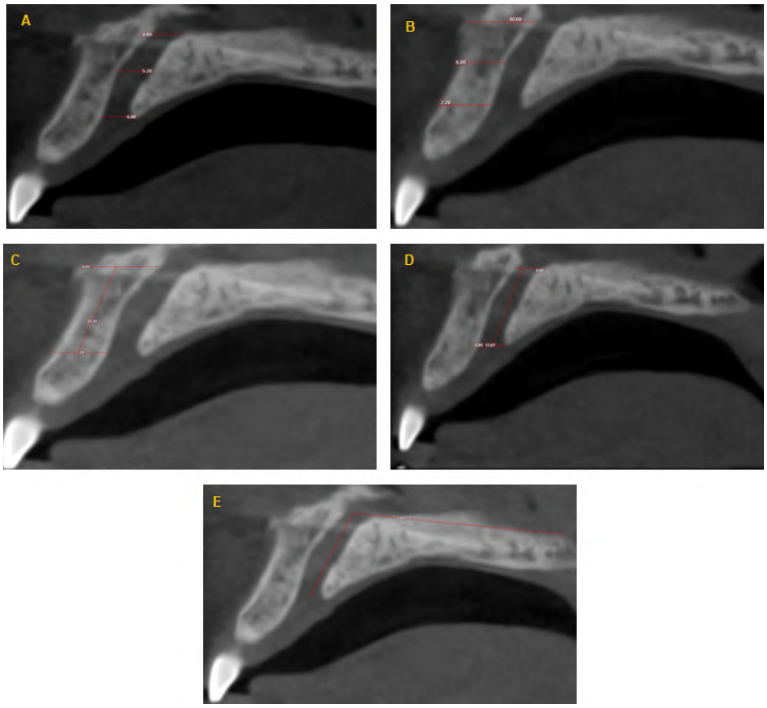

Fig. 9.- CBCT Images of NPC dimensionality in Sagittal section (**A** = Transverse diameter at 3 levels, **B** = Labial Bone Width, **C** = Labial Bone Length, **D** = NPC length, **E** = Angulation of NPC to the hard palate).

ciable aesthetics, phonetics, and functional demands, and an increased willingness to voluntarily participate in the study. This was analogous to the survey performed by Rai et al. (2021), where most of the participants were in the age category of 11 to 30 years, and in the research of Friedreich et al. (2015), where the age demographic of most of the participants was 20 to 29 years old.

The corporeal attributes of the NPC were then contrived on the diagnostic Axial, Coronal, and Sagittal slices of the CBCT images, and were subjected to the following arbitrations:

Axial Section

IF & SF dimension

Males had a transverse IF diameter of 3.57 +/- 1.07 mm, whereas females had a transverse IF diameter of 3.17 +/-1.87 mm in the axial pictures. Males had an IF longitudinal dimension of 3.07 +/- 0.94 mm, while females had a dimension of 2.97 +/- 0.80 mm. Males transverse SF diameters were 3.33+/-1.24 mm and female were 3.40+/-1.27 mm. Male longitudinal SF diameters were 2.83 +/- 0.91 mm, and female were 2.63 +/- 0.76 mm. Comparable values were obtained by Rai et al. (2021), where the mean transverse diameter of IF in males was 3.24 +/-1.03 mm and in females 3.22 +/-0.97 mm. The average longitudinal dimension of IF in males was 3.21 +/- 1.03 mm and 2.83 +/- 0.85 mm in females.

In a discrete analysis by Milanovic et al., (2021), it was noticed that the mean transverse diameter of IF was 3.53 +/- 0.11 mm. In an analysis by Soumya et al. (2019) , the measured transverse diameter of IF in males was 3.25 +/-1.05 mm and in females 3.21 +/-0.92 mm. The longitudinal dimension of IF and both the transverse and longitudinal dimensions of SF were not estimated in these studies.

Apart from the transverse and longitudinal dimensions of the Stensen foramen, there was no statistically significant distinction between the genders and age groups in this study in accordance with the one-way ANOVA test.

These observations are ornately expounded in this study. Despite a vast expanse of literature about CBCT studies on NPC, only this study made a forthright attempt at an appraisal of SF and IF dimensions other than the survey by Rai et al., (2021) where only IF was considered.

Labial Bone Thickness (LBT)

The Labial Bone Thickness was calculated with respect to IF at these 3 points, and the observed values were: 8.0+/-1.46 mm and 7.4+/-1.47 mm at Point A; 8.3+/-1.36 mm and 7.67+/-1.21 mm at Point B; and 8.07+/-1.48 mm and 7.53+/-1.43 mm at Point C in males and females, respectively.

Males and females had labial bone thicknesses of 7.93+/-2.08 mm and 7.07+/-1.81 mm at Point A, 8.73+/-1.63 mm and 8.20+/-1.91 mm at Point B, and 8.23+/-1.83 mm and 7.63+/-1.92 mm at Point C.

These various parameters, which have been appraised in this study, could not be compared with other studies, as none of them are as exhaustive as this study. This study brings to the fore the need for more detailed studies regarding the varying parameters of this one.

Coronal Section

Morphology

The morphology of the NPC was studied and categorised based on Bornstein et al. (2011) who classified them as type A, which has a single canal; type B, which has two parallel canals; and type C, which has variations of the Y type of canal with one oral opening (the Incisive foramen) and two or more nasal openings (the Stensen foramina).

In this study, a single canal of NPC (type A) was widely noted in 50 (83.33%) subjects, followed by a Y-shaped type (type C) in 6 (10%) and a parallel canal (type B) in 4 (6.67%). The most common were a single Stensen foramen and an incisive foramen, followed by two Stensen foramina and one incisive foramen. The parallel type with two Stensen foramina and incisive foramina was the least common finding.

In an analysis guided by Rai et al. (2021), single canals were common (83.2%), followed by parallel (16.4%) and Y-shaped (0.4%). In analogy, the NPC study by Kajan et al. (2015) opined that single-canal (81.8%) was more common than parallel (9.1%) and Y-shaped (9.1%). In the study by Thakur et al. (2013), a single canal was seen in 94.3% of the subjects, followed by a parallel canal in 4.9% and a Y-shaped canal in 0.8%. In a separate survey conducted by Jayasinghe et al. (2020), mainly patients had single canal (48%) or parallel canal (46%), whereas only a small percentage of patients (6%) had Y-shaped canal.

The current study aligns with the above-stated studies in apropos of the presentation of the NPC type in the coronal section.

Interestingly, the analysis by Bahsi et al. (2019) revealed that 63.3% had Y-shaped canals, 39.34% had single canals, and 8.19% had parallel canals. In the study conducted by Khojastepour et al. (2017), Y-shaped canals were marginally more common (47.9%) when compared to single canals (45%), and the least common type were parallel canals (7.1%) in males. Similarly, in females, the most common type of NPC in coronal section was Y-shaped (45.3%), followed by single canal (42.2%) and parallel canal (12.4%). Rao et al. (2018) in their research opined that Y-shaped was the most common (46%), ensued by single (43%) and parallel (11%). According to Jain et al. (2017), the predominant variant was the Y-shaped canal (49.38%).

It can be circumspectly concluded that the morphological characteristics are multifactorial, the result of inter-racial and socio-economic status, and also due to effective methodology.

Sagittal Section

Morphology

The sagittal slices were used to study the morphometrics of the NPC. In 2014, Falci et al. (2013) divided NPC morphologies into six categories: tree branch, cylindrical, banana-like, funnel-like, cone-like, and hourglass-shaped shapes.

The current study found that the most prevalent kind of NPC was funnel-shaped, with 23 (38.33%), followed by cylindrical 19 (31.67%), then hourglass 12 (20%), and spindle 6 (10%).

The outcomes of this study corresponded with the investigation by Rai et al. (2021), which found that NPC with a funnel shape predominated (38.4%), followed by cylinder (38%), hourglass (19.6%), and spindle (4%). This study is also in accordance with other studies: in Milanovic et al. (2021) it was revealed that the funnel shape (35.4%) was the most prevalent forms of NPC, followed by cylindrical (31.0%), hourglass (24.8%), and banana (8.8%) shapes; and in the analysis by Arnaut et al., (2021) the NPC form with the highest representation was the funnel (34.59%), followed by the cylinder (28.57%) and hourglass (24.81%), with only 12.03% of respondents belonged to the banana type; and also in the study done by Thakur et al. (2013) funnel-shaped (38.4%) NPC was most common followed by cylindrical (38.0%) hourglass (19.6%) followed by spindle shaped.

The present study is in fragmentary concord with the analysis done by Jayasinghe et al. (2020): funnel-shaped NPC (38%) were more common, followed by hourglass (26%), spindle (20%), and cylindrical (18%) variants of NPC.

On the contrary, Bahsi et al. (2019) concluded that the cylindrical shape of NPC was more common (26.7%), followed by the hourglass (26.7%), banana (16%), cone-shaped (14.7%), funnel (13.3%), and reverse cone (0.7%). In the survey conducted by Soumya et al. (2019), cylindrical canals were most prevalent, followed by hourglass-, funnel-, and banana-shaped canals. On CBCT pictures of 230 patients, Fernandez-Alonso et al. (2015) identified NPC as 48.2% cylindrical, 30.9% hourglass, 20.5% funnel, and 0.4% banana-like.

Utilizing the Chi square test, it was found that there was no statistically significant difference between the various morphological types in sagittal view among the various age groups, as well as between the sexes with a P value > 0.05. Similarly, Rai et al. (2021) and Jayasinghe et al. (2020) showed no statistical difference with respect to the configuration between different age groups and genders.

The present study is comparable to the preponderance of the studies, except for the studies done by Soumya et al. (2019), Bahsi et al. (2019) and Fernandez-Alonso et al. (2015), which were conducted on Asian, Turkish, and Hispanic populations. Across the literature, evidence both supports and refutes sex differences in the morphometry of NPC (Lake et al., 2018). This disparity warrants for further in-depth research and the systematisation of methodology and protocol in the interpretation of NPC.

Labial Bone Width (LBW)

In this study, mean Labial Bone Width at Level 1 (L1) was **6.70 mm** and **6.27 mm, 6.93 mm** and **6.03 mm** at Level 2 (L2), and at Level 3 (L3) it was **7.80 mm** and **6.93 mm** in males and females, respectively. The labial bone width is a cardinal determining factor in the successful restoration

of the osseous integrity of the maxilla (Lake et al., 2018). The elaborate scrutiny of this study in this aspect at different levels revealed increased width in males as compared with females. In terms of statistics, males had labial bone widths (L2) that were substantially higher than those of females.

In similarity, the study by Bornstein et al. (2011) revealed labial bone width at L1 was **7.12 mm** and **6.01 mm**, **7.26 mm** and **6.05 mm** at L2, and at L3 it was **8.09 mm** and **7.21 mm** in males and females, respectively. The parameter of LBW at L2, which was statistically significant in this study, was in line with the statistically significant parameter of LBW at L2 in the scrutiny conducted by Bornstein et al. (2011), who also had a statistically significant parameter of LBW at the L1 level.

In comparison, a study done by Milanovic et al. (2021) assessed the labial bone width as **7.11 +/- 0.03 mm, 7.52 +/- 0.17 mm,** and **9.22 +/- 0.25 mm** at L1, L2, and L3, respectively. According to Kajan et al. (2015) the average labial bone width was **5.96 +/- 1.5 mm** at Level 1**, 6.82 +/- 1.6 mm** at Level 2, and **6.23 +/- 2.1 mm** at Level 3.

In consensus with this study, the evaluation of NPC conducted by Acar et al. (2015) the LBW was **6.74 mm** and **6.24 mm** at L1; **6.57 mm** and **6.04 mm** at L2; and, **7.21 mm** and **6.53 mm** at L3 level in males and females, respectively.

Khojastepour et al. (2017) measured only the labial bone width in males and females at (L1) 7.36 +/- 1.45 mm and 6.78 +/-1.27 mm, and at (L3) 8.45 +/-2.24 mm and 8.52 +/-2.03 mm, respectively. Albeit, L2 bone width was not prepended, their assessment at L1 and L3 level was analogous to this study.

Only LBW at L2 was measured by Jain et al. (2017) and found to be 5.71 +/- 1.29 mm. LBW at the other two levels was not measured in that study, but nonetheless it was comparable to the L2 dimension of this study. The labial bone width at the level of L1 was only determined to be 6.50 +/-1.52 mm by Soumya et al. (2019) and was comparable with this study. This assessment was done irrespective of the gender of the subjects, and a mean value was expressed.

Dissimilitude in the LBW at different strata can be ascribed to diversification in the shape of the NPC amid different studies. The decorous study of the NPC and its relevance to labial bone width is of utmost importance at Level 2, as any deficit of the bone at that level may hamper the surgical planning and surgical intervention of implant placement. Additional scientific analysis is asked for in this aspect at all three levels, explicitly at the L2 level.

Labial Bone Length (LBL)

In this study, the average labial bone length was 10.57 +/- 2.7 mm in males and 8.57 +/- 2.73 mm in females. The difference was statistically significant ($p < 0.05$), despite certitude that males have structurally longer labial bone length than females.

This parameter was not considered in other studies except by Jain et al. (2017), where it was **17.72 mm** in males and **16.68 mm** in females. The difference in labial bone length for males and females, which is considerably greater compared to this study, can be ascribed to gender specific disparities in facial architecture. The length is salient in apposition to implant emplacement. Exemplary scientific viewpoint regarding the measurement in this aspect of study is preordained.

NPC Length

The average length of the NPC in males was **13.87+/-6.5 mm** and **9.5+/-2.1 mm** in females in this study. There was no statistically significant distinction between the length of the canal in males and females, even though the mean length of the NPC was longer in males.

This was akin to the study done by Rai et al. (2021), where the average linear measure of NPC was in males: **13.60 +/- 2.62 mm** and in females: **11.69 +/- 2.41 mm**. This was closer to the analyses by Jayasinghe et al. (2020), where the average length in males was **13.49 mm** and in females, **10.98 mm,** and by Bahsi et al. (2019), where the average linear measure of NPC noted in men was **12.96 +/- 2.57 mm** and **12.16 +/- 2.45 mm** in women. It was Acar et al. (2015) who, on measuring the length of NPC, found it in males to be **10.20 mm** and in females to be **9.04 mm** on average. In

the Khojastepour et al. (2017) study of NPC, the length in males was higher **(11.46 +/- 2.86 mm)** than in females **(9.37 +/- 2.24 mm)**.

Just a modest body of research, regardless of gender differences, has measured the overall length of NPC. The average NPC length, irrespective of gender difference, in this study was **11.68 +/- 4.30 mm,** which corresponds to hereunder studies. NPC research by Fernandez-Alonso et al. (2015) derived an average length of NPC of **12.28 +/- 2.98 mm**; in the study by Thakur et al. (2013), the average linear measure of NPC was found to be **10.08 +/- 2.25 mm**; and in the scrutiny of NPC by Milanovic et al. (2021), **10.26 mm** was the average length of NPC. Similarly, the average length of NPC in the study by Rao et al. (2018) was 10.32 +/- 2.70 mm, compared to 11.13 +/-3.23 mm in the study by Jain et al. (2017) and 9.9 +/- 2.6 mm in the study by Liang et al. (2009). The study by Arnaut et al. (2021) showed a mean length of **10 mm** with a wide scope of **8-16 mm,** and it was **16.33 mm** in the study by Almery et al. (2015), with the right canal being somewhat longer than the left canal. Additionally, the length of the NPC also varies based on the height of the maxillary bone (Lake et al., 2018).

The results of this study are consistent with the majority of earlier investigations. Despite racial disparities and tooth presence or absence, the measurement method may have a substantial role in the variability in canal length among studies.

Transverse Diameter of NPC

Depending upon the NPC morphology in the sagittal slices, this study implied that there were notable variations in the size of NPC at IF, SF, and mid-level. The mean transverse diameter of NPC at IF level (Level A) was **3.27+/-0.94 mm** and **2.67+/-0.82 mm**; at mid-level (Level B) was **2.67+/-1.02 mm** and **2.5+/-0.77 mm;** and at SF level (Level C) was **2.93+/-1.08 mm** and **2.5+/-0.9 mm** in men and women, respectively. Using the one-way ANOVA test, all metrics with p values > 0.05 showed no evidence of a significant difference between age and gender groups, with the exception of level C diameter in sagittal view.

Similitude was noted in the analysis by Thakur et al. (2013), where the average transverse diameters at Level A, Level B, and Level C were **3.15 mm, 2.32 mm,** and **2.86 mm,** respectively, and by Jayasinghe et al. (2020) the mean transverse diameter of NPC at Level A was **3.03 mm**, at Level B **2.37 mm,** and at Level C **2.85 mm**, respectively.

Analogous results were obtained in an analysis by Rai et al. (2021), where the transverse diameter at Level A was **3.61+/-1.17 mm** and **3.31+/-1.06 mm**, **2.34+/-1.04 mm** and **2.12+/-0.99 mm** at Level B, and at Level C it was **3.35+/-1.86 mm** and **3.18+/-1.62 mm** in males and females, respectively.

Kajan et al. (2015) computed the NPC at all three levels and proffer the results as **3.53 +/- 1.1 mm**, **2.35 +/- 1.1 mm**, and **3.8 +/- 2.3 mm,** respectively.

A plethora of studies have estimated the dimensions only at Level A and C, and the measurements are akin to the dimensions **3.27 +/- 94 mm** and **2.67 +/- 0.82 mm** for males and **2.93 +/-1.08 mm** and **2.5 +/- 0.9 mm** for females, respectively, estimated in this study.

A study by Khojastepour et al. (2017) revealed that the mean diameter of NPC was 3.40 +/-1.08 **mm** and **2.97 +/- 0.91 mm** at Level A and **3.39 +/- 1.55 mm** and **2.98 +/- 1.45 mm** at Level C in males and females, respectively. In an analysis by Acar et al. (2015), it was found that the average diameter at Level A was **4.14 mm** in men and **3.72 mm** in women. The average diameter at Level C in men was **3.12 mm** and **3.03 mm** in women. Bornstein et al. (2011) also determined that the mean transverse dimension of NPC at Level A was **4.45 mm** and **4.38 mm** and **3.65 mm** and **3.37 mm** at Level C in males and females, respectively. Jain et al. (2017) enunciated the average transverse diameter of NPC at Level A and Level C to be **4.53 mm** and **3.98 mm;** also **3.63 mm** and **3.19 mm** in men and women, respectively.

In the scrutiny by Milanovic et al. (2021), the average transverse diameter of the NPC at Level A was **5.04 +/- 0.12 mm** and at Level C, **2.93 +/- 0.01 mm,** and in the Bahsi et al. (2019) study, the transverse diameter of the NPC at Level A was **6.71 +/- 1.50 mm** in men and **6.23 +/-1.28 mm** in women, and at Level C, **4.25 +/-1.15 mm** in men and **4.01 +/-0.99 mm** in women. The transverse dimension of the NPC at level B was not contemplated in some of these studies.

Soumya et al. (2019), with their scrutiny of the transverse dimension of NPC only at Level A, inferred the computation as **3.23 +/- 0.89 mm** in men and **2.99 +/- 1.0 mm** in women. This finding is in accordance with the measurements of this study.

Morphological differences in NPC and racial differences in facial structure are important factors contributing to measurement variation between males and females at different levels. However, these measurements obtained in this study match the preponderance of other studies. However, the disparity with other studies may be epithetical to the morphological disparity in NPC along with the genealogical contrast in facial architecture amid different genders at different strata. It also appears that the diameter increases in pathologies that results in structural deficits of the maxilla such as, trauma, cyst formation and tooth loss (Lake et al., 2018).

Angulation of NPC to hard palate

The average angulation of NPC with respect to the hard palate noted in this study was **119+/-9.0 degrees** in males and **154.43+/-21.3 degrees** in females. The average orientation in females is greater than the average inclination in males, so statistically there is absolutely no dissimilarity between men and women.

This was in comparison to the study done by Jayasinghe et al. (2020), where the mean inclination of the NPC was **115.69 degrees,** and women had a greater mean inclination **(117.43 degrees)** than men (**113.67 degrees),** but it was not statistically significant.

Similarly, in the syudy by Bahsi et al. (2019), the NPC angle in males was 105.45 +/- 7.72 degrees and in females it was 105.98 +/- 7.77 degrees, with no statistically significant difference.

Similarly, in the study done by Rai et al. (2021), the inclination was **77.04 +/- 44.05 degrees** in males and **87.15 +/- 39.67 degrees** in females.

In the study done by Thakur et al. (2013), the incline angle was **63 +/-8.03 degrees** with respect to the horizontal flush hard palate plane, heedless of the gender of the sample subjects.

The NPC angulation noted in the study by Jain et al. (2017) was **67.98 degrees** in females and **73.45 degrees** in males, with an average of **69.32 +/- 7.70 degrees.**

Various researchers have employed different anatomical landmarks to arrive at the angulation of the NPC with respect to the hard palate. Complementary values of angular measurements were noticed when the anterior nasal spine or posterior nasal spine were used by the researchers. The contradictory findings pertaining to the angulation of NPC in the studies emphasise the requirement of a standard protocol for the adoption of a particular anatomical landmark (the anterior or posterior nasal spine) as a basis for measuring the angulation.

This study made an attempt at sequencing the definition of the various parameters in the analysis of NPC, elaborated on the importance of NPC and its complex anatomy in the anterior maxilla, and emphasised the chartering a protocol for the same.

In tour d'horizon, the study's findings suggest that the investigation of topographic details, obtained with a precise approach, offers useful insight into the different relationships between the NPC and the anterior maxilla structures. The consistency of the observed interpretations of labial bone width, labial bone length, transverse diameter of the NPC, and angulation of the NPC might be appropriate as a preliminary evaluation to understand the primary importance of the architectural and semantic attributes of the Nasopalatine canal to aid in the diagnosis and treatment of pathologies and reconstructive surgeries involving the midfacial region, including dental implants, particularly for surgeons using an expeditious approach. This three-dimensional surveillance of NPC for its anatomical interpretation and acreage facilitates the discernment while planning complex surgeries in the anterior maxilla and hence circumvents untoward complications and necessitate for impending explicit scientific analysis of NPC with respect to genealogical, racial, dentate status, and age transition.

ACKNOWLEDGEMENTS

Authors are grateful to all the patients who gave written consent to compile this scientific typescript and to herald the same. Authors like to thank all co-workers for helping them with this project.

REFERENCES

ACAR B, KAMBUROĞLU K (2015) Morphological and volumetric evaluation of the nasopalatinal canal in a Turkish population using cone-beam computed tomography. *Surg Radiol Anat,* 37(3): 259-265.

AL-AMERY SM, NAMBIAR P, JAMALUDIN M, JOHN J, NGEOW WC (2015) Cone beam computed tomography assessment of the maxillary incisive canal and foramen: considerations of anatomical variations when placing immediate implants. *PloS One*, 10(2): e0117251.

ARNAUT A, MILANOVIC P, VASILJEVIC M, JOVICIC N, VOJINOVIC R, SELAKOVIC D, ROSIC G (2021) The shape of nasopalatine canal as a determining factor in therapeutic approach for orthodontic teeth movement - A CBCT study. *Diagnostics*, 11(12): 2345.

BAHŞI I, ORHAN M, KERVANCIOĞLU P, YALÇIN ED, AKTAN AM (2019) Anatomical evaluation of nasopalatine canal on cone beam computed tomography images. *Folia Morphol*, 78(1): 153-162.

BORNSTEIN MM, BALSIGER R, SENDI P, VON ARX T (2011) Morphology of the nasopalatine canal and dental implant surgery: a radiographic analysis of 100 consecutive patients using limited cone-beam computed tomography. *Clin Oral Implants Res*, 22(3): 295-301.

ETOZ M, SISMAN Y (2014) Evaluation of the nasopalatine canal and variations with cone-beam computed tomography. *Surg Radiol Anat*, 36(8): 805-812.

FALCI SG, VERLI FD, CONSOLARO A, SANTOS CR (2013) Morphological characterization of the nasopalatine region in human fetuses and its association to pathologies. *J Appl Oral Sci*, 21: 250-255.

FERNÁNDEZ-ALONSO A, SUÁREZ-QUINTANILLA JA, RAPADO-GONZÁLEZ O, SUÁREZ-CUNQUEIRO MM (2015) Morphometric differences of nasopalatine canal based on 3D classifications: descriptive analysis on CBCT. *Surg Radiol Anat*, 37(7): 825-833.

FRIEDRICH RE, LAUMANN F, ZRNC T, ASSAF AT (2015) The nasopalatine canal in adults on cone beam computed tomograms–A clinical study and Review of the literature. *In Vivo*, 29(4): 467-486.

JAIN NV, GHARATKAR AA, PAREKH BA, MUSANI SI, SHAH UD (2017) Three-dimensional analysis of the anatomical characteristics and dimensions of the nasopalatine canal using cone beam computed tomography. *J Maxillofacial Oral Surg,* 16(2): 197-204.

JAYASINGHE RM, HETTIARACHCHI PV, FONSEKA MC, NANAYAKKARA D, JAYASIGHE RD (2020) Morphometric analysis of nasopalatine foramen in Sri Lankan population using CBCT. *J Oral Biol Craniofacial Res*, 10(2): 238-240.

KAJAN ZD, KIA J, MOTEVASSELI S, REZAIAN SR (2015) Evaluation of the nasopalatine canal with cone-beam computed tomography in an Iranian population. *Dent Res J*, 12(1): 14-19.

KHOJASTEPOUR L, HAGHNEGAHDAR A, KESHTKAR M (2017) Morphology and dimensions of nasopalatine canal: a radiographic analysis using cone beam computed tomography. *J Dent (Shiraz)*, 18(4): 244-250.

LAKE S, IWANAGA J, KIKUTA S, OSKOUIAN RJ, LOUKAS M, TUBBS RS (2018) The incisive canal: a comprehensive review. *Cureus*, 10(7): e3069.

LIANG X, JACOBS R, MARTENS W, HU Y, ADRIAENSENS P, QUIRYNEN M, LAMBRICHTS I (2009) Macro-and micro-anatomical, histological and computed tomography scan characterization of the nasopalatine canal. *J Clin Periodontol*, 36(7): 598-603.

MILANOVIC P, SELAKOVIC D, VASILJEVIC M, JOVICIC NU, MILOVANOVIĆ D, VASOVIC M, ROSIC G (2021) Morphological characteristics of the nasopalatine canal and the relationship with the anterior maxillary bone - a cone beam computed tomography study. *Diagnostics*, 11(5): 915.

RAI S, MISRA D, MISRA A, KHATRI M, KIDWAI S, BISLA S, JAIN P (2021) Significance of morphometric and anatomic variations of nasopalatine canal on cone-beam computed tomography in anterior functional zone-A retrospective study. *Ann Maxillofac Surg*, 11(1): 108-114.

RAO JB, TATUSKAR P, PULLA A, KUMAR N, PATIL SC, TIWARI I (2018) Radiographic assessment of anatomy of nasopalatine canal for dental implant placement: a cone beam computed tomographic study. *J Contemp Dental Pract*, 19(3): 301-305.

SAFI Y, MOSHFEGHI M, RAHIMIAN S, KHEIRKHAHI M, MANOUCHEHRI ME (2017) Assessment of nasopalatine canal anatomic variations using cone beam computed tomography in a group of Iranian population. *Iranian J Radiol*, 31: 14(1).

SOUMYA P, KOPPOLU P, PATHAKOTA KR, CHAPPIDI V (2019) Maxillary incisive canal characteristics: a radiographic study using cone beam computerized tomography. *Radiol Res Pract,* 2019: 6151253.

THAKUR AR, BURDE K, GUTTAL K, NAIKMASUR VG (2013) Anatomy and morphology of the nasopalatine canal using cone-beam computed tomography. *Imag Sci Dentistry*, 43(4): 273-281.

Anatomical Sciences from a translational perspective: Bibliometric analysis

Pablo Álvarez[1], Arturo Argüello[2], Marta Reyes[3]

[1] *Innovation and Technology Transfer Unit Instituto de Investigación Biosanitaria de Granada, Granada, Spain*
[2] *Technology Transfer Office of the Andalusian Public Health System, Andalusian Public Foundation Progress and Health, Sevilla, Spain*
[3] *Hospital Santa Ana Motril, Granada, Spain*

SUMMARY

In the field of human morphology, despite its growing interest in translational anatomy research, its contributions are often unknown. Scientific articles and patents are highly reliable sources of knowledge for measuring scientific progress and technology transfer. The aim of this article is a bibliometric study of the potential of anatomical translational research. Our methodological framework has consisted of a combination of the analysis of two variables: 1) academic papers, and 2) patents of anatomical scientific achievements. The established time range has been 2000-2020 and the database used The Lens (https://www.lens.org), establishing "anatomical science" as the keyword. In the systematic analysis, 11,547 scientific documents and 1,511 patent registrations have been carried out; inclusion criteria were applied to both groups to identify their quantitative and qualitative trends. Our results identified that scientific articles on translational anatomical achievements have an exponential growth rate similar to the growth of patent applications for translational anatomical sciences. The maximum number of contributions of journal articles and patents corresponds to the temporal range of 2010 and 2020, with 2020 being the most productive year; academic documents represented 54.90% and patents produced represented 45.08%, which are significant data if they are compared with the year 2000, when the respective percentages were 76.40% and 23.50%, an indicator of a clear increase in the culture of patentability and the growing interest in translational anatomical research. The records of granted patents were 747 and 487 patent applications, which are significant data for the growth of the culture of patentability as well as the quality of the patents, since those granted represent 60.40%. These results identify the strong growth of anatomical science and its interest in the transfer of scientific achievements.

Key words: Bibliometrics analysis – Anatomical scientific production – Anatomical patents – Translation of knowledge

INTRODUCTION

The relevance of Anatomy has been maintained throughout history because it has proven to be a science whose usefulness is fundamental and essential for medical practice. Centuries ago, Hippocrates emphasized this importance: "The nature of the body is the beginning of science medicine" (Campohermoso et al., 2014).

Corresponding author:
Pablo Álvarez. Innovation and Technology Transfer Unit Instituo de Investigación Biosanitaria de Granada. Spain. Phone: +34 608376697. E-mail: palvarez@fibao.es ORCID No: 0000-0001-6405-8066

Submitted: December 19, 2022. **Accepted:** January 21, 2023

https://doi.org/10.52083/DLWG3599

In the last 20 years, the advancement of science and technology and its transfer has improved the living conditions of citizens through the design of mechanisms capable of changing our environment and generating answers to questions raised (Fernández-Sánchez et al., 2020, Burget et al., 2017). In contemporary societies, there has been a global interest in strengthening the connections between scientific achievements and the problems of daily practice, obtaining an exponential development in translational research (Straus et al., 2011).

On the other hand, scientometrics allows the quantitative analysis of the documentary contributions of a certain science (Álvarez et al., 2014; Álvarez et al., 2022), which enables the development of different scientometric indicators (Rojas-Montesino et al., 2022). This is the criterion that we have followed in this article.

Bibliometric tools make it possible to accurately identify the information published around a thematic area and analyze its scientific and technological specificities. Current web tools make it possible to carry out more efficient and precise searches that facilitate better and more efficient meta-analyses (Chua et al., 2021). The measurement and evaluation of research performance focuses on metrically analyzing the scientific literature in a specific field of knowledge (Mingers et Leydesdorff, 2015). In this work, we have carried out a bibliometric analysis of the literature published in the field of achievements of the anatomical sciences following the studies of Aleshire (1970) and Muñoz-Leija et al. (2022). "Unlike the traditional or narrative review, the systematic review uses a more rigorous and well-defined approach to analyze the literature in a specific thematic area"; that is why systematic reviews are used in order to answer well-focused questions, and using systematic and explicit methods help identify, select, and critically evaluate research being conducted.

Consequently, we follow the guidelines for systematic review of the literature established by Al-Qaysi et al. (2020), and Al-Emran et al. (2018).

In the field of morphology in general and that of human morphology in particular, despite its growing prominence (Aránega, 2022), the knowledge and application of anatomical translational research is often unknown because it is loosely articulated.

Anatomical research affects the resolution of biosanitary problems that require different diagnostic and therapeutic solutions with an interdisciplinary approach, where the role of anatomical knowledge is very important. Throughout time, anatomists with their scientific achievements have contributed significantly to the understanding and resolution of medical-surgical problems, although it is true that, in general, the rate of growth and production of basic translational research had not had the same rate of growth compared to basic translational research in other disciplines of Medicine.

At present, this trend has changed and anatomical researchers have assumed the importance of translational research; therefore, it has become a common component in scientific production that their scientific contributions can also have clinical utility, developing stable and effective collaborations. between basic and clinical sciences.

Translational research or applied research is making its way decisively in the academic world and has become a focus of attention in many academic circles.

Therefore, this work supposes, in the field of anatomical research, a reflective analysis on translational research and responsible innovation that is carried out in the translational anatomical area, during the period 2000-2021. We have analyzed scientometrically the scope and dimension of translational anatomical research through a systematic bibliometric study of the contributions of scientific papers and patent applications carried out in the last two decades. We intend to shed light on some of the keys to the biomedical translation of the scientific achievements obtained in the field of anatomy.

MATERIALS AND METHODS

Design and Planning

To carry out the study, a systematic review of the literature was used as a strategy to identify both

A.-the most relevant scientific documents on Anatomical Science and B.- Patent records produced.

Systematic reviews of the literature are the most widely used tool (MubarakAli et al., 2022; Heo et al., 2022) to identify, evaluate and interpret the data that we want to study, available in a given period of time and a field of research specific.

The review that has been carried out has taken into account the criteria of Kitchenham et al. (2010). First, we established the search strategy, selected the databases, chose the keywords and the temporal space, and proceeded to collect the results. Then the inclusion and exclusion criteria were applied, and we collected and identified the documents. Finally, the data were coded and evaluated and analyzed.

Search Criteria and Resources

The selection has been made based on the documents that are part of the scientific production in Academic Works and Patent literature in the anatomical sciences:

Keyword: *"anatomical science".*

Temporal space: *2000-2020.*

Exclusion criteria: *Documents published on dates other than those established in our study and not focused on the established keywords.*

Search strategy

Database: The Lens

Lens is an academic database and metasearch engine that brings both academic papers and patents together into a unified and separate system, as each type of document has its place on the results page.

Lens enables document analysis to create an open mapping of the world of knowledge- driven innovation. All the software that comprises the Lens platform itself is open source and uses different databases that bring together academic documents and patents in a unified and separate system, incorporating more tools that allow viewing the interaction of academic document citations and patent registration, and providing innovative solutions (Ezeamuzie et al., 2022; Castelló-Cogollos et al., 2018) The Lens is considered the "most comprehensive scholarly literature database, surpassing in width and depth two leading databases (Web of Science and Scopus)" (Dash and Kalamdhad, 2022). It is the search engine for academic documents and patents that support the implementation of metadata standards and offers interaction with other sources of information, both scientific and technological (Penfold, 2020; Jefferson et al., 2021). That is why we have used this database, due to the fact that it provides specific and complementary information that allows researchers' access to full text documents and allows locating book citations, theses, and reports, among others.

Regarding the search for patents, The Lens provides precise information on patents applied for and granted.

Data Extraction and Verification

The data of the documents that met the criteria based on the keyword were extracted independently by 2 of our authors and divided into two groups.

A.-Scientific documents B.- Patent documents

In the two groups, the collection and evaluation of the scientific publications as well as the patents produced were carried out using the most current quantitative and qualitative bibliometric indicators (Durieux and Gevenois, 2010).

To carry out the main purpose of this work, several steps were followed; the flowchart of Fig. 1 shows the route of the bibliographic search and the respective selection of the analyzed document.

Data mining and Selection

Bibliometric analysis

A.-Academic Works

Quantitative Analysis

The published academic documents were selected and the collected data were organized and processed to obtain a quantitative representation of the distribution and evolution of the academ-

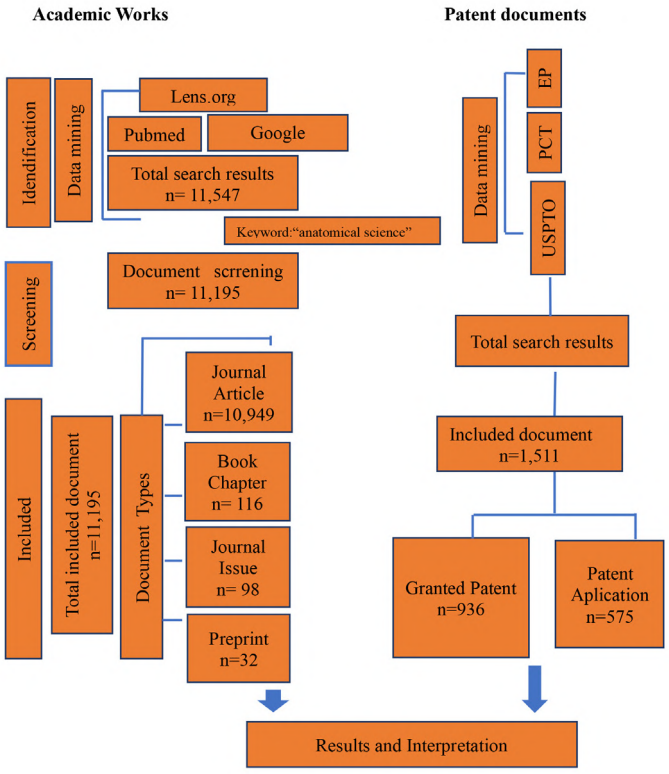

Fig. 1.- Flowchart of the development of the work: Route of the bibliographic search and the respective selection of the academic documents and of Patents analyzed.

ic documents produced in the established time range. Documents included: Journal Article, Book, Chapter Book, Report, Conference, Proceedings Article, Dissertation, Preprint and News.

Qualitative Analysis

For the qualitative analysis, the documents were divided according to the type of article published in indexed journals and with the impact factor of Books Chapter, Journal Issue and Preprint. This criterion has been used because it is currently one of the most widely used bibliometric quality indicators (Torres-Salinas et al., 2009).

To obtain Trends evidence, the distribution of the number of documents was also analyzed according to the main fields of study in which the academic documents were published. Likewise, the most active authors, the most productive academic institutions in translation of the achievements of morphological knowledge, as well as the journal with the largest number of articles, were also selected and analyzed to obtain evidence of their trend.

B.- Human Anatomy Patents

Likewise, the selection of scientific patent registries was carried out to obtain a quantitative representation of patents focused on anatomical sciences in the established period of time.

The Total Patent Documents corresponded to: Application Patent, Granted Patent, Search Report, Amended Application that were used for the quantitative analysis.

The qualitative analysis has been made based on two variables: Patent Application, Granted Patent, as these two variables constitute patentability standards (De Rassenfosse and Jaffe, 2018).

To obtain evidence of their success trend, the distribution of the number of records according to their legal status was also analyzed: active, pending, discontinued, expired, inactive and patented, the most active authors, the institutions were also selected and analyzed. Most productive academic institutions, the Top Agents & Attorney and the Top Proprietary Institutions in translation of the achievements of morphological knowledge to obtain evidence of their evolutionary trend of progress.

RESULTS

A.- Academic Works

Once the search was carried out in the indicated databases, 11,547 documents produced and published in the period of time analyzed were obtained. Total documents include: Journal Article, Book Chapter, Journal Issue, Preprint, Report, Book and Conference Proceedings.

Quality filters were applied to the total of 11,547 documents to analyze them qualitatively and draw conclusions about the research trend on Anatomical Achievements.

The qualitative analysis showed n=11,195 of total documents and are distributed: Journal Article n=10,949, Book Chapter n=116 Journal Issue n=98 and Preprint n=32, its evolution is reflected in the temporal range analyzed in Fig. 2a.

The quantitative analysis indicates that the most significant growth occurs in the decade 2010-2020 and the most productive year is 2020, with 1,103 documents, which represents 9,9 % of the total production (Fig. 2b).

Likewise, the study showed that the Research and Preprint Articles obtained a total of 8,602 citations. The top most active authors of research papers (Fig. 3a and Table 1) were: R Shane Tubbs (649), Marios Loukas (584), Joe Iwanaga (209), Paul R Manger (190), Rod J Oskouian (166) and the 5 most active journals are: *Progress of Anatomical Sciences* (1347), *Anatomical Sciences Education* (871), *Anatomical Science International* (813), *Clinical Anatomy* (293) and *Anatomical Sciences Education* (236) (Fig. 3b, Fig. 4a). The institutions that produced the most scientific papers and in which fields of study they were selected (Fig. 3c): our results show that the most productive university is St. George's University, with a total of 864 contributions, University of Louisville, with 827 research articles; University of Missouri and University of the Witwatersrand contributed 627 and 619 respectively.

Top Journals by Publisher has been *Anatomical Sciences Education*, from the Wiley Online Library publishing house, and *Anatomical Science International*, from the Springer publishing house: both journals multiply by three the number of articles published in *Clinical Anatomy*, which is the third of the Top Journals by Publisher.

The most active countries were: United States (4,206), Iran (2,369), Grenada (845), South Africa (667), Japan (646) and China (631) (Fig. 4b).

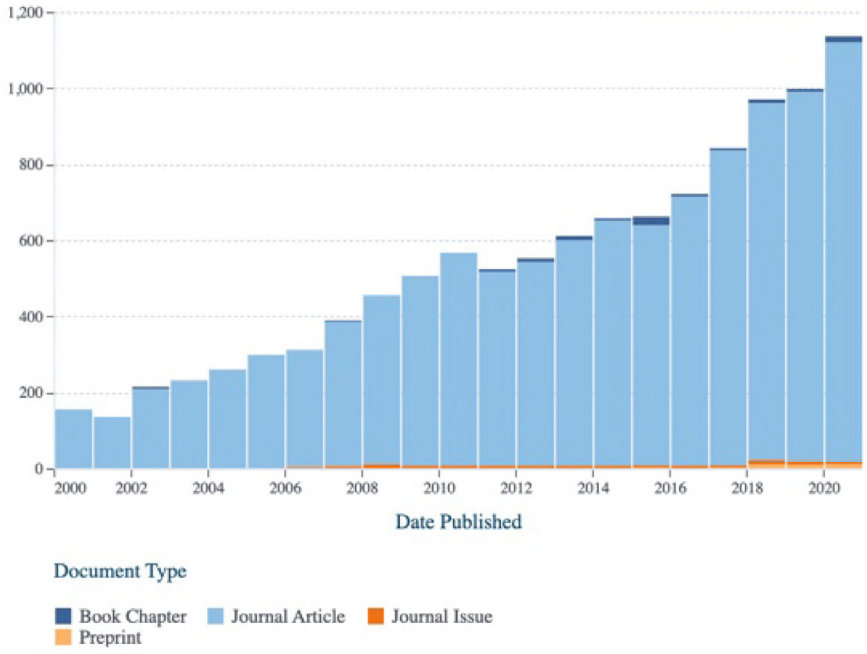

Fig. 2a.- Journal Article, Book Chapter, Journal Issue and Preprint over time.

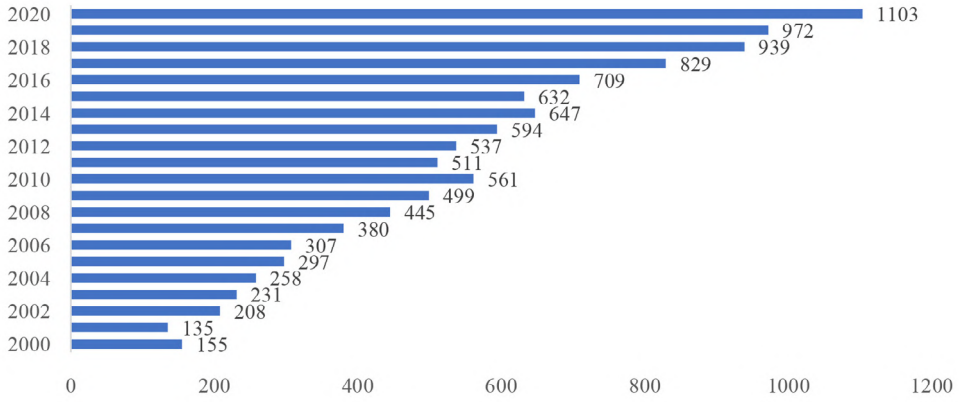

Fig. 2b.- Journal Article: annual distribution in the period 2000-2020.

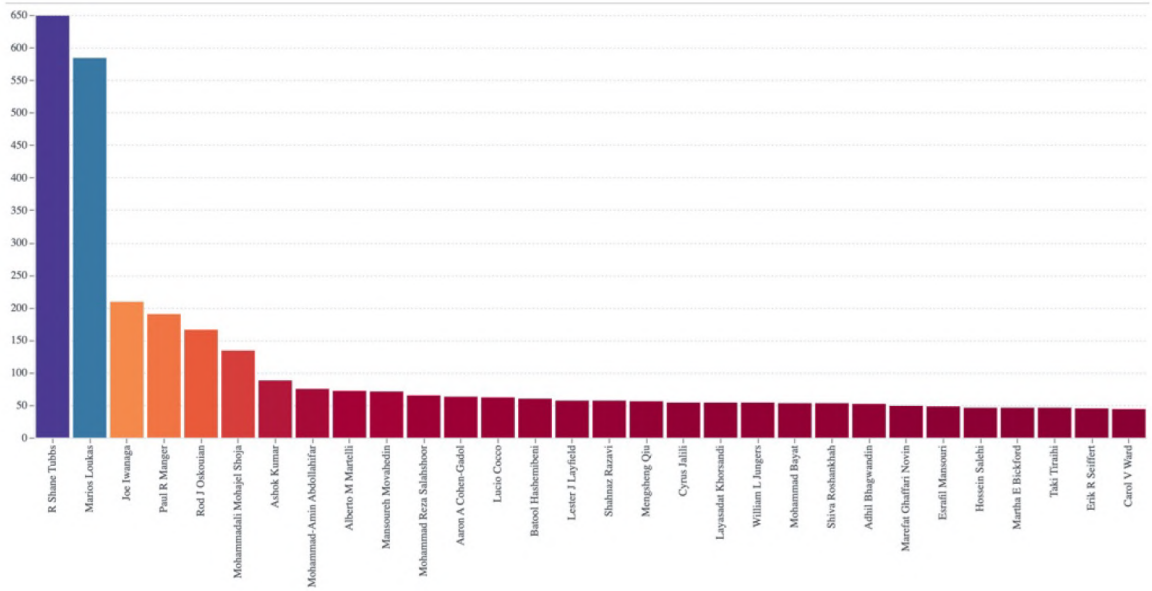

Fig. 3a.- Most productive Authors.

Table 1. Ten top scholarly paper authors and patent inventors.

Top 10 academic papers authors	Top 10 patent inventors
R Shane Tubbs	Baker Joffre B
Marios Lukas	Azamián Bobak Robert
Joe Iwanaga	Cronin Maureen
Pablo R. Pesebre	Coe Jonathan Allen
Rod J. Oskouian	Vafai Scott Bradley
Mohammadali Mohajel Shoja	Giljohann David
Ashok Kumar	Kamboj Rajender Kumar
Mohammad-Amin Abdollahifar	Karche Navnath Popat
Mohammad Reza Salahshoor	Karche Navnath Popat
Aaron A. Cohen-Gadol	Makarov Vladímir

B.- Human Anatomy Patents

Data processing of the patent documents obtained: the total search results were 1,314 documents and they were analyzed quantitatively and qualitatively with the objective of drawing conclusions about the evolution of the patentometry trend of anatomical scientific achievements.

The total 1,314 documents include: Patent Application, Granted Patent, Search Report, Amended Application, Amended Patent. Fig. 5a reflects the Total Patent Documents and their Annual Distribution.

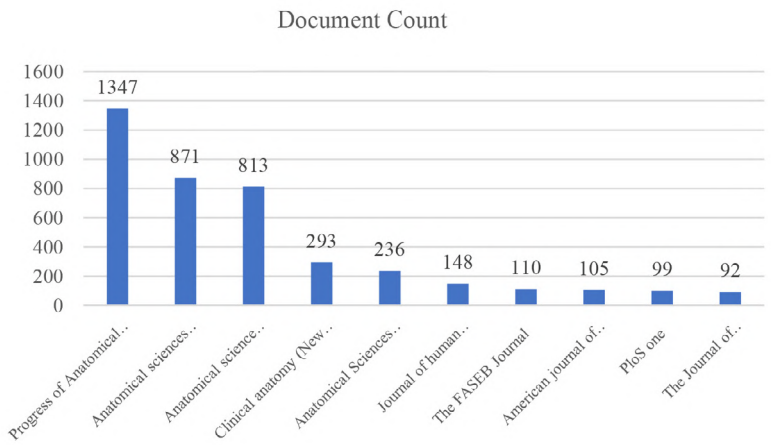

Fig. 3b.- Top Journals by Publisher.

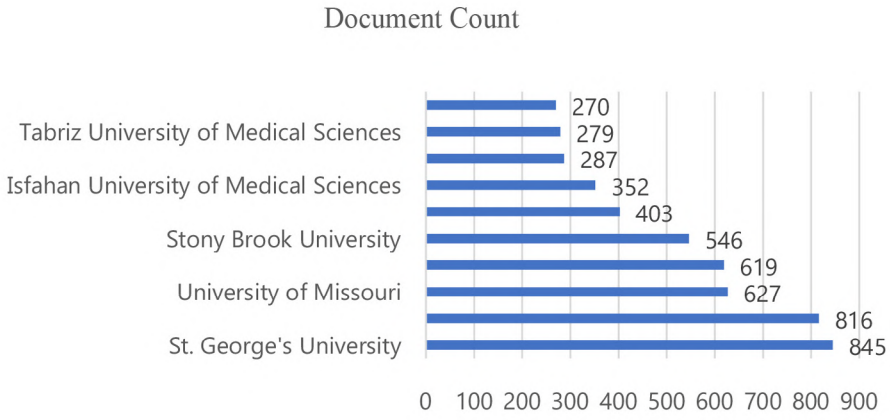

Fig. 3c.- Most Active Academic Institutions.

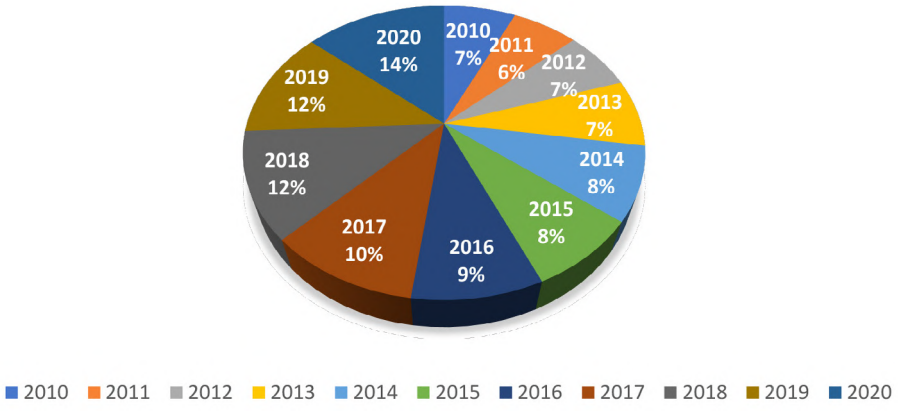

Fig. 4a.- Journal Article: annual percentage distribution in the period 2010-2020.

The results show that the year 2000 accounted for 0.05% of the total applications, while 2020 has accounted for 6.87%, evidencing an upward progression of patents.

The quantitative data are found in Fig. 6a, showing that there are 936 granted patent registrations and 575 patent applications (Fig 7a). The quantitative evolution by years is shown in Fig. 5b, and

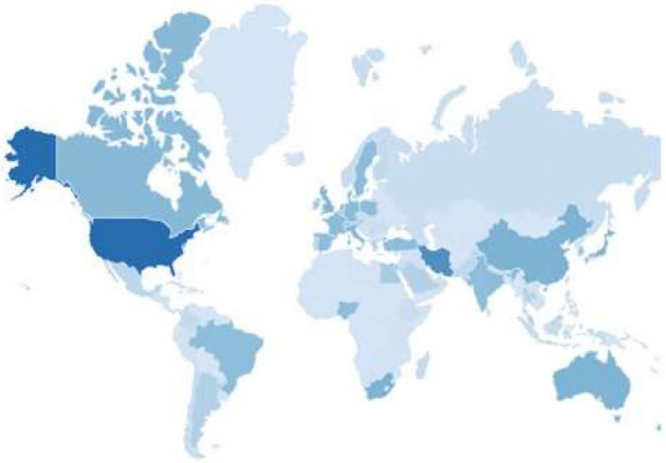

Fig. 4b.- Most active Countries.

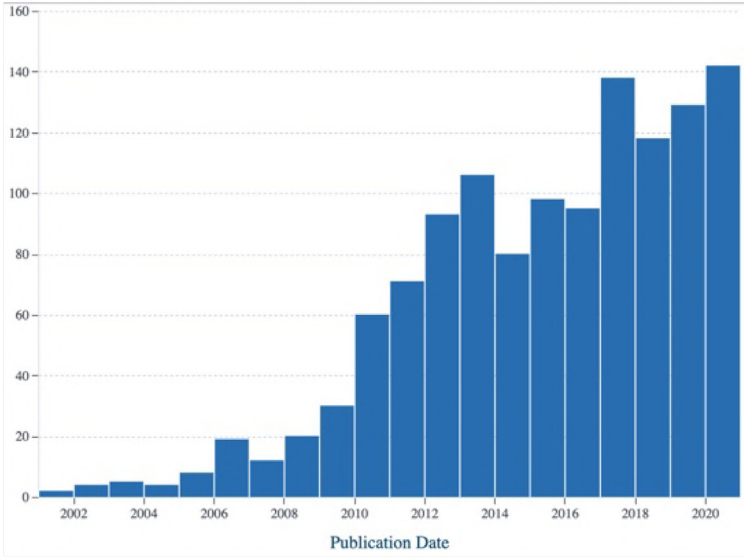

Fig. 5a.-Patent Documents over time.

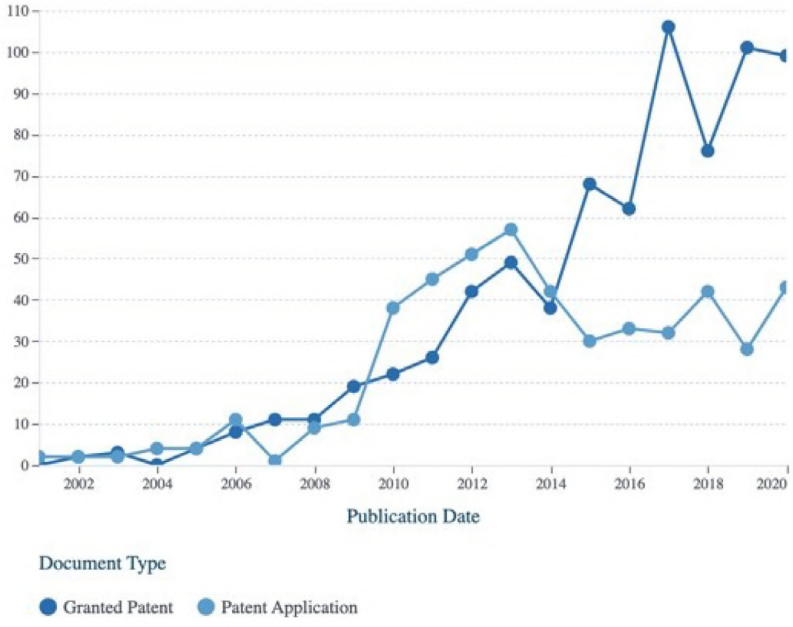

Fig. 5b.- Granted Patent and Applicant Patent over time.

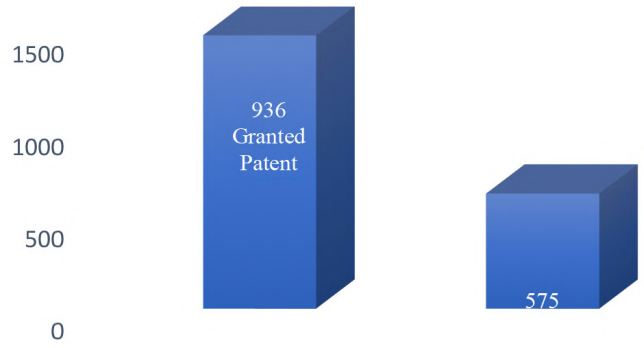

Fig. 6a.- Total Granted Patent and Applicant Patent.

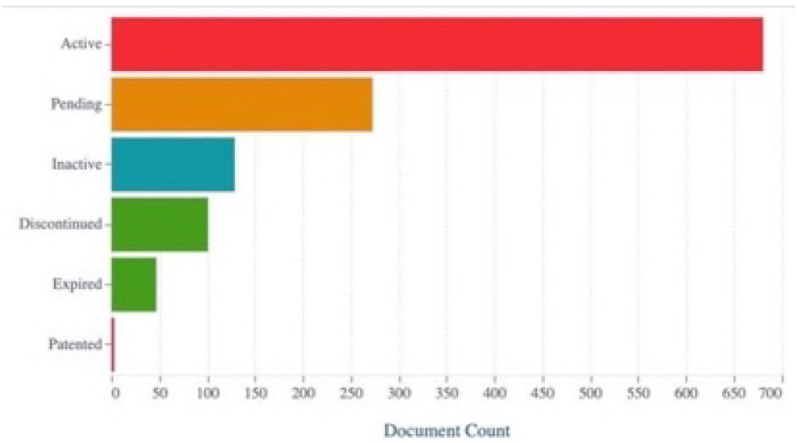

Fig. 6b.- Legal status of all Patents.

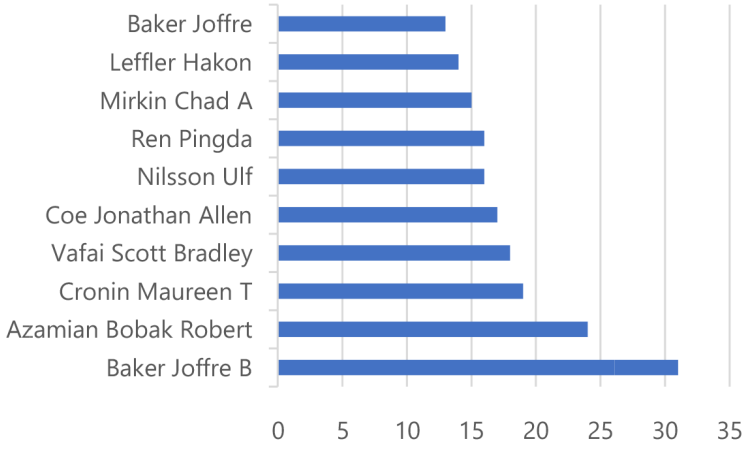

Fig. 6c.- Most Active Patent Inventors.

Fig. 7a shows the percentage of Patents Granted and Patent Applications.

The results that included Application Patent and Granted Patent as quality indicators shows that the time range between 2010 and 2020 constitutes the one with the highest growth. Likewise, this period is where the greatest balance between the number of patents applied for and granted per year occurs, which indicates the quality of the applications, since the percentage of patents grant-

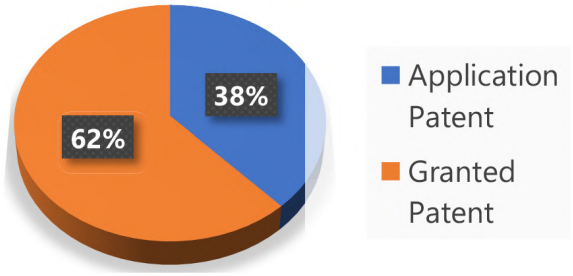

Fig. 7a.- Granted Patent and Application Patent: % Distribution.

ed increases. The results show that the decade between 2010 and 2020 is when the most important success rate is generated both for application patent documents and for granted patents. Specifically, it is demonstrative in the year 2020: of the total patent documents, 69% are granted patents and 31% are application patent.

The legal status analysis showed that most of the patents are active, representing 51% of the total patent and 22% are pending. (Table 2).

Table 2. Legal status patents: Document Count %.

Legal Status	Document Count%
Active	51%
Pending	22%
Inactive	10,5%
Discontinued	8,2%
Expired	3,8%
Patented	0,3%

The Most Active Patent Inventors analysis showed the 10 most productive patent authors (Fig. 6c and Table 1), heading this ranking Baker Joffre B from the Medical University of California and occupying tenth place Makarov Vladimir L from the University of Michigan.

The results of this study have shown that the top five companies in patent applications have been: Genomic Health INC (45), Infinity Pharmaceuticals INC (18), Metavention INC (18), California University (18) and Northwestern University (16) (Fig. 7b, Fig. 8a). Similarly, the top companies Owner of patents were: Infinity Pharmaceuticals INC (24), Metavention INC (24), Genomic Health INC (22) (Fig. 7c, Fig. 8b). The United States of America leads the position of the most active countries in patents (Fig. 9a).

In the analysis of selected patents, we have detected that purely anatomical articles, such as 'A review of the thoracic splanchnic nerves and celiac ganglia' (Loukas et al., 2010) is cited in the text of 32 patents, several of them related to nerve splenic ablation, neuromodulation of the adrenal gland or liver.

The article 'EMG activity of trunk muscles and torque output during isometric axial rotation exertion: a comparison between back pain patients and matched controls' (Ng et al., 2002) is cited for 15 patents, mainly sensors for pain management. Also, the article 'Convergence and cross talk in urogenital neural circuitries' (Hubscher et al., 2013) is cited for 14 patents related to the therapy of stimulation.

The article 'The clinical anatomy of the internal thoracic veins' (Loukas et al., 2007), where the author describes the pattern of branching and adequacy of the internal thoracic veins, is cited for 14 patents related to the implantation of medical devices in the thoracic cavity. Recently in 2022, patents: Azygos, Intercostal and/or Internal Thoracic Vein Implantation and Use of Medical Devices applied for by Cardiac Pacemakers Inc, whose inventors are Reddy et al., designed a method of treating a patient by implanting electrodes in the internal thoracic veins and the azygos, implantable cardiac pacing or monitoring system.

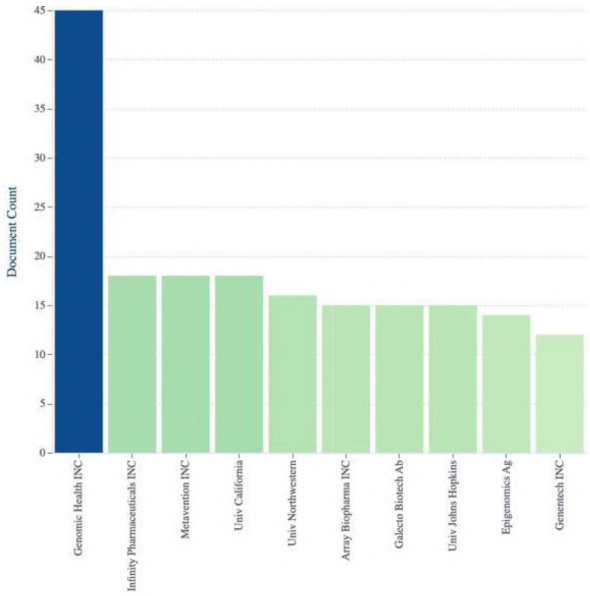

Fig. 7b.- Top applicant companies / institutions.

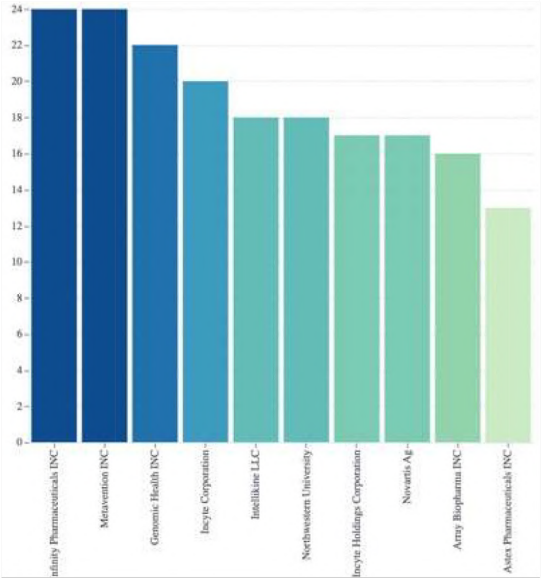

Fig. 7c.- Top owners companies / institutions.

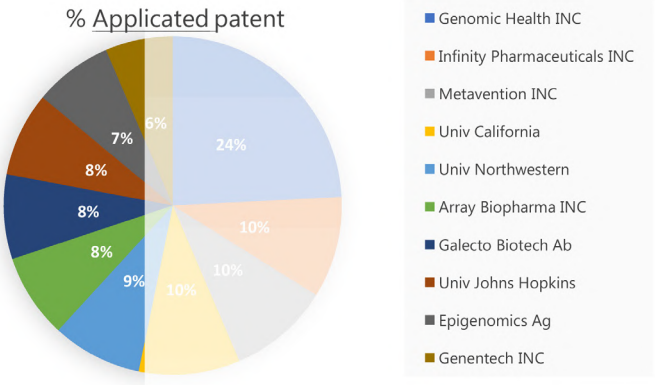

Fig. 8a.- Total companies/ institutions: % of applications.

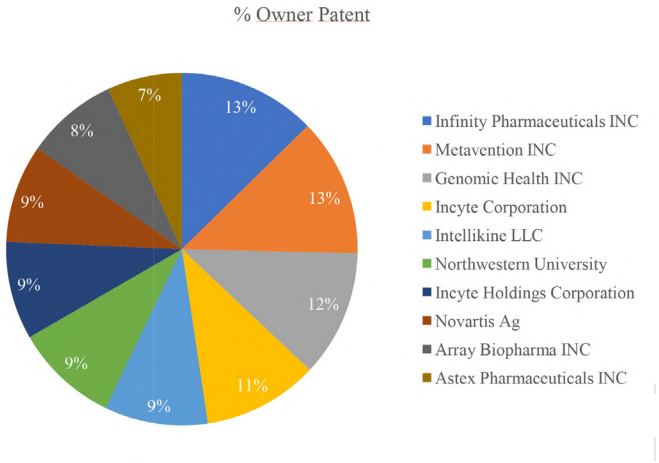

Fig. 8b.- Total company/ institutions: % Ownership.

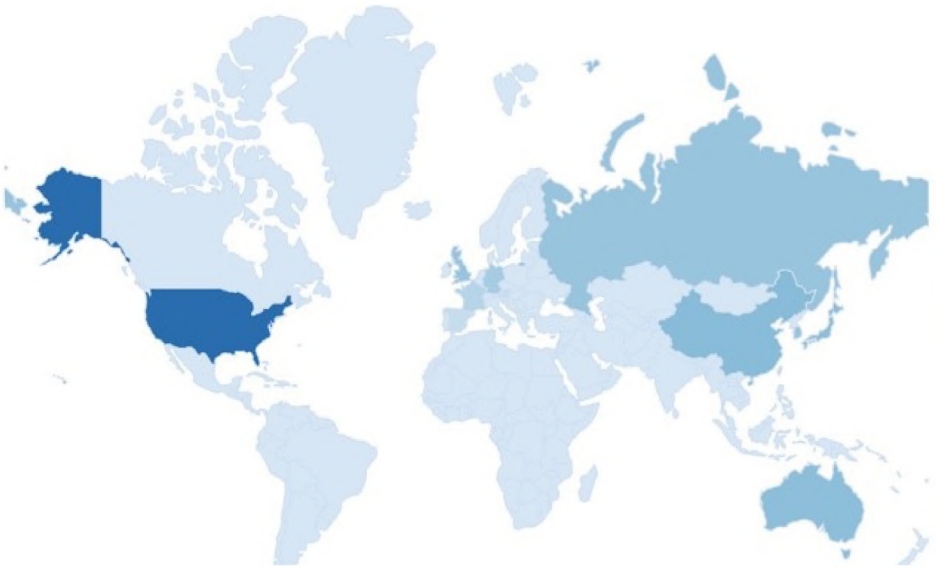

Fig. 9a.- Most active Countries in patents.

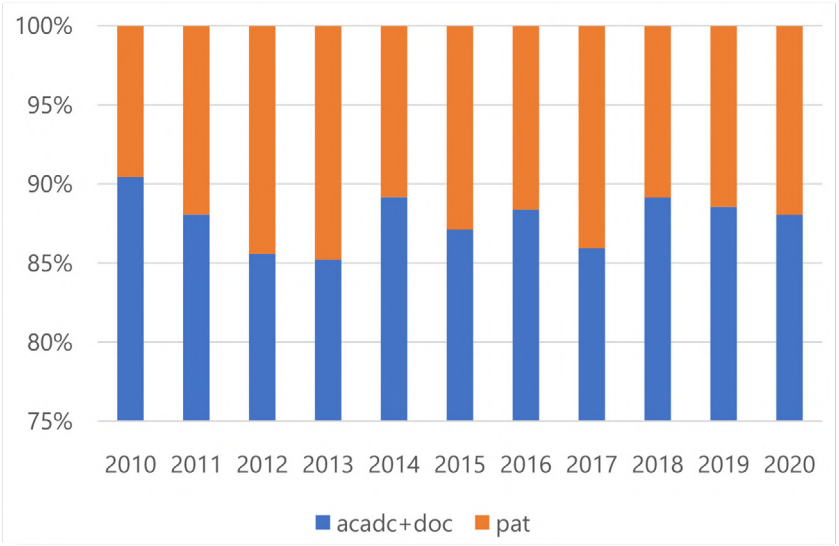

Fig. 9b.- Evolution of % growth in Academic Papers and Patents: 2010-2020.

DISCUSSION

We have carried out a bibliometric analysis on the current state of the latest developments in the academic literature on anatomical scientific papers and patents around "anatomical science" using The Lens database to develop an informed roadmap on this topic, and, to the highest extent possible, stimulate future anatomical research so that it is relevant to biomedical transfer (Bozeman and Boardman, 2014; Franchi, 2020).

The rigorous analysis of the development of human anatomical science as translational science has allowed us to demonstrate that it establishes a direct relationship with the growth of the anatomical patent.

The quantitative and qualitative analysis of the literature of journal articles and patent documents on anatomical science allows us to conclude that the increases in the number of patents have been related to the number of journal articles, this being an irrefutable proof. This article shows that the subject of translational anatomical research must be analyzed in consideration of two elements, (1) academic documents, and (2) patents, since these two variables actively participate in the generation and transfer of anatomical knowledge, and through patents it is possible to commercialize the results of the research, contributing achievements to biomedical innovation and increasing the diagnostic and therapeutic utility of the practice of Medicine. Results are in line with previous research (Franchi, 2020), which indicate that the achievements in the field ofanatomical science are part of a dynamic ecosystem, with actors at the individual level, i.e., researchers, and at an institutional level, i.e., organizations and academic institutions.

The systematic review of the academic documents of translational anatomical achievements showed an evident growth in the period analyzed, the production being very significant in the decade 2010-2020 (Fig. 2a, Fig 2b), especially for documents in Journal Article format and published in journals with a high impact factor– a specific quality indicator data. The number of Journal Article documents represents 78.55% and shows a clear predominance of all academic articles produced, the most productive author being R Shane Tubbs with 649.

Journal articles were mainly published in *Progress of Anatomical Sciences* (n=1,347), *Anatomical Sciences Education*, (n=871), *Anatomical Sciences* (n=813), and *Clinical Anatomy* (n=293).

Analyzing the five most productive countries, the United States is in first place (4,206), representing 48.16% of the total. We select the most productive universities based on scientific articles the field of study (Fig. 4b). The results showed that the 10 main countries had 77.93% of the production of scientific documents and that the most efficient top university is St. George's University, with n=845 contributions. Patent documents have grown significantly in the two decades analyzed, and, based on the inclusion criteria applied, patent applications represented 38,1% of the total and granted patents 61,9% (Fig 7a) – these data are equivalent to those shown in patentability in other areas.

The patent success rate is evident and is based on data on the growth evolution of granted patents compared to those applied for, which follow an increasing evolution (Fig 5b). This increase in granted patents is evidence of the scientific and methodological rigor of the requested patents, hence its high grant rate.

The inventor with the highest number of published patents was Baker Joffre B, School of Medicine, University of California, followed by Azamián Bobak Rober, Cronin Maureen T company: Affymetrix, Santa Clara, California, Coe Jonathan Allen and Vafai Scott Bradley (Fig. 6c).

The most active geographical territory in patents: the bibliometric analysis carried out showed that the most productive jurisdiction has been the USA, with Europe in third place.

The analysis relative to the percentage relationship between the number of articles published and the number of patent applications per year (Table 3) shows that, in 2020, academic documents represented 54.90% and patents produced 45.08%, significant data, sinc,e when compared with the year 2000, the respective percentages were 76.40% and 23.50%, data, indicating a clear

increase in the culture of patentability and the growing interest in translational anatomical research. These results agree with those provided by Fadavi and Mansouri, A. (2022) and demonstrate a sustained growth in the period bewteen 2000 and 2020.

Table 3. Percentage distribution of Academic and Patent Documents by year analyzed.

Year	Acad Doc.	Pat. Doc.
2000	76,40%	23,50%
2001	70,00%	30,00%
2002	52,94 %	47,07%
2003	50,00%	50,00%
2004	44,26%	55,73%
2005	52,33%	47,66%
2006	47,50%	52,50%
2007	54,68%	45,31%
2008	49,52%	50,47%
2009	50,32%	49,67%
2010	56,57%	43,42%
2011	63,86%	36,13%
2012	71,23%	28,76%
2013	73,20%	26,79%
2014	59,74%	33,25%
2015	59,55%	40,44%
2016	69,11%	30,89%
2017	69,86%	30,13%
2018	70,75%	29,24%
2019	68,13%	31,86%
2020	54,90%	45,08%

It should be noted that the decade 2010-2020, which is the most active in the number of contributions to the journal of articles and in the registration of patents (Fig. 9b), indicates that the trend for the interest of the culture of the translation of scientific texts achievements is increasing exponentially. Therefore, it seems that researchers are increasingly assuming that you first apply for a patent and then submit your scientific achievements to a qualified journal, which could partly explain the results shown in this article.

We want to point out that the identification of the main productive authors in scientific articles and patent applications (Table 1) allows researchers to find possible collaborators among the most prolific authors and to know the leading journals in the publication of articles, useful information for the publication of your future research.

Through the analysis of application patent activity in the area of atomic science, this study shows the trend of patent success in this field, as the number of applications for patents and granted patents increases significantly and annually.

Therefore, it can be considered that the contribution of useful anatomical research increases exponentially, this being a relevant fact and showing the growing interest and positive assessment of modern society for scientific achievements. It has been the coronavirus pandemic that has highlighted the value of translational research, which has led to rethinking the approach toward assessing and enhancing the effectiveness of scientific advances.

In order to discuss the findings of the study based on its possible limitations, we consider that the findings of our study should continue with future research, and it would be interesting to know the parameters analyzed based on the subject areas addressed to the different pathologies. In order to discuss the possible limitations of this study, we consider that the findings of our study should continue with future research and it would be interesting to know the parameters analyzed based on particular subject areas of the different pathologies.

CONCLUSIONS

The analysis of the development of Human Anatomy as a translational science has allowed us to show how the progress of anatomical science and its achievements are closely related to the diagnostic, prognostic and therapeutic problems of complex diseases. In the same way, these results show that the anatomical researcher and his scientific achievements play an important role in the efficient resolution of medical practice, connecting anatomical achievements with the possibility of being part of the solution of medical problems.

ACKNOWLEDGEMENTS

Special thanks to Marta Reyes for her participation in this work, noting that it is part of her doctoral thesis.

REFERENCES

AL-EMRAN M, MEZHUYEV V, KAMALUDIN A, SHAALAN K (2018) The impact of knowledge management processes on information systems: A systematic review. *Int J Inf Manag*, 43: 173-187.

ALESHIRE RA (1970) Planning and Citizen Participation. *Urban Aff Rev*, 5: 369-393. AL-QAYSI, N, MOHAMAD-NORDIN N, AL-EMRAN M (2020) A systematic review of social media acceptance from the perspective of educational and information systems theories and models. *J Educ Comput Res*, 57: 2085-2109.

ÁLVAREZ P, BOULAIZ H, VÉLEZ C, RODRÍGUEZ-SERRANO F, ORTIZ R, MELGUIZO C, CARRILLO E, MARTÍNEZ-AMAT A, PRADOS J (2014) Qualitative and quantitative analyses of anatomists' research: evaluation of multidisciplinarity and trends in scientific production. *Scientometrics*, 98: 447-456.

ÁLVAREZ P, ARGÜELLO A, REYES M, SORIANO A (2022) Análisis bibliométrico de la producción científica en torno a la investigación responsable en diferentes áreas de conocimiento. *Revista Cubana de Información en Ciencias de la Salud*, 33(1).

ARÁNEGA A (2022) Anatomy and the future: opportunities as translational science. *Eur J Anat*, 26: 145-147.

BURGET M, BARDONE E, PEDASTE M (2017) Definitions and conceptual dimensions of responsible research and innovation: A literature review. *Sci Eng Ethics*, 23(1): 1-19.

BOZEMAN B, BOARDMAN C (2014) *Research collaboration and team science: A state-of-the-art review and agenda* (Vol. 17). New York: Springer.

CAMPOHERMOSO RODRÍGUEZ OF, SOLIZ SOLIZ R, CAMPOHERMOSO RODRÍGUEZ O, ZÚÑIGA CUNO W (2014) Hipócrates de Cos, Padre de la Medicina y de la Ética Médica Hippocrates, Father of Medicine and Medical Ethics. *Cuad Hosp Clínicas*, 55: 59-68.

CASTELLÓ-COGOLLOS L, SIXTO-COSTOYA A, LUCAS-DOMÍNGUEZ R, AGULLÓ-CALATAYUD V, DIOS JG DE, ALEIXANDRE-BENAVENT R (2018) Bibliometría e indicadores de actividad científica (XI). Otros recursos útiles en la evaluación: Google Scholar, Microsoft Academic, 1findr, Dimensions y Lens.org. *Acta Pediátrica Esp*, 76: 123-130.

CHUA LK, JIMENEZ-DIAZ J, LEWTHWAITE R, KIM T, WULF G (2021) Superiority of external attentional focus for motor performance and learning: Systematic reviews and meta-analyses. *Psychol Bull*, 147: 618-645.

DASH S, KALAMDHAD AS (2022) Systematic bibliographic research on eutrophication-based ecological modelling of aquatic ecosystems through the lens of science mapping. *Ecol Model*, 472: 110080.

DE RASSENFOSSE G, JAFFE AB (2018) Are patent fees effective at weeding out low-quality patents? *J Econ Manag Strategy*, 27: 134-148.

DURIEUX V, GEVENOIS PA (2010) Bibliometric indicators: quality measurements of scientific publication. *Radiology*, 255: 342-351.

EZEAMUZIE NO, LEUNG JS, TING FS (2022) Unleashing the potential of abstraction from cloud of computational thinking: A systematic review of literature. *J Educ Comput Res*, 60: 877-905.

FADAVI HOSEINI F, MANSOURI A (2022) The role of articles in science-technology relationship: a topic analysis of non-patent literature (NPL) references. *Ser Rev*, 48: 137-150.

FERNÁNDEZ-SÁNCHEZ H, KING K, ENRÍQUEZ-HERNÁNDEZ CB (2020) Revisiones sistemáticas exploratorias como metodología para la síntesis del conocimiento científico. *Enfermería universitaria*, 17(1): 87-94.

FRANCHI T (2020) The impact of the Covid-19 pandemic on current anatomy education and future careers: A student's perspective. *Anat Sci Educ*, 13(3): 312-315.

HEO J, MURALE DP, YOON HY, ARUN V, CHOI S, KIM E, LEE JS, KIM S (2022) Recent trends in molecular aggregates: An exploration of biomedicine. *Aggregate*, 3: e159.

HUBSCHER CH, GUPTA DS, BRINK TS (2013) Convergence and cross talk in urogenital neural circuitries. *J Neurophysiol*, 110: 1997-2005.

JEFFERSON OA, LANG S, WILLIAMS K, KOELLHOFER D, BALLAGH A, WARREN B, SCHELLBERG B, SHARMA R, JEFFERSON R (2021) Mapping CRISPR-Cas9 public and commercial innovation using The Lens institutional toolkit. *Transgenic Res*, 30: 585-599.

KITCHENHAM B, PRETORIUS R, BUDGEN D, PEARL BRERETON O, TURNER M, NIAZI M, LINKMAN S (2010) Systematic literature reviews in software engineering – A tertiary study. *Inf Softw Technol*, 52: 792-805.

LOUKAS M, TOBOLA MS, TUBBS RS, LOUIS RGJ, KARAPIDIS M, KHAN I, SPENTZOURIS G, LINGANNA S, CURRY B (2007) The clinical anatomy of the internal thoracic veins. *Folia Morphol*, 66: 25-32.

MINGERS J, LEYDESDORFF L (2015) A review of theory and practice in scientometrics. *Eur J Oper Res*, 246: 1-19.

MUBARAKALI D, KIM H, VENKATESH PS, KIM J-W, LEE S-Y (2022) A systemic review on the synthesis, characterization, and applications of palladium nanoparticles in biomedicine. *Appl Biochem Biotechnol*, doi:10.1007/s12010-022- 03840-9.

PENFOLD R (2020) Using the Lens database for staff publications. *J Med Libr Assoc JMLA*, 108: 341.

ROJAS-MONTESINO E, MÉNDEZ D, ESPINOSA-PARRILLA Y, FUENTES E, PALOMO I (2022) Analysis of scientometric indicators in publications associated with healthy aging in the world, period 2011-2020. *Int J Environ Res Public Health,* 19(15): 8988.

STRAUS SE, TETROE JM, GRAHAM ID (2011) Knowledge translation is the use of knowledge in health care decision making. *J Clin Epidemiol*, 64: 6-10.

TORRES-SALINAS D, RUIZ-PÉREZ R, DELGADO-LÓPEZ-CÓZAR E (2009) Google Scholar como herramienta para la evaluación científica. *El Prof Inf*, 18: 501-510.

Patterns of variability of the shape of the human hand

Alexander Ermolenko

Doctor Chuchkalov Ulyanovsk Regional Clinical Center of Specialized Types of Medical Care, Ulyanovsk, Russian Federation

SUMMARY

The differences between the hands of men and women are mainly observed in the difference in the ratio of the lengths of the index and ring fingers (ratio 2d:4d) or in the difference in the proportional ratios of longitudinal and transverse dimensions, identified using classical morphometry methods, which give only indirect ideas about variations in the shape of the hand. The object of this study was digital images of radiographs of the right hands of 50 men and 50 women, on which 20 landmarks were located, the configuration and two-dimensional coordinates of which were studied using geometric morphometry methods.

The predominance of the general variability of the hand's shape was associated with a combined multidirectional transformation in the space of the elements of the II-V rays of the hand relative to the longitudinal axis with simultaneous compression or stretching of the shape relative to the transverse axis. At the same time, men have a stretching of the shape of the hand from the IV-V rays and compression from the II-III rays, while women have reverse changes. The relationship between the shape and size of the hand, regardless of gender, is minimal – 5.82% and 3.93% of hand allometry were detected in men and women, respectively. This study shows that the shape of the hand is markedly different in men and women, which indicates a significant sexual dimorphism affecting this trait. Based on the detected sexual differences, it is possible to distinguish the male and female morphological type of the hands.

Key words: Human hand – Shape variability – Sexual dimorphism – Geometric morphometry

INTRODUCTION

Hands are vital anatomical parts for humans, as they are used to grip manipulate and shape various objects of the environment. Being an important part of the upper limbs and giving the latter functional completeness, human hands have some differences in men and women (Khanpetch et al., 2012). One of the factors determining the size and shape of the hands is gender. Studies show that men have bigger hands than women of the same height (Case and Ross, 2007). A comparative analysis of the size of the hands also demonstrates that the length of the hand is longer in men than in women, while the same ratios were found for the metacarpal bones and phalanges of the fingers (Hsiao et al., 2015). In addition, one of the differences between the hands of men and women is the ratio of the lengths of the index and ring fingers (2d:4d ratio) – in men, the length of the ring finger prevails over the length of the index finger, while in women the opposite ratio is observed (Sanfilippo et al., 2013; de Sanctis et al., 2017; Ernsten et al.,

Corresponding author:
Alexander Ermolenko. 28 Koryukin st., Ulyanovsk, Russian Federation, 432063. Phone: +79372753757. E-mail: osteon@yandex.ru

Submitted: December 3, 2022. **Accepted:** February 2, 2023

https://doi.org/10.52083/EJRV7551

2021). To study the variability of the hand associated with gender, the following are used: subjective criteria based on morphological features and objective criteria based on size analysis, including various measurements and indices (Kanchan and Krishan, 2011; Kondo et al., 2017). Despite numerous studies, single works are devoted to the analysis of the shape of the hand of a modern person in the context of sexual differences (Sanfilippo et al., 2013; Karakostis et al., 2018).

Anthropometry (Kanchan and Krishan, 2011; de Sanctis et al., 2017), osteometry (Cihák, 1972), morphometry of photographs (Jakubietz et al., 2005) or digital images of hands (Hsiao et al., 2015; Kim et al., 2018; Ernsten et al., 2021), as well as morphometry according to radiography data are used to assess the shape and size of the hand (Kondo et al., 2017). However, classical anthropometric measurements of the hands have a number of disadvantages due to the different index of soft tissues in men and women, as well as measurement errors (Kanchan and Krishan, 2011).

In addition, most studies of the hand have focused on the morphological features of individual segments or bones of the hand related to size, and the components of the shape change of the latter have been underestimated due to conceptual difficulties in quantifying such an abstract concept as shape. Attempts to describe the shape of the hand based on data obtained using classical morphometric methods are indirect – there is no analysis of the shape as such, and it is impossible to assess spatial morphological changes and the geometry of the object under study as a whole (Klingenberg, 2011).

Given the differences between the hands of men and women observed in previous studies, the question arises whether a more detailed analysis of the variations in the morphology of the hand using methods based on geometric morphometry can provide an understanding of the sexual differences in the shape of the hand from radiography data.

MATERIALS AND METHODS

Sample

The object of the study was digital images of radiographs of the right hands (anteroposterior projection, fingers in the position of bringing) of 100 adults (50 men and 50 women) from the archive of the Department of Radiation diagnostics of the Doctor Chuchkalov Ulyanovsk Regional Clinical Center of Specialized Types of Medical Care. The criteria for inclusion in the study were the absence of integrity disorders, developmental anomalies, deformities and bone and joint pathology of the hands. The average age of men was 46.3±1.1 years, and women - 49.2±0.9 years.

Digitization and locating landmarks

In Adobe Photoshop CS6 13.0.1 (Adobe Systems Incorporated Co., USA), digital images of radiographs were edited so that the middle of the metacarpophalangeal joints of the middle finger on each image coincided. On each digital image of the radiograph of the hand there are 20 landmarks in the Cartesian coordinate system using the on-screen digitizer TPSdig2 (Fig. 1, Table 1) (Rohlf, 2015).

Table 1. Definition of landmarks located on digital images of radiographs of hands.

Landmarks	Description
1	Second carpometacarpal joint
2	Metacarpophalangeal of the index finger
3	Proximal interphalangeal joint of the index finger
4	Distal interphalangeal joint of the index finger
5	Tip of the distal phalanx of the index finger
6	Third carpometacarpal joint
7	Metacarpophalangeal of the middle finger
8	Proximal interphalangeal joint of the middle finger
9	Distal interphalangeal joint of the middle finger
10	Tip of the distal phalanx of the middle finger
11	Fourth carpometacarpal joint
12	Metacarpophalangeal of the ring finger
13	Proximal interphalangeal joint of the ring finger
14	Distal interphalangeal joint of the ring finger
15	Tip of the distal phalanx of the ring finger
16	Fifth carpometacarpal joint
17	Metacarpophalangeal of the ring finger
18	Proximal interphalangeal joint of the little finger
19	Distal interphalangeal joint of the little finger
20	Tip of the distal phalanx of the little finger

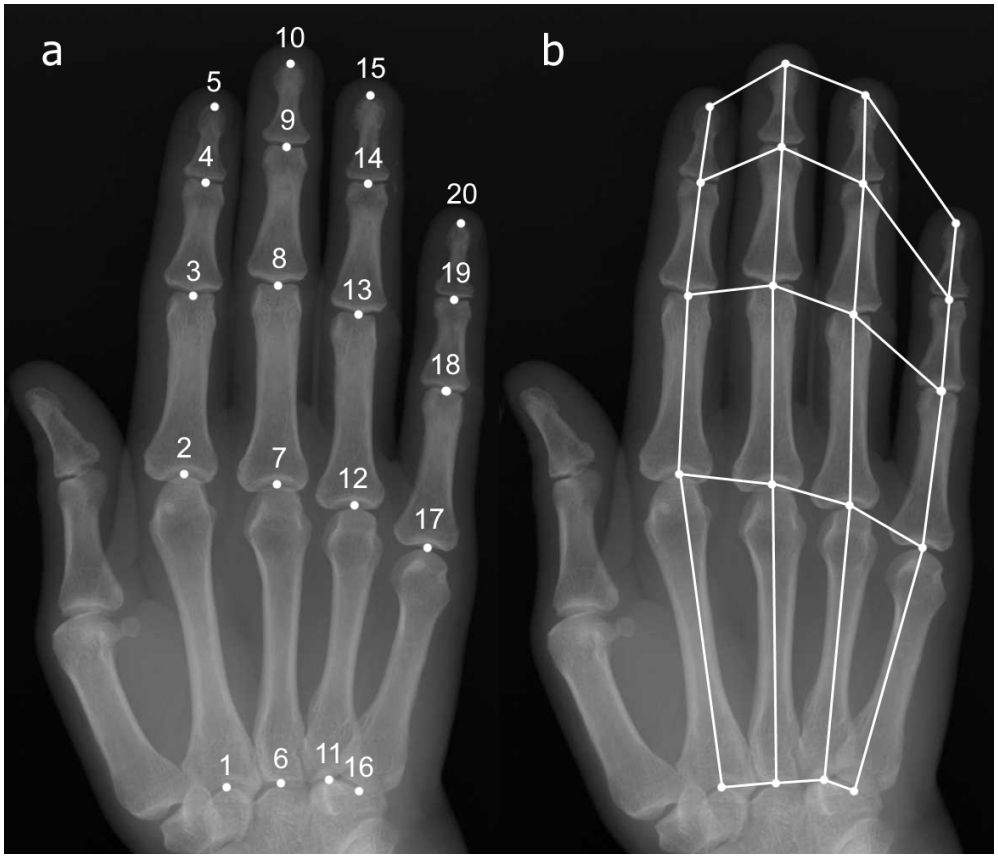

Fig. 1.- Landmark locations (**a**) and wireframe diagram of linked landmarks (**b**).

Geometric morphometrics and statistical analysis

The analysis of hand shapes was carried out using MorphoJ 1.07a (Klingenberg, 2011). In order to eliminate the effects not related to the shape of the hands (position, orientation, scale) and optimal alignment of the configuration of landmarks in the general space of the shape, the configurations of two-dimensional coordinates (n=100) were subjected to generalized Procrustean analysis (GPA). The general variability of the shape of the hands in space relative to each other to assess the similarity or difference in the sample under study was studied using principal component analysis (PCA). The size of the studied hands was expressed in the form of centroid size (CS), as the most common size estimation indicator used in geometric morphometry. To determine the effect of size on the shape (allometry) of the hand, a multidimensional regression was performed, where the CS was used as an independent variable as a size variable, and Procrustean coordinates as a shape variable as a dependent variable (Klingenberg, 2016). In addition, a permutation test was performed using 10 000 iterations to assess the significance of the effect of size on shape. Discriminant function analysis (DFA) was performed to compare the differences between male and female hands. The significance of differences between two groups was assessed using the Mann-Whitney U test for independent variables. The significance level of $p<0.05$ was assumed to be statistically significant.

RESULTS

Among the configurations of hand shapes after GPA, the proportion of total shape variability was determined, taken into account by each main component (PC) from the resulting eigenvalues (total eigenvalues=0.00165468) (Fig. 2). The first main component (PC1) describes 32.4% (eigenvalue=0.00058184) of the total variability of the shape of the hand; the second main component (PC2) describes 20.3% (eigenvalue=0.00029552) of the total variability of the shape of the hand; the remaining 34 PCs were ignored.

The PCA results demonstrate that the main deformations of the hand shape are observed along the PC1 axis regardless of gender, and the dif-

ferences along the PC2 axis are less pronounced (Fig. 3). PC1 describes the space of forms associated with the morphological type of the hand – the configurations of landmarks distributed in the direction of lower values (PC1-) have a more elongated contour of II-III fingers and a shortened contour of IV-V fingers, while the configurations of landmarks distributed in the direction of higher values (PC1+), on the contrary, have a more elongated contour of IV-V fingers and a shortened contour of II-III fingers. PC2 describes the shape space associated with the transverse and longitudinal proportions of the hand – the configurations of landmarks distributed in the direction of lower values (PC2-) have somewhat narrow and elongated shapes (simultaneous compression of the shape in the transverse and stretching in the longitudinal axis), while the configurations of landmarks distributed in the direction of higher values (PC2+) have shorter and wider shapes (simultaneous stretching of the shape in the transverse and compression in the longitudinal axis).

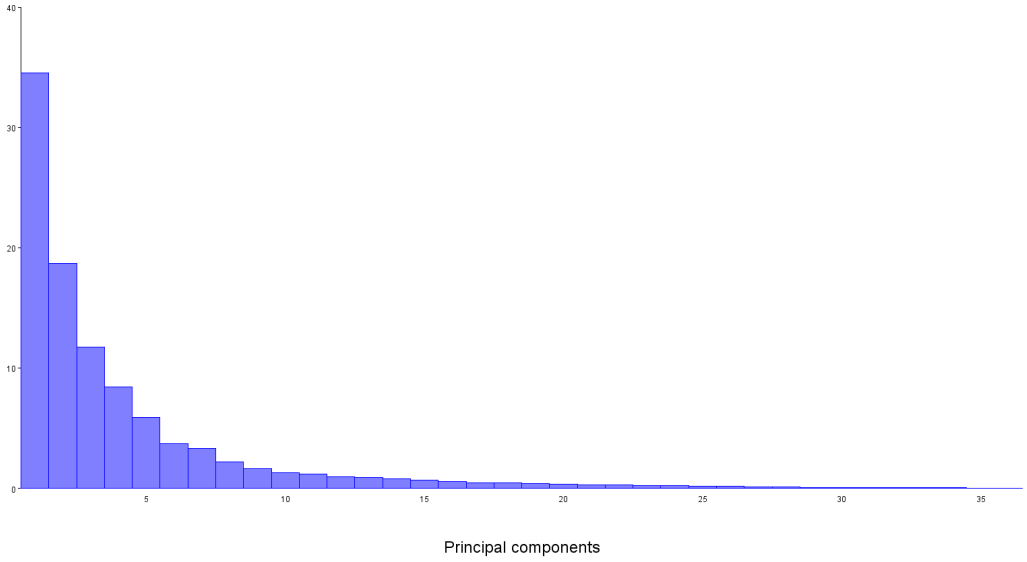

Fig. 2.- Proportion of the total hand shape variance explained by each PC.

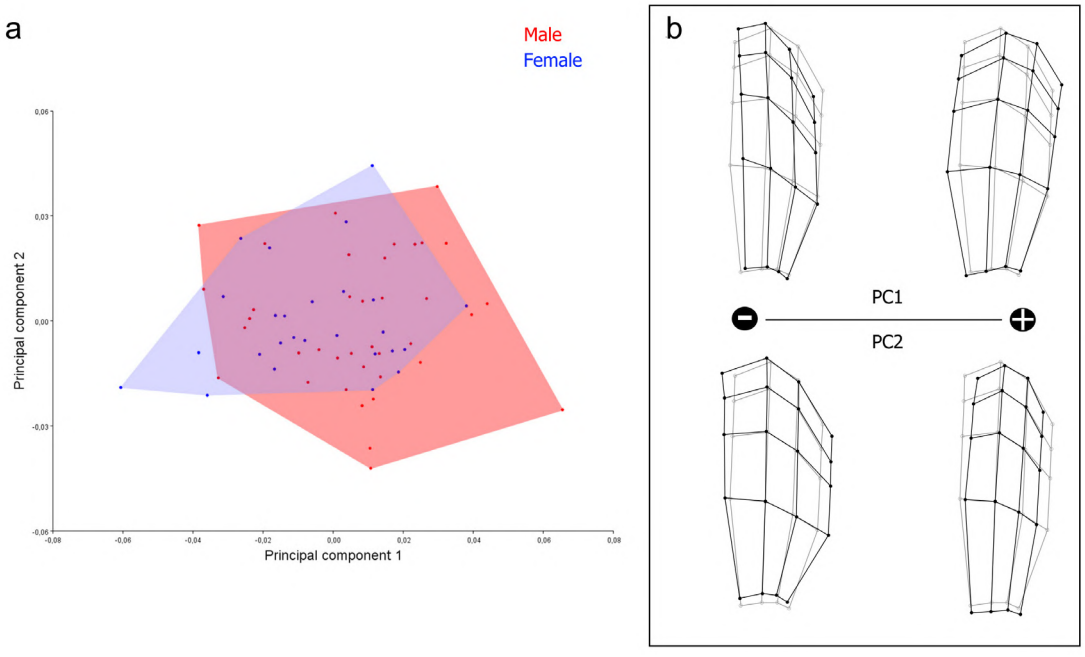

Fig. 3.- Patterns of changes in the configurations of the hand in the morphospace (**a**). Changes in the shape of the hand relative to the average configuration along the axes PC1 and PC2 (magnitude -0.1 and +0.1 for PC1 and PC2, respectively) based on the data of the covariance matrices of procrustean coordinates (**b**).

In men, the shape of the hand is wider relative to the average configuration than in women (Fig. 4). The width of the hand in both men and women is determined by the location of the distal epiphyses of the second and fifth metacarpal bones (landmarks 2 and 17). The smallest differences in shape configurations were found for the segments of the third and fourth rays of the hand (landmarks 6-15).

According to the results of the DFA, statistically significant differences were revealed between the hands of men and the hands of women (the measure of distance is the distance of the Procrustes distance, the distance of Mahalanobis=3.09, T^2=238, p<0.001). The demarcation point is 0.018. Therefore, values of the size of the Procrustes distance exceeding this value indicate male hands, while smaller values are estimated as female (Fig. 5).

The accuracy of the hand shape classification according to the DFA results reaches 86% for men and 80% for women. The cross-validation procedure gives exactly the same results (p <0.0001 with 1000 repetitions) (Table 2).

Table 2. Percentage of hands of men and women correctly and erroneously distributed using the analysis of canonical variations.

Sex	Distribution based on hand shape data	
	Correct distribution, n	Incorrect distribution, n
Male	43	7
Female	40	10

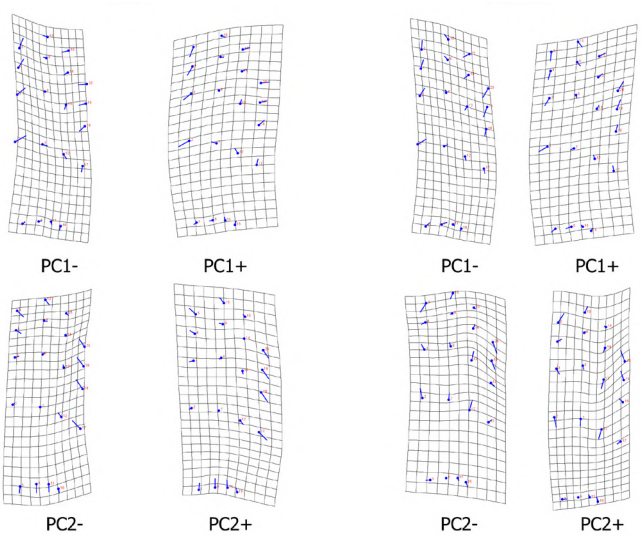

Fig. 4.- The space of hands shapes with corresponding landmarks.

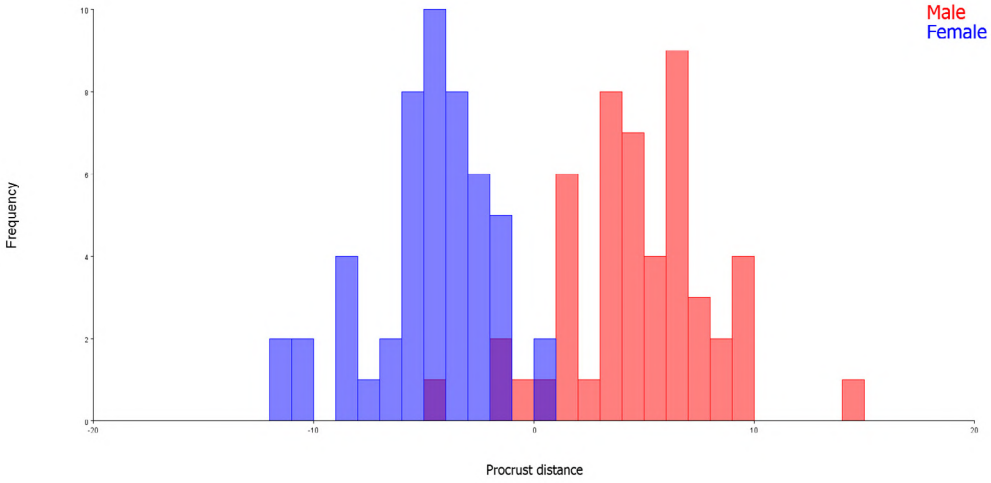

Fig. 5.- Sexual differences between the hands.

When comparing the CS of the hands, statistical sexual differences were revealed (Table 3). Multivariate regression showed 5.82% and 3.93% allometry of the hands in men and women, respectively, with a significant permutation value ($p < 0.0001$) (Fig. 6).

Table 3. Descriptive statistics for CS (in mm) and results for average differences.

Sex	CS		Mann-Whitney U Test		
	Me	IQR	U	Z	p value
Male	53.78	5.99	372	6.05	0.0001
Female	47.57	4.37			

important step in assessing the sexual differences in the shape of the hand in humans. However, the preliminary preparation of digital images of the studied objects before the location of landmarks (alignment of samples), the limited use of the obtained quantitative data in cladistic analysis, the inability to generate new data that are not related to the shape are somewhat narrowing the limits of GMM capabilities.

Nevertheless, the results of this study demonstrate how the spatial orientation of the II-V metacarpal bones and phalanges of the II-V fingers affects the shape of the hand in men and women.

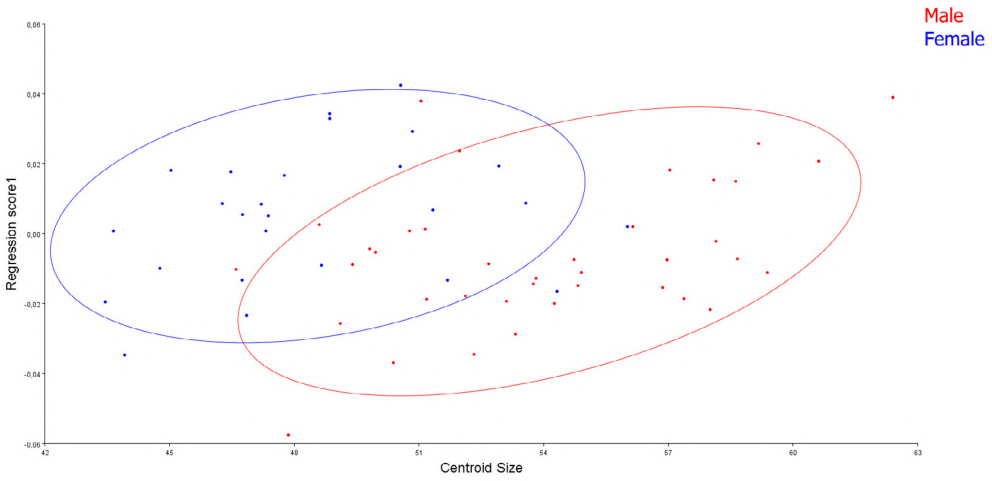

Fig. 6.- Regression of relative deformation estimates by CS. A plot summarizing the relationship between size change and shape.

DISCUSSION

Apparently, this is the first publication in which geometric morphometric methods (GMM) are used to study the sexual differences in the shape of a person's hand according to radiography. In previous studies, it was shown that the differences between the hands of men and women are mainly observed in the difference in the ratio of the lengths of the index and ring fingers (2d:4d ratio), or in the difference in the proportional ratios of longitudinal and transverse dimensions revealed using classical morphometry methods, which give only indirect ideas about variations in the shape of the hand. Thus, the use of GMM is an

Changes in the shape of the hands of men and women consist in its uniform transformation in space relative to the longitudinal (geometry changes are associated with the morphological type of the hand – a combined multidirectional stretching / compression of the shape of elements II and IV-V rays of the hand relative to each other) and transverse (geometry changes are associated with the brachycheiria-dolichocheiria pattern). It is assumed that genetic determination (HOXa and HoxD) against the background of effects caused by different concentrations of steroid hormones in the blood of a pregnant woman leads to sexu-

al dimorphism of fetal finger length (de Sanctis et al., 2017).

The study showed the presence of differences both in the shape of the hands and in their CS, which characterizes men's hands as larger compared to women's. These sex differences may be due to the action of prenatal sex hormones of developing gonads (Blecher and Erickson, 2007). The regression of the apical ectodermal ridge observed at the beginning of the second trimester of pregnancy, located at the distal end of the rudiment of each limb with the formation of hand rays and subsequent interdigital apoptosis under the influence of androgenic stimulation proportional to both the level of androgens in the blood and individual sensitivity to these hormones, causes a different ratio of fingers during their development (Breedlove, 2010).

The results of the study demonstrate a minimal degree of allometry, while in men it is slightly higher than in women. This is consistent with the data that in the process of ontogenesis, despite the fact that the size of the hands varies by several orders of magnitude (from several tenths of a millimeter to several millimeters), their proportionality, including shape, does not change so much – the hands of human embryos are similar to the hands of an adult (Hattori, 1986). The general similarity of the proportions of the fetal and adult hands does not exclude minor changes in the shape and proportions of the hand during ontogenesis, as well as individual differences in these changes (Cihák, 1972). Another form of sexual dimorphism, manifested as previously indicated in the form of uniform transformation, are differences in the relative width of the hand, which may be due to allometry, since the size of the hand correlates with changes in the relative width of the hand – large hands, regardless of gender, are somewhat wider (Jakubietz et al., 2005). The results obtained by us – i.e., that the male hand is somewhat wider than the female hand – are consistent with the results of traditional morphometry (Xiao et al., 2015). The transformation of the hand observed in postnatal ontogenesis in the form of transverse compression (both in men and women) due to more intensive growth of the hand in length than in width, both in men and women, maintains positive dynamics and reaches a maximum during puberty. One of the important aspects of sexual dimorphism of the hand shape is that the differences associated with gender are the result of both uniform shape transformation and the result of proximal-distal displacement of the hand rays relative to the width of the latter – since the fourth and fifth rays are displaced more distally, the hand becomes relatively wider. It is possible that the detected sex differences in the shape of the hand reflect the different effects of genetic and hormonal factors affecting the development of the hand at different stages of embryogenesis.

Thus, GMM can be an assessment of the morphology of the hand by extracting shape variability at various scales and analyzing their relationship. In addition, the results of this study may be useful in the development of algorithms for assessing gender in forensic medicine and in biometric authentication systems. It is likely that with a larger number of participants in the study, it would be possible to study the age-related aspects of hand shape variations in men and women. In addition, it is of interest how changes in the geometry of the configurations of individual parts of the hand (the pastern, the distal part of the hand, which is formed by the fingers) in men and women affect the shape of the hand as a whole.

ACKNOWLEDGEMENTS

The author expresses gratitude to the radiology department of the Doctor Chuchkalov Ulyanovsk Regional Clinical Center of Specialized Types of Medical Care for providing digital images of hand radiographs.

REFERENCES

ARNOLD AP (2009) The organizational-activational hypothesis as the foundation for a unified theory of sexual differentiation of all mammalian tissues. *Horm Behav*, 55(5): 570-578.

BLECHER SR, ERICKSON RP (2007) Genetics of sexual development: a new paradigm. *Am J Med Genet A*, 143A(24): 3054-3068.

BREEDLOVE SM (2010) Minireview: Organizational hypothesis: instances of the fingerpost. *Endocrinology*, 151(9): 4116-4122.

CASE DT, ROSS AH (2007) Sex determination from hand and foot bone lengths. *J Forensic Sci*, 52(2): 264-270.

CIHÁK R (1972) Ontogenesis of the skeleton and intrinsic muscles of the human hand and foot. *Ergeb Anat Entwicklungsgesch*, 46(1): 5-194.

DE SANCTIS V, SOLIMAN AT, ELSEDFY H, SOLIMAN N, ELALAILY R, DI MAIO S (2017) Is the second to fourth digit ratio (2D:4D) a biomarker of sex-steroids activity? *Pediatr Endocrinol Rev*, 14(4): 378-386.

ERNSTEN L, KÖRNER LM, HEIL M, RICHARDS G, SCHAAL NK (2021) Investigating the reliability and sex differences of digit lengths, ratios, and hand measures in infants. *Sci Rep*, 11(1): 10998.

HATTORI K (1986) Tubular hand bone growth during the latter half of the prenatal period: an allometric analysis. *Am J Phys Anthropol*, 71(4): 417-422.

HSIAO H, WHITESTONE J, KAU TY, HILDRETH B (2015) Firefighter hand anthropometry and structural glove sizing: a new perspective. *Hum Factors*, 57(8): 1359-1377.

JAKUBIETZ RG, JAKUBIETZ MG, KLOSS D, GRUENERT JG (2005) Defining the basic aesthetics of the hand. *Aesthetic Plast Surg*, 29(6): 546-551.

KANCHAN T, KRISHAN K (2011) Anthropometry of hand in sex determination of dismembered remains – A review of literature. *J Forensic Leg Med*, 18(1): 14-17.

Karakostis FA, Lorenzo C, Moraitis K (2017) Morphometric variation and ray allocation of human proximal hand phalanges. *Anthropol Anz*, 74(4): 269-281.

Karakostis FA, Hotz G, Scherf H, Wahl J, Harvati K (2018) A repeatable geometric morphometric approach to the analysis of hand entheseal three-dimensional form. *Am J Phys Anthropol*, 166(1): 246-260.

KHANPETCH P, PRASITWATTANSEREE S, CASE DT, MAHAKKANUKRAUH P (2012) Determination of sex from the metacarpals in a Thai population. *Forensic Sci Int*, 217(1-3): 229.e1-229.e8.

Kim W, Kim YM, Yun MH (2018) Estimation of stature from hand and foot dimensions in a Korean population. *J Forensic Leg Med*, 55: 87-92.

KLINGENBERG CP (2011) MorphoJ: an integrated software package for geometric morphometrics. *Mol Ecol Resour*, 11(2): 353-357.

Klingenberg CP (2016) Size, shape, and form: concepts of allometry in geometric morphometrics. *Dev Genes Evol*, 226(3): 113-137.

Kondo M, Ogihara N, Shinoda K, Anada S, Ito K, Murata M, Tanaka T, Takai S, Matsu ' ura S (2017) Sexual dimorphism in the human hand proportion: A radiographic study. *Bull Natl Mus Nat Sci Ser D*, 43: 1-6.

Rohlf FJ (2015) The TPS series of software. *Hystrix, the Italian Journal of Mammalogy*, 26(1): 9-12.

Sanfilippo PG, Hewitt AW, Mountain JA, Mackey DA (2013) A geometric morphometric assessment of hand shape and comparison to the 2D:4D digit ratio as a marker of sexual dimorphism. *Twin Res Hum Genet*, 16(2): 590-600.

Complete thyrohyoid calcification: a case from the 18th century and literature review

Laura Canales[1], Assumpció Malgosa[1], Josep Liria[1], Jose-Ramón Sañudo[2], Albert Isidro[1,3]

[1] Unitat d'Antropologia Biològica. Departament de Biologia Animal, Biologia Vegetal i Ecologia, Universitat Autònoma de Barcelona, Spain

[2] Departamento de Anatomía y Embriología Humanas. Facultad de Medicina. Universidad Complutense, Madrid, Spain

[3] Hospital Universitari del Sagrat Cor de Barcelona, Spain

SUMMARY

Calcifications in the thyrohyoid ligament are uncommon and usually involve triticeal cartilage. This report analyzes an uncommon thyrohyoid ossification in an individual from the 18th century. To study this ossification, an X-ray analysis was made and the measurements of the different segments of the bone were taken to compare to other cases. The radiographic images show a complete thyrohyoid ossification arising from the great horn of the hyoid with the non-clear presence of the triticeal cartilage. This form is rarely taken into account in typology studies so far, although its etiology is theorized. Different types of calcifications must be considered when clarifying terminologies, investigating their etiology, and whether they involve the triticeal cartilage. Literature review has been carried out to clarify the different types of calcifications in the thyrohyoid ligament and its terminology.

Key words: Hyoid – Cartilage calcification – Triticeal cartilage – Lateral thyrohyoid ligament – Paleopathology

INTRODUCTION

The hyoid bone is located at the upper neck above the thyroid cartilage and is attached to its nearby structures by a large number of muscles and ligaments (Ito et al., 2012). Aside from minor anatomical variations, X-ray examinations usually show calcifications derived from those connections (Di Nunno et al., 2004). Its detection and proper identification can be challenging, and it is important not to misdiagnose them with other calcifications in oral soft tissue or serious pathological conditions (Ahmad et al., 2005; Vatansever et al., 2018; Barut et al., 2020). In this regard, clinical studies done so far have focused on describing the calcifications of the carotid, the triticeal cartilage, and the thyroid, but few cases of ossifications of the entire thyrohyoid ligament have been reported (Porrath, 1969; Di Nunno et al., 2004; Alqahtani et al., 2016; Wilson et al., 2017).

Here we present an anomalous ossification that arises from the greater horn of the hyoid (GHH) and is not tied to the superior cornu of the thyroid (SCT). It was found in an archaeological skeleton of the 18th century and it only matches with another case ever described in the current literature (Klinefelter, 1952). The ambiguous identification

Corresponding author:
Albert Isidro. Hospital Universitari del Sagrat Cor, C/Viladomat 288, 08029, Barcelona, Spain. Phone: 691501692. E-mail. aisidro.cot@gmail.com

Submitted: July 11, 2022. **Accepted:** December 29, 2022

https://doi.org/10.52083/MZZJ8543

of the triticeal cartilage (TC) in the present case has orientated the discussion on the types of thyrohyoid calcifications that are normally strictly related to the presence of this cartilage.

MATERIALS AND METHODS

The case presented here was found during the archaeological excavation of the ancient church of Santa Maria de Besora (Barcelona) (Busquets and Malgosa, 2020). Inside the church were the graves of the clergy who had served there. One of them was an 80-year-old presbyter from the 18th century, who had an anomalous hyoid bone (Fig. 1). In the laboratory, no other pathologies were found in the skeleton apart from age-related calcifications, such as those of the thyroid and costochondral ones.

Regarding the study of bone morphology, an X-ray image was taken to identify the presence or absence of bone structures within the calcification. In order to understand this abnormal formation and its implications, the existing literature was reviewed.

RESULTS

The hyoid bone of the Santa Maria de Besora individual (Fig. 2) has both GHH fused to the body and no lesser horns are observed, although this is not an abnormal condition (Parsons, 1909; Porrath, 1969). The left GHH is not completely preserved, and the distal part of the ramus is missing. The right GHH presents an ossification forming a bony structure emerging from the tip and descending vertically towards the SCT. The descending segment has a wide end in which a rounded indent can be identified in the center; this indicates that the bone ends at that point, and it is probably forming a joint in discontinuity with the SCT.

The right GHH measures 0.55x3.25 cm and the vertical segment 0.70x3.05 cm (Fig. 3A). The width of the descending segment is 0.70cm, but it widens to 1.50 cm at the joint with the thyroid. The width (2.80 cm) and height (1 cm) of the body of the hyoid are within the range of the measurements for males (Ito et al., 2012; Parsons, 1909). The left GHH is partially missing but shows differences in thickness with the right GHH; the pre-

Fig. 1.- a) Excavated skeleton from Santa Maria de Besora church and **b)** Enlarged image of the hyoid *in situ*.

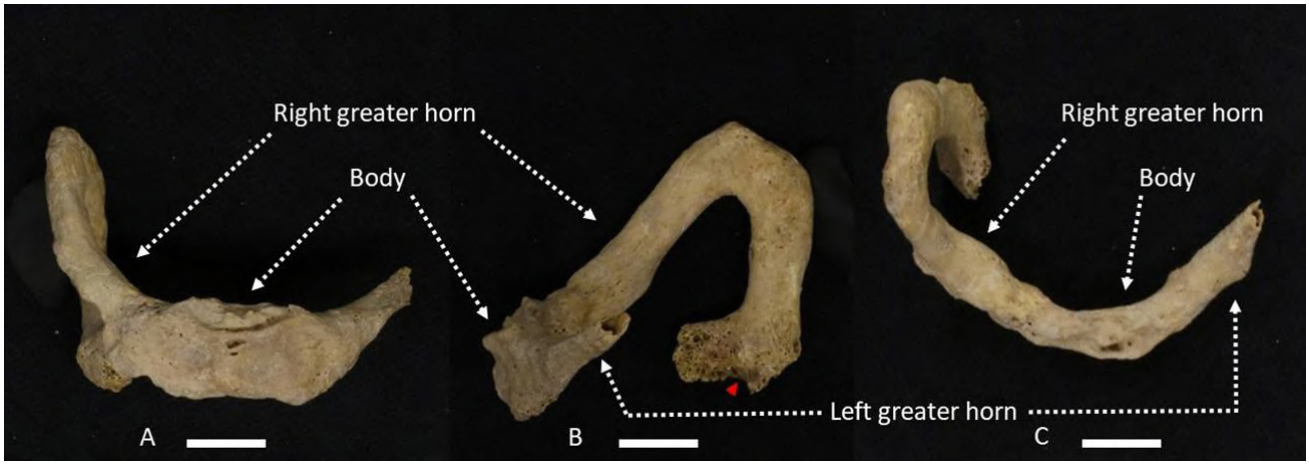

Fig. 2.- a) Frontal view of the hyoid, **b)** lateral left view, c) superior view. Rounded indent of the wide end pointed in red.

served left part is 0.25 cm thick, while the right horn at the same point is 0.65 cm.

This abnormality in the hyoid is associated with the calcification of the thyroid cartilage that only preserves the left superior cornu, and it displays a normal appearance. No other calcifications are observed related to the hyoid or the styloid process.

The X-ray study (Fig. 3B) shows the bone continuity of the right GHH and the anomalous descending segment. The bone density distinguishes the point where the GHH ends, and the ossified segment start, because the GHH is more radio-opaque. It also shows a decrease in bone density in the widened distal part of the segment, which has broken edges except for the rounded indent in the center. Although the X-ray image shows other bone density variations, such as transverse lines at the proximal part of the calcified segment, the outline of the TC is not firmly defined, and its presence cannot be confirmed. Despite density variations, the thickness of the calcification is uniform and the rounded central indent distinguishes it from the SCT. Its calcification in continuity with the thyrohyoid ligament is ruled out.

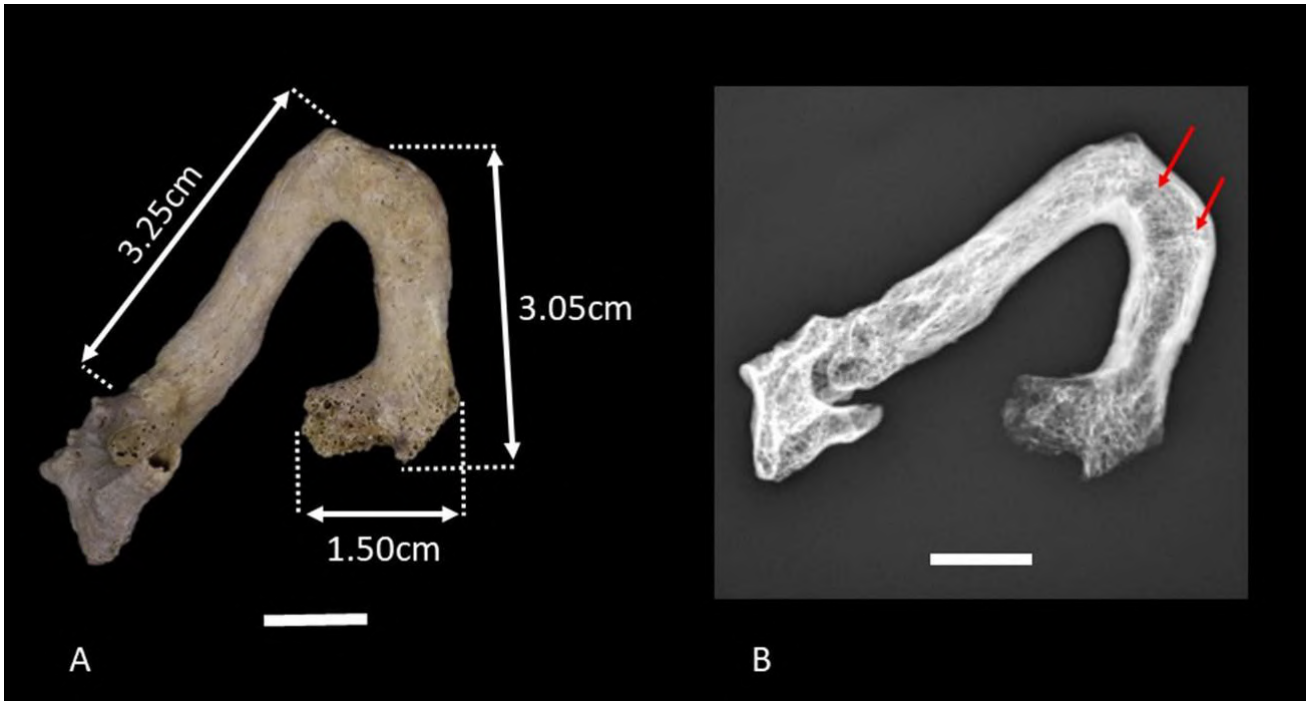

Fig. 3.- a) Measurements of the hyoid, **b)** X-ray image of the hyoid of the continuity of cancellous bone and two transverse lines (arrows).

DISCUSSION

The hyoid bone consists of a body, two greater horns and two lesser horns and it is connected to the structures of the neck by a large number of muscles and ligaments attached to its surface (Fig. 4) (Parsons, 1909; Ito et al., 2012). The anatomical complexity of this apparatus and its abnormalities, calcifications, and embryological disorders are still under study, especially those concerning the infrahyoid area (Porrath, 1969; Alsarraf et al.,1998).

On the bottom surface of the hyoid, the thyrohyoid membrane covers the space between the hyoid and the thyroid cartilage (Di Nunno et al., 2004). The thyrohyoid ligament is located in the posterior border of this membrane, extending from the end of the GHH to the tip of the SCT (Ahmad et al., 2005). The TC is located within this cord-like ligament. It is a small oval-shaped nodule of hyaline cartilage which tends to calcify and whose function is unknown, although it is supposed to reinforce the thyrohyoid ligament (Standring et al., 2008; Alqahtani et al., 2016; Vatansever et al., 2018). This cartilage has focused the investigations concerning calcifications on the infrahyoid area (Barut et al., 2020). These have shown that the TC is not a constant structure: its prevalence is variable just like its appearance and ossification patterns (Ahmad et al., 2005; Alqahtani et al., 2016; Wilson et al., 2017; Pinheiro et al., 2018; Vatansever et al., 2018; Barut et al., 2020). The lack of information on this piece of the human body has led experts to explore the calcifications involving it, and to find out whether its presence leads more often to abnormal calcifications in the thyrohyoid area (Vatansever et al., 2018).

The case reported here shows a calcification of the right lateral thyrohyoid ligament in continuity with the right GHH, but the presence of the TC is not clear. Thyrohyoid ligament calcifications are mostly related to the presence of the TC, although there is no consensus on all typologies; very few mention complete thyrohyoid ligament calcifications (Pinheiro et al., 2018). This information gap is due to the lack of reported cases of this type of calcification that is only referenced as a possible abnormality (Soerdjbalie-Maikoe and Van Rijn, 2008; Alqahtani et al., 2016), but has never been demonstrated and, therefore, studied.

The review of specific literature about calcifications of the thyrohyoid ligament (Porrath, 1969; Kainz et al., 1990; Avrahami et al., 1994; Urben and Ransom, 1999) provides only one clinical case with the same X-ray characteristics as the Besora hyoid. Klinefelter (1952) presents the case of an anomalous hyoid bone related to a large hyoid body and calcification of the stylohyoid and thyrohyoid ligaments. The radiologic study showed

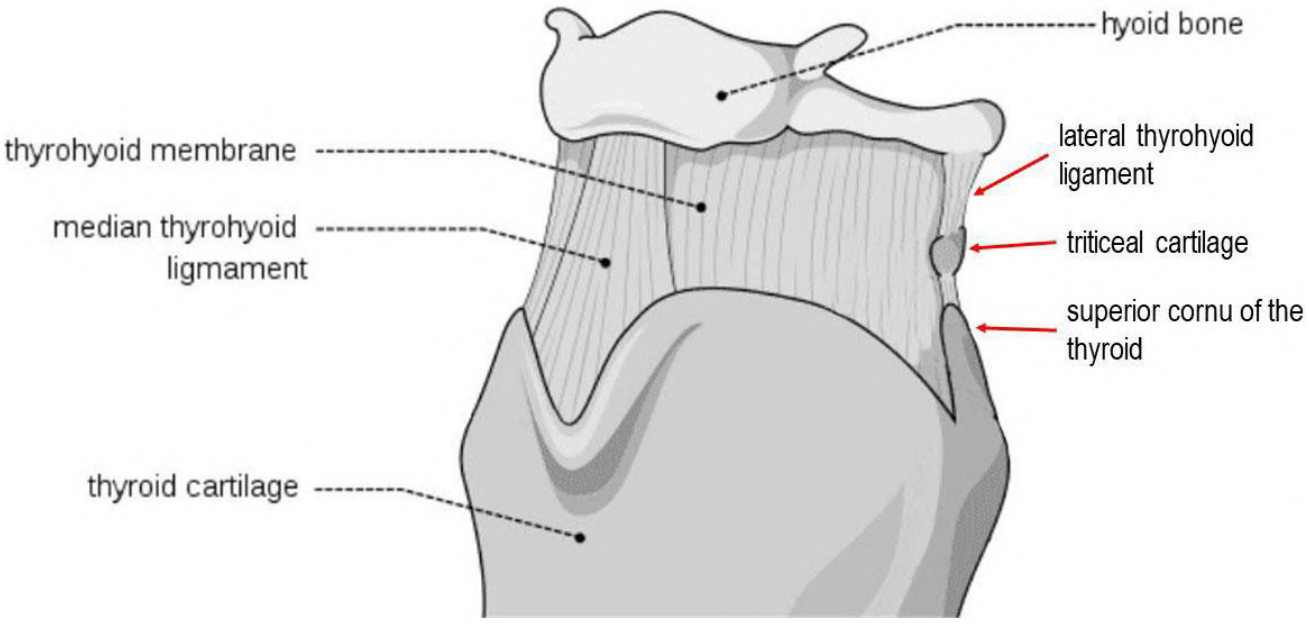

Fig. 4.- Larynx external en.svg by Olek Remesz (wiki-pl: Orem, commons: Orem) / CC-BY-SA 2.5, 2.0, 1.0. Modified from the original.

a right GHH formed by a horizontal segment and a descending one in a 7-shaped fused bone. The descending segment formed a joint with the enlarged SCT. The shape and the measurements of the GHH and the vertical segment are similar to our case; however, the body of the Besora hyoid is within the ranges for men, and no calcifications of the styloid were found. The fact that the preserved part of the left GHH presented normal measures leads us to assume that, just like in Klinefelter's case, the calcification of the thyrohyoid is unilateral. This abnormality was diagnosed as an anomalous hyoid without penetrating or perforating ossifications, and there is no mention of the presence of the TC or a complete thyrohyoid calcification (Klinefelter 1952).

Although we cannot prove the presence of the TC, most of the published articles regarding the etiology of the calcifications of the thyrohyoid ligament involve this cartilage. We must take them into account, since the TC could be also present in the case described here. Until now, the most commonly documented variation reported in clinical and forensic cases shows a bone articulating the GHH and the SCT with synovial joints (Ilankovan, 1987; Alsarraf et al., 1998; Joshi et al., 2014; Wilson et al., 2017; Pinheiro et al., 2018). In these cases, a calcification of the thyrohyoid ligament (Ilankovan, 1987) or an enlarged ossified TC (Alsarraf et al., 1998) was diagnosed, but there are no known causes for these calcifications. It has been hypothesized that calcification processes of the TC could be linked to age, and so the thyrohyoid calcifications could follow this trend, as has been proposed (Avrahami et al., 1994; Harrison, 1995; Di Nunno et al., 2004). Nevertheless, the degree of calcification of the TC has been proven to have no relationship with age (Vatansever et al., 2018). Furthermore, the age disparity between our case and that of Klinefelter's shows that the age criterion cannot be applied to this type of calcification either. Another variation that has been reported in fewer cases is the direct articulation of GHH with SCT without the presence of the TC (Dwight, 1907; de Bakker et al., 2019).

There are disorders described such as congenital malformations of the thyrohyoid apparatus that can lead to calcified anatomical variations (Ilankovan, 1987; Urben and Ransom, 1999; Soerdjbalie-Maikoe and Van Rijn, 2008). One of them is the embryological separation of the TC from the SCT: it was proposed that the presence of the TC resulted in a short SCT, but it has been proved that there is no correlation between the presence of the TC and a short SCT (Wilson et al., 2017). In our report, the calcification arises from the tip of the GHH, and it is in discontinuity with the SCT, forming probably a widened joint. Therefore, we can rule out that it started from the bottom up, creating a continuity of the thyroid with the TC or the thyrohyoid ligament.

Several studies affirm that another described disorder is the failure of the disconnection of the GHH and the SCT when thyroid chondrification begins. It is said that it can cause a total ossification of the thyrohyioid ligament (Soerdjbalie-Maikoe and Van Rijn, 2008; Alqahtani et al., 2016). However, in a research of the existing literature, this embryological variant is not described (van den Broek and Brinkman, 1979). Only Porrath (1969) includes Klinefelter's case variation and proposes an embedded TC that has failed in segmentation of the thyrohyoid ligament during fetal processes, causing a hyothyroid bar. This nomenclature has been used to describe cases of embedded TC and also in direct connections between the GHH and the SCT (de Bakker et al., 2019). This bar originates from an irregular embryological process of TC formation in which cartilaginous components persist in the lateral thyrohyoid ligament (Porrath, 1969).

The diagnoses of the thyrohyoid abnormalities are diverse and some authors have tried to establish a unified nomenclature (Wilson et al., 2017; Pinheiro et al., 2018). As Wilson et al. (2017) propose, it could be a "persistent thyrohyoid cartilage" that has failed to regress into a TC, similar to the hyoid apparatus seen in some mammals. Pinheiro et al. (2018) suggest the nomenclature of "lateral thyrohyoid ossification" when describing synovial joint cases. These generic names do not contemplate the possibility of different types of calcifications of the thyrohyoid ligament, and cases like Klinefelter's or the one presented here are not considered.

The hyoid of Besora does not clearly present the TC; there is a direct bone fusion with the

right GHH and probably a joint is observed with the SCT. Therefore, it may resemble the variation described by Porrath or it could be a calcification of the thyrohyoid ligament without the TC, a variation that has been proposed but not proved. It may be the confirmation of the complete thyrohyoid calcification proposed, because of the embryological failure of the separation of the GHH and the SCT. The calcifications of the thyrohyoid ligament are diverse, and those involving the synovial joints must not be the only ones considered. This case can inspire the search for the causes of this calcification and the differentiation with the synovial joint calcification cases which need surgical intervention. Investigations of calcifications involving TC and the thyrohyoid ligament are far from being resolved, not only the different types but also the etiologies that can lead to these calcifications.

ACKNOWLEDGEMENTS

The authors thank the *Fundació del Conjunt Monumental del Castell de Besora* for its support in this work, and Carlos García Mallo for the RX images.

REFERENCES

AHMAD M, MADDEN R, PEREZ L (2005) Triticeous cartilage: prevalence on panoramic radiographs and diagnostic criteria. *Oral Surg Oral Med Oral Pathol Oral Radiol Endodontol,* 99(2): 225-230.

ALQAHTANI E, MARRERO DE, CHAMPION WL, ALAWAJI A, KOUSOUBRIS PD, SMALL JE (2016) Triticeous cartilage CT imaging characteristics, prevalence, extent, and distribution of ossification. *Otolaryngol Head Neck Surg (United States),* 154(1): 131-137.

ALSARRAF R, MATHISON S, FUTRAN N (1998) Symptomatic presentation of an enlarged, ossified triticeal cartilage. *Am J Otolaryngol - Head Neck Med Surg*, 19(5): 339-341.

AVRAHAMI E, HAREL M, ENGLENDER M (1994) CT evaluation of displaced superior cornu of ossified thyroid cartilage. *Clin Radiol*, 49(10): 683-685.

BARUT O, AHLQVIST J, GAROFF M, JOHANSSON E, JOHANSSON M, WESTER P, JÄGHAGEN E (2020) Levring calcifications in the neck region of patients with carotid artery stenosis: A computed tomography angiography study of topographic anatomy. *Oral Surg Oral Med Oral Pathol Oral Radiol,* 129(5): 523-530.

BUSQUETS F, MALGOSA A (2020) Besora's Castle monumental complex. Archaeology and Paleontology Campus – UAB Barcelona. https://www.uab.cat/web/seus/presentacio/presentacio-1345831858471.html Accessed December 9, 2022.

DE BAKKER BS, DE BAKKER HM, SOERDJBALIE-MAIKOE V, DIKKERS FG (2019) Variants of the hyoid-larynx complex, with implications for forensic science and consequence for the diagnosis of Eagle's syndrome. *Sci Rep*, 9(1): 1-10.

DI NUNNO N, LOMBARDO S, COSTANTINIDES F, DI NUNNO C (2004) Anomalies and alterations of the hyoid-larynx complex in forensic radiographic studies. *Am J Forensic Med Pathol,* 25(1): 14-19.

DWIGHT T (1907) IX Stylo-hyoid ossification. *Ann Surg,* 46(5): 721-735.

HARRISON DFN (1995) The Anatomy and Physiology of the Mammalian Larynx. Cambridge: Cambridge University Press.

ILANKOVAN V (1987) An anomaly of the thyro-hyoid articulation. *J Laryngol Otol*, 101(9): 959-961.

ITO K, ANDO S, AKIBA N, WATANABE Y, OKUYAMA Y, MORIGUCHI H, YOSHIKAWA K, TAKAHASHI T, SHIMADA M (2012) Morphological study of the human hyoid bone with three-dimensional CT images – Gender difference and age- related changes. *Okajimas Folia Anat Jpn*, 89(3): 83-92.

JOSHI MM, JOSHI SD, JOSHI SS (2014) Prevalence and variations of cartilago triticea. *Int J Anat Res*, 2(3): 474-477.

KAINZ J, FRIEDRICH G, ANDERHUBER F (1990) Zwei atavistische Merkmale des Kehlkopfskelettes. *Cells Tissues Organs,* 137(2): 103-108.

KLINEFELTER EW (1952) The anomalous hyoid; review of the literature and report of a case. *Radiology,* 58(2): 224-227.

PARSONS FG (1909) The topography and morphology of the human hyoid bone. *J Anat Physiol*, 43: 279-290.

PINHEIRO J, CASCALLANA JL, LOPEZ DE ABAJO B, OTERO JL, RODRIGUEZ-CALVO MS (2018). Laryngeal anatomical variants and their impact on the diagnosis of mechanical asphyxias by neck pressure. *Forensic Sci Int*, 290: 1-10.

PORRATH S (1969) Roentgenologic considerations of the hyoid apparatus. *Am J Roentgenol Radium Ther Nucl Med*, 105(1): 63-73.

SOERDJBALIE-MAIKOE V, VAN RIJN RR (2008) Embryology, normal anatomy, and imaging techniques of the hyoid and larynx with respect to forensic purposes: A review article. *Forensic Sci Med Pathol*, 4(2): 132-139.

STANDRING S, ELLIS H, HEALY J, JOHNSON D, WILLIAMS A (2008) Gray's Anatomy, The Anatomical Basis of Clinical Medicine. UK: Elsevier Health Sciences.

URBEN SL, RANSOM ER (1999) Fusion of the thyrohyoid interval in a patient with a thyroglossal duct cyst. *Otolaryngol - Head Neck Surg*, 120(5): 757-759.

VAN DEN BROEK P, BRINKMAN WFB (1979) Congenital laryngeal defects. *Int J Pediatr Otorhinolaryngol*, 1(1): 71-78.

VATANSEVER A, DEMIRYÜREK D, TATAR I, ÖZGEN B (2018) The triticeous cartilage - Redefining of morphology, prevalence and function. *Folia Morphol*, 77(4): 758-763.

WILSON I, STEVENS J, GNANANANDAN J, NABEEBACCUS A, SANDISON A, HUNTER A (2017) Triticeal cartilage: the forgotten cartilage. *Surg Radiol Anat*, 39: 1135-1141.

Facial, lingual, and infraorbital artery calcification: A rare incidental radiographic finding

Karthikeya Patil, C.J. Sanjay, Eswari Solayappan, Namrata Suresh

Department of Oral Medicine and Radiology, JSS Dental College and Hospital, JSS Academy of Higher Education and Research, Mysore - 570 015, India

SUMMARY

Identifying calcification of arteries in the head and neck region may aid in the diagnosis of advanced systemic conditions. In contrast, failure to recognize them can result in incorrect diagnoses and ineffective treatments. Radiographic analyses can be used to detect such calcifications. This report focuses on calcifications discovered in the facial, lingual, and infraorbital arteries following a routine dental care panoramic radiograph. This report is particularly notable because it is the second in the literature to highlight the calcification of all three arteries.

Key words: Arteriosclerosis – Medial calcinosis – Panoramic radiograph

INTRODUCTION

A comprehensive understanding of anatomy and its variations is the basis for a precise diagnosis and treatment strategy; failing in this respect may lead to misdiagnosis and undesirable treatment. Clinicians appreciate the external anatomy upon clinical examination; however, the internal anatomy necessitates further investigation, specifically radiography.

Routine radiographic evaluations show clues to some systemic conditions. Appreciation of sporadic incidental findings in the radiographic image is crucial to the patient's health care. Nevertheless, a thorough history and clinical examination in conjunction with radiographic imaging often aid in recognizing the underlying specific systemic diseases. Panoramic radiographs for primary screening are an excellent tool for detecting structural changes and soft tissue calcification due to their accessibility, affordability, and reliability.

This report represents a rare instance of a male patient exhibiting soft tissue calcification in branches of the external carotid artery detected by panoramic radiography. There are scanty reports in the scientific literature concerning calcification of the facial artery, lingual artery, maxillary artery, etc., in the head and neck region. To date, only two cases of calcification involving the infraorbital artery have been reported. This article reports a rare third instance of the calcification of the infraorbital artery and a second case in the scientific literature reporting the calcification of three arteries: the facial, the lingual, and the infraorbital artery.

Corresponding author:
Dr. C.J. Sanjay. Department of Oral Medicine and Radiology, JSS Dental College and Hospital, JSS Academy of Higher Education and Research, Mysore - 570 015, India. Phone: +91 97425 65566. E-mail: drsanjaycj_dch@jssuni.edu.in ORCID ID: 0000-0003-2830-1481

Submitted: December 12, 2022. **Accepted:** January 18, 2023

https://doi.org/10.52083/IYAU7211

CASE REPORT

A 67-year-old male patient presented with the chief complaint of swelling in the right lower third of his face that had been present for one week and was gradually increasing. This was preceded by a toothache in the right lower back tooth region two weeks prior. The patient presented with a medical history of Type II diabetes mellitus and hypertension for the past 15 years, along with chronic renal disease, for which he had been undergoing haemodialysis twice a week for the past 5 years. He was on medication for diabetes (glipizide and metformin), hypertension (telmisartan), and renal disease (furosemide and allopurinol). In addition, the patient was also on pantoprazole 40 mg (once daily) for oesophageal reflux and calcium supplements (calcitriol and cholecalciferol). The patient's blood work showed elevated levels for the following parameters: serum creatinine level was 7.2 mg/dL (normal range: 0.5 to 1.1 mg/dL); gamma-glutamyl transpeptidase level was 140 U/L (normal range: 3-35 U/L); lipase level was 440 U/L (normal range: 0 to 60 U/L); ferritin level was 589 ng/mL (normal range: 12 to 200 ng/mL); total triglycerides: 254 mg/dL (normal range: 25 to 200 mg/dL); Random blood sugar: 240 mg/dL.

On examination, the facial asymmetry was very noticeable on the right side. There was a large, diffuse swelling on the right side of the face that was about 3.4 cm long and went from 1.5 cm below the right infraorbital margin to the lower edge of the mandible. Anteroposterior, from the right commissure of the lip, till 0.5 cm away from the angle of the mandible. The skin over the swelling was smooth and glossy, and there was no pus discharge or sinus opening.

Intraoral examination revealed deep dental caries involving the left maxillary central and lateral incisors, left mandibular second premolar and third molar, and right mandibular first and third molar, along with a grossly decayed right mandibular second molar with tenderness noted in the buccal vestibule. Generalized gingival recession and gingival inflammation were also observed. The upper and lower arches were partially edentulous. Deep dental caries in the right first, second, and third molars was diagnosed, leading to submandibular and submental space infections. A preliminary panoramic radiograph was advised, which depicted deep dental caries in the right mandibular first molar and a homogenous periapical radiolucency with a well-defined sclerotic border. The right mandibular second and third molars were grossly decayed, with features of chronic periapical abscesses. Generalized horizontal and vertical alveolar bone loss was observed with the normal trabecular pattern in both the maxilla and mandible.

This case presented an incidental finding near the angle, and the body of the mandible bilaterally had a radiopaque "tram track" or "pipeline" or "rail track" arrangement that emerged beneath the angle and the body of the mandible, followed a tortuous course, wrapping over to the hyoid bone. This calcification turned an S-bend (two loops), first winding down over the submandibular gland fossa and then up over the base of the mandible (Fig. 1). Bilaterally towards the ramus of the mandible, a tortuous upward loop of calcification was evident. The calcification extended laterally towards the left ramus of the mandible and the coronoid notch, at the levels of C1, C2, and C3. Unique to this case was the calcification running towards the left infraorbital rim and crossing the pterygomaxillary fissure. This uniform line mimics soft tissue calcification.

DISCUSSION

Arteries are vital components of the circulatory system, primarily transporting oxygenated blood from the heart to various parts of the body. They are made up of three layers: the tunica intima, media, and adventitia, which are comprised of smooth muscles that allow constriction and dilation via parasympathetic nervous system signals. Over the years, the arteries undergo age- or health-related issues that may lead to the thickening of arterial walls. Dystrophic calcifications in the arteries of the head and neck region, which manifest as atherosclerosis or arteriosclerosis, are extremely rare. Atherosclerosis is the constriction of arteries caused by a persistent inflammatory condition that leads to the accumulation of cholesterol, fatty substances, cellular waste products, calcium, and fibrin, which form a plaque within the large and medium-sized arteries (Castling et al., 2015).

Arteriosclerosis, on the other hand, usually affects the small arteries (Diehm et al., 2013). It is believed that "intimal fibromuscular tissue" or "hyaline" deposits in small arteries, with one or two layers of smooth muscle cells, lead to the thickening of the arterial wall (Fishbein and Fishbein, 2015). In 1903, arterial calcification was first described by Monckeberg as the calcification of tunica media, an intermediate layer of the artery wall composed of smooth muscle and elastic fibers, which was then referred to as "Monckeberg sclerosis or medial calcinosis" (Tahmasbi-Arashlow et al., 2016; Castling et al., 2015). Monckeberg medial calcinosis, unlike atherosclerosis, does not impede the arterial lumen; rather, there is a loss of vascular elasticity and compliance due to substantial perfusion reduction and clinically significant coronary and peripheral artery disease.

The extracellular matrix, as well as cells of the media or intima of the vascular endothelium, are thought to be the cause of vascular calcification. These are the sites where hydroxyapatite with a significant level of crystallization tends to deposit, eventually leading to vascular calcification (Tahmasbi-Arashlow et al., 2016). Atherosclerotic lesions are greatly influenced by genes involved in lipoprotein metabolism. For instance, deficiency of apolipoprotein E (ApoE), a protein necessary for the liver's clearance of chylomicron and very-low-density lipoprotein (VLDL) remnants, can lead to the formation of atherosclerotic lesions (Schinke et al., 1998).

Calcification of the "cheek arteries" was the first instance of calcification in the arteries of facial tissues, as described by Ennis and Burket (1942). These calcifications are usually an indication of the severity and progression of conditions such as diabetes, hyperparathyroidism, coronary artery disease, chronic renal disease, and arteriosclerosis. Furthermore, this condition has been linked to hypervitaminosis D, hyperlipidaemia, aging, chronic inflammation, and autoimmune diseases such as systemic lupus erythematosus (Prasad et al., 2015).

One such condition of arteriosclerosis is medial calcinosis, which is associated with end-stage renal impairment. Even though the cause of medial calcinosis is unknown, vascular smooth muscle cells in the tunica media have been identified as the major cells involved in its formation. In longitudinal studies, the prevalence of medial calcinosis was found to be 6.9% in females and 13.3% in males (Byon and Chen, 2015). Vascular calcification was found in nearly 40% of chronic renal disease patients compared to 13% of controls, as per the study by Russo et al. (2004). The Centers for

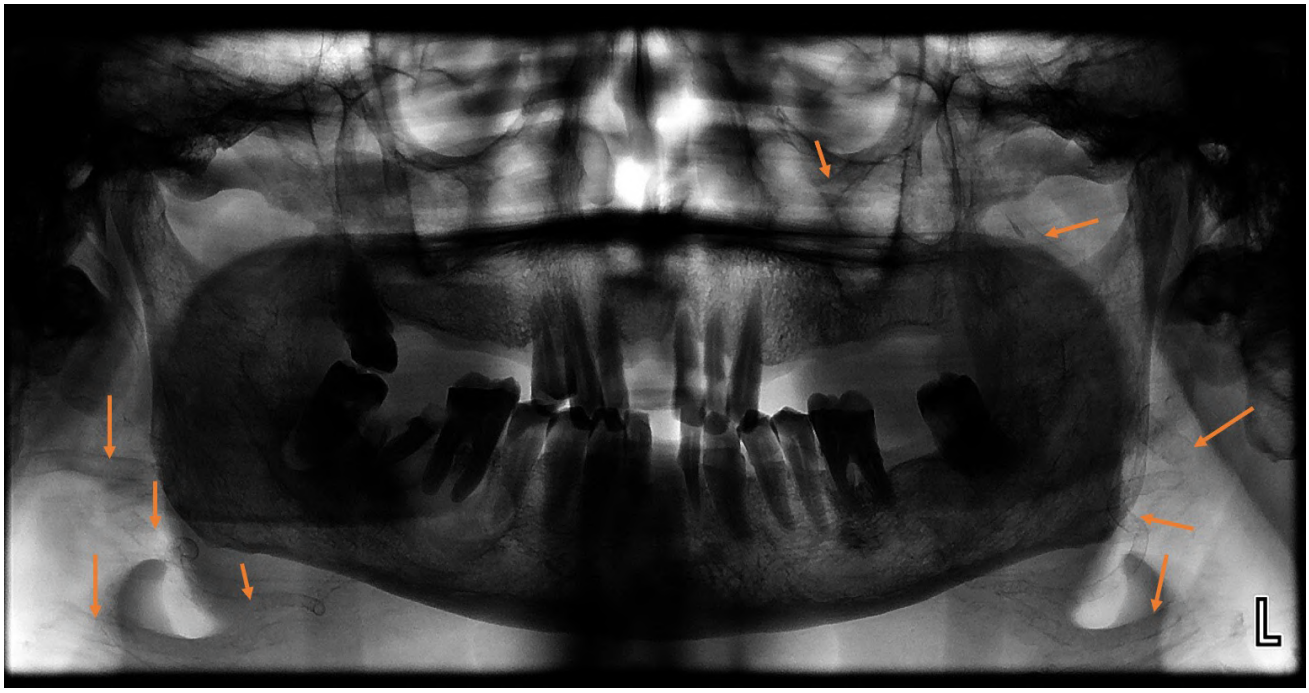

Fig. 1.- Panoramic radiograph shows an inverted-tone image depicting *tram line, pipestem, or tram track* calcification.

Disease Control and Prevention observed in 2021 that 36.8% of diabetic patients aged 20 years and older had chronic renal disease. In 2018, Frazier et al. published the first case report of infraorbital artery calcification in a patient with chronic renal disease and diabetes mellitus. According to Kramer et al. (2005), patients with chronic renal disease and diabetes are significantly more likely to present with medial calcinosis, which is consistent with the current report. Such calcifications are rarely visible on radiographs. When Miles and Craig (1983) examined 2422 panoramic radiographs taken between January 1980 and August 1981 at a Veterans Administration Centre, they discovered six cases of facial artery calcification. Furthermore, Brooks et al. (2022) reported a second incidence of facial and infraorbital artery calcification in a panoramic radiograph. On a radiograph, medial calcinosis appears as paired linear areas of calcification in soft tissue, which have been referred to as "pipeline," "tunnel track," "pipe stem," "railroad track," and "tram line"-like appearances when viewed longitudinally, as well as a circular calcification in a cross-sectional view (Castling et al., 2015).

When vascular smooth muscle cells were cultured with high phosphate concentrations in an in vitro study (Speer et al., 2009), vascular calcifications were observed, indicating that these types of calcifications can be observed in patients with hyperphosphatemia. This was a similar presentation in a 64-year-old male with type II diabetes mellitus, chronic renal disease, hyperphosphatemia, hypercalcemia-related illness, secondary hyperparathyroidism, and kidney failure, in addition to calcification of the lingual artery, facial artery, internal maxillary artery, transverse facial artery, and superficial temporal artery (Macdonald et al., 2012). In this report, similar results were found. The patient had type II diabetes, high blood pressure, chronic kidney failure, and high phosphate levels. There were also calcifications in the infraorbital, facial, and lingual arteries (Fig. 2).

To the best of our knowledge, after a thorough search, this is the third well-documented instance of reporting infraorbital artery calcification in scientific literature. Anatomical features, morphological changes, and extensions may all be seen by 3-D scans, which also reveal the structure's form, origin, location, and relations to associated structures and help in further investigations.

This report emphasizes the significance of identifying the incidental finding of medial calcinosis and its clinical implications in terms of the patient's general health, as nine out of ten individuals with chronic kidney disease are unaware of their ailment. This was easily accomplished by a panoramic radiograph, which is a well-recognized, valuable, and widely utilized diagnostic radiograph for routine day-to-day dental examinations, making it an invaluable tool for identi-

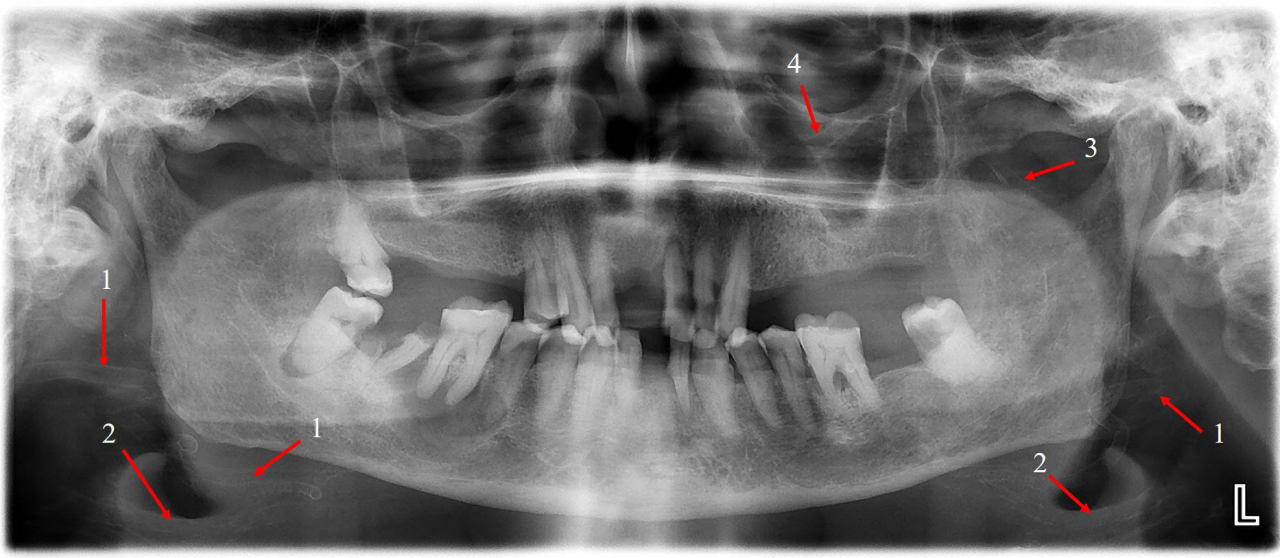

Fig. 2.- Panoramic radiograph shows the tracing of calcification. - Arrow 1 denotes a facial artery; Arrow 2, a lingual artery; Arrow 3, a maxillary artery; and Arrow 4, an infraorbital artery.

Table 1. Incidence and prevalence of calcification in radiographs. PET- Positron emission tomography; CT- Computed tomography; CBCT- Cone beam computed tomography.

S.NO	AUTHOR & YEAR	AGE & GENDER	PATIENT MEDICAL HISTORY	RADIOGRAPHIC IMAGING	RADIOGRAPHIC FINDING
1.	Ennis & Burket, 1942	Not mentioned	Not mentioned	Panoramic	Calcification of cheek artery
2.	Hays et al. 1966	60/ Male	Diabetes mellitus	Periapical and occlusal roentgenogram	Calcification of Facial artery
3.	Miles & Craig, 1983	Median age was 61 years	Hyperparathyroidism Coronary artery disease, and Diabetes mellitus	Panoramic and intraoral	6 case of Calcification of facial artery
4.	Suarez-Cunqueiro et al. 2002	69/Male	Hyperparathyroidism, Renal insufficiency, Hypothyroidism	Panoramic	Calcification of right facial artery Left maxillary, facial and lingual artery
5.	MacDonald et al. 2012	64/Male	Chronic kidney disease, Hyperparathyroidism	Panoramic and CT	Calcification of bilaterally lingual artery, facial artery, the internal maxillary artery, the transverse facial artery and the superficial temporal artery.
6.	Tahmasbi-Arashlow et al. 2016	65/Male	End-stage renal disease, Hyperthyroidism, type 2 Diabetes mellitus, Hypertension, Atrial fibrillation, and secondary Hyperparathyroidism	Panoramic, bitewing, PET, CT	Calcification of bilateral lingual and facial artery
7.	Omami, 2018	59//Male	Diabetes mellitus, Hypertension and kidney transplantation.	Panoramic and CBCT	Calcification of facial artery
8.	Frazier et al. 2018	64/Male	Not mentioned	Panoramic, CBCT	Calcification of facial artery and infraorbital arteries
9.	Fitzgerald et al. 2021	78/Male	Diabetes mellitus, Hypertension, Coronary heart disease	Panoramic, bitewing.	Calcification of facial and maxillary artery
10.	Brooks et al. 2022	90/Female	Hypertension, Hypercholesterolemia	Panoramic	Calcification of facial and infraorbital artery
11.	Current case, 2022	67/Male	Hypertension, Diabetes mellitus, Chronic renal failure	Panoramic	Calcification of facial, Lingual, Infraorbital artery

fying such serious underlying medical conditions and preventing catastrophic adverse events in patients' healthcare.

CONCLUSION

Variations in the normal anatomy may indicate the existence of serious, undiagnosed medical conditions. These variations are often incidental findings on radiographs, and failure to recognize them endangers the patient's health by concealing the situation's critical complexity. Hence, before commencing any invasive procedures, the practitioner obtained a clue about the patient's health status from this atypical picture with calcification.

REFERENCES

BROOKS JK, SHIN K, PRICE JB (2022) Occult Mönckeberg medial calcinosis of the facial and infraorbital arteries in an elderly edentulous patient. *Spec Care Dentist*, 42(6): 642-645.

BYON CH, CHEN Y (2015) Molecular mechanisms of vascular calcification in chronic kidney disease: the link between bone and the vasculature. *Curr Osteoporos Rep*, 13(4): 206-215.

CASTLING B, BHATIA S, AHSAN F (2015) Mönckeberg's arteriosclerosis: vascular calcification complicating microvascular surgery. *Int J Oral Maxillofac Surg,* 44(1): 34-36.

CENTERS FOR DISEASE CONTROL AND PREVENTION (2021) Chronic Kidney Disease in the United States, 2021. Atlanta, GA: US Department of Health and Human Services, Centers for Disease Control and Prevention.

ENNIS L, BURKET L (1942) Calcified vessels of the cheeks: demonstration by means of dental roentgenograms. *Ann Dent*, 1: 111-113.

FISHBEIN MC, FISHBEIN GA (2015) Arteriosclerosis: facts and fancy. *Cardiovasc Pathol*, 24(6): 335-342.

FITZGERALD J, ZIEGLER ME, GREEN PT, NEVILLE BW (2021) Calcified facial and maxillary arteries: Incidental radiographic findings

indicative of Mönckeberg arteriosclerosis. *J Am Dent Assoc*, 152(11): 943-946.

FRAZIER JJ, CASIAN R, BENSON BW (2018) Mönckeberg medial calcinosis of the infraorbital arteries: a first case report. *Oral Surg Oral Med Oral Pathol Oral Radiol*, 125(2): e31-e35.

HAYS JB, GIBILISCO JA, JUERGENS JL (1966) Calcification of vessels in cheek of patient with medial arteriosclerosis. *Oral Surg Oral Med Oral Pathol*, 21(3): 299-302.

KRAMER H, TOTO R, PESHOCK R, COOPER R, VICTOR R (2005) Association between chronic kidney disease and coronary artery calcification: the Dallas Heart Study. *J Am Soc Nephrol*, 16(2): 507-513.

MACDONALD DS, ZHANG L, GU Y (2012) Calcification of the external carotid arteries and their branches. *Dentomaxillofac Radiol*, 41(7): 615-618.

MILES DA, CRAIG RM (1983) The calcified facial artery. A report of the panoramic radiographic incidence and appearance. *Oral Surg Oral Med Oral Pathol*, 55(2): 214-219.

OMAMI G (2018) Calcification of the stylohyoid complex in Libyans. *Saudi Dent J*, 30(2): 151-154.

PLUMP AS, SMITH JD, HAYEK T (1992) Severe hypercholesterolemia and atherosclerosis in apolipoprotein E deficient mice created by homologous recombination in ES cells. *Cell,* 71(2): 343-353.

RUSSO D, PALMIERO G, DE BLASIO AP, BALLETTA MM, ANDREUCCI VE (2004) Coronary artery calcification in patients with CRF not undergoing dialysis. *Am J Kidney Dis*, 44(6): 1024-1030.

SCHINKE T, MCKEE MD, KIVIRANTA R, KARSENTY G (1998) Molecular determinants of arterial calcification. *Ann Med*, 30(6): 538-541.

SPEER MY, YANG HY, BRABB T (2009) Smooth muscle cells give rise to osteochondrogenic precursors and chondrocytes in calcifying arteries. *Circ Res*, 104(6): 733-741.

SUAREZ-CUNQUEIRO MM, DUKER J, LIEBEHENSCHEL N, SCHÖN R, SCHMELZEISEN R (2002) Calcification of the branches of the external carotid artery detected by panoramic radiography: a case report. *Oral Surg Oral Med Oral Pathol Oral Radiol Endod*, 94(5): 636-640.

TAHMASBI-ARASHLOW M, BARGHAN S, KASHTWARI D, NAIR MK (2016) Radiographic manifestations of Mönckeberg arteriosclerosis in the head and neck region. *Imaging Sci Dent*, 46(1): 53-56.

Velamentous cord insertion - Gross and histological examination

Fariha Sabeen

Department of Anatomy, Mahatma Gandhi Memorial Medical College, Jharkhand, India

SUMMARY

Velamentous cord insertion is an abnormal cord insertion in which the umbilical vessels diverge as they traverse between the amnion and chorion before reaching the placenta. The present case study is an incidental finding during a cesarean section. A 30-year-old woman with 37 weeks of pregnancy, gravid 1, presented with bleeding per vagina. Previous ultrasonography reports confirmed the presence of a low-lying placenta. However, the site of cord insertion was not mentioned in her reports. On cesarean section, a healthy male baby was delivered. The placenta had velamentous cord insertion. Approximately 12 cm of vessels traversed the membranes.

In the present case study, the umbilical cord was thoroughly examined, both grossly and histologically. For better understanding, the umbilical cord was also compared with a normal umbilical cord. Morphologically, the length and diameter of the cord were in normal range and blood vessels were patent. Histologically, the slides showed the absence of Wharton's jelly on the cord.

Velamentous cord insertion can lead to many unwanted complications like preterm birth, post-partum hemorrhage, and even fetal death. Abdominal ultrasound can be used to visualize the insertion of the cord; however, it often goes unnoticed, as the insertion site is usually obscured by the fetus. Moreover, maternal obesity and posterior placenta make the diagnosis even more difficult. This case study highlights the necessity to pre-diagnose velamentous cord insertion. It can be done with the help of trans-vaginal ultrasound and color Doppler imaging of the cord vessels.

Key words: Umbilical cord – Velamentous cord insertion – Color Doppler imaging – Histology of umbilical cord – Placenta – Umbilical vessels

INTRODUCTION

Velamentous cord insertion is an abnormal cord insertion in which the umbilical vessels diverge as they traverse between the amnion and chorion before reaching the placenta. Membranous umbilical vessels at the placental insertion site are the main characteristics. The remainder of the cord is usually normal. Because of the lack of protection from Wharton's jelly, these vessels are prone to compression and rupture, especially when they are located in the membranes covering the cervical ostium. Umbilical cord insertion with great clinical significance. Umbilical cord forms a connecting link between fetus and the placenta through which fetal blood flows to and from placenta. The extension of the cord is dull white, moist and covered by amnion through which umbilical vessels can be seen, which is often consid-

Corresponding author:
Dr. Fariha Sabeen. Senior Resident, Department of Anatomy, Mahatma Gandhi Memorial Medical College, Jharkhand, India. E-mail: dfariha@gmail.com

Submitted: January 9, 2023. **Accepted:** February 4, 2023

https://doi.org/10.52083/YTKG6205

ered as fetal membrane (Eastman and Hellman, 2022).

According to Dattary and Charavarty (2009), the umbilical cord is attached to the placenta at varying positions. Central attachment of the cord is usually considered normal, but eccentric attachment also mostly results in uneventful delivery. Eccentric attachment refers to the lateral insertion of the umbilical cord at a distance more than 2 cm away from the placental margin. Majority of the placentas present with eccentric attachment of the cord, i.e., 73%. The incidence of central attachment of the cord and marginal and velamentous insertion was described (Soernes and Bakke, 1986). Almost 1% of cases of singleton deliveries have velamentous cord insertion[4]. These data are summarized in Table 1. Interestingly, velamentous cord occurs much more frequently with twins and is observed in as many as 15 percent of monochorionic twin gestations (Sepulveda et al., 2003).

Table 1. Incidence of attachment of the cord.

Central	18%
Eccentric	73%
Battledore	7%
Velamentous	1– 2%

Velamentous type of cord insertion is of considerable practical importance, because the umbilical vessels are separated in the membrane at a distance from the placental margin which they reach, surrounded only by a fold of amnion (Fig. 1).

CASE REPORT

A 30-year-old woman with 37 weeks of pregnancy, gravid 1, presented to the Obstetrics and Gynecology Emergency Department with a complaint of bleeding per vagina. Her previous ultrasonography reports showed the presence of a live fetus with a single posterior, low-lying placenta. There was no history of any transvaginal ultrasound and color Doppler imaging, so the site of insertion of the cord was not known. To prevent any further complications, a cesarean section was scheduled. A healthy male baby was delivered. A posterior discoid placenta with velamentous cord insertion and 12 cm of vessels traversing in membranes were observed. However, no neonatal complications or obstetric complications like vasa previa were recorded. Apgar scores were 9 and 10 at 1 and 5 min, respectively.

The umbilical cord was grossly examined for:

- Length
- Diameter
- Cut sections for the patency of vessels.
- Site of Insertion of the cord

As velamentous insertion of cord is an absolute indication for histological examination of the cord, so histological slides were prepared from the cut sections. For better understanding, slides were prepared from normal umbilical cords also, and both were compared.

All the steps of tissue processing were done – tissue cutting and fixation – A 1 x 1 cm sized tissue was taken from near the center of the cord. These tissues were fixed in 10% formalin in separate containers and were labeled. Tissue fixation was done for 1-2 days.

- Rinsing: The tissue was rinsed in running tap water.
- Dehydration: Tissue was subjected to ascending grades of alcohol, ie, 50%, 70%, 90% and absolute alcohol, for 24 h each.
- Clearing: Clearing was done by methyl benzoate for 24 h.
- Embedding: Impregnation of the tissue by a solid medium, paraffin wax, was done. Wax blocks were prepared and kept on cold plate.
- Trimming: Paraffin embedded blocks were trimmed by a sharp knife leaving an edge of 2-3 mm.
- Section cutting: Sections were cut approximately 7 µm thick and ribbons were made. Ribbons were floated on hot water bath. Sections were taken on a slide and kept on a hot plate for drying. Slides were stored in boxes.
- Staining: Slides were stained routinely by hematoxylin and eosin.
- The stained slides were observed under light microscope.

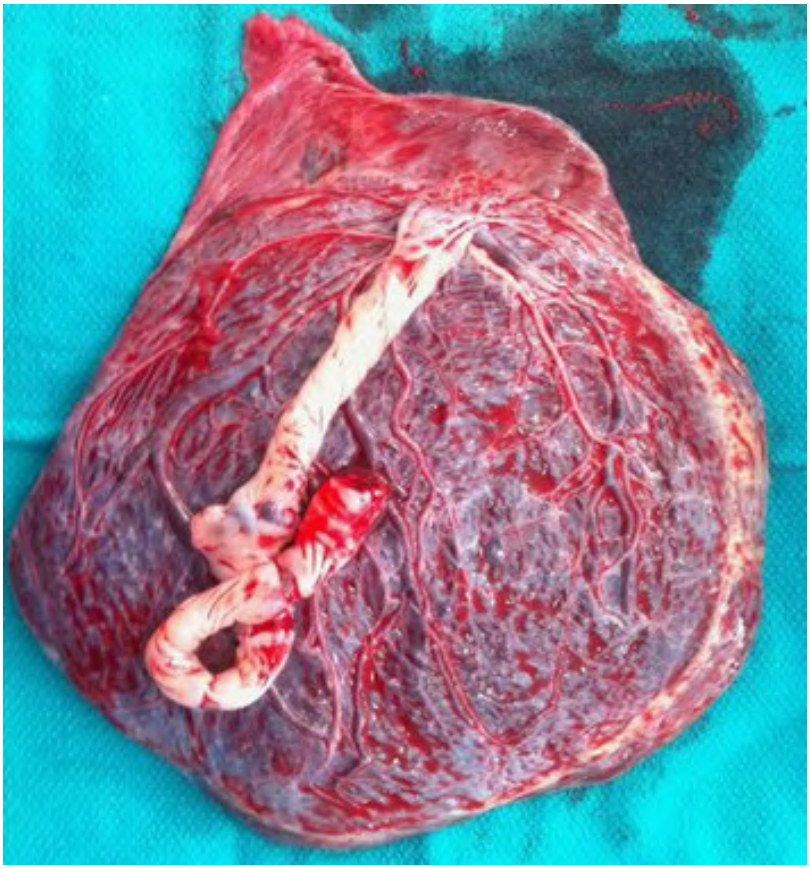

Fig. 1.- Velamentous insertion of cord.

RESULTS

In the present case, both the length of the umbilical cord attached to the fetus and the length of the umbilical cord attached to the placenta were measured and added to calculate the total length of the umbilical cord. The cord was 36 cm long and the diameter of the cord was 1 cm.

Histology slides prepared of the normal case were found to be free of any abnormalities. A cross-section of the umbilical cord of the normal case showed the amniotic membrane (Fig. 2), mucoid connective tissue (Wharton's jelly) (Fig. 3), two umbilical arteries and one umbilical vein (Figs. 2,3,4).

On the other hand, Wharton's jelly was absent in the histology slides prepared of the velamentous cord. But there was no abnormality in the number of vessels. Two umbilical arteries and one umbilical vein were present. Arteries and vein were lined by endothelium. The internal elastic lamina was present in the intima and inner media, both of which were thicker in arteries than in vein.

DISCUSSION

The average length of umbilical cord is 55 cm with the range of 30-100 cm, hence the length of the cord, 36 cm, falls within normal range. Eastman and Hellman (2022) described the diameter of the umbilical cord ranged between 1-1.25 cm. Hence, the diameter, 1 cm, can also be considered to be in a normal range.

Frequently, placental or cord abnormalities are a leading cause of perinatal deaths. An emergency cesarean section is still needed in a lot of uneventful pregnancies. More than half cases of uneventful pregnancies are associated with placental or umbilical cord abnormalities (Hasegawa et al., 2006). A recent report indicated that 85% of obstetricians in England and Wales stated that velamentous cord insertion is not routinely screened during anomaly scanning (Ioana and Wayne, 2010).

According to Pal (2013) in his Textbook of Histology, the umbilical cord extends between placenta and fetus. It brings the oxygenated blood

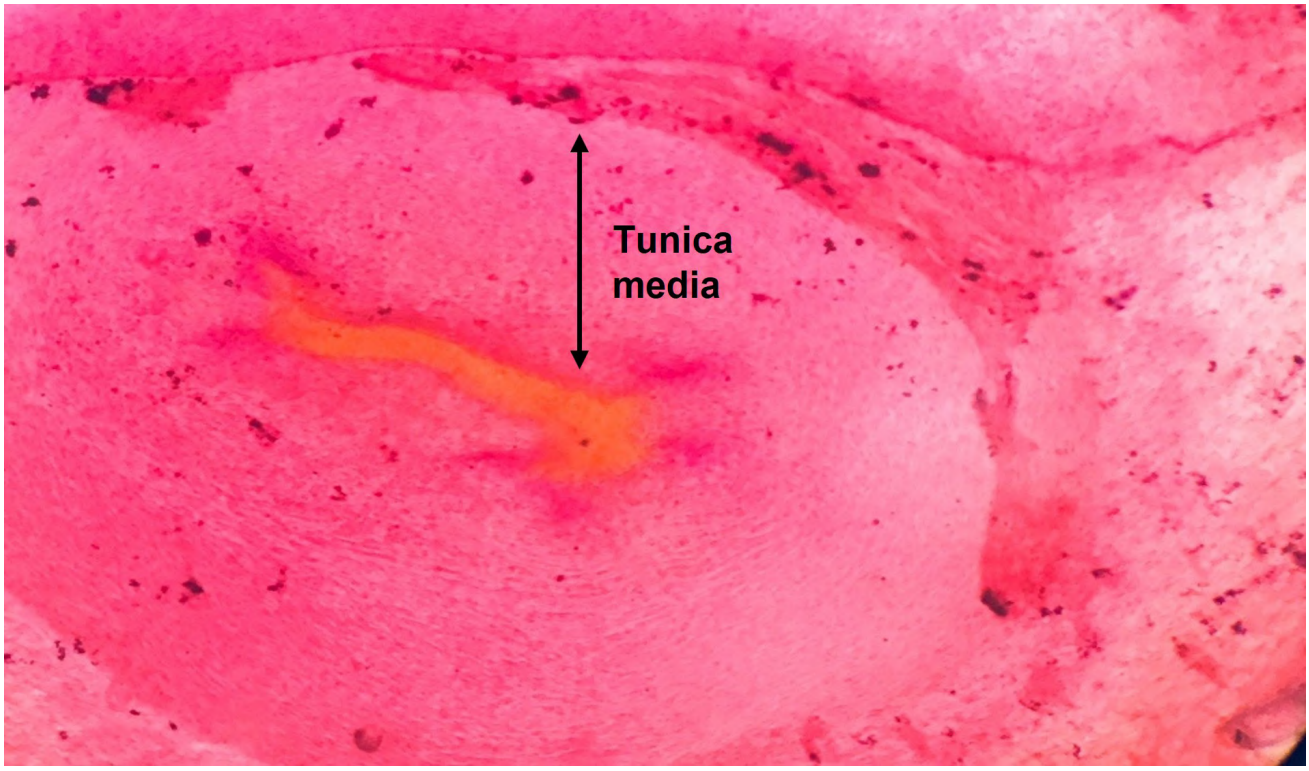

Fig. 2.- Slide of umbilical cord showing umbilical artery with thick tunica media.

from placenta to fetus through a single umbilical vein, and carries deoxygenated blood to placenta through two umbilical arteries. A cross-section of the umbilical cord shows the amniotic membrane covering the umbilical cord (Hasegawa et al., 2006). Thus, the cord is lined by flattened amniotic epithelial cells (Pal, 2013).

Deep to epithelial lining, umbilical cord contains mucoid connective tissue (Wharton's Jelly). The Wharton's Jelly consists of highly branched fibro-

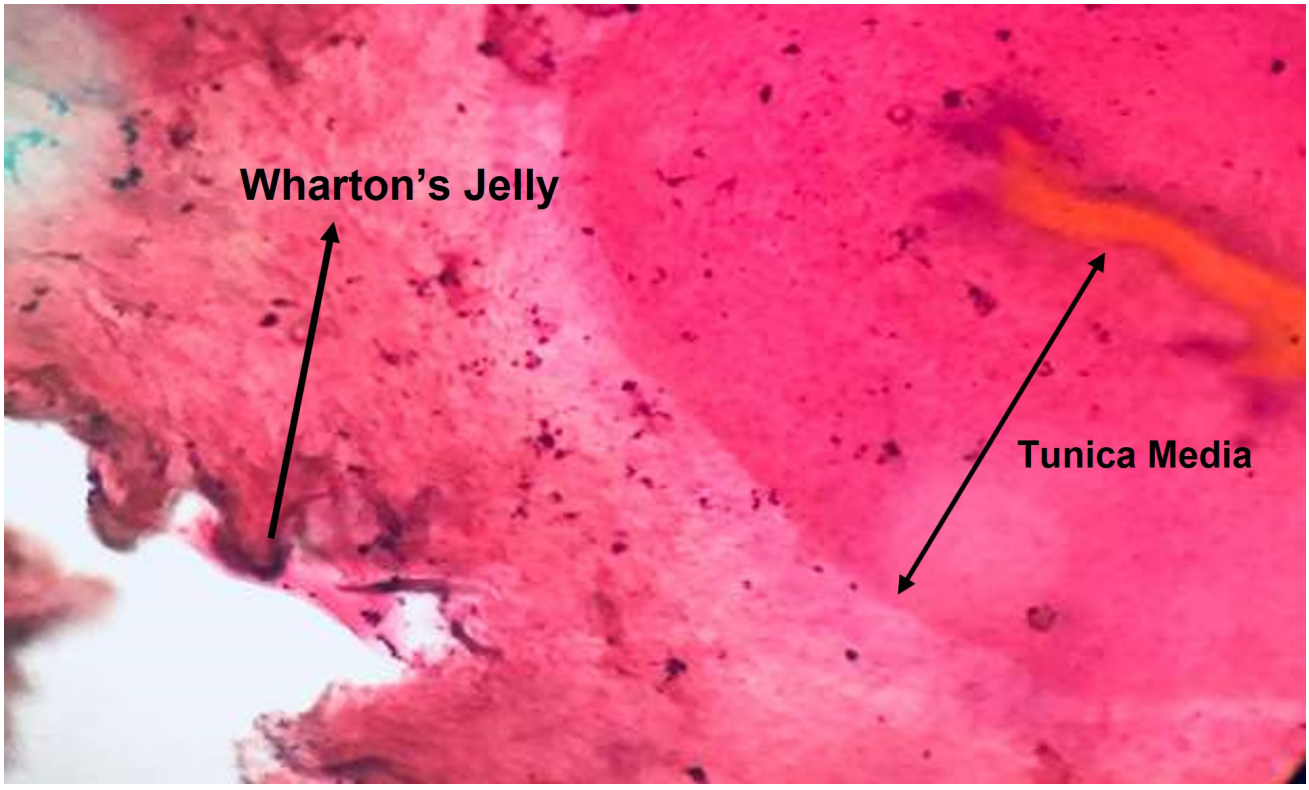

Fig. 3.- Slide of normal umbilical cord showing Wharton's Jelly.

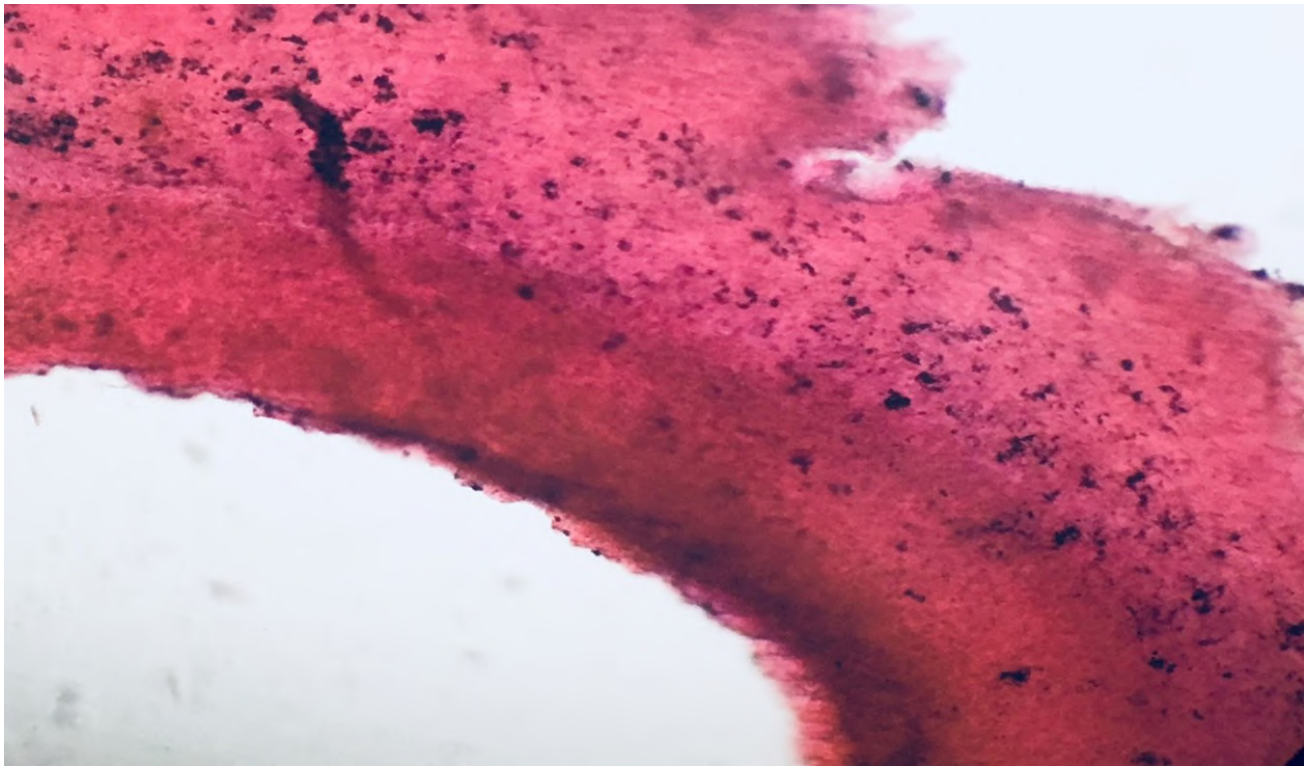

Fig. 4.- Slide of umbilical cord showing umbilical vein with thin tunica media.

blasts, collagen fibers and ground substance. The fibroblasts are widely separated from each other because of ground substance. In the connective tissue, there is presence of two umbilical arteries and one umbilical vein. The umbilical arteries are thick walled and show wavy internal elastic lamina and narrow lumen. The vein is thin walled with wide lumen (Pal, 2013).

Abnormal cord insertion is usually associated with adverse neonatal outcomes. In velamentous cord insertion, vessels from the umbilical cord run through part of the chorionic membrane rather than directly into the placenta. Thus, the blood vessels are not protected by Wharton's jelly within the cord, making fetal hemorrhage more likely to occur when the fetal membranes rupture (Antonette, 2022).

With the help of the present case study, the author tries to throw some light on the importance of pre-diagnosis of velamentous cord insertion. In this particular case, velamentous cord insertion was not identified prenatally, and it was diagnosed only during the intrapartum period. The author strongly recommends transvaginal ultrasound along with color Doppler scan in every pregnancy to avoid any unexpected consequences. On histological evaluation, it was confirmed that Wharton's jelly was absent from the cord, which makes it more vulnerable to hemorrhage. Although this case had a favorable outcome, velamentous cord insertion must be ruled out in early gestation itself. Women diagnosed with velamentous cord insertion may be counseled about the condition and potential courses of action, including preterm delivery or caesarean section.

ACKNOWLEDGEMENTS

The author would like to express thanks to the Department of Obstetrics and Gynecology (MGM Medical College and Hospital) for the permission to collect the placenta.

The author also owes a big thank-you to colleagues at the Department of Pathology (MGM Medical College and Hospital) for their great help whenever needed. Due permission was taken from the Ethical Society of MGM Medical College and Hospital.

REFERENCES

ANTONETTE T (2022) Vasa Previa. *MSD Manual.*

DATTARY S, CHARAVARTY S (2009) Holland and Brews*, Manual of Obstetrics,* 4th edit., Elsevier, India.

EASTMAN N, HELLMAN L (2022) Development and anatomy of placenta. In*: William's Obstetrics,* 26th edit. Appleton Century Crofts Inc, New York.

HASEGAWA J, MATSUOKA R, ICHIZUA K, SEZIKAWA A, OKAI T (2006) Velamentous cord insertion: significance of prenatal detection to predict perinatal complications. *Taiwan J Obstet Gynecol*, 45(1): 21-25.

IOANA C, WAYNE C (2010) Diagnosis and management of vasa previa: a questionnaire survey. *Ultrasound Obstet Gynecol*, 35(2): 205-209.

PAL GP (2013) *Textbook of Histology,* 3rd edit., pp 40-41.

SEPULVEDA W, ROJAS I, ROBERT JA, SCHNAPPC, ALCALDE JL (2003) Prenatal detection of velamentous insertion of the umbilical cord: a prospective color Doppler ultrasound study. *Ultrasound Obstet Gynecol,* 21(6): 564-569.

SOERNES T, BAKKE T (1986) The length of human umbilical cord in vertex and breech presentations. *Am J Obstet Gynaecol,* 154: 1086-1087.

ANTONIO DE GIMBERNAT Y ARBOS (1734-1816)

Pedro Mestres Ventura

Institute of Anatomy and Cell Biology, Laboratory of Electron Microscopy, Medical School, University of Saarland, Homburg Saar, Germany

Languages*: Spanish and Catalan. Versions in English and German are in preparation.*
Publisher*: Arola-Editors (Tarragona, Spain), 2022.*

Antonio de Gimbernat y Arbós is probably one of the figures in Spanish medicine about whom more has been written. This is the newest biography about this great historical figure born in Cambrils (Tarragona, Spain), and surely is a special one because it was made by Dr. Mestres, a native Cambrilense, passionate about his land, his people, history in general and that of medicine in particular, a prestigious and renowned anatomist and connoisseur to perfection of Gimbernat's field of work of who for many years has studied his life and work.

This book was born from the commitment to write a new biography of this figure, which arose in 2016 during the symposium held in Cambrils to commemorate the bicentenary of the death of Gimbernat that was organized by Dr. Mestres (Pedro Mestres Ventura, 2016).

The book traces a chronological account of Gimbernat's life that begins with the origins (chapter one) and the character's childhood and youth (chapter two). In these chapters, the author gives us a portrait of Cambrils and Catalan society at the time when Gimbernat, in the bosom of a wealthy family, began his compulsory studies in a fairly planned manner. The third chapter explains Gimbernat's journey to Cádiz, where he enrolled in the Royal College of Surgery of Cádiz (1756), and where he met another great surgeon who would influence him in his career: Pere Virgili. In the fourth chapter, we can see Gimbernat moving to Barcelona with the help of Virgili to start his work at the Royal College of Surgery of Barcelona. The fifth chapter narrates perhaps the most transcendent years in Gimbernat's professional life, i.e., his stay in several European countries, subsidized by King Charles III of Spain, with the aim of returning to Spain after having learned the most recent advances in the field of anatomy and surgery in order to improve the health of the population. It was precisely in London, on April 25, 1777, where he was able to explain his technical innovation on crural hernia surgery during a lecture of eminent professor John Hunter. The sixth and seventh chapters deal with the most important episodes of Gimbernat's career in Madrid after his European tour. Here we see how he was entrusted with the creation and subsequent direction of the Royal College of Surgery of Madrid, was appointed surgeon of the King's Chamber, and subsequently first Royal Surgeon and, as a result of this, president of all the surgical colleges in Spain. The eighth chapter shows us Gimbernat in decline, losing influence and reputation, especially due to some controversial decisions of a political nature during the Napoleonic invasion; to all this must be added a progressive but significant physical de-

https://doi.org/10.52083/TKFP3489

terioration and serious economic problems. The ninth chapter reviews his published and unpublished works, which include the most recognized of all: the *New Method of Operating the Crural Hernia* (1793). Finally, the tenth chapter, titled "Gimbernat in images", illustrates all known images of the surgeon, whether in drawing, engraving, painting, bust or medallion.

By reading this book, we easily realize that we are dealing with a character with an enormous capacity for work, a great intelligence, a facility for learning, a deep and wide knowledge in many aspects of medicine (including the field of pharmacology), and above all a great commitment to the profession.

The book, besides being recognized for his important discoveries in the anatomy of the human body and his ability to apply them to the improvement of surgical operations, shows us Gimbernat's capacities as a health "manager", at a time when "everything was to be done" in this field, improving education and medical training and the structures on which the organization of professionals and medicine itself had to be based.

With regard to the writing of the book, we can say that the book contents a rich bibliography presented in a very accessible way that allows an easy and agile reading of the text. In this sense, the chronological method, while interspersing the most personal aspects with the purely scientific, together with an impeccable contextualization of everything that is narrated (from the socio-political atmosphere of the time, the medical science of the 18th century and because of the intrigues between characters and institutions in which Gimbernat participated in the midst of the struggle to impose his criteria and of course, his power and prominence), make this book not only interesting for specialists in Gimbernat's work, but also for all those interested in medicine in general, as well as in history and biographies.

Prof. José R. Sañudo

Dept. of Anatomy, Faculty of Medicine

Universidad Complutense, Madrid, Spain

REFERENCE

MESTRES VENTURA P (Guest editor) (2016) Honoring Don Antonio de Gimbernat, Anatomist and Surgeon (1734-1816) Cambrils (Tarragona), 19 November. Bicentenary of Gimbernat's death. *Eur J Anat*, 20 Supplement 1.

Index of Contents of the Supplement:

European Journal of Anatomy